Guidelines for Analysis Methods and Construction Engineering of Curved and Skewed Steel Girder Bridges

DETAILS

185 pages | 8.5 x 11 | PAPERBACK
ISBN 978-0-309-25839-5 | DOI 10.17226/22729

AUTHORS

White, Donald W.; Coletti, Domenic; Chavel, Brandon W.; Sanchez, Andres; Ozgur, Cagri; Chong, Juan Manuel Jimenez; Leon, Roberto T.; Medlock, Ronald D.; Cisneros, Robert A.; Galambos, Theodore V.; Yadlosky, John M.; Gatti, Walter J.; and Kowatch, Gary T.

NATIONAL COOPERATIVE HIGHWAY RESEARCH PROGRAM

NCHRP REPORT 725

Guidelines for Analysis Methods and Construction Engineering of Curved and Skewed Steel Girder Bridges

Donald W. White
GEORGIA INSTITUTE OF TECHNOLOGY
Atlanta, GA

Domenic Coletti
HDR ENGINEERING, INC.
Raleigh, NC

Brandon W. Chavel
HDR ENGINEERING, INC.
Chicago, IL

Andres Sanchez
HDR ENGINEERING, INC.
Pittsburgh, PA

Cagri Ozgur and Juan Manuel Jimenez Chong
PAUL C. RIZZO ASSOCIATES, INC.
Pittsburgh, PA

Roberto T. Leon
VIRGINIA POLYTECHNIC INSTITUTE AND STATE UNIVERSITY
Blacksburg, VA

Ronald D. Medlock and Robert A. Cisneros
HIGH STEEL STRUCTURES, INC.
Lancaster, PA

Theodore V. Galambos
UNIVERSITY OF MINNESOTA
Minneapolis, MN

John M. Yadlosky
HDR ENGINEERING, INC.
Pittsburgh, PA

Walter J. Gatti
TENSOR ENGINEERING
Indian Harbor Beach, FL

Gary T. Kowatch
THE MARKOSKY ENGINEERING GROUP
Youngwood, PA

Subscriber Categories
Bridges and Other Structures • Highways

Research sponsored by the American Association of State Highway and Transportation Officials
in cooperation with the Federal Highway Administration

TRANSPORTATION RESEARCH BOARD

WASHINGTON, D.C.
2012
www.TRB.org

NATIONAL COOPERATIVE HIGHWAY RESEARCH PROGRAM

Systematic, well-designed research provides the most effective approach to the solution of many problems facing highway administrators and engineers. Often, highway problems are of local interest and can best be studied by highway departments individually or in cooperation with their state universities and others. However, the accelerating growth of highway transportation develops increasingly complex problems of wide interest to highway authorities. These problems are best studied through a coordinated program of cooperative research.

In recognition of these needs, the highway administrators of the American Association of State Highway and Transportation Officials initiated in 1962 an objective national highway research program employing modern scientific techniques. This program is supported on a continuing basis by funds from participating member states of the Association and it receives the full cooperation and support of the Federal Highway Administration, United States Department of Transportation.

The Transportation Research Board of the National Academies was requested by the Association to administer the research program because of the Board's recognized objectivity and understanding of modern research practices. The Board is uniquely suited for this purpose as it maintains an extensive committee structure from which authorities on any highway transportation subject may be drawn; it possesses avenues of communications and cooperation with federal, state and local governmental agencies, universities, and industry; its relationship to the National Research Council is an insurance of objectivity; it maintains a full-time research correlation staff of specialists in highway transportation matters to bring the findings of research directly to those who are in a position to use them.

The program is developed on the basis of research needs identified by chief administrators of the highway and transportation departments and by committees of AASHTO. Each year, specific areas of research needs to be included in the program are proposed to the National Research Council and the Board by the American Association of State Highway and Transportation Officials. Research projects to fulfill these needs are defined by the Board, and qualified research agencies are selected from those that have submitted proposals. Administration and surveillance of research contracts are the responsibilities of the National Research Council and the Transportation Research Board.

The needs for highway research are many, and the National Cooperative Highway Research Program can make significant contributions to the solution of highway transportation problems of mutual concern to many responsible groups. The program, however, is intended to complement rather than to substitute for or duplicate other highway research programs.

NCHRP REPORT 725

Project 12-79
ISSN 0077-5614
ISBN 978-0-309-25839-5
Library of Congress Control Number 2012942265

COPYRIGHT INFORMATION

NOTICE

The project that is the subject of this report was a part of the National Cooperative Highway Research Program, conducted by the Transportation Research Board with the approval of the Governing Board of the National Research Council.

The members of the technical panel selected to monitor this project and to review this report were chosen for their special competencies and with regard for appropriate balance. The report was reviewed by the technical panel and accepted for publication according to procedures established and overseen by the Transportation Research Board and approved by the Governing Board of the National Research Council.

The opinions and conclusions expressed or implied in this report are those of the researchers who performed the research and are not necessarily those of the Transportation Research Board, the National Research Council, or the program sponsors.

The Transportation Research Board of the National Academies, the National Research Council, and the sponsors of the National Cooperative Highway Research Program do not endorse products or manufacturers. Trade or manufacturers' names appear herein solely because they are considered essential to the object of the report.

Published reports of the

NATIONAL COOPERATIVE HIGHWAY RESEARCH PROGRAM

are available from:

Transportation Research Board
Business Office
500 Fifth Street, NW
Washington, DC 20001

and can be ordered through the Internet at:

http://www.national-academies.org/trb/bookstore

Printed in the United States of America

THE NATIONAL ACADEMIES

Advisers to the Nation on Science, Engineering, and Medicine

The **National Academy of Sciences** is a private, nonprofit, self-perpetuating society of distinguished scholars engaged in scientific and engineering research, dedicated to the furtherance of science and technology and to their use for the general welfare. On the authority of the charter granted to it by the Congress in 1863, the Academy has a mandate that requires it to advise the federal government on scientific and technical matters. Dr. Ralph J. Cicerone is president of the National Academy of Sciences.

The **National Academy of Engineering** was established in 1964, under the charter of the National Academy of Sciences, as a parallel organization of outstanding engineers. It is autonomous in its administration and in the selection of its members, sharing with the National Academy of Sciences the responsibility for advising the federal government. The National Academy of Engineering also sponsors engineering programs aimed at meeting national needs, encourages education and research, and recognizes the superior achievements of engineers. Dr. Charles M. Vest is president of the National Academy of Engineering.

The **Institute of Medicine** was established in 1970 by the National Academy of Sciences to secure the services of eminent members of appropriate professions in the examination of policy matters pertaining to the health of the public. The Institute acts under the responsibility given to the National Academy of Sciences by its congressional charter to be an adviser to the federal government and, on its own initiative, to identify issues of medical care, research, and education. Dr. Harvey V. Fineberg is president of the Institute of Medicine.

The **National Research Council** was organized by the National Academy of Sciences in 1916 to associate the broad community of science and technology with the Academy's purposes of furthering knowledge and advising the federal government. Functioning in accordance with general policies determined by the Academy, the Council has become the principal operating agency of both the National Academy of Sciences and the National Academy of Engineering in providing services to the government, the public, and the scientific and engineering communities. The Council is administered jointly by both Academies and the Institute of Medicine. Dr. Ralph J. Cicerone and Dr. Charles M. Vest are chair and vice chair, respectively, of the National Research Council.

The **Transportation Research Board** is one of six major divisions of the National Research Council. The mission of the Transportation Research Board is to provide leadership in transportation innovation and progress through research and information exchange, conducted within a setting that is objective, interdisciplinary, and multimodal. The Board's varied activities annually engage about 7,000 engineers, scientists, and other transportation researchers and practitioners from the public and private sectors and academia, all of whom contribute their expertise in the public interest. The program is supported by state transportation departments, federal agencies including the component administrations of the U.S. Department of Transportation, and other organizations and individuals interested in the development of transportation. **www.TRB.org**

www.national-academies.org

COOPERATIVE RESEARCH PROGRAMS

CRP STAFF FOR NCHRP REPORT 725

Christopher W. Jenks, *Director, Cooperative Research Programs*
Crawford F. Jencks, *Deputy Director, Cooperative Research Programs*
Waseem Dekelbab, *Senior Program Officer*
Danna Powell, *Senior Program Assistant*
Eileen P. Delaney, *Director of Publications*
Hilary Freer, *Senior Editor*

NCHRP PROJECT 12-79 PANEL
Field of Design—Area of Bridges

Edward P. Wasserman, *Modjeski and Masters, Nashville, TN* (Chair)
David J. Kiekbusch, *Wisconsin DOT, Madison, WI*
Paul V. Liles, Jr., *Georgia DOT, Atlanta, GA*
Thomas P. Macioce, *Pennsylvania DOT, Harrisburg, PA*
Gichuru Muchane, *North Carolina DOT, Raleigh, NC*
Hormoz Seradj, *Oregon DOT, Salem, OR*
Yuan Zhao, *Texas DOT, Austin, TX*
Fassil Beshah, *FHWA Liaison*
Frederick Hejl, *TRB Liaison*

FOREWORD

By Waseem Dekelbab
Staff Officer
Transportation Research Board

This report contains guidelines on the appropriate level of analysis needed to determine the constructability and constructed geometry of curved and skewed steel girder bridges. Required plan details and submittals are included in the guidelines. When appropriate in lieu of a 3D analysis, the guidelines also introduce improvements to 1D and 2D analyses that require little additional computational costs. The report will be of immediate interest to bridge and construction engineers.

Curved and skewed steel girder bridges can experience significant three-dimensional deflections and rotations. These deformations should be considered in design and in the detailing of cross-frames and the fit-up of cross-frames during erection. The consequences of ignoring these deformations include potential fit-up problems during girder erection, over-run or under-run of deck thicknesses, misalignment of deck joints, mismatched stages in staged construction projects, deviations from intended deck cross-slopes and profiles, and unintended dead load stresses in the structural components. Depending on the severity of the bridge geometric conditions, a simple analysis solution may be adequate, or a more refined analysis may be required.

In addition, curved and skewed steel deck-girder bridges may be unstable during erection. The behavior of these structures at various stages of construction can be quite complex. Depending on the specific configuration of the structure, different levels of analysis techniques may be required to adequately assess the stability of the structure and the possible need for temporary shoring, bracing, or other means to ensure stability during erection. Longer spans, more severe curvature, and more severe skew exacerbate the magnitude of the above effects and may lead to construction problems, claims, and accidents. Therefore, greater attention to erection engineering analysis, preparation of erection plans, and review of erection plans is needed as a function of the span length, horizontal curvature, and magnitude of the skew.

Research was performed under NCHRP Project 12-79 by Dr. Donald W. White, School of Civil and Environmental Engineering at the Georgia Institute of Technology, Atlanta, GA. The objectives of NCHRP Project 12-79 were to develop (1) guidance on selecting analytical methods for design and (2) recommendations on the level of erection analysis, erection plan detail, and submittals for skewed and/or horizontally curved steel deck-girder bridges.

A number of deliverables are provided as appendices. Only Appendix A—Glossary of Key Terms Pertaining to Cross-Frame Detailing and Appendix B—Recommendations for Construction Plan Details and Level of Construction Analysis are published herein. Other

appendices are not published but are available on the TRB website by searching on *NCHRP Report 725*. These appendices are titled as follows:

- APPENDIX C—Evaluation of Analytical Methods for Construction Engineering of Curved and Skewed Steel Girder Bridges
- APPENDIX D—Benchmark Problems
- APPENDIX E—Executive Summaries of Study Bridges
- APPENDIX F—Early Correspondence with Owners and Agencies
- APPENDIX G—Owner/Agency Policies and Procedures
- APPENDIX H—Design Criteria for New Bridge Designs
- APPENDIX I—Extended Summaries of Study Bridges
- APPENDIX J—Bridge Drawings
- APPENDIX K—Organization of Electronic Data

CONTENTS

Note: Many of the photographs, figures, and tables in this report have been converted from color to grayscale for printing. The electronic version of the report (posted on the Web at www.trb.org) retains the color versions.

AUTHOR ACKNOWLEDGMENTS

The research reported herein was performed under NCHRP Project 12-79 by the School of Civil and Environmental Engineering at the Georgia Institute of Technology, Atlanta, Georgia. The Georgia Institute of Technology was the contractor for this study, with the Georgia Tech Research Foundation serving as the Fiscal Administrator.

Dr. Donald W. White, professor, Georgia Institute of Technology, was the project director and principal investigator. Mr. Domenic Coletti, PE, senior professional associate, HDR Engineering, Inc., was the co-principal investigator. The research involved a substantial collaborative effort among Georgia Tech; HDR Engineering; Markosky Engineering Group, Inc.; High Steel Structures, Inc.; Tensor Engineering; and Dr. Theodore V. Galambos. The authors of this report were Dr. White, Mr. Coletti, Dr. Brandon W. Chavel, PE, professional associate, HDR Engineering; Dr. Andres Sanchez, bridge designer, HDR Engineering (formerly graduate research assistant, Georgia Tech); Dr. Cagri Ozgur, engineering associate II, Paul C. Rizzo Associates, Inc. (formerly graduate research assistant, Georgia Tech); Dr. Juan Manuel Jimenez Chong, project engineering associate, Paul C. Rizzo Associates (formerly graduate research assistant, Georgia Tech); Dr. Roberto T. Leon, PE, professor, Virginia Polytechnic Institute and State University (formerly professor, Georgia Tech); Mr. Ronald D. Medlock, PE, director-technical services, High Steel Structures; Mr. Robert A. Cisneros, PE, chief engineer, High Steel Structures; Dr. Galambos, professor emeritus, University of Minnesota; Mr. John M. Yadlosky, PE, senior professional associate and vice president, HDR Engineering; Mr. Walter J. Gatti, president, Tensor Engineering; and Mr. Gary T. Kowatch, PE, project manager, Markosky Engineering Group.

The Tennessee Department of Transportation (TDOT) provided substantial supplementary funding for field instrumentation of Bridge EICCR22a by the Georgia Institute of Technology research team for the purpose of verifying the veracity of the 3D FEA models as a standard for comparison of 1D and 2D methods. TDOT, Bell and Associates Construction L.P., and Powell Construction Co., Inc., provided substantial assistance to the field study. The supplementary funding from TDOT and the cheerful assistance from all of the above parties are gratefully acknowledged.

SUMMARY

Guidelines for Analysis Methods and Construction Engineering of Curved and Skewed Steel Girder Bridges

Horizontally curved and/or skewed bridges generally exhibit significant torsional displacements. Twisting of the girders, and of the overall bridge as a structural system, is unavoidable in these structures. Steel I-girder and tub-girder bridges have performed well in a vast majority of the cases involving horizontal curvature and skew in highway bridge engineering. Indeed, they are arguably the premier design option for handling of curved and skewed roadway alignments. However, in situations where problems have occurred, they often have been during, or related to, the construction. Furthermore, these problems often have involved issues in addressing the torsional response.

Within the structural design profession, little has been published in the way of guidelines or recommendations on the level of structural analysis sufficient for the construction engineering of curved and skewed steel I- and tub-girder bridges. The key construction engineering considerations for these types of structures include the following:

1. The prediction of the deflected geometry at the intermediate and final stages of the construction,
2. Determination and assessment of cases where the stability of a structure or unit needs to be addressed,
3. Identification and alleviation of situations where fit-up may be difficult during the erection of the structural steel, and
4. Estimation of component internal stresses during the construction and in the final constructed configuration.

Bridges with significant span lengths, curvature, and/or skew generally require detailed planning of the erection procedures and sequences such that lifting and assembly of their spatially deformed components is achievable. Conversely, shorter bridges with minor curvature and skew can be built with less attention to the construction engineering. With respect to all of the above considerations, it is important that an appropriate level of analysis is applied for the task at hand.

This research has systematically evaluated the accuracy of various 1D (line-girder analysis based) as well as 2D-grid structural analysis procedures to assess when the simplified 1D and 2D methods are sufficient and when 3D methods may be more appropriate for prediction of the constructability and of the constructed geometry of curved and/or skewed steel girder bridges. Both steel I-girder and tub-girder bridges are addressed. A method of estimating the accuracy of conventional 1D line-girder and 2D-grid procedures as a function of the bridge geometry is provided. In addition, a number of improvements to conventional line-girder and 2D-grid methods of analysis are developed, which provide substantial benefits at little

additional computational cost. Furthermore, cases where locked-in forces from steel dead load fit (SDLF) or total dead load fit (TDLF) detailing of cross-frames should be considered using an accurate 2D-grid or 3D finite element analysis are explained, and procedures for incorporating the corresponding initial lack-of-fit displacements in these analysis methods are provided. Finally, the project has developed guidelines on the level of construction analysis, plan detail, and submittals for curved and skewed steel girder bridges. These guidelines are suitable for direct incorporation into specifications or other guideline documents.

CHAPTER 1

Background

1.1 Problem Statement

At larger span lengths, tighter curvatures and/or sharper skews, assurance of fit-up, control of the component stresses, and control of the constructed geometry are critical attributes in the construction engineering of steel girder bridges. Significantly curved and/or skewed bridges generally exhibit significant torsional deformations, along with associated significant cross-frame forces, potential for uplift at bearings, and other effects. These attributes must be considered in the design, detailing, and construction of these structures. Conversely, straight bridges with negligible skew respond predominantly in a manner involving vertical girder displacements with little or no torsional response.

Bridge engineers have a wide array of approximate and refined analysis and design tools at their disposal for the assessment of constructability. It is important that the right tool is selected for the job at hand. Furthermore, it is essential that construction plans and submittals adequately convey the information necessary to build a given structure safely without unnecessary delays or rework. With regard to these attributes, the key construction engineering considerations for steel I- and tub-girder bridges are as follows:

- **Prediction of the deflected geometry at the intermediate and final stages of the construction.** During steel erection stages, it can be necessary in some cases to limit the structural displacements to avoid fit-up difficulties. In addition, it is particularly important for the engineer to be able to predict the deflected geometry under the steel dead load, prior to the placement of the deck concrete, as well as under the total dead load, after placement of the deck and various appurtenances. It should be noted that, in general, there is no such thing as a "conservative" prediction of the structural displacements. Over-prediction of the displacements can be just as bad as under-prediction when considering the control of the constructed geometry. The deflections during the concrete deck placement generally need to be evaluated to assess that the deck thickness, cross-slopes, superelevations, and grade are within tolerances, the dead load rotations are limited at the bearings, the separate units are sufficiently aligned at deck joints, and the separate phases are matched in phased construction projects.

Detailers and fabricators use long-established practices for various types of steel structures in which they detail and fabricate the steel components such that the parts do not fit together when they are in their unloaded (unstressed and undeformed) geometry. This initial lack of fit of the undeformed components is used to compensate for some of the displacements that occur under load, and it can facilitate or hinder the assembly of the unshored, partially shored, or shored structure depending on the procedures and the erection conditions. In curved and/or skewed I-girder bridges, the corresponding practices are commonly termed *steel dead load fit* (*SDLF*)

4 Guidelines for Analysis Methods and Construction Engineering of Curved and Skewed Steel Girder Bridges

or *total dead load fit* (*TDLF*) detailing of the cross-frames. These detailing methods entail the fabrication of the cross-frames in a geometry that does not fit-up with the connection work points on the initially fabricated (cambered and plumb) girders. The corresponding internal locked-in forces twist the girders in a direction opposite to that corresponding to the torsional displacements under the bridge steel or total dead load. Due to the combined dead load and locked-in force effects, the girders deflect into a position where their webs are approximately plumb under the steel dead load, for SDLF, or under the total dead load, for TDLF. In certain cases, the dead load and locked-in force effects approximately cancel each other, such that the net final stresses due to the torsional deformations are approximately zero; however, in other cases these internal effects are additive (i.e., the locked-in forces increase the internal stresses).

Numerous bridges also are built in which all the components are detailed ideally to fit-up in their undeformed geometry. This method of detailing is commonly referred to as *no-load fit (NLF)*. When NLF detailing is used, the girders are plumb in the theoretical zero load condition when connected to the cross-frames, but due to the torsional deformations, they deflect into a position in which their webs are out of plumb, or laid over, under the action of the steel and total dead loads.

There are various advantages and disadvantages to all of the above methods of detailing, and generally, different methods work well for different bridge types and geometries. Furthermore, it is important to note that the above descriptions are from the perspective of the structural analysis and behavior of steel I-girder bridges. However, the detailer and the fabricator do not conduct any structural analysis. When SDLF or TDLF detailing is used, the detailer and fabricator work solely with the specified steel dead load and total dead load cambers of the girders. The specified steel or total dead load cambers are subtracted from the initially fabricated (cambered and plumb) girder geometries and the cross-frames are detailed to fit between the girders in the anticipated plumb steel or total dead load final geometry. The torsional interactions between the individual girders and the overall structural system, via the attached cross-frames as the structure deforms under the loads, is only indirectly and approximately considered.

SDLF and TDLF detailing are very effective at achieving *approximately* plumb steel girder webs at the targeted dead load condition. However, the resulting effects on the structural responses are quite complex and are generally not well understood. This has led to the current state of practice where the AASHTO LRFD Specifications (AASHTO, 2010) Article C6.7.2 state that for curved I-girder bridges, " . . . the Engineer may need to consider the potential for any problematic locked-in stresses in the girder flanges or the cross-frames or diaphragms. . . ." However, due to the lack of detailed knowledge of the locked-in stresses that can be generated, no guidance is provided regarding when the influence of these stresses needs to be considered in the design. The de facto standard practice is that these effects are rarely, if ever, included in design calculations. That is, the implicit assumption in the structural design of steel I-girder bridges is no-load fit (NLF). The components are implicitly assumed to fit-up perfectly in their undeformed condition under zero load. As a result, regardless of the level of sophistication of the structural analysis, the structural displacements, internal forces, and internal stresses used in current practice are in error to the extent that the locked-in responses due to SDLF or TDLF detailing are important.

The lack of understanding of SDLF and TDLF detailing effects has led, in some instances, to conflicting job requirements, such as stating that TDLF detailing should be used and that the I-girder webs should be plumb under the steel dead load condition, or stating that no significant locked-in forces shall be generated and that the I-girder webs should be plumb in the final dead load condition. The I-girder webs can be plumb only under one loading due to the fact that curved and skewed bridges displace torsionally under load. SDLF detailing targets approximately plumb webs in the steel dead load condition, while TDLF detailing targets approximately plumb webs under the final dead load. However, these detailing practices produce locked-in forces due to the corresponding fabricated initial lack of fit between the undeformed (cambered and plumb)

no-load geometry of the girders and the fabricated geometry of the cross-frames. These forces can be both additive and subtractive with the dead load forces in the structure.

Appendix A provides summary definitions of key terms pertaining to cross-frame detailing. It is essential that the reader understand these definitions to facilitate study and interpretation of the corresponding results and discussions throughout this report.

- **Determination and assessment of cases where stability effects may be important.** In curved and/or skewed structures, stability effects show up as significant second-order amplification of the displacements and the corresponding internal forces and stresses. In cases where they experience significant stability-related limit states, curved and skewed structures do not exhibit a "bifurcation" from a primary load-displacement response. Rather, the structural displacements increase at an increasing rate as the stability limit of the structure is approached. In cases where the structure is stability critical, second-order amplification can significantly impact the prediction and control of the constructed geometry. In girder bridge structures, large second-order amplification generally should be avoided in the structure's final constructed condition as well as during the concrete deck placement. However, the engineer needs to be able to anticipate and/or predict a problem in order to prevent it. Lastly, it is important to note that large second-order amplification may not present any significant problem during intermediate stages of steel erection, unless the amplified displacements lead to difficulty with fit-up of the structural components.
- **Identification and alleviation of situations where fit-up may be difficult during the erection of the structural steel.** Due to a combination of (1) structural component or unit weights, (2) the deflections of the steel components under their self-weight during a specific erection stage, as well as (3) the stiffnesses of the components (i.e., the component resistances to being deformed by come-alongs, jacks, cranes, etc. such that their connections can be made), some situations involving tight curves, sharp skews, and/or long spans may be particularly problematic for the erector to fit the structural components together. These situations generally must be identified and addressed by the development of suitable erection plans. It is well known that TDLF detailing of the cross-frames in I-girder bridges tends to increase the forces required for fit-up. This is because the cross-frames do not fit together with the girders (without some force fitting) until the girder total dead load vertical deflections have occurred in the final constructed configuration (including the influence of the concrete slab weight). The girders are not yet subjected to the total dead load, nor are they connected together in the final constructed geometry, during a given intermediate steel erection stage.

In cases where cross-frames or other secondary framing must be included in shop assembly, the fabricator is not likely to choose TDLF. Inclusion of such framing in a shop assembly is rare and only necessary in complex framing situations, such as a single-point urban interchange (SPUI), where girders of varying lengths and curvature are joined by multiple short, stiff diaphragms. For such situations, the fabricator will likely choose SDLF or NLF so that the steel can be assembled in the yard without the weight of the deck present. In such cases, it is good for the erector to be aware of the assembly requirements so that the field assembly procedure can closely mimic the shop support conditions inasmuch as the jobsite conditions will allow.

- **Estimation of component internal stresses during construction and in the final constructed condition.** AASHTO LRFD Article 6.10.3 requires various checks of factored forces and stresses in steel girder bridges during construction. These include the following:
  1. Prevention of any nominal yielding under factored loads (neglecting initial steel residual stress effects) during the construction.
  2. Checking of strength limit states, which in some cases, can occur prior to nominal yielding of the structural components.

6 Guidelines for Analysis Methods and Construction Engineering of Curved and Skewed Steel Girder Bridges

3. Prevention of girder web bend buckling or shear buckling during the construction, such that the out-of-plane deflections of the (initially out-of-flat) girder webs are limited.
4. Limiting of girder flange lateral bending stresses (to $0.6F_y$) to ensure the applicability of the AASHTO resistance equations for the girder strength limit states, and practically, to limit the magnitude of the flange lateral bending deformations.
5. Control of tensile stresses in the concrete deck, to limit the potential for significant deck cracking.

Generally speaking, the structural analysis used for assessing the construction conditions must be sufficiently accurate such that, at the least, all major contributors to the structural responses are accounted for (including all major contributions to the structural displacements, e.g., any significant deformations in attachment details). It is important for engineers to understand if, and when, the responses of curved and/or skewed steel girder bridges are impacted significantly by (1) SDLF or TDLF detailing effects and/or (2) structural stability (i.e., second-order amplification) effects, in addition to the primary effects associated with the bending and twisting of these structures under load.

- **Development of sufficient construction plans and submittals.** Given the application of a sufficient level of structural analysis for a given job, it is also important that the construction plans and procedures contain adequate detail to properly convey the job requirements as a function of the bridge and construction complexity. Bridges with significant span lengths, curvature, and/or skew generally require detailed planning of the erection procedures and sequences such that lifting and assembly of their spatially deformed components is achievable. Longer bridges typically require placement of the deck concrete in multiple stages. Setup of the concrete from prior stages and, in some cases, during the current stage, can have a significant influence on the final geometry and the ultimate performance of the structure. Conversely, shorter bridges with minor curvature and skew can be built with less attention to the construction engineering. With respect to all of the above considerations, it is important that an appropriate level of effort is applied for the task at hand. More complete guidelines are needed in current practice (2012) regarding the level of construction analysis, plan detail, and submittals for curved and/or skewed steel girder bridge structures.

1.2 Current Knowledge

Substantial progress has been achieved in recent years with the streamlining and unification of the AASHTO LRFD (2010a and b) provisions for general steel girder bridges. These Specifications provide more organized and explicit guidance on design for constructability than ever before. Also, recent AASHTO/NSBA Guidelines and Guide Specifications (AASHTO/NSBA, 2003, 2006, 2007, and 2011) provide numerous useful and important recommendations. In addition, many state DOTs have developed substantial constructability guidelines, such as PennDOT (2004), TxDOT (2005), and NCDOT (2006). However, while these documents provide important recommendations applicable to curved and/or skewed steel girder bridges, they target a broad range of steel bridge construction. The construction engineering of highly curved and/or skewed bridges is a highly specialized topic. NCHRP Project 12-79 seeks to develop recommendations that can be fully integrated with the present Specifications and Guidelines to better address the unique attributes of curved and/or skewed steel girder bridges.

In recent years, the capabilities for simulation of physical tests using advanced 3D finite element analysis (FEA) has progressed to the point that, in numerous areas, the results from physical experiments can be reproduced readily and quite reliably. There is great potential for advanced 3D FEA simulation methods to be used as a tool for more comprehensive assessment of various levels of analysis and calculation suitable for design. Nevertheless, similar to the

results from experimental testing, the results from an FEA test simulation are only as good as the accuracy of

- The detailed geometry (e.g., plate thicknesses, deck-slab thicknesses, haunch depths, girder web depths, bearing heights, bearing plan locations, etc.),
- The load and displacement boundary conditions, including any thermal loading conditions where important, and bearing restraints with finite stiffness or flexibility where important,
- The assumed initial conditions (e.g., initial residual stresses, geometric imperfections, any lack of fit between components in their unloaded condition, etc.),
- The constitutive relationships for the various constituent materials, including attributes such as early stiffness and strength gain of the deck concrete at a given casting stage, or between stages when the deck is placed sequentially in multiple stages, creep and shrinkage deformations of the concrete, concrete micro-cracking in tension, and concrete tension stiffening due to interaction with the deck reinforcing steel, and
- The kinematic assumptions and/or constraints imposed by structural theories and/or associated with the assumed interconnection between various components (e.g., the modeling of stay-in-place metal deck forms tied to the girders by flexible strap details; also, the composite interconnection between the steel girders and the concrete slab, including local short-term and creep deformation of the concrete in the vicinity of shear studs etc., particularly if accounting for early concrete stiffness gains).

The consideration of above attributes should not detract from the use of advanced 3D FEA test simulations. In many respects, the above attributes are more easily specified, controlled, and quantified in sophisticated 3D FEA models than in physical tests. Also, in certain situations, many of the above attributes have an inconsequential effect on the structural response. However, similar to successful experimental testing procedures, the execution of refined test simulations requires great care in the creation and setup of the models. This is particularly the case where advanced simulation capabilities are not facilitated well by simplified computer user interfaces. As stated well by Hall et al. (1999), "3D FEA models are not all the same."

The current knowledge about the true accuracy of different methods of analysis for curved and/or skewed steel girder bridges is limited. NCHRP Project 12-79 provided an opportunity to gain substantial insights into the behavior of curved and skewed steel bridge structures, as well as the accuracy of various methods of analysis for these structures, by comparing the results from practical design-analysis methods to the results from refined 3D FEA test simulations. The NCHRP Project 12-79 research is the first time that the overall analysis and construction engineering of curved and/or skewed steel girder bridges has been studied in a systematic manner, considering a large sample of bridges representative of the range of structures encountered in practice, to develop improved guidelines for practice.

1.3 Objectives and Scope of This Research

The objectives of NCHRP Project 12-79 are to provide the following:

1. An extensive evaluation of when simplified 1D or 2D analysis methods are sufficient and when 3D methods may be more appropriate for prediction of the constructability and of the constructed geometry of curved and/or skewed steel girder bridges, and
2. A guidelines document providing recommendations on the level of construction analysis, plan detail, and submittals for curved and skewed steel girder bridges suitable for direct incorporation into specifications or guidelines.

Both I- and tub-girder bridges are addressed.

8 Guidelines for Analysis Methods and Construction Engineering of Curved and Skewed Steel Girder Bridges

The first major objective starts with the assessment of the accuracy of "base" or "conventional" 1D (line-girder) and 2D-grid methods of analysis, representing current standards of care in the profession. These assessments lead to the identification of a number of important improvements that can be made to the current simplified methods of analysis. Various improvements are addressed that

1. Are easy to implement in structural engineering practice, and
2. Result in substantial improvements in the ability of the methods to capture the physical responses with minimal additional calculation effort.

In recognition of the importance of integration with structural analysis and design software in structural engineering practice, specific considerations with respect to software implementation also are addressed. The identification of when stability effects (i.e., second-order amplification effects) are significant, as well as the calculation of these effects when they are important, is considered. In addition, a thorough evaluation of the influence of steel dead load fit (SDLF) and total dead load fit (TDLF) detailing of the cross-frames in steel I-girder bridges is conducted. The research focused on the first objective is summarized in the NCHRP Project 12-79 Task 8 report, "Evaluation of Analytical Methods for Construction Engineering of Curved and Skewed Steel Girder Bridges," Appendix C of the contractors' final report.

The second major objective is addressed by the NCHRP Project 12-79 Task 9 report "Recommendations for Construction Plan Details and Level of Construction Analysis," which is included as Appendix B of this document. The Task 9 report provides a detailed description of considerations necessary for the development of construction plans. This information is provided in a specification format, complete with a commentary. In addition, the Task 9 report synthesizes key recommendations from the Task 8 research into a specification form.

1.4 Organization of This Report

Chapter 2 of this report provides a brief overview of the research approach used in NCHRP Project 12-79. Chapter 3 highlights the major findings from this research and their applications.

Section 3.1 summarizes the results from the core NCHRP Project 12-79 research involving the assessment of the "base" or "conventional" 1D line-girder and 2D-grid methods of analysis, representing the current standards of care in the profession. A matrix of scores is provided, indicating the general accuracy of each of the methods for determining different types of responses. This section also gives several examples of how the matrix of scores should be applied.

Section 3.2 discusses detailed results behind the assessment of the conventional analysis methods in Section 3.1 and focuses on key improvements that can be made to the current simplified methods of analysis identified in Task 8 of the NCHRP Project 12-79 research. Section 3.3 then summarizes essential results from the portion of the NCHRP Project 12-79 research focused on evaluating the influence of steel dead load fit (SDLF) and total dead load fit (TDLF) methods of detailing the cross-frames in steel I-girder bridges. This is followed by Section 3.4, which gives a synthesis of the overall pros and cons of no-load fit (NLF), steel dead load fit (SDLF), and total load fit (TDF) detailing of cross-frames, and Section 3.5, which provides a few basic recommendations for selection of cross-frame detailing methods in I-girder bridges. Chapter 3 concludes with Section 3.6, which highlights key construction engineering recommendations captured in NCHRP Project 12-79 Task 9.

Chapter 4 emphasizes the most important findings of the NCHRP Project 12-79 research, provides specific recommendations for application and implementation of the findings, and describes areas where further research would be valuable.

Appendix A provides summary definitions of key terms pertaining to cross-frame detailing. It is essential that the reader understand these definitions to facilitate study and interpretation of the corresponding results and discussions throughout this report. Appendixes B and C contain the reports for Tasks 8 and 9, addressing the two major objectives of the NCHRP Project 12-79 research. In addition, Appendix D contains a Task 7 report that provides specific written documentation on three of the 76 bridges considered in the NCHRP Project 12-79 studies. Appendix E provides a short summary of each of the bridges studied by the NCHRP Project 12-79 researchers, emphasizing the primary considerations addressed by each bridge. Appendixes F and G, respectively, show an early survey sent to owners/agencies in July 2008 and provide a brief summary of policies and practices pertaining to the analysis and design of curved and/or skewed steel girder bridges at the beginning of the NCHRP Project 12-79 research. Appendix H summarizes the criteria used for the parametric study bridges designed and evaluated during the core NCHRP Project 12-79 research. The parametric study designs were developed to reflect a comprehensive range of potential curved and/or skewed steel girder bridge attributes and geometries based on current practices. Appendix I provides a more detailed summary of results for each of the existing, example, and parametric bridges studied by the project, while Appendix J provides the engineering drawings for all of the bridges. Detailed electronic data from the complete set of analysis studies is available as one of the project's Task 8 products. Finally, Appendix K explains the organization of the project electronic data. Please note that Appendixes C through K are not published herein but are available at the TRB website by searching on *NCHRP Report 725*.

CHAPTER 2

Research Approach

This chapter provides a brief summary of the approach used in addressing the objectives of the NCHRP Project 12-79 research. The primary project tasks were:

- Task 1. Review and evaluation of pertinent research,
- Task 2. Synthesis of owner/agency policies,
- Task 3. Identification of existing bridges,
- Task 4. Identification of geometric factors,
- Task 5. Selection of range and levels of geometric factors,
- Task 6. Selection of existing and parametric design bridges,
- Task 7. Analytical studies,
- Task 8A. Data reduction and assessment of analysis procedures,
- Task 8B. Development of improvements to simplified methods, and
- Task 9. Development of guidelines.

The following descriptions are organized and arranged in the order of these tasks.

2.1 Review and Evaluation of Pertinent Research

The first task of the research was to review and evaluate pertinent domestic and international research on the basis of applicability, conclusiveness of findings, and usefulness for the development of guidance for selecting analytical methods for the construction engineering of curved and/or skewed steel girder bridges. An extensive bibliography of the pertinent research was developed, including abstract summaries of research in progress, conference and workshop presentation slides, research reports, and archival journal papers. The references were scanned, indexed, and loaded into an internal database for ease of document access. The bibliography was focused primarily on references since 1993. Since Zureick et al. (1994) developed a comprehensive bibliography of the published literature on curved I- and box-girder bridges before 1994, the bibliography focused only on references not identified by the earlier bibliography for any citations prior to 1994.

2.2 Synthesis of Owner/Agency Policies and Practices

The second project task was to synthesize current owner/agency policies and practices related to the construction engineering, construction plan preparation, and construction plan review for the above structure types. During this task, the project team coordinated its work with the

AASHTO/NSBA Steel Bridge Collaboration Task Group 13, which conducted a "Survey of Current Practice in Steel Girder Design" during the early stages of the NCHRP Project 12-79 research. The project team also conducted its own survey, which was sent to the 50 state bridge engineers and bridge engineering contacts as well as the Commonwealth of Puerto Rico, the District of Columbia, and the bridge engineering contacts of various other owner agencies. The mailing, (see Appendix F of the contractors' final report), included a short slide presentation summarizing the focus of Project 12-79, requested pertinent bridge cases (descriptions and plans) encountered in the recipient's practice that fit the criteria highlighted in the slides (summarized in the third project task below), and asked for input on state policies and practices regarding analysis methods and construction engineering of curved and/or skewed steel girder bridges.

Thirty-one responses were received. Of these, 20 provided one or more bridges that fit the criteria provided with the mailing, 12 states provided specific input regarding their policies and practices, and 9 states responded but indicated that they did not have any relevant information to provide. In addition to the specific request regarding state policies and practices, the project team researched various state policies and practices available via the Web. Appendix G of the contractors' final report contains a summary of the policies and practices from several representative states. The results of the AASHTO/NSBA Steel Bridge Collaboration Group Task Group 13 (TG13) Survey of Current Practice also are discussed in this appendix. The TG13 and Project 12-79 efforts were complementary to one another, with the TG13 efforts focusing on synthesis of current practices and practical recommendations concerning analysis methods, while the Project 12-79 focus was directed at identifying specific representative bridges and specific state policies and practices.

2.3 Identification of Existing Bridges

During Task 3, the project collected more than 130 representative curved and/or skewed steel girder bridges based on a specific set of selection criteria. These included the bridges provided by the states as well as bridges from the professional practice of the project team members and various consultants contacted by the project team.

The primary criteria posed for the collection of existing bridges were:

- Availability of quality field instrumentation data, or at least field observations, particularly during intermediate stages of construction,
- Availability of detailed construction and erection plans, and
- Successful construction but with significant challenges or concerns about the state of stress, etc.

Cases involving generally acknowledged poor practices, such as the inappropriate use of oversize holes or inadequate attachment of cross-frames leading to loss of control of the structural geometry, were specifically ruled out from consideration.

One of the key existing bridges identified for the NCHRP Project 12-79 studies was an eight-span curved I-girder fly-over ramp in Nashville, Tennessee, in which the Tennessee Department of Transportation gave the Georgia Institute of Technology researchers the opportunity to instrument and monitor the girders throughout the erection of the steel and the placement of the concrete deck. The results of this research are documented in Dykas (2012).

The collected bridges, which are documented in the project's Task 8 report (Appendix C of the contractors' final report), showed a wide diversity in span arrangements, span lengths, span-to-width ratios, horizontal curvature, skew angles, and skew patterns (i.e., radial, non-radial, parallel, and non-parallel supports). In the Task 8 report, the collected bridges are summarized

12 Guidelines for Analysis Methods and Construction Engineering of Curved and Skewed Steel Girder Bridges

succinctly in the form of sketches of their overall plan geometry, along with a title block listing specific bridge geometric parameters.

2.4 Identification of Geometric Factors

In its fourth task, the project team developed a list of various geometric factors that potentially could have a significant impact on the accuracy of simplified methods of analysis. It was clear that if NCHRP Project 12-79 was to consider analysis accuracy for curved and/or skewed steel I- and tub-girder bridges, then the project would need to consider the following factors in the design of its parametric studies:

- Some measure of the horizontal curvature and
- Some quantification of the skew magnitude and pattern.

Furthermore, it was apparent that the bridge responses, and hence the analysis accuracy, can be affected significantly by the magnitude of the span lengths as well as the span length-to-width ratios. Longer span bridges tend to be affected more substantially by dead load effects, potentially resulting in more significant stability considerations during construction. In addition, beyond a certain span length, I-girder bridges are more likely to need partial or full-span horizontal flange-level bracing systems to ensure adequate stability and sufficient resistance to lateral loads during construction. Flange lateral bracing systems cause corresponding portions of the structure to act as "pseudo-box girders," fundamentally changing the behavior of the structural system. Furthermore, longer span bridges generally exhibit larger overall deflections. These larger overall deflections can lead to larger relative deflections at certain locations in the structural system, which can sometimes be problematic during construction. Longer span bridges often have a smaller ratio of the girder spacing relative to the girder depths, and typically have larger girder depth-to-flange-width ratios. These attributes can fundamentally affect various relative deflections in the structure as well as the local and overall behavior and analysis accuracy at the different stages of construction.

In addition, the bridge span length-to-width ratios can significantly impact the influence of skew. Skewed bridges with smaller span length-to-width ratios tend to have more significant load transfer to the bearing lines across the width of the structure and hence more significant "nuisance stiffness" effects that need to be addressed in the design. Furthermore, relatively narrow horizontally curved bridges experience a greater torsional "overturning component" of the reactions, which tends to increase the vertical reactions on the girders farther from the center of curvature and decrease the vertical reactions on the girders closer to the center of curvature. Of equal or greater importance, these types of bridges potentially can experience significant global second-order amplification of their displacements. In addition, relatively wide horizontally curved bridges can have more substantial concerns related to overturning at intermediate stages of the steel erection, prior to assembly of the girders across the full width of the bridge cross-section. These spans become more stable as additional girders are erected and connected by cross-frames across the width of the bridge. Wide horizontally curved bridges also can cause greater concerns associated with overturning forces during deck placement.

Lastly, it was apparent that the bridge responses (and the analysis accuracy) can be significantly affected by whether the spans are simply supported or continuous. Simple-span bridges tend to have larger deflections for a given geometry and potentially can be more difficult to handle during construction. Although simple-span girders can see negative bending during erection (due to lifting or temporary support from holding cranes, etc.), continuous spans have more significant negative bending considerations. Furthermore, particularly in I-girder bridges,

continuous-span bridges can have significant interactions between adjacent spans with respect to both major-axis bending as well as the overall torsional response.

All of the above factors can have a substantial influence on the many detailed structural attributes of steel I-girder and tub-girder bridges. Also, there can be significant interactions between these factors in terms of their influence on the bridge responses, as well as the accuracy of different bridge analysis methods.

If one considers the many detailed attributes of steel I- and tub-girder bridge structural systems and their members and components addressed subsequently, the combinations and permutations of potential bridge designs become endless. Hence, it was decided that the most practical way of covering the design space of curved and/or skewed I-girder and tub-girder bridges was to consider a range of practical combinations and permutations of the following primary factors:

- Span length of the bridge centerline, L_s,
- Deck width normal to the girders, w, (in phased construction projects, w is determined separately for each bridge unit),
- Horizontal curvature, of which the most appropriate characterization is discussed below,
- Skew angle of the bearing lines relative to the bridge centerline, θ (equal to zero for bridges in which the bearing lines are not skewed),
- Skew pattern of the bearing lines, of which the most appropriate characterization is discussed below, and
- Span type, simple and various types of continuous spans.

2.5 Selection of Range and Levels of Geometric Factors

As part of its fifth task, the project team compiled a summary of the range of values encountered for the above primary factors, as well as for various other geometric factors, considering the existing bridges collected in Task 3. This summary is documented in the project's Task 8 research report (see Appendix C of the contractors' final report). Given, this summary and the project team's knowledge of maximum practical limits on the values, the primary factor ranges and levels shown in Table 2-1 were selected.

Several nomenclature terms for categorizing the collected existing bridges as well as the bridges studied analytically in the project research appear in Table 2-1. These are the terms ICCR, TCCR, ICSS, TCSS, ICCS, and TCCS. The complete categories and their designations, which are used extensively throughout the remainder of this report, are as follows for the I-girder bridges:

- Simple-span, straight, with skewed supports (ISSS),
- Continuous-span, straight, with skewed supports (ICSS),
- Simple-span, curved, with radial supports (ISCR),
- Continuous-span, curved, with radial supports (ICCR),
- Simple-span, curved, with skewed supports (ISCS), and
- Continuous-span, curved, with skewed supports (ICCS).

The same designations are used for the tub-girder bridges, except the first letter in the designation starts with a "T" rather than an "I."

A specific geometric factor used to characterize the bridge horizontal curvature is introduced in Table 2-1. This is the bridge torsion index:

$$I_T = \frac{s_{ci}}{s_{ci} + s_{co}} \qquad \text{Eq. 1}$$

14 Guidelines for Analysis Methods and Construction Engineering of Curved and Skewed Steel Girder Bridges

Table 2-1. Primary factor ranges and levels for the NCHRP Project 12-79 main analytical study.

Factor	I-girder bridges	Tub-girder bridges
Type of span	Simple, 2-span continuous, and 3-span continuous with one balanced end span and one end span equal in length to the main center span. Use the above 3-span continuous bridges as base ICCR and TCCR cases. Consider both 2- and 3-span continuous bridges for the ICSS and TCSS cases. Consider only 2-span continuous cases for the ICCS and TCCS designs. Consider at least one 2-span continuous bridge with a significant unbalance between the span lengths.	
Maximum span length of bridge centerline, L_s	150, 225, and 300 ft. for simple spans 150, 250, and 350 ft. for continuous spans (measured along the curve)	
Deck width, *w*	30 ft. (1 to 2 traffic lanes + shoulders and barriers) 80 ft. (4 to 5 traffic lanes + shoulders and barriers	30 ft. (1 to 2 traffic lanes + shoulders and barriers)
Torsion Index, I_T	0.58 to 0.71 for ISCR bridges 0.66 to 0.88 for ICCR bridges	0.72 to 0.87 for TSCR bridges 0.69 to 1.14 for TCCR bridges
Skew angle relative to the bridge centerline, θ	20^o, 35^o, 50^o, and 70^0 but with θ at the inside edge of the deck $\leq 70^o$ in curved spans	15^o and 30^o, plus additional sensitivity studies with variations up to ±15° from zero skew
Skew pattern	Consider the ± combinations of skew angles shown in Figure 2-1 (for straight bridges) and Figure 2-2 (for curved bridges), but using θ = 35 and 70^o for I-girder bridges and θ = 15 and 30^o for tub-girder bridges. Limit the ratio of the span lengths along the edges of the deck, L_2/L_1, to a maximum value of 2.0 in all cases. Limit the difference in orientation of adjacent bearing lines to a maximum of 90^o in all cases. Give preference to typical (i.e., non-exceptional) bridge geometries.	

The terms in this equation, illustrated in Figure 2-3, are:

- s_{ci}, the distance between the centroid of the deck and the chord between the inside fascia girder bearings, measured at the bridge mid-span perpendicular to a chord between the intersections of the deck centerline with the bearing lines, and
- s_{co}, the distance between the centroid of the deck and the chord between the outside fascia girder bearings, measured at the bridge mid-span perpendicular to a chord between the intersections of the deck centerline with the bearing lines.

The torsion index I_T is an indicator of the overall magnitude of the torsion within a span. It is a strong indicator of the tendency for uplift at the bearings under the nominal (unfactored) dead loads. This parameter was selected over various other factors that could be used to characterize the horizontal curvature effects on the bridge behavior and analysis accuracy, because it can be used to set minimum practical values for the radius of curvature of a span for a given deck width.

A value of $I_T = 0.5$ means that the centroid of the deck area is mid-way between the chords intersecting the outside and inside bearings. This is the ideal case where the radius of curvature

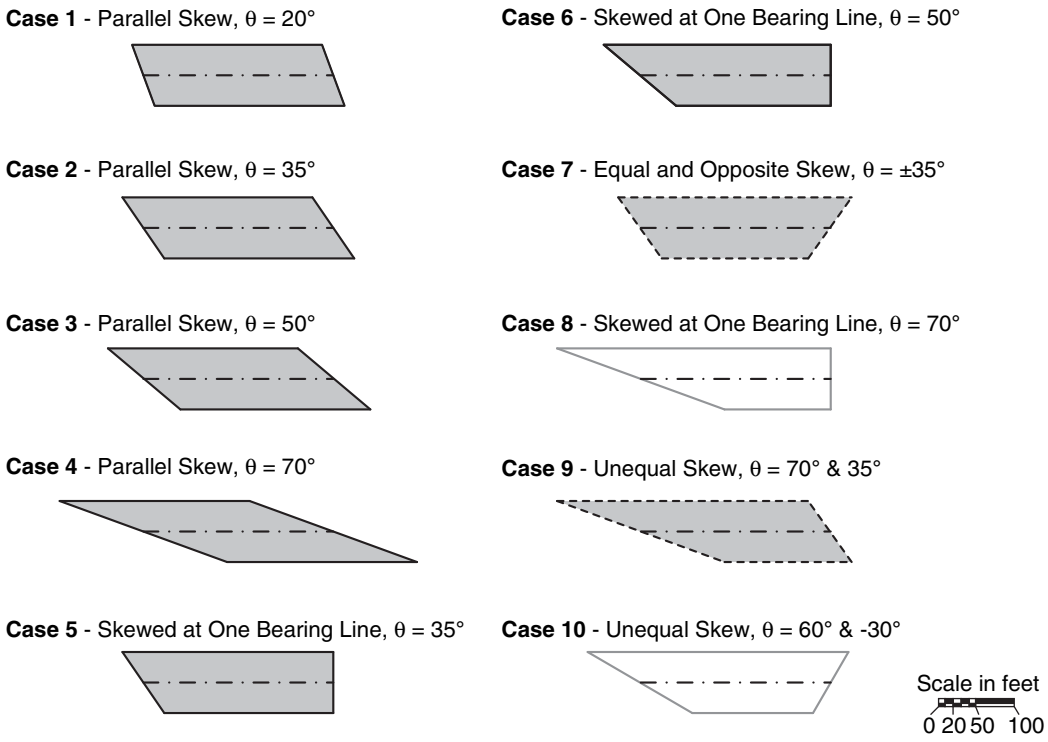

Figure 2-1. Potential skew combinations for straight I-girder bridge spans with w = 80 ft. and L_s = 250 ft. (sketches with a dashed border are considered unusual; unshaded sketches with a grey border are considered exceptional).

is equal to infinity and the skew is zero, (i.e., a straight tangent bridge). A value of $I_T = 1.0$ means that the centroid of the deck area is located at the chord line between the outside bearings. This implies that the bridge is at incipient overturning instability, by rocking about its outside bearings under uniform self-weight. For a curved radially supported span, the denominator in Equation 1, $s_{ci} + s_{co}$, is equal to $w_g \cos(L_s/2R)$, where w_g is the perpendicular width between the fascia girders.

The NCHRP Project 12-79 research identified that simple-span I-girder bridges with $I_T \geq 0.65$ are often susceptible to uplift at the bearings under nominal (unfactored) dead plus live load. Similarly, for simple-span tub-girder bridges with single bearings on each tub, $I_T = 0.87$ was identified as a limit beyond which bearing uplift problems are likely. The maximum values of 0.71 and 0.87 for the ISCR and TSCR bridges shown in Table 2-1 are similar to, and the same as, these values respectively. Continuous-span bridges can tolerate larger I_T values due to the continuity with the adjacent spans. Therefore, the maximum I_T values shown in Table 2-1 are larger for the ICCR and TCCR bridges.

Figures 2-1 and 2-2 are referenced in Table 2-1 for the consideration of the skew pattern in straight and curved bridges, respectively.

2.6 Selection of Existing and Parametric Design Bridges

Task 6 of the NCHRP Project 12-79 research involved the selection of various existing and parametric design bridges for detailed analytical study. The project's Task 8 research report provides a detailed discussion of the considerations in the selection of the study bridges. An initial preliminary selection of these bridges was conducted at the start of Task 7 of the

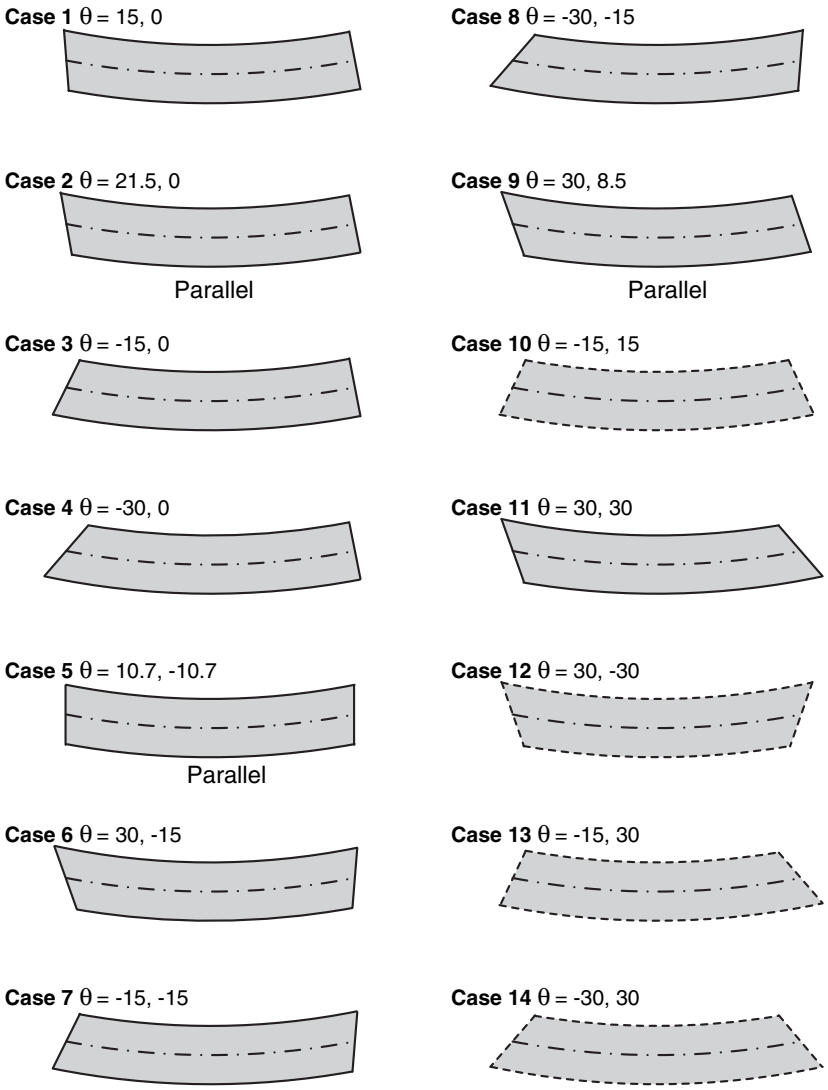

Figure 2-2. Example potential skew and horizontal curvature combinations for curved tub-girder bridge spans with w = 30 ft., L_s = 150 ft., and R = 400 ft. (sketches with a dashed border are considered unusual).

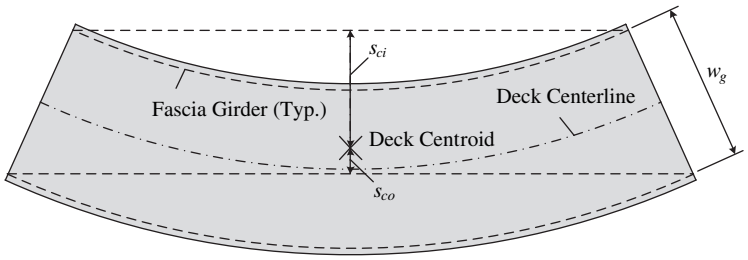

Figure 2-3. Illustration of parameters used in calculating I_T.

research (i.e., the specific analytical studies discussed in the next section). These selections were revisited and revised at various subsequent stages, based on information learned during the analytical studies. A total of 58 I-girder and 18 tub-girder bridges were considered by the project at the completion of its analytical studies. In addition, another 10 tub-girder bridges were studied that involved taking several of the above tub-girder bridges and varying the skew angle at one of the bearing lines to study the sensitivity of the bridge response and the analysis accuracy to skew effects. Of the 86 total bridges studied, 16 were existing I-girder bridges and 5 were existing tub-girder bridges. In addition, three of the I-girder bridges and two of the tub-girder bridges studied were detailed example designs taken from prior AISI, NSBA, NCHRP, and NHI developments.

Throughout the project documentation, the various bridges are referred to by their category (e.g., ISCR, ICCS, TCCS, etc.), preceded by the letters:

- E if the structure is an "existing" bridge,
- X if the structure is an AISI, NSBA, NCHRP, or NHI "example" bridge, and
- N if the structure is a "new" parametric bridge design.

A unique number is appended to the end of the designation to arrive at the specific bridge name. Therefore, for example, the 8-span continuous I-girder ramp flyover in Nashville, Tennessee, studied by the NCHRP project team, has the designation EICCR22a (the number "22a" was selected in this case to group this bridge with other Tennessee EICCR bridges considered within the project research without modifying the numbers that had already been assigned to the other EICCR bridges).

For all of the above bridges, the erection sequences used in the bridge construction were considered, or hypothetical erection sequences were developed where the specific erection sequences were not known. Various critical stages of the construction were then selected for study. In general, from 4 to 10 construction stages were selected for analysis with each bridge. As a result, more than 500 construction stages were considered in total, including the execution of multiple analysis methods for each stage.

For the $58 - 16 - 3 = 39$ additional "new" I-girder bridges and the $28 - 10 - 5 - 2 = 11$ "new" tub-girder bridges, hypothetical parametric designs were developed by the practicing design members of the project team. These $39 + 11 = 50$ bridges were complete designs satisfying the current AASHTO LRFD Specifications requirements. Specific supplementary criteria used for the design of these parametric bridges are explained in Appendix H of the contractors' final report. It is important to note that the results of simply varying design parameters without checking Specification requirements can be misleading. The AASHTO requirements were satisfied for the parametric study bridges such that the research could establish appropriate relationships between bridge design variables and recommended levels of analysis and construction engineering effort.

It should be noted that the study of 86 different bridges, as well as more than 500 construction stages, is not enough to develop a relevant data set for valid statistical assessment of analysis accuracy, given the vast range of potential situations that can be encountered during construction. However, the evaluations of the accuracy are certainly a large representative sample of the results that can be encountered in professional practice. Furthermore, a major focus of the project research, in Task 8 below, was the identification of mechanistic causes of the errors observed in the simplified analysis calculations, as well as the development of specific improvements to the simplified methods. By adopting this approach in the project research, various improvements were identified that are relatively easy to implement and lead to substantial gains in the general accuracy of the simplified methods.

2.7 Analytical Studies

Task 7 of the NCHRP Project 12-79 research involved the development and execution of a large number of analysis studies aimed at identifying when simplified 1D and 2D analysis methods are sufficient for the evaluation of the constructability and the prediction of the constructed geometry of curved and/or skewed steel girder bridges. Results from the Task 7 research are provided in written report form for three benchmark cases extracted from the larger studies. This report is included as Appendix D of the contractors' final report.

Three main levels of design analysis were considered in the NCHRP Project 12-79 research: 1D or line-girder analysis, 2D-grid (or grillage) analysis, and general 3D finite element analysis (FEA). The specifics of the methods evaluated in each of these categories are summarized in the sections below. Chapter 2 of the Task 8 project report, Appendix C to the contractors' final report, provides a more detailed description of each of the methods.

2.7.1 1D Line-Girder Analysis

The first level of analysis targeted in the NCHRP Project 12-79 research was a conventional line-girder analysis including approximations such as the V-load (Richardson, Gordon & Associates, 1976; USS, 1980; Grubb, 1984; Poellot, 1987) and M/R (Tung and Fountain, 1970) methods to account for horizontal curvature effects. For these 1D solutions, a commonly available commercial line-girder analysis program, STLBRIDGE (Bridgesoft, 2010) was used to analyze the behavior for straight skewed I- and tub-girder bridges. The 1D analysis of curved, and curved and skewed, I-girder bridges was based on the V-load method using the software VANCK (NSBA, 1996).

The 1D analysis of curved and skewed tub-girder bridges was based on a line-girder analysis coupled with supplementary calculations implemented by the project team based on the M/R Method. In addition, a useful method developed in the NCHRP Project 12-79 research for estimating the internal torque due to skew was implemented within the calculations for skewed tub-girder bridges. The recommended procedure is summarized subsequently in Section 3.2.6 of this report.

Furthermore, for the estimation of the flange lateral bending stresses and the bracing forces in tub-girder bridges, the component force equations developed originally by Fan and Helwig (1999 and 2002), supplemented by additional equations presented in Helwig et al.(2007) for the calculation of external intermediate cross-frame forces and the top flange lateral bracing (TFLB) system strut forces in Pratt systems, are used. Section 2.7 of the Task 8 report provides a detailed summary of these equations.

Lastly, one additional improvement developed in the NCHRP Project 12-79 research is included in the calculation of the top flange average longitudinal normal stresses in tub-girder bridges. An additional local "saw-tooth" contribution to these stresses that comes from the longitudinal component of the TFLB diagonal forces is included in the project calculations. These additional "saw-tooth" stresses are discussed in Section 3.2.6 of this report.

2.7.2 2D-Grid Analysis

To evaluate conventional 2D-grid methods of analysis, two commercially available software packages, employed by many bridge designers, were used to analyze the behavior of the same bridges considered with the above 1D methods: the software MDX (MDX, 2011) for analysis using a conventional 2D-grid approach, and a subset of the capabilities of the general-purpose LARSA-4D (LARSA, 2010) software for analysis using a conventional 2D-frame approach. In

the subsequent presentations in this report, the LARSA-4D software is referred to as Program P1 and the MDX software is referred to as Program P2.

The 2D-frame model is referred to as such, even though the nodes in this model have 6 degrees of freedom (dofs) (3 translations and 3 rotations), because the entire structural model is created in a single horizontal plane. As discussed in Section 2.3 of the NCHRP Project 12-79 Task 8 report (see Appendix C to the contractors' final report), if the structural model is constructed all in one plane with no depth information being represented, and if the element formulation does not include any coupling between the traditional 2D-grid dofs and the other dofs (which is practically always the case), 2D-frame models do not provide any additional forces or displacements beyond those provided by ordinary 2D-grid solutions. Assuming gravity loading normal to the plane of the structure, all the displacements at the three additional nodal dofs in the 2D-frame solution are zero. All of these conditions are satisfied by the LARSA-4D models developed in the NCHRP Project 12-79 research. Therefore, the 2D-frame and 2D-grid procedures are conceptually and theoretically synonymous. Unfortunately, the programs typically do not provide identical results for various reasons, some of which are addressed in the subsequent discussions.

For the estimation of the flange lateral bending stresses and the bracing component forces in tub-girder bridges, NCHRP Project 12-79 used the same component force equations described above for the 1D-methods in its 2D-grid solutions.

In a limited number of cases, 2D-grid calculations for the staged placement of the concrete deck were evaluated in the NCHRP Project 12-79 research. These calculations were conducted using a refinement on the basic 2D-grid modeling approach implemented in the MDX software system. For these calculations, once the deck was made composite with the girders in a staged construction analysis, the composite deck was modeled using a flat shell finite element model and the girders were represented by 6 dof per node frame elements with an offset relative to the slab. This modeling procedure is commonly referred to as a plate and eccentric beam (PEB) approach. In the PEB analyses of staged deck placement conducted by the project team, the concrete was assumed to be fully effective at the beginning of the stage just after the one in which it is placed.

In addition, a limited number of additional "specialized" 2D-grid solutions were performed in the NCHRP Project 12-79 research using the first-order analysis capabilities of a thin-walled open-section (TWOS) frame element implemented in the educational program MASTAN2 (MASTAN2, 2011; McGuire et al., 2000). The TWOS frame element in MASTAN2 contains a seventh nodal warping degree of freedom, or a total of 14 nodal dofs per element. The specific element implemented in the MASTAN2 software, discussed in detail in McGuire et al. (2000), assumes a doubly symmetric cross-section such that the girder cross-section shear center is at the same position as the cross-section centroid. Therefore, the element is strictly not capable of representing the detailed response of singly symmetric bridge I-girders. However, in the 2D-grid models created with the MASTAN2 element, all the girder and cross-frame reference axes were modeled at the same planar elevation, and no depth information (e.g., bearing position relative to the reference axis of the girders, load height above the girder reference axis, etc.) was included in the model. As such, only the three conventional 2D-grid dofs plus the additional warping dof have non-zero displacement values and the influence of the shear center height relative to the height of the cross-section centroid does not enter into the first-order TWOS 2D-grid solutions.

2.7.3 3D Finite Element Analysis

The ABAQUS software system was used to conduct linear elastic (first-order) design-analysis solutions as well as detailed geometric nonlinear (second-order) elastic "simulation" studies in the NCHRP Project 12-79 research. Furthermore, for selected cases from the full suite of 86

20 Guidelines for Analysis Methods and Construction Engineering of Curved and Skewed Steel Girder Bridges

bridges considered in the NCHRP Project 12-79 analytical studies, ABAQUS was used to conduct full nonlinear (material and geometric nonlinear) test simulations. Where possible, extant bridges were evaluated, and if those bridges had been instrumented, the test simulation results were validated against measured responses. The ABAQUS geometric nonlinear solutions were taken as the benchmarks to which all the simplified elastic analysis solutions were compared. Furthermore, the ABAQUS full nonlinear test simulation models were utilized as "virtual experiments" to evaluate questions such as the influence of different practices on the structural capacity of the physical bridges.

Generally speaking, any matrix analysis software where the structure is modeled in three-dimensions may be referred to as a three-dimensional finite element analysis (3D FEA). The NCHRP Project 12-79 research adopts the more restrictive definition of 3D FEA stated by AASHTO/NSBA G13.1 (2011). According to G13.1, an analysis method is classified as 3D FEA if:

1. The superstructure is modeled fully in three dimensions,
2. The individual girder flanges are modeled using beam, shell, or solid type elements,
3. The girder webs are modeled using shell or solid type elements,
4. The cross-frames or diaphragms are modeled using truss, beam, shell, or solid type elements as appropriate, and
5. The concrete deck is modeled using shell or solid elements (when considering the response of the composite structure).

Section 2.8 of the Project Task 8 report (Appendix C to the contractors' final report) provides a detailed description of the specific finite element modeling procedures employed for the elastic first- and second-order 3D FEA solutions as well as the full nonlinear test simulations conducted in the NCHRP Project 12-79 research.

One additional 3D FEA solution (using a less restrictive definition of the term) is employed for limited additional checking and verification of the above linear elastic and geometric nonlinear 3D FEA solutions in the NCHRP Project 12-79 research. This approach involves a second TWOS frame element implemented in the GT-Sabre software (Chang, 2006; Chang and White, 2008). The GT-Sabre TWOS frame element formulation accommodates the geometrically nonlinear modeling of singly symmetric I-girders, where the cross-section shear center and centroid are located at different elevations. In addition, in the GT-Sabre software, all of the girder reference axes (taken as the shear-center axis) are modeled at their correct physical elevations, and all of the individual cross-frame members are modeled explicitly at their precise elevation in the physical bridge. The connection of these components to the girder reference axes is accomplished by the use of rigid offsets. Furthermore, the height of the girder reference axes above the bearings is modeled by rigid offsets, and the load height of the slab dead weight effects is included in the element formulation. Therefore, the GT-Sabre model captures all the essential three-dimensional attributes of the structure geometry. This approach is referred to as a TWOS 3D-frame method in the project's Task 8 report. Specific comparisons of the geometric nonlinear results from GT-Sabre and ABAQUS are discussed subsequently in Section 3.2.4 of this report.

2.8 Data Reduction and Assessment of Analysis Procedures

Task 8A of the NCHRP Project 12-79 research involved extensive data reduction and interpretation of the results from the various studies of Task 7. The detailed results of this research are documented in the Task 8 report, "Evaluation of Analytical Methods for Construction Engineering of Curved and Skewed Steel Girder Bridges," Appendix C to the contractors' final report. Key results from this task are summarized in Chapter 3 of this report.

2.9 Development of Improvements to Simplified Methods

Task 8B of the NCHRP Project 12-79 research involved the identification of various shortcomings of the conventional simplified analysis methods studied in Tasks 7 and 8A and the development of specific improvements to these methods that lead to significantly better accuracy at little additional effort or cost. Specific calculations, as well as important considerations in the software implementation of these methods, were addressed.

Several of the key improvements for the analysis of tub-girder bridges have already been outlined in Sections 2.7.1 and 2.7.2, and, with the exception of the saw-tooth top-flange major-axis bending stress effects, were included as part of the "conventional" analysis calculations evaluated in Tasks 7 and 8 of the research. This is because these improvements are all implemented as part of 1D line-girder calculations as well as "post-processing" calculations to determine top flange lateral bending stresses and bracing component forces given the internal major-axis bending moments and torques determined either from the 1D or 2D analysis procedures. These improvements are discussed in more detail in Section 3.2.6 of this report.

The key improvements for the analysis of I-girder bridges require implementation within software if they are to be used efficiently in design practice. Furthermore, it is valuable to illustrate the critical inadequacies of the conventional methods to emphasize the importance of making the recommended improvements. Therefore, for I-girder bridges, the above Tasks 7 and 8 focus on evaluation of the accuracy of the simplified methods without the benefit of these improvements. The critical shortcomings of the conventional models and the essential improvements developed in the NCHRP Project 12-79 research are as follows:

- **The conventional 2D-grid models used in current practice substantially underestimate the girder torsional stiffnesses in I-girder bridges.** This is because the software considers only the St. Venant torsional stiffness of the girders. The contribution of warping torsion to the girder responses is generally neglected. It is interesting to note that competent structural engineers would never discount the girder warping rigidity EC_w, and thus use only the girder St. Venant torsional stiffness GJ, when evaluating the lateral-torsional buckling (LTB) resistance of I-girders. Doing so would underestimate the girder LTB resistances in practical constructed geometries so drastically that the I-girders would become useless. Yet, it is common practice to completely discount the girder warping rigidity when conducting a structural analysis. This practice generally results in dramatic over-estimation of the structural displacements when curved I-girders are modeled with nodes along the arc between the cross-frame locations. Furthermore, it tends to discount the significant transverse load paths in highly skewed bridges, since the girders are so torsionally soft (in the structural model) that they are unable to accept any significant load from the cross-frames causing torsion in the girders. As such, the cross-frame forces can be under-estimated to a dramatic extent.

In the Project 12-79 Task 8B research, this limitation is addressed by the development of an *equivalent St. Venant torsion constant* that accounts approximately for the girder stiffness from warping torsion. Section 3.2.2 of this report makes the case for this essential improvement.

- **The conventional 2D-grid models commonly use an equivalent beam stiffness model for the cross-frames that substantially misrepresents the cross-frame responses.** Fortunately, in many I-girder bridges, cross-frame deformations are small enough compared to the girder displacements such that the cross-frames perform essentially as rigid components in their own plane. However, in cases of significantly skewed I-girder bridges having "nuisance stiffness" transverse load paths (Krupicka and Poellot, 1993) and/or in general wide I-girder bridges, the deformations of the cross-frames can be a significant factor in the overall bridge response.

22 Guidelines for Analysis Methods and Construction Engineering of Curved and Skewed Steel Girder Bridges

The Project 12-79 Task 8B research addressed this issue by the development of equivalent beam elements that capture the "exact" in-plane response for various cross-frame configurations. Section 3.2.3 of this report makes the case for this essential improvement.

- **The conventional 2D-grid models do not address the calculation of girder flange lateral bending in skewed I-girder bridges.** The current AASHTO LRFD Specifications Article C6.10.1 states:

  > In the absence of calculated values of f_ℓ from a refined analysis, a suggested estimate for the total f_ℓ in a flange at a cross-frame or diaphragm due to the use of discontinuous cross-frame or diaphragm lines is 10.0 ksi for interior girders and 7.5 ksi for exterior girders. These estimates are based on a limited examination of refined analysis results for bridges with skews approaching 60 degrees from normal and an average D/b_f ratio of approximately 4.0. In regions of the girders with contiguous cross-frames or diaphragms, these values need not be considered. Lateral flange bending in the exterior girders is substantially reduced when cross-frames or diaphragms are placed in discontinuous lines over the entire bridge due to the reduced cross-frame or diaphragm forces. A value of 2.0 ksi is suggested for f_ℓ, for the exterior girders in such cases, with the suggested value of 10 ksi retained for the interior girders. In all cases, it is suggested that the recommended values of f_ℓ be proportioned [apportioned] to dead and live load in the same proportion as the unfactored major-axis dead and live-load stresses at the section under consideration. An examination of cross-frame or diaphragm forces is also considered prudent in all bridges with skew angles exceeding 20 degrees.

The above recommendations are intended as coarse estimates of the total unfactored stresses associated with the controlling strength load condition. Hence, for an example location in a straight skewed bridge governed by the STRENGTH I load combination, with discontinuous cross-frames over only a portion of the bridge and with a ratio of dead load stress to total stress (dead plus live load) of ⅓, the nominal total *dead load* flange lateral bending stress in the exterior girders may be taken as 7.5 ksi × ⅓ = 2.5 ksi. If discontinuous cross-frame lines are used throughout the entire bridge, then using this same example dead-to-live-load ratio, f_ℓ may be taken equal to 2.0 ksi × ⅓ = 0.7 ksi. In both of these cases, the dead load f_ℓ values may be taken as 10.0 × ⅓ = 3.3 ksi on the interior girders.

In lieu of using a more rational method of determining the flange lateral bending effects, the NCHRP Project 12-79 research recommends that the value of f_ℓ from the above AASHTO (2010) provisions should be combined additively with the results from other estimates for the effects of overhang bracket loads and horizontal curvature when using 1D (line-girder) and 2D-grid analysis methods. However, the variety of geometries and framing conditions in highway bridges is extensive, involving a large range of skew, length, width, number of spans, and curvature combinations. Therefore, the above recommendations are very coarse estimates. Section 3.2.4 describes a method to more closely predict the f_ℓ stresses caused by skew effects within a 2D-grid analysis.

- **None of the analysis calculations commonly employed in current bridge design practice address the calculation of internal locked-in forces due to cross-frame detailing.** Yet, AASHTO (2010) Article C6.7.2 states that for curved I-girder bridges, " . . . the Engineer may need to consider the potential for any problematic locked-in stresses in the girder flanges or the cross-frames or diaphragms . . . " This article goes on to state, "The decision as to when these stresses should be evaluated is currently a matter of engineering judgment. It is anticipated that these stresses will be of little consequence in the vast majority of cases and that the resulting twist of the girders will be small enough that the cross-frames or diaphragms will easily pull the girders into their intended position and reverse any locked-in stresses as the dead load is applied." This statement reflects a limited understanding of the detailed behavior associated with the locked-in forces due to steel dead load fit (SDLF) or total dead load fit (TDLF) detailing of the cross-frames. One major misconception in this statement is that these forces are canceled by the dead load effects calculated by the 2D-grid analysis or 3D FEA. This implicit assumption

is false. The 2D-grid and 3D FEA calculations, conducted without the modeling of initial lack-of-fit effects, only give the internal forces in the bridge associated with no-load fit (NLF) detailing. Any locked-in forces, due to the lack of fit of the cross-frames with the girders in the undeformed geometry, add to (or subtract from) the forces determined from the 2D-grid or 3D FEA design analysis. Fortunately, at many locations in a given bridge, the SDLF or TDLF detailing effects tend to be opposite in sign to the internal forces due to the dead loads. Therefore, the 2D-grid or 3D FEA solutions for the stresses at these locations are conservative (potentially, undesirably so). However, there are important locations where the SDLF or TDLF detailing effects and the dead load effects can be additive. These locations depend on the characteristics of the bridge geometry.

Substantial effort was invested in the NCHRP Project 12-79 research to thoroughly evaluate the detailed behavior associated with the conceptually simple SDLF and TDLF detailing of the cross-frames in steel I-girder bridges. Sections 3.3 through 3.5 highlight the major findings and applications of this work. However, possibly the most important point related to the locked-in forces caused by SDLF and TDLF detailing is that they can be included in 2D-grid or 3D FEA calculations with relative ease and with little computational expense. Section 3.2.5 discusses how these locked-in force effects can be included in both of these types of analysis.

- **Little guidance is available in the current literature on methods that can be used to estimate fit-up forces.** In order to evaluate the potential for fit-up difficulties in the field for a given steel erection stage, generally, the engineer must conduct some evaluation of the corresponding fit-up forces. Better and more complete guidelines for conducting these types of analysis would be very useful. Section 3.3.5 of this report highlights major NCHRP Project 12-79 Task 8B findings that address this need.

2.10 Development of Guidelines for the Level of Construction Analysis, Plan Detail, and Submittals

The tenth task of the NCHRP Project 12-79 studies involved the development of guidelines for the level of construction analysis, plan detail, and submittals for curved and skewed steel girder bridges. As noted previously, this major objective of the project is addressed by the Task 9 report "Recommendations for Construction Plan Details and Level of Construction Analysis," which is included as Appendix B of this document. Section 3.6 of this report outlines the major recommendations from these guidelines.

CHAPTER 3

Findings and Applications

3.1 Evaluation of Conventional Simplified Analysis Methods

A substantial number of studies were conducted as part of NCHRP Project 12-79 to determine the ability of approximate 1D and 2D methods of analysis to capture the behavior predicted by refined 3D finite element models.

This chapter summarizes the findings and applications from the above research. Section 3.1.1 first addresses procedures for checking of (and in many cases, preventing) large second-order amplifications. Once these considerations are addressed, attention can be focused on selecting a suitable method of analysis for estimating the primary (i.e., first-order) forces, stresses, and displacements. Section 3.1.2 presents an overall scoring matrix for use in selecting the appropriate analysis type for I-girder bridges. Sections 3.1.3 and 3.1.4 provide examples illustrating how the scoring matrix should be used. Sections 3.1.5 and 3.1.6 parallel the above sections and focus on tub-girder bridges.

Sections 3.1.2 through 3.1.6 focus on the evaluation of conventional methods of 1D line-girder and 2D-grid analysis (i.e., methods of 1D line-girder and 2D-grid analysis representative of the current standards of care in the bridge design profession). However, as noted in the statement of the objectives and scope of this research (Section 1.3) and in the summary of Task 8B of the project, development of improvements to simplified methods (see Section 2.9), substantial research effort was devoted to identifying the major causes of shortcomings in the conventional methods and to the development of easily implemented, low-cost solutions that provide substantial improvements to these methods. Sections 3.2 through 3.4 describe these improvements.

The ultimate goal of the NCHRP Project 12-79 research is to provide substantive recommendations on the level of construction analysis, plan detail, and submittals for curved and skewed steel girder bridges. The project's Task 9 report, "Recommendations for Construction Plan Details and Level of Construction Analysis," included as Appendix B of this document, addresses this goal. Section 3.6 of this chapter provides an overview of this guidelines document.

3.1.1 Checking for (and Preventing) Large Second-Order Amplification

3.1.1.1 Global Second-Order Amplification

In certain situations, steel I-girder bridges can be vulnerable to overall (i.e., global) stability-related failures during their construction. The noncomposite dead loads must be resisted predominantly by the steel structure prior to hardening of the concrete deck. Relatively narrow

I-girder bridge units (i.e., units with large span-to-width ratios) may be susceptible to global stability problems rather than cross-section or individual unbraced length strength limit states (Yura et al., 2008).

Furthermore, due to second-order lateral-torsional amplification of the displacements and stresses, the limit of the structural resistance may be reached well before the theoretical elastic buckling load. Therefore, in curved and/or skewed bridge structures sensitive to second-order effects, simply ensuring that the loads for a given configuration are below an estimated global elastic buckling load is not sufficient. Large displacement amplifications can make it difficult to predict and control the structure's geometry during construction well before the theoretical elastic buckling load is reached.

Possible situations with the above characteristics include widening projects on existing bridges, pedestrian bridges with twin girders, phased construction involving narrow units, and erection stages where only a few girders of a bridge unit are in place. In all of these cases, the problem unit is relatively long and narrow.

The NCHRP Project 12-79 research recommends a simple method that can be used to alert the engineer to undesired response amplifications due to global second-order effects. The linear response prediction obtained from any of the first-order analyses can be multiplied by the following amplification factor:

$$AF_G = \frac{1}{1 - \frac{M_{\max G}}{M_{crG}}} \qquad \text{Eq. 2}$$

where M_{maxG} is the maximum total moment supported by the bridge unit for the loading under consideration, equal to the sum of all the girder moments, and

$$M_{crG} = C_b \frac{\pi^2 sE}{L_s^2} \sqrt{I_{ye} I_x} \qquad \text{Eq. 3}$$

is the elastic global buckling moment of the bridge unit (Yura et al., 2008). In Equation (2.25), C_b is the moment gradient modification factor applied to the full bridge cross-section moment diagram, s is the spacing between the two outside girders of the unit, E is the modulus of elasticity of steel,

$$I_{ye} = I_{yc} + \frac{b}{c} I_{yt} \qquad \text{Eq. 4}$$

is the effective moment of inertia of the individual I-girders about their weak axis, where I_{yc} and I_{yt} are the moments of inertia of the compression and tension flanges about the weak-axis of the girder cross-section respectively, b and c are the distances from the mid-thickness of the tension and compression flanges to the centroidal axis of the cross-section, and I_x is the moment of inertia of the individual girders about their major-axis of bending (i.e., the moment of inertia of a single girder).

Yura et al. (2008) developed Equation 3 considering multiple girder systems with up to four girders in the cross-section of the bridge unit. The individual girders were assumed to be prismatic and all the girders were assumed to have the same cross-section. The engineer must exercise judgment in applying this equation to general I-girder bridge units with stepped or other non-prismatic cross-sections, as well as cases where the different I-girders have different cross-sections.

26 Guidelines for Analysis Methods and Construction Engineering of Curved and Skewed Steel Girder Bridges

In addition to providing an estimate of the second-order effects on the overall girder displacements, Equation 2 also can be used to predict potential increases in the girder stresses. Hence, to address potential second-order amplification concerns with narrow structural units, the results of an approximate 1D or 2D analysis should be amplified, using Equation 2, prior to conducting the constructability checks required by AASHTO LRFD Article 6.10.3. The limit states in Article 6.10.3 are:

- Nominal initial yielding due to combined major-axis bending and flange lateral bending,
- Strength under combined major-axis and flange lateral bending,
- Bend buckling or shear buckling of the girder webs,
- Reaching a flange lateral bending stress of $0.6F_y$, and
- Reaching the factored tensile modulus of rupture of the concrete deck in regions not adequately reinforced to control the concrete crack size.

Section 2.9 of the NCHRP Project 12-79 Task 8 report provides a detailed example showing the results of these calculations for an example narrow bridge unit that experienced construction difficulties (over-rotation of the bridge cross-section) during the deck placement.

The NCHRP Project 12-79 research suggests that Equation 2 should be used to detect possible large response amplifications during preliminary construction engineering. If the amplifier shows that a structure will exhibit significant nonlinear behavior during the deck placement, then in many cases, the scheme adopted for the construction should be revisited. In these cases, by conducting a detailed 3D FEA of the suspect stages, one often may find that the physical second-order amplification is somewhat smaller than predicted by the above simple estimate. If the second-order amplification is still relatively large in the more refined model, one should consider reducing the system response amplification by providing shoring or by bracing off of adjacent units. If AF_G from Equation 2 is less than approximately 1.1, it is recommended that the influence of global second-order effects may be neglected.

If it is found necessary to construct a structure that has potentially large response amplification during the deck placement, the engineer should perform a final detailed check of the suspect stages using a second-order (geometric nonlinear) 3D FEA. (It is recommended that this scenario with an AF_G larger than approximately 1.25 should be considered as requiring an accurate second-order 3D FEA.) In addition, it will be necessary to ensure that the deck placement does not deviate from the assumptions of the analysis in any way that would increase the second-order effects. Obviously, in most cases, it is best to stay away from these issues.

Substantial second-order effects during the steel erection may be a concern in some situations; however, particularly during the earliest stages of the steel erection, if the steel stresses are small and if the influence of the displacements on fit-up is not a factor, large second-order amplification of the deformations typically does not present a problem.

Steel tub girders generally have as much as 100 to more than 1,000 times the torsional stiffness of a comparable I-girder section. Therefore, when steel tub girders are fabricated with proper internal cross-frames to restrain their cross-section distortions as well as a proper top flange lateral bracing (TFLB) system, which acts as an effective top flange plate creating a pseudo-closed cross-section with the commensurate large torsional stiffness, lateral-torsional buckling is rarely a concern. Furthermore, second-order amplification in bridge tub girders is rarely of any significance even during lifting operations and early stages of the steel erection. However, overturning stability of curved tub girders, or tub-girder bridge units, can be a significant issue if it is not properly identified and addressed. Overturning stability considerations are addressed in Section 3.1.1.3.

3.1.1.2 Second-Order Amplification of Flange Lateral Bending between Cross-Frame Locations

Design-analysis compression flange lateral bending estimates usually are based on a first-order analysis. They do not consider any potential amplification of the bending between cross-frame locations due to second-order effects. That is, they do not consider equilibrium on the deflected geometry of the structure in the evaluation of the stresses. The corresponding "local" second-order flange lateral bending stresses (local to a given unbraced length between cross-frames) can be estimated by multiplying the first order f_ℓ values by the following amplification factor discussed in Article 6.10.1.6 of the AASHTO LRFD Specifications:

$$AF = \frac{0.85}{1 - f_b / F_{cr}} \geq 1.0 \qquad \text{Eq. 5}$$

where F_{cr} is the *elastic* lateral-torsional buckling stress for the compression flange, based on the unbraced length L_b between the cross-frames, and f_b is the maximum major-axis bending stress in the compression flange within the targeted unbraced length. It should be noted that when Equation 5 gives a value less than 1.0, AF must be taken equal to 1.0; in this case, the second-order amplification of the flange lateral bending is considered negligible.

When determining the amplification of f_ℓ in horizontally curved I-girders, White et al. (2001) indicate that for girders with $L_b/R \geq 0.05$, F_{cr} in Equation 5 may be determined using $KL_b = 0.5L_b$. For girders with $L_b/R < 0.05$, they recommend using the actual unsupported length L_b in Equation 5. The use of $KL_b = 0.5L_b$ for $L_b/R \geq 0.05$ gives a better estimate of the amplification of the bending deformations associated with the approximate symmetry boundary conditions for the flange lateral bending at the intermediate cross-frame locations and assumes that an unwinding stability failure of the compression flange is unlikely for this magnitude of the girder horizontal curvature. Figure 3-1 illustrates the flange lateral deflections associated with the horizontal curvature effects, as well as the unwinding stability failure mode for a straight elastic member.

3.1.1.3 Overturning Stability

Two straight dashed lines are drawn along the length direction of the plan sketches in Figure 3-2. One of the dashed lines is the chord between the fascia girder bearings on the outside of the curve. The other is the chord between the fascia girder bearings on the inside of the curve. Also shown on the plan sketches is the symbol "x," which indicates the centroid of the deck area (and hence the approximate centroid of dead weight of the structure). For bridges that are more highly curved (smaller R), the centroid (x) is closer to the outside chord line. If the curvature is

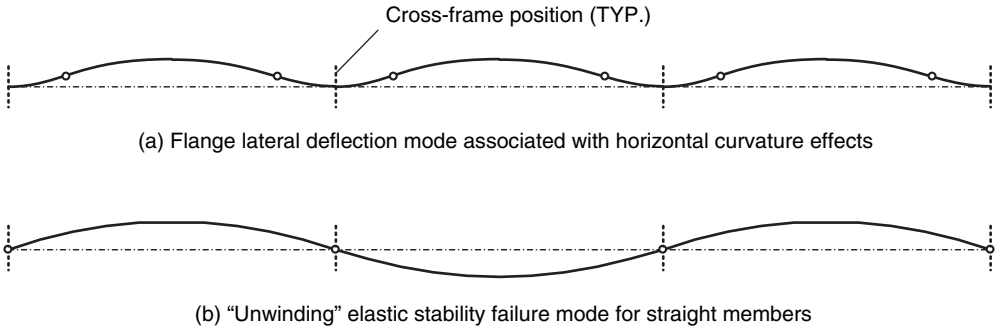

Figure 3-1. Second-order elastic deflection of a horizontally curved flange versus the unwinding stability failure mode of the compression flange in a straight member.

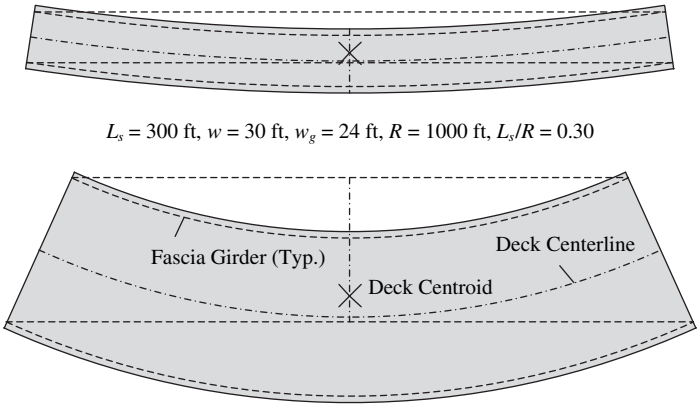

Figure 3-2. Plan geometries of two representative simple-span horizontally curved bridges with L_s = 300 ft.

such that the centroid is positioned directly over the outside chord line, then all the bridge reactions have to be zero except for the reactions at the outside bearings. That is, the bridge unit is at the verge of tipping about its outside bearings (assuming a single span, simply supported ends, and no hold-downs at the other bearings). This is obviously an extreme condition. Even a bridge with a much smaller curvature (larger radius of curvature) would require hold-downs at bearings closer to the center of curvature to handle uplift and equilibrate (or balance) the structure weight. The more common practice is to avoid uplift at any of the bearings.

As noted previously in Section 2.5, the bridge torsion index I_T provides a rough indication of the tendency for uplift at the bridge bearings. I_T is equal to 1.0 for the extreme hypothetical case where the deck centroid is located on the chord between the bearings on the outside of the curve, as discussed previously. It is equal to 0.5 for a straight bridge with zero skew. The NCHRP Project 12-79 research studies identified that simply supported I-girder bridges with $I_T \geq 0.65$ are often susceptible to uplift at some of the bearings under the nominal (unfactored) dead plus live loads. Similarly, for simple-span tub-girder bridges with single bearings on each tub, $I_T = 0.87$ was identified as a limit beyond which bearing uplift problems are likely. Continuous-span bridges can tolerate larger I_T values due to the continuity with adjacent spans.

It should be emphasized that I_T is only a rough indicator of uplift or overturning problems. It is relatively easy to calculate, but it is based on the idealization that the structure weight is uniformly distributed over the slab area. Also, when considering intermediate stages of the steel erection, it should be noted that until all the girders are erected and connected together sufficiently with cross-frames, the width of the bridge cross-section is only equal to the perpendicular distance between the connected girders on the inside and the outside of the curve. (I_T can be determined using this approximation for intermediate stages of the steel erection.) In addition, it should be noted that individual spans of continuous-span bridges may be supported essentially in a simple-span condition during some of the intermediate steel erection stages. Lastly, it should be noted that on highly curved bridge units, it may be useful to start the placement of the deck concrete on the inside of the curve to avoid a potential bearing uplift or overturning stability issue.

3.1.2 Selection of Analysis Methods for I-Girder Bridges

A quantitative assessment of the accuracy of conventional 1D line-girder and 2D-grid analysis methods was obtained in the NCHRP Project 12-79 research by identifying several error measures

that compared the conventional approximate (1D and 2D method) solutions to 3D FEA benchmark solutions. Using these quantitative assessments, the simplified methods of analysis were graded based on a scoring system developed to provide a comparative evaluation of the accuracy of each analysis method with regard to its ability to predict various structural responses.

Table 3-1 summarizes the results for the various methods and responses monitored for I-girder bridges. The grading rubric was as follows:

- A grade of A is assigned when the *normalized mean error* is less than or equal to 6 percent, reflecting excellent accuracy of the analysis predictions.

Table 3-1. Matrix for recommended level of analysis—I-girder bridges.

Response	Geometry	Worst-Case Scores		Mode of Scores	
		Traditional 2D-Grid	1D-Line Girder	Traditional 2D-Grid	1D-Line Girder
Major-Axis Bending Stresses	C ($I_C \leq 1$)	B	B	A	B
	C ($I_C > 1$)	D	C	B	C
	S ($I_S < 0.30$)	B	B	A	A
	S ($0.30 \leq I_S < 0.65$)	B	C	B	B
	S ($I_S \geq 0.65$)	D	D	C	C
	C&S ($I_C > 0.5$ & $I_S > 0.1$)	D	F	B	C
Vertical Displacements	C ($I_C \leq 1$)	B	C	A	B
	C ($I_C > 1$)	F	D	F	C
	S ($I_S < 0.30$)	B	A	A	A
	S ($0.30 \leq I_S < 0.65$)	B	B	A	B
	S ($I_S \geq 0.65$)	D	D	C	C
	C&S ($I_C > 0.5$ & $I_S > 0.1$)	F	F	F	C
Cross-Frame Forces	C ($I_C \leq 1$)	C	C	B	B
	C ($I_C > 1$)	F	D	C	C
	S ($I_S < 0.30$)	NA[a]	NA[a]	NA[a]	NA[a]
	S ($0.30 \leq I_S < 0.65$)	F[b]	F[c]	F[b]	F[c]
	S ($I_S \geq 0.65$)	F[b]	F[c]	F[b]	F[c]
	C&S ($I_C > 0.5$ & $I_S > 0.1$)	F[b]	F[c]	F[b]	F[c]
Flange Lateral Bending Stresses	C ($I_C \leq 1$)	C	C	B	B
	C ($I_C > 1$)	F	D	C	C
	S ($I_S < 0.30$)	NA[d]	NA[d]	NA[d]	NA[d]
	S ($0.30 \leq I_S < 0.65$)	F[b]	F[e]	F[b]	F[e]
	S ($I_S \geq 0.65$)	F[b]	F[e]	F[b]	F[e]
	C&S ($I_C > 0.5$ & $I_S > 0.1$)	F[b]	F[e]	F[b]	F[e]
Girder Layover at Bearings	C ($I_C \leq 1$)	NA[f]	NA[f]	NA[f]	NA[f]
	C ($I_C > 1$)	NA[f]	NA[f]	NA[f]	NA[f]
	S ($I_S < 0.30$)	B	A	A	A
	S ($0.30 \leq I_S < 0.65$)	B	B	A	B
	S ($I_S \geq 0.65$)	D	D	C	C
	C&S ($I_C > 0.5$ & $I_S > 0.1$)	F	F	F	C

[a] Magnitudes should be negligible for bridges that are properly designed & detailed. The cross-frame design is likely to be controlled by considerations other than gravity-load forces.

[b] Results are highly inaccurate due to modeling deficiencies addressed in Ch. 6 of the NCHRP 12-79 Task 8 report. The improved 2D-grid method discussed in this Ch. 6 provides an accurate estimate of these forces.

[c] Line-girder analysis provides no estimate of cross-frame forces associated with skew.

[d] The flange lateral bending stresses tend to be small. AASHTO Article C6.10.1 may be used as a conservative estimate of the flange lateral bending stresses due to skew.

[e] Line-girder analysis provides no estimate of girder flange lateral bending stresses associated with skew.

[f] Magnitudes should be negligible for bridges that are properly designed & detailed.

- A grade of B is assigned when the normalized mean error is between 7 percent and 12 percent, reflecting a case where the analysis predictions are in "reasonable agreement" with the benchmark analysis results.
- A grade of C is assigned when the normalized mean error is between 13 percent and 20 percent, reflecting a case where the analysis predictions start to deviate "significantly" from the benchmark analysis results.
- A grade of D is assigned when the normalized mean error is between 21 percent and 30 percent, indicating a case where the analysis predictions are poor, but may be considered acceptable in some cases.
- A score of F is assigned if the normalized mean errors are above the 30 percent limit. At this level of deviation from the benchmark analysis results, the subject approximate analysis method is considered unreliable and inadequate for design.

The normalized mean error used in the assessment of the above grades is calculated as

$$\mu_e = \frac{1}{N \bullet R_{FEAmax}} \sum_{i=1}^{N} e_i \qquad \text{Eq. 6}$$

where N is the total number of sampling points along the bridge length in the approximate model, R_{FEAmax} is the absolute value of the maximum response obtained from the FEA, and e_i is the absolute value of the error relative to the 3D FEA benchmark solution at point *i:*

$$e_i = \left| R_{approx} - R_{FEA} \right| \qquad \text{Eq. 7}$$

The summation in Equation 6 is computed for each girder line along the full length of the bridge. The largest resulting value is reported as the normalized mean error for the bridge. The error measure μ_e is useful for the overall assessment of the analysis accuracy since this measure is insensitive to local discrepancies, which can be due to minor shifting of the response predictions, etc. The normalized local maximum errors, e_i/R_{FEAmax}, generally are somewhat larger than the normalized mean error. Also, in many situations, unconservative error at one location in the bridge leads to comparable conservative error at another location. Hence, it is simpler to not consider the sign of the error as part of the overall assessment of the analysis accuracy.

In Table 3-1, the scoring for the various measured responses is subdivided into six categories based on the bridge geometry. These categories are defined as follows:

- Curved bridges with no skew are identified in the geometry column by the letter "C."
- The curved bridges are further divided into two subcategories, based on the connectivity index, defined as:

$$I_C = \frac{15000}{R(n_{cf}+1)m} \qquad \text{Eq. 8}$$

where R is the minimum radius of curvature at the centerline of the bridge cross-section in feet throughout the length of the bridge, n_{cf} is the number of intermediate cross-frames in the span, and m is a constant taken equal to 1 for simple-span bridges and 2 for continuous-span bridges. In bridges with multiple spans, I_C is taken as the largest value obtained from any of the spans.

- Straight skewed bridges are identified in the geometry column by the letter "S."
- The straight skewed bridges are further divided into three subcategories, based on the *skew index*:

$$I_S = \frac{w_g \tan\theta}{L_s} \qquad \text{Eq. 9}$$

where w_g is the width of the bridge measured between fascia girders, θ is the skew angle measured from a line perpendicular to the tangent of the bridge centerline, and L_s is the span

length at the bridge centerline. In bridges with unequal skew of their bearing lines, θ is taken as the angle of the bearing line with the largest skew.
- Bridges that are both curved and skewed are identified in the geometry column by the letters "C&S."

Two letter grades are indicated for each of the cells in Table 3-1. The first grade corresponds to the worst-case results encountered for the bridges studied by NCHRP Project 12-79 within the specified category. The second grade indicates the mode of the letter grades for that category (i.e., the letter grade encountered most often for that category).

It is useful to understand the qualifier indicated on the "C&S" bridges, i.e., "($I_C > 0.5$ & $I_S > 0.1$)" in Table 3-1. If a bridge has an $I_C < 0.5$ and an $I_S > 0.1$, it can be considered as a straight-skewed bridge for the purposes of assessing the expected analysis accuracy. Furthermore, if a bridge has an $I_C > 0.5$ and an $I_S \leq 0.1$, it can be considered as a curved radially supported bridge for these purposes.

Table 3-1 can be used to assess when a certain analysis method can be expected to give acceptable results. The following examples illustrate how this table should be used.

3.1.3 I-Girder Bridge Level of Analysis Example 1

Consider a horizontally curved steel I-girder bridge with radial supports, "very regular" geometry (constant girder spacing, constant deck width, relatively uniform cross-frame spacing, etc.), and $I_C < 1$, for which the engineer wants to perform a traditional 2D-grid analysis to determine the forces and displacements during critical stages of the erection sequence. (It should be noted that if I_C is calculated for an intermediate stage of the steel erection in which some of the cross-frames have not yet been placed, the number of intermediate cross-frames n_{cf} in Equation 8 should be taken as the number installed in the erection stage that is being checked. In addition, the radius of curvature R and the constant m should correspond to the specific intermediate stage of construction being evaluated, not the bridge in its final erected configuration.)

For the girder major-axis bending stresses and vertical displacements (f_b and Δ), the results are expected to deviate somewhat from those of a 3D analysis in general, since a worst-case score of B is assigned in Table 3-1 for these response quantities. The worst-case normalized mean error in these results from the 2D-grid analysis will typically range from 7 percent to 12 percent, compared to the results from a refined geometric nonlinear benchmark 3D FEA. However, one can expect that for most bridges, the errors will be less than or equal to 6 percent, based on the mode score of A for both of these responses.

Therefore, in this example, if the major-axis bending stresses and vertical displacements are of prime interest, a 2D-grid model should be sufficient if worst-case errors of approximately 12 percent are acceptable. Given that the bridge has "very regular" geometry, it is likely that the f_b and Δ errors are less than or equal to 6 percent. (The worst-case score is considered as the appropriate one to consider when designing a bridge with complicating features such as a poor span balance, or other "less regular" geometry characteristics.)

It is important to note that the engineer can compensate for potential unconservative major-axis bending stress errors in the design by adjusting the performance ratios targeted for the construction engineering design checks. For example, for the above bridge, the engineer may require that the performance ratios be less than or equal to 1/1.12 = 0.89 or 1/1.06 = 0.94 for the girder flexural resistance checks to gain further confidence in the adequacy of the resulting design. Conversely, over-prediction or under-prediction of the vertical displacements can be equally bad. Nevertheless, 12 percent or 6 percent displacement error may be of little consequence if the magnitude of the displacements is relatively small, or if the deflections are being calculated at an early stage of

the steel erection and it is expected that any resulting displacement incompatibilities or loss of geometry control can be subsequently resolved. However, if the magnitude of the displacements is large, or if it is expected that the resulting errors or displacement incompatibilities may be difficult to resolve, the engineer should consider conducting a 3D FEA of the subject construction stage to gain further confidence in the calculated displacements. This step in the application of Table 3-1 is where the bridge span length enters as an important factor, since longer-span bridges tend to have larger displacements.

It should be noted that compared to the creation of 3D FEA models for overall bridge design, including the calculation of live-load effects, the development of a 3D FEA model for several specific construction stages of potential concern involves a relatively small amount of effort. This is particularly the case with many of the modern software interfaces that facilitate the definition of the overall bridge geometry.

For calculation of the girder flange lateral bending stresses and the cross-frame forces in the above example bridge, the worst-case errors are expected to be larger, on the order of 13 percent to 20 percent (corresponding to a grade of C for both of these responses). However, the mode score is B, and since the bridge has a very regular geometry, it is likely that the normalized mean error in the flange lateral bending stresses and cross-frame forces is less than 12 percent. If these errors are acceptable in the engineer's judgment, then the 2D-grid analysis should be acceptable for the construction engineering calculations. As noted above, the engineer can compensate for these potential errors by reducing the target performance indices. In addition, with respect to the flange lateral bending stress, it should be noted that the f_ℓ values are multiplied by ⅓ in the AASHTO ⅓ rule equations. Therefore, the errors in f_ℓ have less of an influence on the performance ratio than errors in f_b when considering the strength limit state. When checking the AASHTO flange yielding limit for constructability, both f_ℓ and f_b have equal weights though. Based on these considerations, the simplest way to compensate for different potential unconservative errors in the f_ℓ and f_b values is to multiply the calculated stresses from the 2D-grid analysis by 1.20 and 1.12 (or 1.12 and 1.06) respectively prior to checking the performance ratios.

3.1.4 I-Girder Bridge Level of Analysis Example 2

Consider a straight steel I-girder bridge, with skewed supports and a skew index $I_s = 0.35$ (corresponding to the intermediate erection stage being evaluated), for which the engineer wants to perform a traditional 2D-grid analysis to determine the forces and displacements.

After reviewing Table 3-1, it is observed that for the major axis bending stresses and vertical deflections, a worst-case score of B is shown for straight skewed I-girder bridges with $0.30 < I_S \leq 0.65$. Furthermore, it can be observed that the mode of the scores for these bridge types is a B for the major-axis bending stresses and an A for the vertical displacements. Therefore, a properly prepared conventional 2D-grid analysis would be expected to produce major-axis bending stress and vertical deflection results that compare reasonably well with the results of a second-order elastic 3D FEA, such that the normalized mean error would be expected to be less than or equal to 12 percent.

If the layout of the cross-frames in the skewed bridge is such that overly stiff (nuisance) transverse load paths are alleviated, the engineer may expect that the error in the displacement calculations may be close to 6 percent or less. In this case, the engineer should be reasonably confident in the 2D-grid results for the calculation of the displacements. As noted in the previous example, the potential unconservative errors in the stresses can be compensated for in the construction engineering design checks; however, positive or negative displacement errors are equally bad.

The girder layover (i.e., the relative lateral deflection of the flanges) at the skewed bearing lines is often of key interest in skewed I-girder bridges. Table 3-1 shows that the girder layover calculations essentially have the same magnitude of error (i.e., the same resulting grades, as the girder vertical displacements). This is because properly designed and detailed skewed bearing line cross-frames are relatively rigid in their own planes compared to the lateral stiffness of the girders. Hence, the girder layovers are essentially proportional to the girder major-axis bending rotations at the skewed bearing lines.

For the calculation of the cross-frame forces and/or the girder flange lateral bending stresses in the above example, one should observe that the conventional 2D-grid procedures are entirely unreliable. That is, the scores in Table 3-1 are uniformly an F. The reason for this poor performance of the traditional 2D-grid methods is the ordinary modeling of the girder torsional properties using only the St. Venant torsional stiffness *GJ*/*L*. The physical girder torsional stiffnesses are generally much larger due to restraint of warping (i.e., flange lateral bending) effects. In addition, for wide skewed bridges and/or for skewed bridges containing specific overly stiff (nuisance) transverse load paths, the limited accuracy of the cross-frame equivalent beam stiffness models used in conventional 2D-grid methods may lead to a dramatic loss of accuracy in the cross-frame forces.

Lastly, conventional 2D-grid methods generally do not include any calculations of the girder flange lateral bending stresses due to skew. Hence, the score for the calculation of the flange lateral bending stresses is also an F in Table 3-1.

3.1.5 Selection of Analysis Methods for Tub-Girder Bridges

Similar to the I-girder bridges, a quantitative assessment of the analysis accuracy of tub-girder bridges was obtained in the NCHRP Project 12-79 research by focusing first on the normalized mean errors in the approximate (1D and 2D method) solutions for the girder major-axis bending stresses, internal torques and vertical displacements, compared to benchmark 3D FEA results. Using the quantitative assessments, the various methods of analysis were assigned scores in the same manner as the scoring for the I-girder bridge responses. Table 3-2 summarizes the scores for the above responses in tub-girder bridges.

Table 3-2. Matrix 1 for recommended level of analysis—tub-girder bridges.

Response	Geometry	Worst-Case Scores		Mode of Scores	
		2D-P1	1D-Line Girder	2D-P1	1D-Line Girder
Major-Axis Bending Stresses	S	B	B	A	B
	C	B	C	A	B
	C&S	B	C	B	B
Girder Torques	S	F	F	D	F
	C	D	D	A	B
	C&S	F	F	A	B
Vertical Displacements	S	B	B	A	A
	C	A	B	A	A
	C&S	B	B	A	A
Girder Layover at Bearing Lines	S	B	B	A	A
	C	NA[a]	NA[a]	NA[a]	NA[a]
	C&S	B	B	A	A

[a] Magnitudes should be negligible where properly designed and detailed diaphragms or cross-frames are present.

34 Guidelines for Analysis Methods and Construction Engineering of Curved and Skewed Steel Girder Bridges

It is interesting that the Table 3-2 scores for the major-axis bending stresses and vertical displacements are relatively good. However, the worst-case scores for the internal torques are generally quite low. These low scores are largely due to the fact that the internal torques in tub-girder bridges can be sensitive to various details of the framing, such as the use and location of external intermediate cross-frames or diaphragms, the relative flexibility of these diaphragms as well as the adjacent internal cross-frames within the tub girders, skewed interior piers without external cross-frames between the piers at the corresponding bearing line, incidental torques introduced into the girders due to the specific orientation of the top flange lateral bracing system members (particularly for Pratt-type TFLB systems), etc. Jimenez Chong (2012) provides a detailed evaluation and assessment of the causes for the errors in the girder internal torques for the tub-girder bridges considered in the NCHRP Project 12-79 research.

Similar to the considerations for I-girder bridges, the external diaphragms and/or cross-frames typically respond relatively rigidly in their own plane compared to the torsional stiffness of the girders (even though the tub-girder torsional stiffnesses are significantly larger than those of comparable I-girders). Therefore, the girder layovers at skewed bearing lines tend to be proportional to the major-axis bending rotation of the girders at these locations. As a result, the errors in the girder layover calculations obtained from the approximate methods tend to be similar to the errors in the major-axis bending displacements.

The connectivity index, I_C, does not apply to tub-girder bridges. This index is primarily a measure of the loss of accuracy in I-girder bridges due to the poor modeling of the I-girder torsion properties. For tub-girder bridges, the conventional St. Venant torsion model generally works well as a characterization of the response of the pseudo-closed section tub girders. Hence, I_C is not used for characterization of tub-girder bridges in Table 3-2. Furthermore, there is only a weak correlation between the accuracy of the simplified analysis calculations and the skew index I_S for tub-girder bridges. Therefore, the skew index is not used to characterize tub-girder bridges in Table 3-2 either. Important differences in the simplified analysis predictions do exist, however, as a function of whether the bridge is curved, "C," straight and skewed, "S," or curved and skewed, "C&S." Therefore, these characterizations are shown in the table.

It should be noted that there was a measureable decrease in the accuracy of the 2D-grid solutions for the tub-girder bridges obtained with Program P2 compared to Program P1. Since the research team had greater control over the calculations, as well as more detailed information regarding the specifics of the procedures in Program P1, the P1 results are presented in Table 3-2 as being the most representative of the results achievable with a 2D-grid procedure.

In addition to the above assessments, the accuracy of the bracing component force calculations in tub-girder bridges is assessed separately in Table 3-3. It is useful to address the accuracy of these response calculations separately from the ones shown in Table 3-2 since the simplified bracing component force calculations take the girder major-axis bending moments, torques, and applied transverse loads as inputs and then apply various useful mechanics of materials approximations to obtain the force estimates. That is, there are two distinct sources of error in the bracing component forces relative to the 3D FEA benchmark solutions:

1. The error in the calculation of the input quantities obtained from the 1D line-girder or 2D-grid analysis, and
2. The error introduced by approximations in the bracing component force equations.

Chapter 2 of the NCHRP Project 12-79 Task 8 report provides an overview of the bracing component force equations evaluated here, which are used frequently in current professional practice. It should be noted that the calculation of the top flange lateral bending stresses in tub girders is included with the bracing component force calculations. This is because these stresses

Table 3-3. Matrix 2 for recommended level of analysis—tub-girder bridges.

Response	Sign of Error	Geometry	Worst-Case Scores		Mode of Scores	
			2D-P1	1D-Line Girder	2D-P1	1D-Line Girder
TFLB Diagonal Force	Positive (Conservative)	S	D	D	D	C
		C	D	F	B	F
		C&S	D[a]	F	B	F
		Pratt TFLB System	C	F	A	F
	Negative (Unconservative)	S	F[b]	C		
		C	--[c]	--		
		C&S	--	--		
		Pratt TFLB System	--	--		
TFLB & Top Internal CF Strut Force	Positive (Conservative)	S	C	C		
		C	F	F		
		C&S	F	F[d]		
		Pratt TFLB System	F	F		
	Negative (Unconservative)	S	C	C		
		C	--	A		
		C&S	--	C		
		Pratt TFLB System	D	D		
Internal CF Diagonal Force	Positive (Conservative)	S	NA[e]	NA[e]		
		C	F	F		
		C&S	F	F		
		Pratt TFLB System	--	F[f]		
	Negative (Unconservative)	S	NA[e]	NA[e]		
		C	--	--		
		C&S	--	D		
		Pratt TFLB System	B	--		
Top Flange Lateral Bending Stress (Warren TFLB Systems)	Positive (Conservative)	S	C	C		
		C	F	F		
		C&S	F	F[d]		
	Negative (Unconservative)	S	C	C		
		C	--	A		
		C&S	--	C		

[a] Modified from a C to a D considering the grade for the C and the S bridges.

[b] Large unconservative error obtained for bridge ETSSS2 due to complex framing. If this bridge is considered as an exceptional case, the next worst-case unconservative error is -15 % for NTSSS2 (grade = C).

[c] The symbol "--" indicates that no cases were encountered with this score.

[d] Modified from a B to an F considering the grade for the C bridges.

[e] For straight-skewed bridges, the internal intermediate cross-frame diagonal forces tend to be negligible.

[f] Modified from an A to an F considering the grade for the C and C&S bridges.

are influenced significantly by the interaction of the top flanges with the tub-girder bracing systems.

The NCHRP Project 12-79 research observed that in many situations, the bracing component force estimates are conservative relative to the 3D FEA benchmark solutions. Therefore, it is useful to consider a signed error measure for the bracing component force calculations. In addition, the bracing component dimensions and section sizes often are repeated to a substantial degree throughout a tub-girder bridge for the different types of components. Therefore, it is useful to

36 Guidelines for Analysis Methods and Construction Engineering of Curved and Skewed Steel Girder Bridges

quantify the analysis error as the difference between the maximum of the component forces determined by the approximate analysis minus the corresponding estimate from the 3D FEA benchmark, that is:

$$e_{\max} = \left(R_{approx.max} - R_{FEA.max}\right) / R_{FEA.max} \qquad \text{Eq. 10}$$

for a given type of component. The grades for these responses were assigned based on the same scoring system used for the assessments based on the normalized mean error with one exception: Separate grades were assigned for the positive (conservative) errors and for the negative (unconservative) errors in Table 3-3. In situations where no negative (unconservative) errors were observed in all of the bridges considered in a given category, the symbol "—" is shown in the cells of the matrix, and the cells are unshaded.

The mode of the grades is shown only for the top flange diagonal bracing forces in Table 3-3. The mode of the grades for the other component force types is not shown because of substantial positive and negative errors in the calculations that were encountered in general for the tub-girder bridges and because, in cases where a clear mode for the grades existed, the mode of the grades was the same as the worst-case grade.

In addition to the above considerations, it should be noted that current simplified estimates of the tub-girder bridge bracing component forces are generally less accurate for bridges with Pratt-type top flange lateral bracing (TFLB) systems compared to Warren and X-type systems. A small number of tub-girder bridges with Pratt-type TFLB systems were considered in the NCHRP Project 12-79 research. Therefore, the composite scores for these bridges are reported separately in Table 3-3.

3.1.6 Tub-Girder Bridge Level of Analysis Example

Consider a horizontally curved steel tub-girder bridge with a Warren top flange lateral bracing system and skewed supports for which the engineer wants to perform a traditional 2D-grid analysis to determine the forces and displacements during critical stages of the erection sequence. The bridge has a "very regular" geometry (constant girder spacing, constant deck width, a relatively uniform top flange lateral bracing [TFLB] system and internal cross-frame spacing, solid plate end diaphragms, single bearings for each girder, etc.).

A properly prepared 2D-grid analysis would be expected to produce major axis bending stresses and vertical deflections with mean errors less than 12 percent relative to a rigorous 3D FEA solution, since the worst-case score assigned for both of these quantities is a B in Table 3-2 for the subject "C&S" category. Furthermore, it can be observed that the mode of the scores for the vertical displacements is an A; hence, given the "very regular" geometry of the above bridge, it is expected that the vertical displacements most likely would be accurate to within 6 percent.

Unfortunately, the worst-case score is an F for the 2D-grid estimates of the internal torques in the C&S bridges. As noted previously, this low score is due to the fact that the internal torques in tub-girder bridges can be very sensitive to various details of the framing, such as the use and location of external intermediate cross-frames or diaphragms, the relative flexibility of these diaphragms as well as the adjacent internal cross-frames within the tub girders, skewed interior piers without external cross-frames between the piers at the corresponding bearing line, incidental torques induced in the girders due to the specific orientation of the top flange lateral bracing system members (particularly for Pratt-type TFLB systems), etc. Fortunately though, the web and bottom flange shear forces due to the internal torques are often relatively small compared to the normal stresses associated with the major-axis bending response of the

girders. Furthermore, the mode of the scores for the internal torques is an A from Table 3-2. Therefore, the engineer must exercise substantial judgment in estimating what the expected error may be for the internal torque from a 2D-grid analysis and in assessing the impact of this error on the bridge design. As noted for I-girder bridges, one can compensate for any anticipated potential unconservative error in the internal force or stress response quantities by scaling up the corresponding responses by the anticipated error, or by adjusting the target values of the performance ratios.

Based on Table 3-3, the worst-case score for the positive (conservative) error in the calculation of the TFLB diagonal forces in the above example is a D, whereas the mode of the scores is a B. The table shows that no unconservative errors were encountered in this calculation for the tub-girder bridges studied in NCHRP Project 12-79. Since the example bridge is "very regular," the engineer may assume that the TFLB diagonal force calculations are conservative, but reasonably accurate, relative to the refined 3D FEA benchmark values.

For both the TFLB and top internal cross-frame strut forces and the internal cross-frame diagonal forces in C&S bridges, Table 3-3 shows a grade of F for the conservative error. Also, the table shows that no unconservative errors were encountered in the NCHRP Project 12-79 calculations for these responses. Therefore, the engineer can assume that the forces for these components, as determined from a 2D-grid analysis plus the bracing component force equations, are highly conservative. It should be noted that the forces in the top struts of the internal cross-frames near exterior diaphragm or exterior cross-frame locations can be very sensitive to the interaction of the external diaphragm or cross-frame with the girders. These forces should be determined based on consideration of statics at these locations, given the forces transmitted to the girders from the external diaphragm or cross-frame components. NCHRP Project 12-79 did not consider these component forces in its error assessments.

Lastly, Table 3-3 shows that the tub-girder top flange lateral bending stresses tend to be estimated with a high degree of conservatism by 2D-grid methods combined with the bracing component force equations. In addition, no unconservative errors were encountered in the tub-girder bridges studied by NCHRP Project 12-79 for the top flange lateral bending stresses. Therefore, the engineer can also assume that these stress estimates are highly conservative.

3.2 Improvements to Conventional Analysis Methods

Various essential improvements to conventional methods of analysis were developed during the course of the NCHRP Project 12-79 research. In all cases, the project team strived to identify specific sources of errors relative to 3D FEA benchmark solutions and then to develop solutions to these errors by addressing the inadequacies in the conventional models at a fundamental structural mechanics level. In addition, solutions were sought that provided substantial benefits, yet involved little computational expense and were relatively easy to implement in software. The following sections highlight these major improvements.

First, Section 3.2.1 introduces a basic simply supported I-girder bridge used for illustration purposes in a number of the subsequent sections. This bridge was designed and tested at the FHWA Turner-Fairbank Highway Research Center in prior FHWA research (Jung, 2006; Jung and White, 2008). The bridge has substantial horizontal curvature and zero skew. Furthermore, the bridge was designed at, or slightly above, a number of limits in the AASHTO LRFD Design Specifications. Therefore, this structure is particularly sensitive to a number of parameters that influence the accuracy of simplified analysis methods. Because of the fact that the bridge is relatively basic and easily modeled in a short amount of time, due to the sensitivity of the structure to attributes influencing the analysis accuracy, and since the calculations are backed up by a large

number of experimental measurements, this bridge is an excellent case for discussion of analysis error sources as well as analysis improvements.

Section 3.2.1 is followed by four sections that describe four key improvements to conventional 2D-grid analysis methods recommended by the NCHRP Project 12-79 research for I-girder bridges:

1. Use of an equivalent St. Venant torsion constant for the I-girders that accounts approximately for the contribution of warping (i.e., flange lateral bending) to the girder torsional stiffnesses,
2. Use of equivalent beam models for the cross-frames that better capture the true bending and shear racking stiffnesses of various types of cross-frames used in I-girder bridges,
3. Direct calculation of flange lateral bending stresses in skewed or curved and skewed I-girder bridges based on the cross-frame forces calculated from the above improved 2D-grid procedures, and
4. 2D-grid (or 3D FEA) calculation of locked-in forces due to steel dead load fit (SDLF) or total dead load fit (TDLF) detailing of the cross-frames in curved and/or skewed I-girder bridges.

The first three of the above sections focus on the recommended calculations and their implementation, as well as the resulting improvement of the analysis results. However, the fourth of these sections focuses just on the recommended calculations and their implementation. A longer discussion is necessary to convey the detailed characteristics of the locked-in force effects from SDLF or TDLF detailing. These considerations are addressed in depth in Section 3.3.

3.2.1 The FHWA Test Bridge

Figure 3-3 shows key particulars of the geometry for a 90 ft. span curved I-girder bridge tested in 2005 at the FHWA Turner-Fairbank Highway Research Center (Jung, 2006; Jung and White, 2008). This bridge is introduced here because it is used for illustration purposes in a number of the subsequent sections. The reader is referred to the Task 8 report (Appendix C of the contractors' final report), and to Sanchez (2011), Ozgur (2011) and Jimenez Chong (2012) for similar results to those discussed in Sections 3.2.2 through 3.2.6 for a wide range of bridges.

The radius of curvature of the centerline of the FHWA Test Bridge was 200 ft. and the bridge cross-section contained three I-girders spaced at 8.75 ft. Figure 3-4 shows a photo of the bridge after the girders G3 and G2 were placed on the supports and the cross-frames were installed. The fascia girder on the outside of the curve (G1) is blocked on the laboratory floor toward the right-hand side of the photo. It should be noted that the naming of the outside girder as G1 and the inside girder as G3 follows the naming convention adopted within the NCHRP Project 12-79 project research. The above referenced research reports refer to the outside girder as G3 and the inside girder as G1.

The total width of the 8-in. concrete deck was 23.5 ft., with 3.0-ft. overhangs outside the fascia girders. The bridge was constructed using V-type cross-frames composed of circular tube section members. These HSS 5 × ¼-in. members had areas comparable to the member areas that would have been required for this bridge with other more common cross-frame section types. However, the tube-member cross-frames facilitated the measurement of the cross-frame forces, since the tubes were essentially instrumented as load cells.

The FHWA Test Bridge was designed with a number of characteristics that pushed or slightly exceeded the limits of prior AASHTO curved I-girder bridge specifications, as well as some of the limits in the current AASHTO (2010) LRFD Specifications, as follows:

- Intermediate cross-frames were employed at only three cross-sections within the bridge span, resulting in a subtended angle between the cross-frames of $L_b/R = 0.1125$. This is slightly larger than the maximum limit of $L_b/R = 0.10$ specified in AASHTO (2010) Article 6.7.4.2.

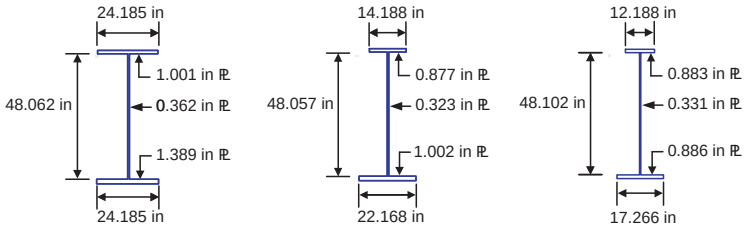

(a) G1 cross-section (b) G2 cross-section (b) G3 cross-section

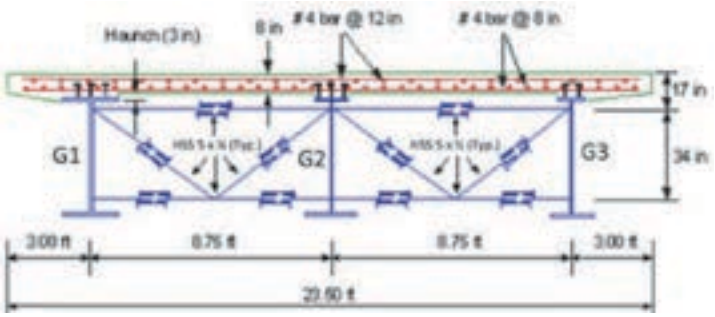

(d) Bridge cross-section

L_s = 90 ft., R = 2000 ft., w = 23.5 ft.

(e) Bridge plan view

Figure 3-3. FHWA Test Bridge (EISCR1) geometry.

Figure 3-4. FHWA Test Bridge (EISCR1) during the steel erection, with cross-frames attached between girders G2 and G3 (Jung, 2006; Jung and White, 2008).

- The fascia girder on the outside of the curve (G1) utilized a hybrid HPS 70W bottom flange. Hybrid curved girders were not permitted in the AASHTO Specifications at the time of the FHWA research. The use of grade 70 steel allowed the bottom flange thickness for Girder G1 to be reduced from approximately 2 in. if grade 50 steel had been used.
- Due to the grade 70 bottom flange on G1, the 48-in. web depth for this girder slightly violates the arc-span length-to-depth requirements in AASHTO (2010) Article 2.5.2.6.3. However, this bridge satisfies the *Span*/800 deflection limit of AASHTO Article 2.5.2.6.2.
- The web slenderness D/t_w of all the girders was close to the AASHTO (2010) limit of 150 for straight and curved transversely stiffened web panels.
- Transverse stiffening of the girder webs varied from a maximum of close to $d_o/D = 3$ in all the girders near the mid-span of the bridge to $d_o/D < 1$ near the supports for Girder G1. Prior AASHTO Specifications have required a much tighter spacing of web transverse stiffeners in curved I-girder webs.
- The top compression flange slenderness $b_{fc}/2t_{fc}$ was slightly larger than 12, which is the maximum limit on the flange slenderness specified in AASHTO LRFD Article 6.10.2.2.
- Both girders G1 and G2 were sized close to the AASHTO (2010) strength limits.

The tight radius of curvature ($R = 200$ ft.) combined with the use of only three intermediate cross-frames ($n_{cf} = 3$) results in a value of I_C of 18.75 from Equation 8 for this bridge in its final constructed condition. Therefore, this bridge significantly exceeds the $I_C \leq 1$ limit utilized for scoring the accuracy of the simplified analysis methods in Table 3-1. As noted previously, the NCHRP Project 12-79 research found that the connectivity index, I_C, tended to correlate well with the magnitude of the errors exhibited by conventional 2D-grid methods.

Figures 3-5 and 3-6 show several photos of the test bridge during its construction.

3.2.2 Improved I-Girder Torsion Model for 2D-Grid Analysis

As noted previously, the conventional use of just the St. Venant term (GJ/L) in characterizing the torsional stiffness of I-girders results in a dramatic underestimation of the true girder

Figure 3-5. FHWA Test Bridge, overhang brackets attached to the fascia girder on the outside of the curve (Girder G1 per the NCHRP Project 12-79 naming convention, Girder G3 in reports and papers on the FHWA research) (Jung, 2006; Jung and White, 2008).

Figure 3-6. FHWA Test Bridge placement of the slab concrete (Jung, 2006; Jung and White, 2008).

torsional stiffness. This is due to the neglect of the contributions from flange lateral bending, that is, warping of the flanges, to the torsional properties. Even for intermediate steel erection stages where some of the cross-frames are not yet installed, the typical torsional contribution from the girder warping rigidity (EC_w) is substantial compared to the contribution from the St. Venant torsional rigidity (GJ). It is somewhat odd that structural engineers commonly would never check the lateral-torsional buckling capacity of a bridge I-girder by neglecting the term EC_w and using only the term GJ. Yet, it is common practice in conventional 2D-grid methods to neglect the warping torsion contribution coming from the lateral bending of the flanges.

The NCHRP Project 12-79 Task 8B research observed that an *equivalent torsion constant*, J_{eq}, based on equating the stiffness GJ_{eq}/L_b with the analytical torsional stiffness associated with assuming warping fixity at the intermediate cross-frame locations and warping free conditions at the simply supported ends of a bridge girder, potentially could result in significant improvements to the accuracy of 2D-grid models for I-girder bridges. This observation was based in part on the prior research developments by Ahmed and Weisgerber (1996), as well as the commercial implementation of this type of capability within the software RISA-3D (RISA, 2011). The term L_b in the stiffness GJ_{eq}/L_b is the unbraced length between the cross-frames.

When implementing this approach, a different value of the equivalent torsional constant J_{eq} must be calculated for each unbraced length having a different L_b or any difference in the girder cross-sectional properties. Furthermore, it is important to recognize that the use of a length less than L_b typically will result in a substantial over-estimation of the torsional stiffness. Therefore, when a given unbraced length is modeled using multiple elements, it is essential that the unbraced length L_b be used in the equations for J_{eq}, not the individual element lengths.

By equating GJ_{eq}/L_b to the torsional stiffness (T/ϕ) for the open-section thin-walled beam associated with warping fixity at each end of a given unbraced length L_b, where T is the applied end torque and ϕ is corresponding relative end rotation, the equivalent torsion constant is obtained as:

$$J_{eq(fx-fx)} = J\left[1-\frac{\sinh(pL_b)}{pL_b}+\frac{[\cosh(pL_b)-1]^2}{pL_b\sinh(pL_b)}\right]^{-1} \qquad \text{Eq. 11}$$

42 Guidelines for Analysis Methods and Construction Engineering of Curved and Skewed Steel Girder Bridges

Similarly, by equating GJ_{eq}/L_b to the torsional stiffness (T/ϕ) for the open-section thin-walled beam associated with warping fixity at one end and warping free boundary conditions at the opposite end of a given unbraced length, one obtains:

$$J_{eq(s-fx)} = J\left[1-\frac{\sinh(pL_b)}{pL_b\cosh(pL_b)}\right]^{-1} \qquad \text{Eq. 12}$$

Section 6.1.2 of the Task 8 report shows a complete derivation of these equivalent torsion constants.

The assumption of warping fixity at all of the intermediate cross-frame locations is certainly a gross approximation. TWOS 3D-frame analysis (see Section 2.7.3 for a description of this terminology) generally shows that some flange warping (i.e., cross-bending) rotations occur at the cross-frame locations. However, the assumption of warping fixity at the intermediate cross-frame locations leads to a reasonably accurate characterization of the girder torsional stiffnesses pertaining to the overall deformations of a bridge unit as long as:

- There are at least two I-girders connected together, and
- They are connected by enough cross-frames such that the connectivity index I_C is less than 20 ($I_C \leq 20$).

Therefore, the FHWA Test Bridge in its final constructed condition represents essentially the maximum limit at which the above approach provides a sufficient solution.

3.2.2.1 Comparison of the Vertical Displacement Results from Various Approaches for the FHWA Test Bridge

Figure 3-7 shows representative results for the vertical displacement of Girder G1 of the FHWA Test Bridge under the nominal (unfactored) total dead load, i.e., the self-weight of the structural steel plus the weight of the concrete deck, with all the loads being resisted by the noncomposite structure. The benchmark 3D FEA prediction, 4.49 in. downward deflection of the centerline of G1 at its mid-span, matches closely with the results from the physical test (Jung, 2006; Jung and White, 2008). Figure 3-8 shows a rendering of the magnified bridge vertical deflections from the 3D FEA solution.

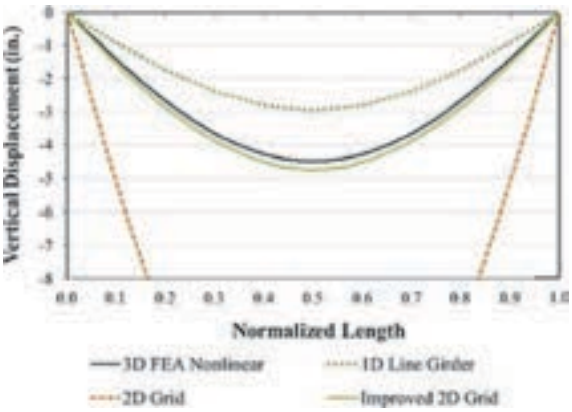

Figure 3-7. FHWA Test Bridge (EISCR1) vertical displacements in fascia girder on the outside of the curve under total dead load (unfactored).

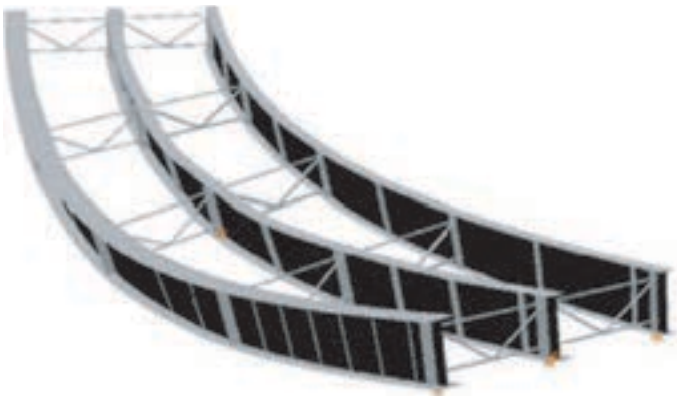

Figure 3-8. Magnified deflected geometry of EISCR1 under total dead load, from 3D FEA (displacements scaled 20x, initial vertical camber not scaled).

The 1D-line girder solution in Figure 3-7 is obtained using the V-load method, applying the primary loads as well as the V-loads to Girder G1 on the outside of the horizontal curve, and analyzing the uniaxial bending deformations of the member subjected to these loads. Unfortunately, this solution under-predicts the vertical displacement of Girder G1 by 33.4 percent. The actual displacements are larger due to the coupling between the girder mid-span vertical displacements and the twisting deformations, particularly the twisting deformations of the girder near the supports. That is, the twisting of the girder near the supports produces corresponding additional vertical displacements at the mid-span.

In the 2D-grid analyses, the girders are modeled by four elements within each of their unbraced lengths, with the nodes being positioned along the circular arc between the cross-frames. Only one conventional 2D-grid solution is shown in the plot. However, essentially the same results are obtained by models built in MDX and LARSA-4D, as well as one other 2D-grid model created using a third independent code for this problem. The improved method of modeling the cross-frames discussed in Section 3.2.3 is employed for all the 2D-grid solutions discussed in this section.

One can observe that the improved 2D-grid solution, based on the use of J_{eq}, predicts a slightly larger mid-span displacement of Girder G1 than obtained in the 3D FEA solution (4.73 in. versus 4.49 in.). Furthermore, it should be noted that the benchmark 3D FEA solution shown here includes geometric nonlinearity. However, if the 3D FEA simulation model is run as a geometrically linear (first-order analysis) solution, the mid-span displacements reduce to only 4.40 in. Therefore, the second-order effects on the vertical displacements are only about 2 percent for this structure and loading. The improved 2D-grid solution over-estimates the 3D FEA linear elastic solution by 7.5 percent and over-predicts the 3D FEA geometric nonlinear benchmark solution by 5.3 percent.

Conversely, the conventional 2D-grid solutions predict a displacement of 15.37 in. at the mid-span of G1, 342 percent larger than the benchmark result. Obviously, this discrepancy between the 2D-grid prediction and the physical result is some cause for concern.

Table 3-4 summarizes the above numerical results and presents a number of additional solutions for the vertical displacement of Girder G1. The only solution that is dramatically in error is the conventional 2D-grid solution discussed above. Interestingly, if the girders are modeled using only one straight conventional element between each of the cross-frames, the predicted displacement is 4.35 in. (3.1 percent smaller than the benchmark solution). Furthermore, the same

Table 3-4. FHWA Test Bridge (EISCR1) mid-span vertical displacement of Girder G1 (ΔG1) under total dead load (unfactored) for different 2D-grid girder discretizations and idealizations, cross-frames modeled using shear deformable beam element (ΔG1 = 4.49 in., second-order 3D FEA; ΔG1 = 4.40 in., first-order 3D FEA).

2D-grid discretization and idealization	Δ_{G1} (in.)
Four conventional elements within each L_b, nodes located on the circular arc	15.37
One conventional element within each L_b, straight between each CF	4.35
Four conventional elements within each L_b, straight between each CF	4.35
Four elements within each L_b, nodes located on the circular arc, using J_{eq}	4.73
Four elements within each L_b, straight between each CF, using J_{eq}	4.28
One element within each L_b, straight between each CF, using J_{eq}	4.28
Four TWOS beam elements within each L_b, nodes located on the circular arc	4.42
Four TWOS beam elements within each L_b, straight between each CF	4.34
Four TWOS beam elements within each L_b, nodes located on the circular arc, warping fixed at the intermediate CF locations	4.32
Four TWOS beam elements within each L_b, straight between each CF, warping fixed at the intermediate CF locations	4.28
Four TWOS beam elements within each L_b, nodes located on the circular arc, all girder J values taken equal to zero	4.43
One TWOS beam element within each L_b, straight between each CF	4.38
One TWOS beam element within each L_b, straight between each CF, warping fixed at the intermediate CF locations	4.32

displacement solution is obtained if the girders are modeled with four elements positioned along the straight chord between each of the cross-frames. If the improved 2D-grid model is used with only one straight element between each of the cross-frames, or with four elements positioned along the straight chord between each of the cross-frames, the predicted displacement is 4.28 in. (4.7 percent smaller than the benchmark solution).

One solution to the above problem that some engineers might consider is to simply never represent any unbraced length with the nodes positioned along the curved arc of an I-girder member when using conventional methods. However, this can lead to an awkward handling of situations where the same model is used to analyze girders with different numbers of cross-frames inserted in the structure at an early intermediate stage of construction. In addition, a common practice for modeling of staged deck placement in 2D-grid programs such as MDX is to use conventional frame elements to model portions of the bridge that are not yet composite, but then to connect these elements to a plate representation of the slab once the slab has been activated for a given stage. Usually, it is desirable to use more than one plate element within each unbraced length for modeling of the structure in its composite condition. Furthermore, it is desirable to model the slab with nodes along arcs about the center of curvature (assuming a circular arc). Therefore, it is desirable to also position the I-girder element nodes along the circular arcs between the cross-frames.

Several additional 2D-grid solutions are provided at the bottom of Table 3-4 using the TWOS frame element in MASTAN2 (MASTAN2, 2011; McGuire et al., 2000). The reader is referred to Section 2.7.2 for a discussion of the meaning of a TWOS 2D-grid analysis. One can observe that this element predicts a displacement of 4.42 in. (1.6 percent smaller than the benchmark solution) when four elements are used between each of the cross-frames and the nodes are positioned along the circular arc, whereas a displacement of 4.34 in. (3.3 percent smaller than the benchmark solution) is obtained when four elements are used with the nodes positioned along a straight chord between the cross-frames.

Another interesting solution is one obtained using the TWOS frame element if the warping is artificially fully fixed at the intermediate cross-frame locations rather than being modeled as a

continuous function along the girder lengths. In this case, the displacement prediction is reduced to 4.28 in. (4.5 percent smaller than the benchmark displacement). This demonstrates the accuracy of assuming full fixity at these locations, subject to the limitations discussed in the development of the improved 2D-grid procedure (i.e., at least two I-girders connected together, and $I_C \leq 20$). The accuracy of these solutions is not influenced significantly if the girders are modeled using only one element between the cross-frames for the evaluation of the non-composite behavior of this bridge.

Lastly, it is interesting to investigate the influence of completely neglecting the St. Venant torsional contribution to the stiffness within the Mastan TWOS 2D-grid analysis. In this case, the solution with four elements modeled along the circular arcs between the cross-frames increases from 4.42 in. to 4.43 in. The torsional stiffness of the I-girders is dominated by the restraint of flange warping, once the girders are sufficiently connected together such that I_C is less than approximately 20. It should be noted that if the improved 2D-grid model is used to predict the vertical displacements for the girder pair G2-G3, connected together by the bearing-line cross-frames and only a single intermediate cross-frame, the results are very poor. In this case, the connectivity index I_C is equal to 38. However, if G2 and G3 are connected together by three intermediate cross-frames, as shown in Figure 3-4, the accuracy of the improved 2D-grid prediction is comparable to that demonstrated above.

One question that could be asked relative to the implementation of the improved 2D-grid model is the following: Will the improved 2D-grid model work properly when used to model composite conditions with a plate-eccentric beam approach? Separate studies conducted in the NCHRP Project 12-79 research indicate that the improved 2D-grid model works sufficiently with a plate representation of the slab as long as one handles the calculation of the girder bottom flange lateral bending stresses properly. Chang and White (2008) have shown in previous research that, if TWOS 3D-frame elements are used to model the steel I-girders, and if these elements are constrained by rigid offsets to a shell representation of the slab, the bottom flange lateral bending stresses predicted by the TWOS element are drastically underestimated. This is because the slab bending stiffness, along with the rigid link of the TWOS element to the slab, essentially prevents any lateral bending of the bottom flange in the TWOS model (unless special procedures are invoked to release the torsional constraint of the TWOS element by the slab model). As noted above, these issues are not encountered for the improved 2D-grid element with the use of J_{eq}, as long as the flange lateral bending stresses (f_ℓ) are calculated properly. The calculation of f_ℓ is addressed subsequently in Section 3.2.4.

3.2.2.2 Mechanical Explanation of the Large Error in the Conventional 2D-Grid Procedure with the Nodes Positioned along a Circular Arc

Consider the idealized 2D-frame representation of an I-girder unbraced length between two cross-frames shown in Figure 3-9. All the degrees of freedom at the end nodes are constrained with

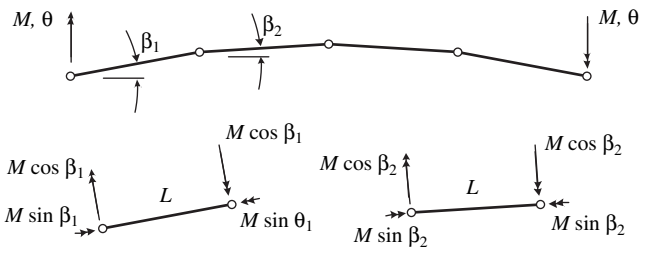

Figure 3-9. Behavior for a chorded representation of a curved girder using four straight elements.

46 Guidelines for Analysis Methods and Construction Engineering of Curved and Skewed Steel Girder Bridges

the exception of the rotational dof corresponding to the applied end moments. In addition, all of the dofs are free at the interior nodes in this model. The reason for the dramatic over-prediction of the vertical displacements by the conventional 2D-grid procedure shown in the previous section is due to the fact that statics requires that a portion of the bending moment transmitted to the elements must be taken by element torsion (when the elements are modeled along a circular arc). However, the torsional stiffness of the elements is drastically underestimated by the St. Venant torsional stiffness GJ/L, where L is the length of each of the individual elements.

The bending end rotations in the idealized problem shown in Figure 3-9 can be calculated with relative ease, using the principle of virtual work, as:

$$1 \cdot \theta = (1 \cdot \sin\beta_1)\frac{(M\sin\beta_1)L}{GJ} + (1 \cdot \cos\beta_1)\frac{(M\cos\beta_1)L}{EI} + (1 \cdot \sin\beta_2)\frac{(M\sin\beta_2)L}{GJ} + (1 \cdot \cos\beta_2)\frac{(M\cos\beta_2)L}{EI} \quad \text{Eq. 13}$$

After some algebra, Equation 13 may be expressed as:

$$\theta = \frac{ML}{EI}\sum_i \left[\frac{EI}{GJ}\sin^2\beta_i + \cos^2\beta_i\right] \quad \text{Eq. 14}$$

Clearly, one can obtain a significant contribution from the torsional term in this equation, i.e., the first term inside the brackets.

If one substitutes the relevant parameters for Girder G1 of the previous problem into Equation 14, i.e., I = 37,600 in^4, J = 29.4 in^4, L = 70.45 in., β_1 = 0.04218 radians and β_2 = 0.01462 radians, along with the yield moment of the G1 cross-section, $M = M_{yG1}$ = 5,564 ft-kips = 66,768 in-kips, one obtains θ = 0.0369 radians. This prediction matches precisely with the first-order elastic MASTAN2 solution for this problem. If the improved 2D-grid procedure with $J_{eq(fx\text{-}fx)}$ = 688.3 in.^{4} is employed, the predicted value for θ is 0.00983 radians. Finally, if the more rigorous TWOS frame element solution is employed, where C_w = 1,662,000 in.^{6} for Girder G1, equal end rotations of θ = 0.00889 radians are obtained. The rotations predicted by the recommended improved 2D-grid model are 10.6 percent larger than the more rigorous predictions from the TWOS frame element. Correspondingly, the conventional 2D-grid solution over-predicts the end rotations by 315 percent.

3.2.2.3 Comparison of the Major-Axis Bending Stresses from Various Approaches for the FHWA Test Bridge

Figures 3-10 and 3-11 show the results from the different methods of analysis for the major-axis bending stresses in the FHWA Test Bridge Girder G1 (on the outside of the horizontal curve) and Girder G3 (on the inside of the horizontal curve) respectively. It should be noted that these results are shown at the factored load level, i.e., 1.5 of the total dead load, associated with the Strength IV loading condition.

One can observe that the major-axis bending stress at the mid-span of Girder G1 is under-predicted by 12.3 percent in the 1D line-girder solution conducted using the V-load method. All of the other solutions are very comparable. Therefore, it can be concluded that the poor vertical displacement estimate for Girder G1 does not impact the accuracy of the conventional 2D-grid estimate of the major-axis bending stress in this problem.

The percentage accuracy of the results is not as good for Girder G3. However one should notice that the scale on the vertical axis of the plot in Figure 3-11 is highly magnified compared to the

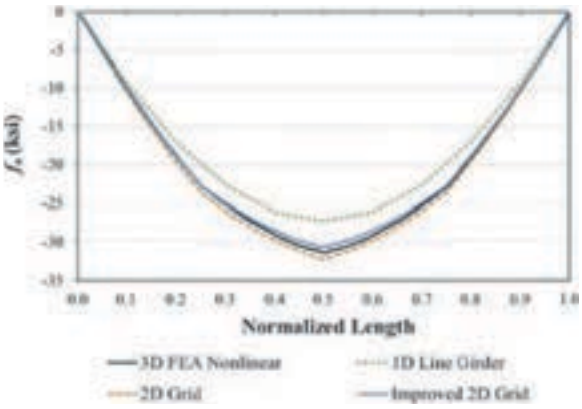

Figure 3-10. FHWA Test Bridge (EISCR1) top flange major-axis bending stresses in the fascia Girder G1 on the outside of the curve under the Strength IV load combination (1.5 × total dead load).

scale in Figure 3-10. It may be more useful to consider the differences between the maximum predicted stresses when considering the errors for Girder G3 in this bridge. The maximum major-axis bending stress in the 3D FEA simulation model is 8.1 ksi. The corresponding maximum predicted by the improved 2D-grid method is 9.9 ksi versus 10.8 ksi by the conventional 2D-grid solution. The 1D line-girder (V-load) solution exhibits the largest error in this problem, predicting a maximum major-axis bending stress of only 4.1 ksi. Furthermore, the 1D solution does not capture any semblance of the shape of the stress diagram from the benchmark.

3.2.3 Improved Equivalent Beam Cross-Frame Models

Figure 3-12 shows the geometry of the V-type cross-frames used in the FHWA Test Bridge. The cross-frames are 34 in. deep and $L = 8.75$ ft. = 105 in. wide between the work points at the girder centerlines. The areas of all the tube members are $A = 3.73$ in.^{2} In this section, various

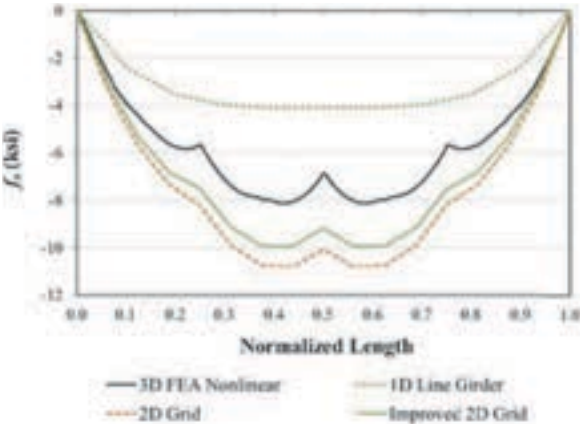

Figure 3-11. FHWA Test Bridge (EISCR1) top flange major-axis bending stresses in the fascia Girder G3 on the inside of the curve under the Strength IV load combination (1.5 × total dead load).

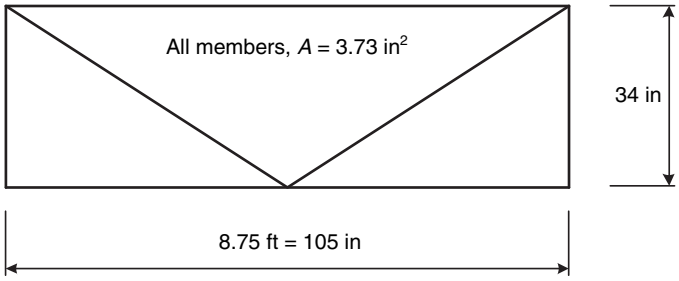

Figure 3-12. Cross-frame configuration, FHWA Test Bridge.

idealized beam solutions are compared to the "exact" equivalent beam stiffnesses of this cross-frame, where the "exact" solutions are taken as the stiffnesses from an explicit truss representation of the cross-frames in their own plane. The most appropriate simplified equivalent beam modeling of the cross-frames becomes apparent by evaluating these results.

3.2.3.1 Equivalent Beam Stiffness Based on the Flexural Analogy Approach

Figure 3-13 illustrates the calculation of the equivalent moment of inertia for the cross-frames in the FHWA Test Bridge using the "flexural analogy" approach discussed as one of two commonly used options in the AASHTO/NSBA (2011) G13.1 document "Guidelines for Steel Girder Bridge Analysis." This is the default option for calculation of the cross-frame equivalent beam stiffness in the MDX software. The lighter arrows in the figure represent displacement constraints at the corner nodes of the cross-frame. The truss support reactions corresponding to the loading applied in the figure are shown with these arrows. The cross-frame is effectively supported as a propped cantilever and is loaded by an end moment at its simply supported end in the flexural analogy approach. It is fixed against rotation and vertical displacement at its left-hand side and restrained against vertical movement at its right-hand side in the figure. A couple composed of equal and opposite unit loads is applied to the top and bottom joints on the right-hand side. The associated horizontal displacements of the truss are determined via a

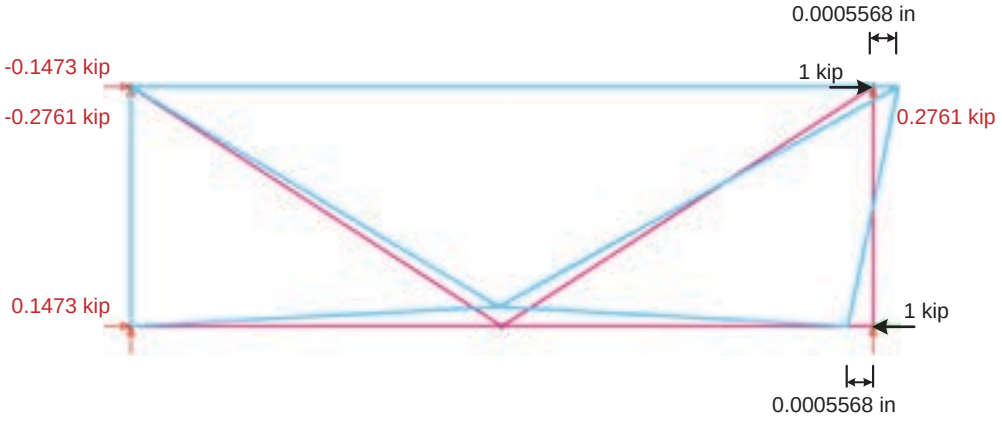

$\theta = 2(0.0005568)/34 = 0.00003275$ radians $= ML/4EI_{eq} = (34)(105)/4(29000)I_{eq}$

$I_{eq} = 940$ in^4

Figure 3-13. Calculation of equivalent moment of inertia based on the flexural analogy method.

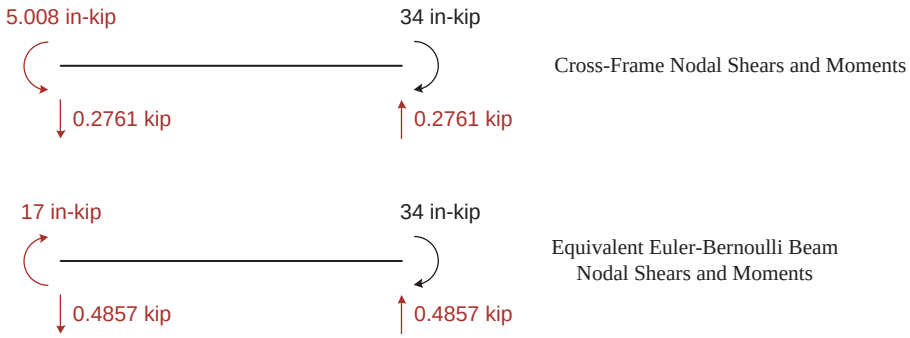

Figure 3-14. Cross-frame nodal shears and moments and equivalent Euler-Bernoulli beam shears and moments based on flexural analogy method.

structural analysis. The equivalent beam moment of inertia, I_{eq}, is then calculated by equating the corresponding rotation at the right-hand side to the Euler-Bernoulli beam rotation $M/(4EI_{eq}/L)$, as shown in the figure.

Figure 3-14 compares the physical cross-frame end shears and moments to the nodal shears and moments in the equivalent Euler-Bernoulli beam. One can observe that the moment induced at the left-hand side of the physical cross-frame is much smaller than the "carry-over moment" of one-half of the applied end moment in the equivalent Euler-Bernoulli beam element. In fact, it is even of the opposite sign. Correspondingly, the vertical shear forces induced in the physical cross-frame are much smaller than the ones associated with the equivalent beam based on the flexural analogy. These smaller internal forces are due to the shear raking deformations in the physical truss system. The equivalent Euler-Bernoulli beam does not consider any beam shear deformations.

3.2.3.2 Equivalent Beam Stiffness Based on the Shear Analogy Approach

Figure 3-15 illustrates the second common method of determining an equivalent beam stiffness discussed by the AASHTO/NSBA (2011) G13.1 document. This approach is termed the shear analogy method. In this approach, the cross-frame is supported as a fixed-fixed beam subjected to a transverse shear force. In the figure, all of the truss dofs are fixed on the left-hand side,

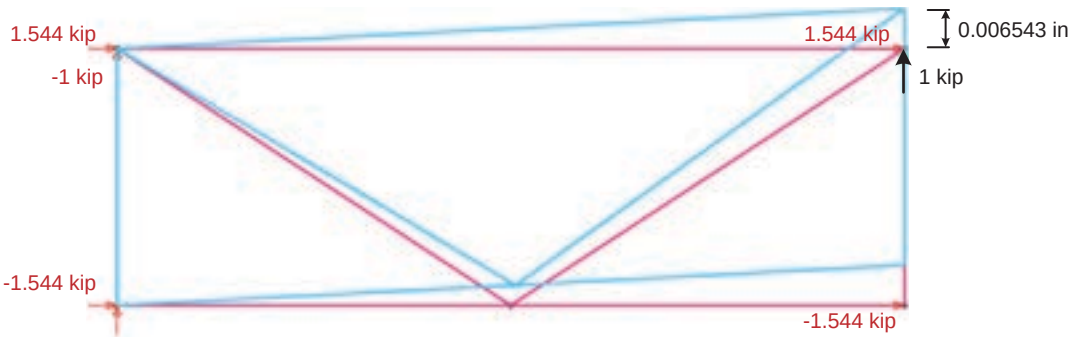

$$\Delta = 0.0006543 \text{ in} = PL^3/12EI_{eq} = (1)(105)^3/12(29000)I_{eq}$$

$$I_{eq} = 508 \text{ in}^3$$

Figure 3-15. Calculation of equivalent moment of inertia based on the shear analogy method.

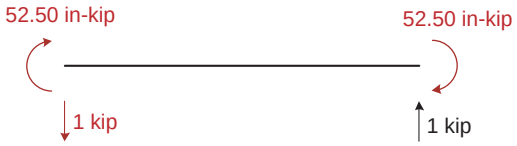

Figure 3-16. Cross-frame nodal shears and moments and equivalent Euler-Bernoulli beam shears and moments based on shear analogy.

the horizontal dofs are constrained on the right-hand side, and the truss is subjected to a unit vertical load on the right-hand side. It should be noted that the vertical members at the sides of the cross-frames represent the stiffness of the girder webs and connection plates, which typically involves a larger effective area than the cross-frame members themselves. The unit load is applied on the right-hand side and the truss is supported on the left-hand side in Figure 3-15 such that no deformations of the end vertical elements come into play. The equivalent beam cross-frame stiffness is obtained by equating the relative end deflection to the Euler-Bernoulli beam solution $P/(12EI_{eq}/L^3)$.

Figure 3-16 shows the nodal shears and moments for both the physical cross-frame and the equivalent Euler-Bernoulli beam in this problem. That is, the nodal shears and moments are identical for the equivalent beam idealization and the physical truss in this case. However, it should be noted that a large portion of the vertical displacement in the physical truss is due to shearing type deformations whereas the Euler-Bernoulli beam does not include any consideration of shear deformations. Therefore, the equivalent moment of inertia is in essence "artificially reduced" to account for these large shearing deformations in the shear analogy approach.

3.2.3.3 Equivalent Beam Stiffness for a Timoshenko Beam Element

Figure 3-17 illustrates the first step of a more accurate approach for the calculation of the cross-frame equivalent beam stiffnesses. This approach simply involves the calculation of an equivalent moment of inertia, I_{eq}, as well as an equivalent shear area A_{seq} for a shear-deformable (Timoshenko) beam element representation of the cross-frame. In this approach, the equivalent

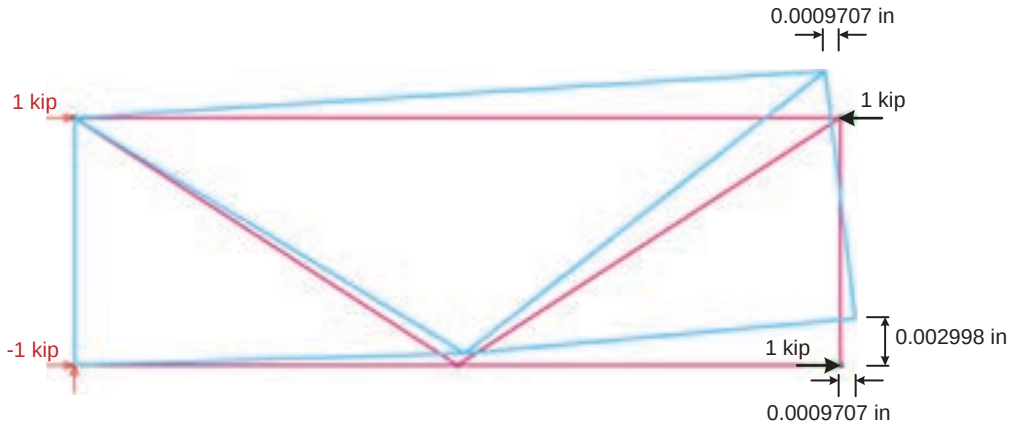

$$\theta = 2(0.0009707)/34 = 0.0000571 = ML/EI_{eq} = 34(105)/29000I_{eq}$$

$$I_{eq} = 2156 \text{ in}^4$$

Figure 3-17. Calculation of equivalent moment of inertia based on pure bending.

moment of inertia is determined first based on pure flexural deformation of the cross-frame (zero shear). The cross-frame is supported as a cantilever at one end and is subjected to a force couple applied at the corner joints at the other end, producing constant bending moment. The associated horizontal displacements are determined at the free end of the cantilever, and the corresponding end rotation is equated to the value from the beam pure flexure solution $M/(EI_{eq}/L)$. One can observe that this results in a substantially larger I_{eq} and that this EI_{eq} represents the "true" flexural rigidity of the cross-frame.

In the second step of the improved calculation, using an equivalent Timoshenko beam element rather than a Euler-Bernoulli element, the cross-frame is still supported as a cantilever but is subjected to a unit transverse shear at its tip. Figure 3-18 shows the corresponding displacements and reactions for this model, as well as the Timoshenko beam equation for the transverse displacement and the solution for the A_{seq} of the FHWA Test Bridge cross-frame.

It should be noted that the end rotation of the equivalent beam in Figure 3-18 is

$$\theta = VL^2/2EI_{eq} - V/GA_{seq}$$

$$= 1(105)^2/2(29000)(2156) - (1)(2.6)/(29000)(2.008) = 0.00004352 \text{ radians}$$

However, from the deflected shape in Figure 3-18, $\theta = 2(0.001499)/34 = 0.00008818$ radians. Therefore, it can be observed that the shear-deformable Timoshenko beam element is not able to match the "exact" kinematics of the cross-frame.

Figure 3-19 compares the physical cross-frame end shears and moments to the nodal shears and moments for the equivalent Timoshenko beam for the case of a propped cantilever subjected to end moment. One can observe that the Timoshenko beam comes much closer to fitting the force response of the cross-frame, compared to the earlier result with the Euler-Bernoulli beam element in Figure 3-14. However, it can be seen that the Timoshenko beam shear forces are still 2.9 percent smaller than those of the physical truss, and the left-hand end moment is 16.5 percent larger than the "actual" left end moment. The left-hand moment is in the correct direction though in Figure 3-19, whereas in the previous Figure 3-14, the left-hand end moment is not even in the correct direction.

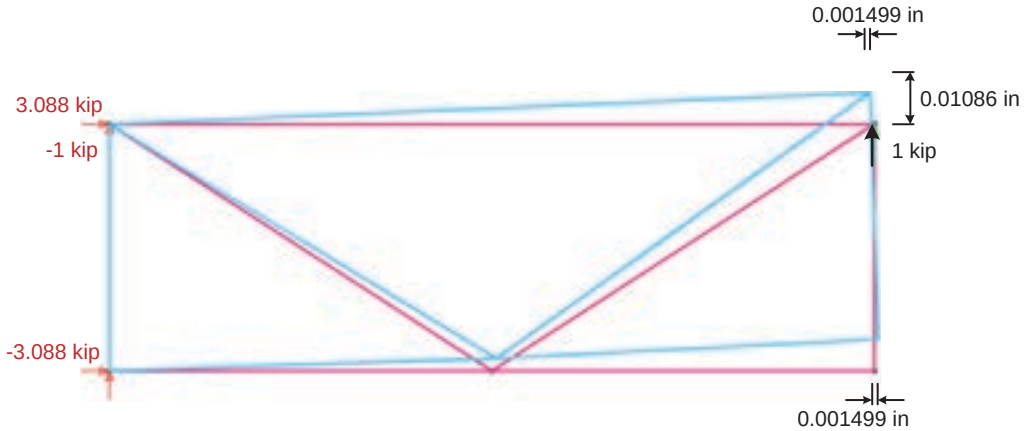

$$\Delta = 0.01086 \text{ in} = VL^3/3EI_{eq} + VL/GA_{eq}$$
$$= 1(105)^3/3(29000)(2156) + (1)(105)(2.6)/29000A_{seq}$$
$$A_{seq} = 2.008 \text{ in}^2$$

Figure 3-18. Calculation of equivalent shear area based on tip loading of the cross-frame supported as a cantilever.

52 Guidelines for Analysis Methods and Construction Engineering of Curved and Skewed Steel Girder Bridges

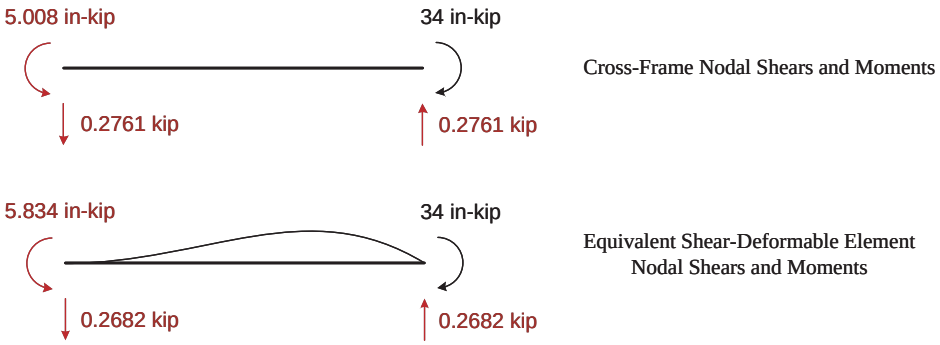

Figure 3-19. Cross-frame nodal shears and moments and equivalent shear-deformable beam shears and moments.

3.2.3.4 Overall Comparison of Cross-Frame Models

Table 3-5 provides a detailed comparison of the force and displacement results for the three different equivalent beam elements described in the above compared to the "exact" results for the physical truss model of the cross-frame from Figure 3-12. All the "exact" solutions are shown in bold. It can be observed that the equivalent Euler-Bernoulli beams are able to fit the exact solution for only one response, whereas the Timoshenko beam is able to fit the exact solution for two responses. Furthermore, the Timoshenko beam provides a closer approximation to the physical truss results in the cases where the fit is not exact. This is due to the fact that the Timoshenko element is able to represent both flexure and shear deformations. The approximations are due in part to the fact that the Timoshenko beam formulation considered here is a close representation of prismatic solid web members. The truss-type cross-frame deformations generally lead to different stiffness results than provided by a prismatic solid web member though.

It can be shown that the Timoshenko beam element provides a closer approximation of the physical cross-frame behavior compared to the Euler-Bernoulli beam for all other types of cross-frames typically used in I-girder bridges as well, including X and inverted V cross-frames with top and bottom chords, as well as X and V cross-frames without top chords. However, similar to the above demonstrations, the Timoshenko beam model is only able to provide an exact fit for two of the five responses listed across the rows of Table 3-5.

Given the "exact" equivalent beam stiffness values developed in the above solutions, the next logical refinement is to develop generic X, V, inverted-V, X without top chord, and V without top chord models with variable width and height and variable cross-section area for the cross-frame members (including different cross-section areas for the different members). Section 6.2.2 of the Task 8 report describes the development of one "exact" equivalent beam element of this form as well as a rather easy implementation of this element as a user-defined element within the LARSA 4D software system. Sanchez (2011) provides detailed developments of this form for all of the above cross-frame types.

3.2.3.5 Influence of the Cross-Frame Equivalent Beam Stiffness Model on the Vertical Displacement Results in the FHWA Test Bridge

Table 3-6 shows the influence of the different equivalent beam stiffness models considered in the above developments on the vertical displacement at the mid-span of the fascia girder (G1) on the outside of the horizontal curve in the FHWA Test Bridge. It can be observed that the 2D-grid model using the Timoshenko equivalent beam element generally provides the best estimate of the models developed in the above section. The results provided by the "exact" equivalent beam model of the test bridge cross-frame are essentially the same as those obtained using the

Table 3-5. Comparison of equivalent beam responses to the physical truss cross-frame model responses for the V-type cross-frame of Figure 3-12.

CF Model	I_{eq} (in^4)	A_{seq} (in^2)	M_{far}/M_{near} propped cantilever subjected to end moment	Transverse deflection of cantilever in pure bending (M = 34 in-k)	Transverse deflection of tip-loaded fixed-fixed member (V = 1 k)	End rotation of propped cantilever (M = 34 in-k)	Cantilever in pure bending, end rotation (M = 34 in-k)
Euler-Bernoulli element with I_{eq} based on flexural analogy	940	NA[a]	+0.5	6.88E-3 inches	3.54E-3 inches	**3.27E-5 radians**[b]	13.1E-5
Euler-Bernoulli element with I_{eq} based on shear analogy	508	NA[a]	+0.5	12.7E-3 inches	**6.55E-3 inches**	6.06E-5 radians	24.9E-5
Timoshenko beam element	2156	2.01	-0.172	**3.00E-3 inches**	6.23E-3 inches	3.28E-5 radians	**5.71E-5 radians**
Physical truss model	--	--	-0.147	**3.00E-3 inches**	**6.55E-3 inches**	**3.27E-5 radians**	**5.71-5 radians**

[a] The shear area is effectively ∞ for the Euler-Bernoulli beam element.

[b] Exact values are shown in bold font.

Timoshenko beam formulation. The predicted mid-span displacement is 8.7 percent larger using the model with the Euler-Bernoulli element based on the shear analogy. This demonstrates that the cross-frame model can have a measurable influence on the prediction of the constructed geometry. The absolute difference in the displacements is relatively small for the test bridge; however, for a longer span, the difference could be more consequential.

The last row of Table 3-6 gives the solution obtained if the cross-frame torsional stiffness is neglected (i.e., $J = 0$) for the cross-frame equivalent beam element. One can observe that this results in little change in the bridge vertical displacement.

3.2.3.6 FHWA Test Bridge Cross-Frame Forces Predicted by Different Methods

Figure 3-20 shows the forces calculated in the two cross-frames at the mid-span of the FHWA Test Bridge from the various methods of analysis. One can observe that, of the various solutions,

Table 3-6. FHWA Test Bridge (EISCR1) mid-span vertical displacement of Girder G1 (Δ_{G1}) under total dead load (unfactored) for different 2D-grid cross-frame idealizations, girders modeled using J_{eq} and four elements in each L_b, nodes located on the circular arc (Δ_{G1} = 4.49 in., second-order 3D FEA; Δ_{G1} = 4.40 in., first-order 3D FEA).

Cross-frame idealization	Δ_{G1} (in.)
Shear-deformable (Timoshenko) beam element – I = 2156 in^4, A_s = 2.01 in^2, J = 39.8 in^4	4.73
Equivalent Euler-Bernoulli beam element based on flexural analogy – I = 940 in^4, A_s = ∞, J = 39.8 in^4	4.87
Equivalent Euler-Bernoulli beam element based on shear analogy – I = 508 in^4, A_s = ∞, J = 39.8 in^4	5.14
Shear deformable (Timoshenko) beam element – I = 2156 in^4, A_s = 2.01 in^2, J = 0 in^4	4.74

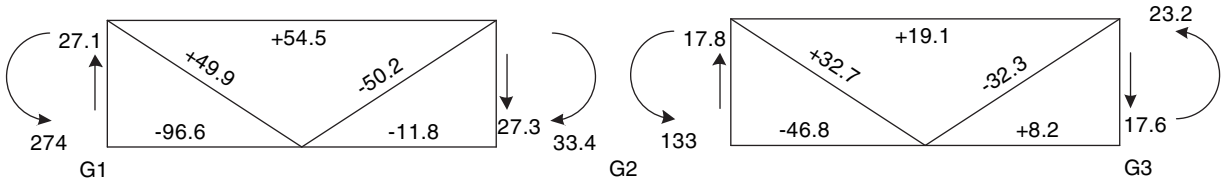

(a) 3D FEA benchmark

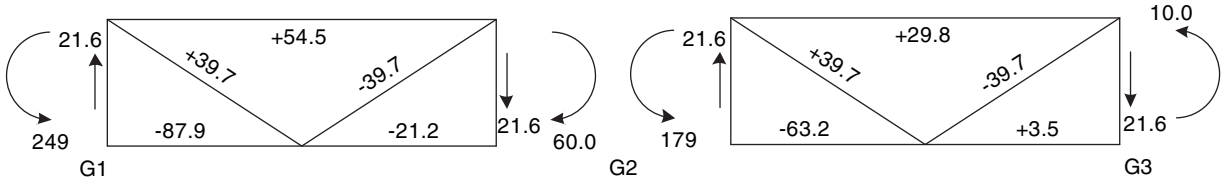

(b) V-Load

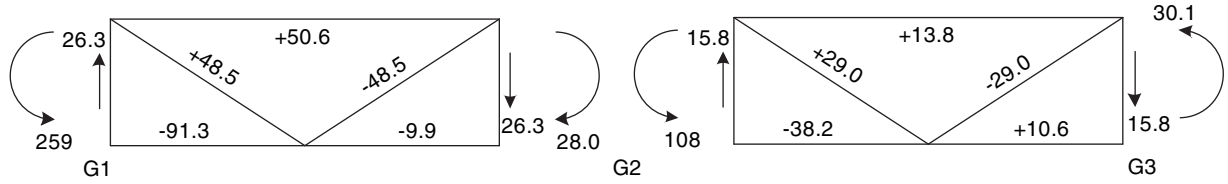

(c) Conventional 2D-grid, cross-frame equivalent beam stiffness based on flexural analogy

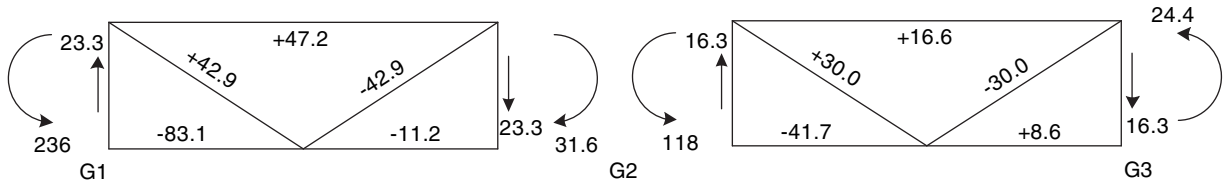

(d) Improved 2D-grid, cross-frame equivalent beam stiffness based on Timoshenko beam model

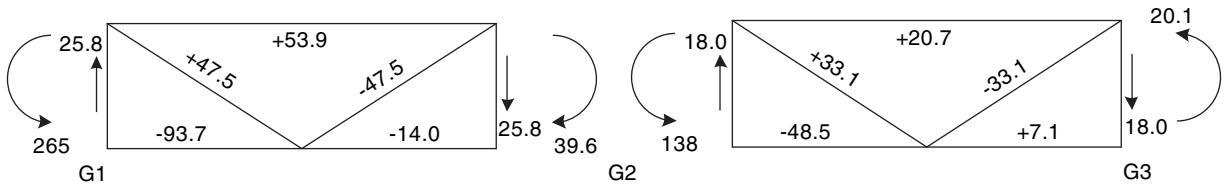

(e) TWOS 2D-grid, cross-frame equivalent beam stiffness based on Timoshenko beam model

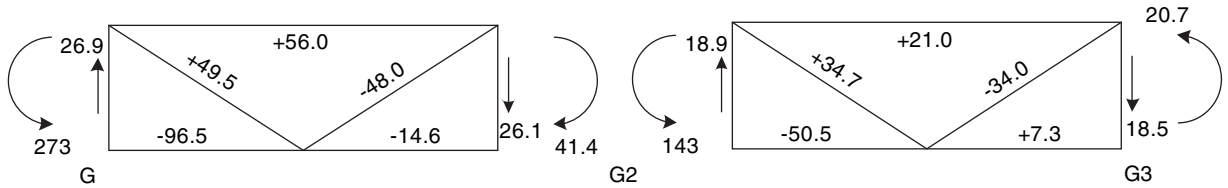

(f) TWOS 3D-frame, explicit modeling of cross-frames by beam and truss elements

Figure 3-20. FHWA Test Bridge (EISCR1) unfactored (nominal) cross-frame dead load forces calculated at mid-span by different methods (units: ft-kip moments, kip forces).

only the TWOS results shown in Figure 3-20e and f give results that never deviate more than 3 kips from the 3D FEA benchmark solution. (The percentage errors can be large even for these solutions in cases where the cross-frame forces are small. However, these percentage errors are not of any consequence when the cross-frame member sizes are repeated throughout the structure and sized for the most critical demand.) The TWOS 3D-frame solution shown in Figure 3-20f gives the best correlation with the 3D FEA benchmark. This is because this is the only "simplified" solution that accounts for:

1. The second-order effects in the calculation of the cross-frame forces (although the second-order effects are only a few percent for this structure and loading, as discussed previously in Section 3.2.2.1), and
2. The location of the various components and entities through the depth of the structure (i.e., the girder centroids and shear centers, the cross-frame depths and locations through the depth of the girders, the load height of the concrete slab, and the location of the bearings relative to the girder centroidal and shear center axes).

Nevertheless, all of the 2D-grid solutions as well as the V-load solution give reasonable results for this bridge. The maximum error in the prediction of the maximum cross-frame bottom chord force is -14.0 percent, corresponding to the improved 2D-grid solution shown in Figure 3-20d, while the maximum error in the maximum cross-frame diagonal force is -20.4 percent, corresponding to the V-load method solution shown in Figure 3-20b. It is clear that the V-load method gives the greatest misrepresentation of the true cross-frame vertical shear forces. This is due to the fact that the V-load method is based on an assumption of "equal vertical stiffness" across all the girders at each of the intermediate cross-frame locations.

The concept of equal vertical stiffness in the above means that, if each girder were considered in isolation, and if a unit load were applied at each girder in succession, the same vertical displacement would be obtained. However, the girders can never be physically isolated from each other in any meaningful way for calculation of these so-called vertical stiffnesses. Isolating the girders requires the application of artificial boundary conditions to them, which changes the way they respond to the load. An implicit assumption of an equal vertical stiffness from each girder is invoked in the derivation of the coefficient C used in calculating the V-load as a function of the number of girders in the bridge system (NHI, 2011). Since the "equal vertical stiffnesses" can never be calculated in any meaningful way, they can never be checked. Conceptually, the girder vertical stiffnesses can be thought of typically as being very different though, even in radially supported bridges with a "very regular" geometry such as the FHWA Test Bridge, at least when the structure is highly curved. This is because the outside girder generally must resist substantially more load.

It should be noted that in the calculation of the results shown for the simplified methods in Figure 3-20b through e, part of the solution involves the calculation of the contribution from the overhang eccentric bracket loads. These load effects are approximated based on the AASHTO LRFD Equation (C-6.10.3.4-2) and are shown in Figure 3-21.

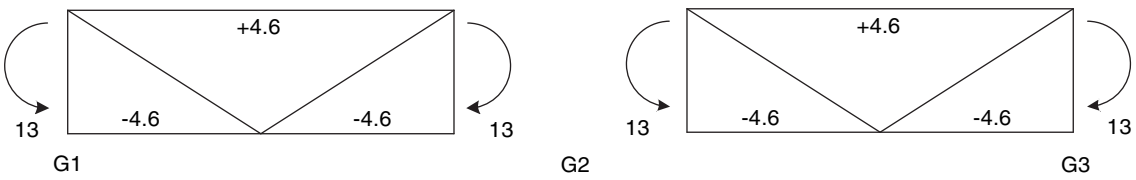

Figure 3-21. FHWA Test Bridge (EISCR1) unfactored (nominal) cross-frame dead load forces due to eccentric bracket loads (units: ft-kip moments, kip forces).

56 Guidelines for Analysis Methods and Construction Engineering of Curved and Skewed Steel Girder Bridges

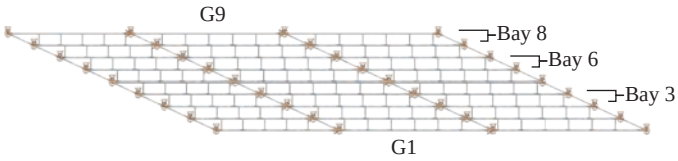

Figure 3-22. Framing plan of Bridge NICSS16.

3.2.3.7 Improved Prediction of Cross-Frame Forces in Skewed I-Girder Bridges

Figure 3-22 shows a sketch of the framing plan for Bridge NICSS16 from the NCHRP Project 12-79 Task 7 analytical studies. This is a continuous-span structure with an extreme parallel skew of its bearing lines of 70°, combined with an 80-ft.-wide deck ($w = 80$ ft.), a perpendicular distance between its fascia girders of $w_g = 74$ ft., and 120-, 150- and 150-ft. span lengths. As a result, its skew index I_S is 1.69 from Equation 9. The skew index captures the tendency for the development of substantial transverse load paths in I-girder bridge structures and is used as a key term in scoring the accuracy of the simplified methods of analysis in Table 3-1. This bridge is framed with staggered cross-frame lines, which reduces the large forces developed particularly in the transverse direction between the obtuse corners of each span. However, these forces still are significant.

Figures 3-23 through 3-25 show the cross-frame forces calculated in Bay 3 (between Girders G2 and G3), Bay 6 (between Girders G3 and G4, and Bay 8 (between Girders G6 and G7)

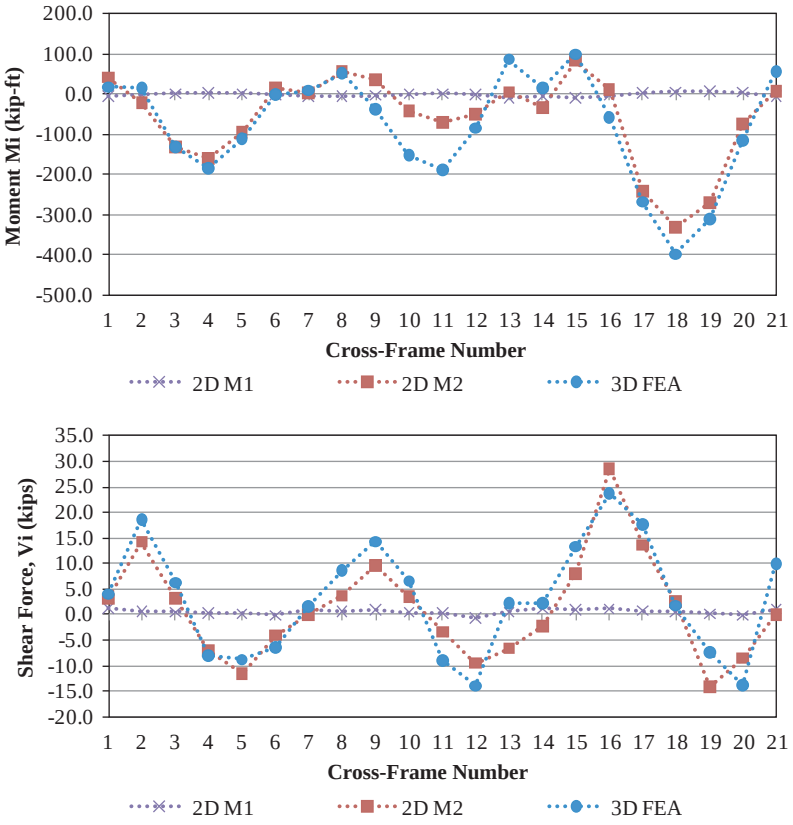

Figure 3-23. Bridge NICSS16 cross-frame forces in Bay 3 (between Girders G3 and G4) under total dead load (unfactored) from conventional 2D-grid analysis (M1), improved 2D-grid analysis (M2), and 3D FEA.

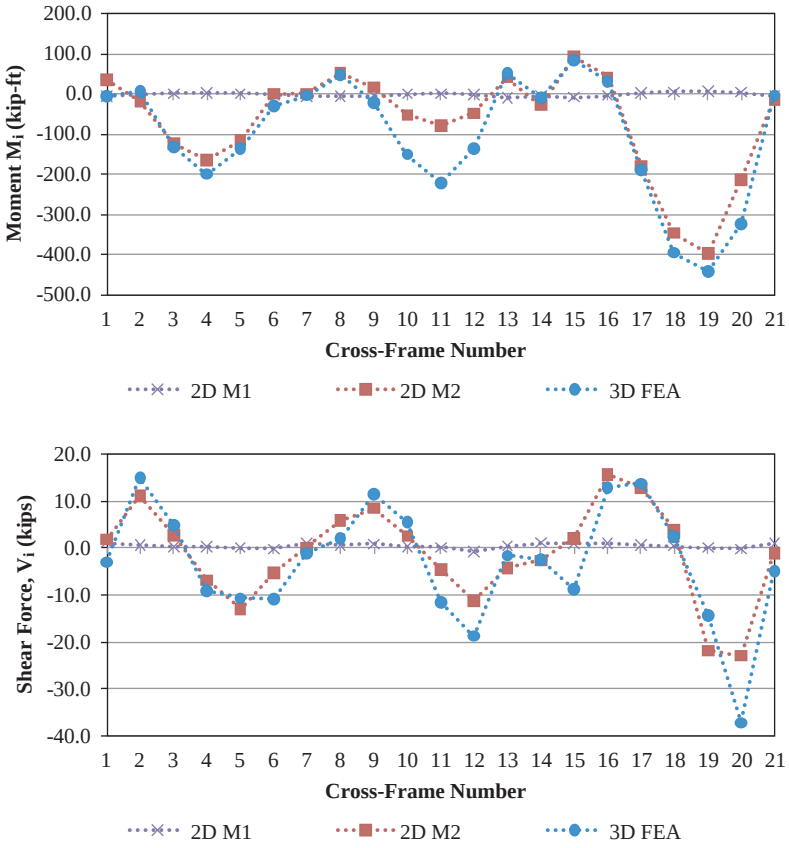

Figure 3-24. Bridge NICSS16 cross-frame forces in Bay 6 (between Girders G6 and G7) under total dead load (unfactored) from conventional 2D-grid analysis (M1), improved 2D-grid analysis (M2), and 3D FEA.

in the Bridge NICSS16 using the conventional 2D-grid approach, the improved 2D-grid method, and the 3D FEA benchmark simulation. The improved 2D-grid solution implemented here uses the J_{eq} girder torsion model discussed in Section 3.2.2 as well as the "exact" equivalent beam element discussed Section 3.2.3 and described in detail in the Task 8 report (Appendix C of the contractors' final report).

The first plot in each of the figures cited above shows the nodal moment at the ends of the cross-frames toward the bottom of the plan view shown in Figure 3-22. The second plot shows the vertical shear transferred by each cross-frame. The horizontal axis shows the cross-frame number within each of the bays, starting from the left-hand end of the bridge in Figure 3-22 and progressing to the right-hand end. The forces are calculated assuming no-load fit detailing of the cross-frames for simplicity of the discussion. Steel dead load fit (SDLF) and total dead load fit (TDLF) detailing effects are addressed subsequently in Sections 3.2.5 and 3.3.

From the above plots, it is apparent that the conventional 2D-grid solution predicts essentially zero cross-frame forces throughout the NICSS16 bridge structure. The primary reason for this behavior is the dramatic under-estimation of the girder torsional stiffnesses due to using only the St. Venant torsional stiffness term (GJ/L) in the 2D-grid idealization. Conversely, the improved 2D-grid method provides a reasonably good estimate of the cross-frame forces in this extreme structure, compared to the benchmark 3D FEA solutions.

The results in Figures 3-23 through 3-25 for the above skewed I-girder bridge, combined with the results in Figure 3-7 for the FHWA Test Bridge highlight the importance of using a

58 Guidelines for Analysis Methods and Construction Engineering of Curved and Skewed Steel Girder Bridges

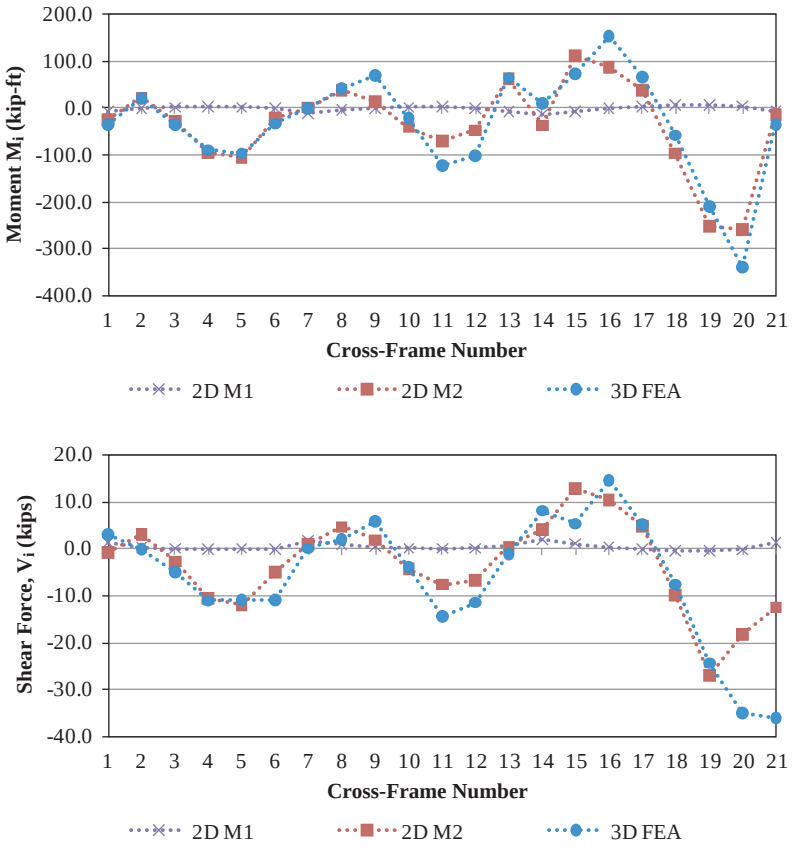

Figure 3-25. Bridge NICSS16 cross-frame forces in Bay 8 (between Girders G8 and G9) under total dead load (unfactored) from conventional 2D-grid analysis (M1), improved 2D-grid analysis (M2), and 3D FEA.

better I-girder torsion model than the simplistic one commonly used in conventional 2D-grid methods. Furthermore, the results in Table 3-6 clearly show the importance of also using a better representation of the cross-frame stiffnesses in bridges where the cross-frame deformations start to have some influence on the overall structure response. Of major importance is the fact that these improvements require little additional computational expense, and their software implementation is relatively straightforward. However, professional software implementation of these methods is essential for them to be used efficiently in practice. Manual calculation and input of the corresponding improvements into the software is too laborious to be workable given common professional time constraints.

3.2.4 Improved Calculation of I-Girder Flange Lateral Bending Stresses from 2D-Grid Analysis

Given the above improvements in the I-girder and cross-frame stiffness representations, it is still essential to address the calculation of the flange lateral bending stresses in curved and/or skewed I-girder bridges. This section recommends specific improvements in these calculations.

Figure 3-26a shows the plan view of Bridge NISSS16 considered in the NCHRP Project 12-79 Task 7 analytical studies. This is a 150-ft. simple-span straight bridge with an 80-ft.-wide deck ($w = 80$ ft.), a perpendicular distance between its fascia girders of 74 ft., and a skew of 50 degrees at its left-hand abutment. These geometry factors produce a skew index of $I_s = 0.59$, placing this

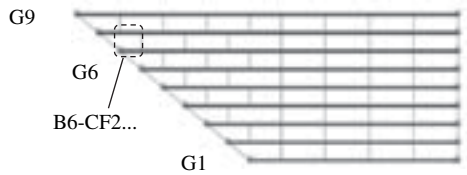

(a) Plan view of Bridge NISSS16

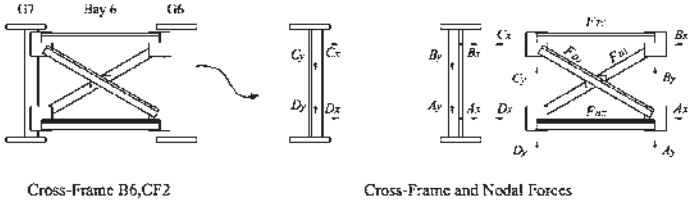

(b) Forces transferred from cross-frame B6-CF2 to Girders G6 and G7

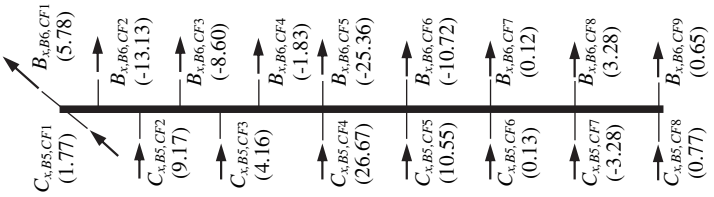

(c) Top flange of Girder G6 subject to the horizontal components of the nodal forces

Figure 3-26. Calculation of lateral bending stresses in the top flange of Girder G6, in Bridge NISSS16 under total dead load (unfactored).

bridge just inside the second category of straight-skewed bridge structures in the scoring system of Table 3-1.

Figure 3-26b illustrates the forces in cross-frame 2 (CF2) of Bay 6 in this structure and the corresponding statically equivalent nodal horizontal and vertical forces transferred to the I-girders at the cross-frame chord levels. These horizontal forces can be transformed to statically equivalent lateral forces applied at the flange levels of the I-girders by determining the couple associated with these horizontal forces and then multiplying the chord-level couple forces by the ratio of the cross-frame depth to the girder depth between the flange centroids, d_{CF}/h. In typical 2D-grid solutions, $C_x = -D_x$ and $B_x = -A_x$, and thus the forces shown in Figure 3-26b are the couple forces.

Figure 3-26c shows the top flange forces applied to Girder G6 in this bridge, determined from the improved 2D-grid method discussed in the previous sections. The forces are still labeled "C_x" and "B_x," for simplicity of the presentation. It should be noted that the chord-level couple forces shown in Figure 3-26b are multiplied by (d_{CF}/h) to determine the flange-level forces.

Given a general statical free-body diagram of a girder flange, such as the one shown for Girder G6 in the figure, one would expect that the subsequent determination of the flange lateral bending stresses is an easy strength of materials calculation. If the girder is also horizontally curved, the equivalent radial lateral loads corresponding to the horizontal curvature can be included in the free-body diagram. Furthermore, eccentric bracket loads from the overhangs can be included on fascia girders.

Unfortunately, the solution for the flange lateral bending stresses is not this simple. The problem is that the girder torsional stiffnesses, upon which the above calculation of the cross-frame

forces is based, include a contribution both from the girder warping torsion as well as the girder St. Venant torsion. As such, a portion of the above forces is transferred (by the interaction of the flange with the girder web) into the internal St. Venant torsion in the girders. More specifically, corresponding small but undetermined distributed lateral forces are transferred to the flange from the web in Figure 3-26c. Because of this effect, if the statical free-body diagram shown in Figure 3-26c is used to calculate the girder flange lateral bending stresses, slight errors accumulate as one moves along the girder length.

Solutions to this problem include:

1. Use the girder torsional rotations and displacements along with the detailed open-section thin-walled beam stiffness model associated with J_{eq} to directly determine the flange lateral bending stresses. This results in an imbalance in the flange lateral bending moments on each side of the intermediate cross-frames (since J_{eq} is based on the assumption of warping fixity at the cross-frame locations). This moment imbalance could be re-distributed along the girder flange to determine accurate flange lateral bending moments. A procedure analogous to elastic moment distribution could be utilized for this calculation. Although this approach is a viable one, it is relatively complex. Therefore, it was not pursued in the NCHRP Project 12-79 research.
2. Focus on an approximate local calculation in the vicinity of each cross-frame, utilizing the forces delivered to the flanges from the cross-frames as shown in Figure 3-26c. Because of its relative simplicity, this approach was selected in the NCHRP Project 12-79 research.

It should be noted that the girder flange lateral bending stresses are calculated directly and explicitly from the element displacements and stiffnesses in the TWOS 2D-grid and TWOS 3D-frame solutions. Therefore, these methods provide the best combination of accuracy and simplicity for the grid or frame element calculation of the flange lateral bending stresses. However, the disadvantage of this approach is the additional complexity of the element formulation and the requirement that an additional warping degree of freedom has to be included in the global structural analysis.

Figure 3-27 illustrates the simplified approach adopted in the NCHRP Project 12-79 research for calculating the I-girder flange lateral bending moments given the statically equivalent lateral loads transferred at the flange level from the cross-frames. The calculation focuses on a given cross-frame location and the unbraced lengths, *a* and *b,* on each side of this location. For simplicity of the discussion, only the force delivered from the cross-frame under consideration

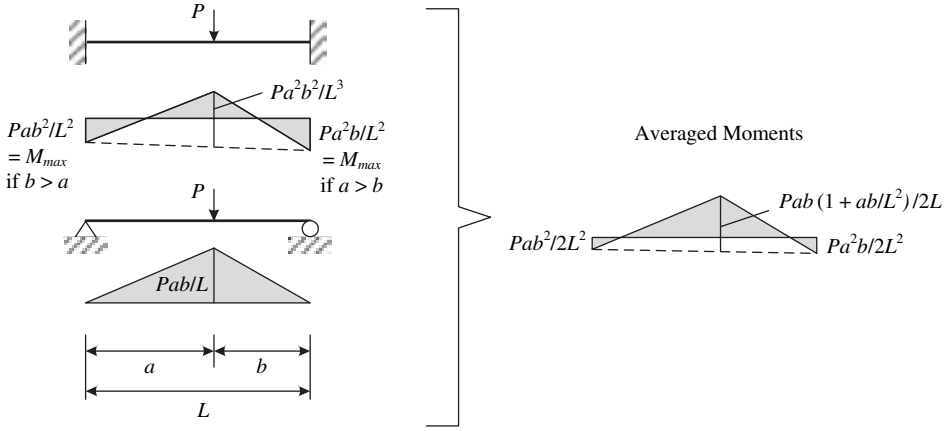

Figure 3-27. Lateral bending moment, M_ℓ in a flange segment under simply supported and fixed-end conditions.

is shown in the figure, and the cross-frame is assumed to be non-adjacent to a simply supported end of the girder. In general, the lateral forces from horizontal curvature effects and/or from eccentric bracket loads on fascia girders also would be included. Two flange lateral bending moment diagrams are calculated as shown in the figure, one based on simply supported end conditions and one based on fixed-end conditions at the opposite ends of the unbraced lengths. For unbraced lengths adjacent to simply supported girder ends, similar moment diagrams are calculated, but the boundary conditions are always pinned at the simply supported end. The cross-frame under consideration is located at the position of the load *P* in the sketches. In many situations, the moments at the position of the load are the controlling ones in the procedure specified below.

Given the moment diagrams for the above cases, the project Task 8B research determined that an accurate-to-conservative solution for the flange lateral bending moments and stresses is obtained generally by:

1. Averaging the above moment diagrams, and
2. Taking the largest averaged internal moment in each of the unbraced lengths as the flange lateral bending moment for that length.

This solution is repeated cross-frame location by cross-frame location along the length of the girders and the largest moment from the two solutions obtained for each unbraced length is taken as the estimate of the flange lateral bending moment in that unbraced length. (For the unbraced lengths at girder simply supported ends, only one solution is performed.)

The above procedure recognizes that the true flange lateral bending moment is bounded by the "pinned" and "fixed" moment diagrams (neglecting the small St. Venant torsional contributions from the interaction with the web) and ensures that the flange lateral bending moments required for static equilibrium are never underestimated. Also, the average of the pinned and fixed moment diagrams is analogous to the use of the approximation $qL_b^2/10$ rather than $qL_b^2/12$ when estimating the flange lateral bending moments due to horizontal curvature, where q is the equivalent flange radial load. In addition, the above solution is insensitive to any inaccuracies in the calculation of the cross-frame forces as described in Sections 3.2.3.6 and 3.2.3.7.

Figure 3-28 illustrates the accuracy associated with using the procedure from Figure 3-27 for the NISSS16 Bridge. One can observe that the flange lateral bending stresses from the 3D FEA simulation model are predicted quite well. The recommended procedure of using the maximum of the internal moments from the calculations for the two adjacent cross-frames for each unbraced

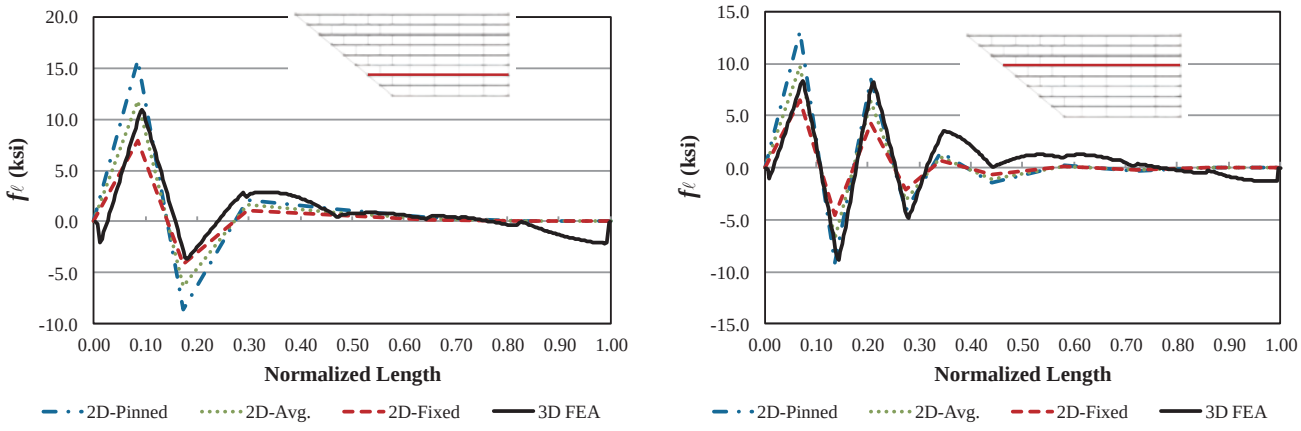

(a) Girder G3 (b) Girder G6

Figure 3-28. Bridge NISSS16 flange lateral bending stresses under total dead load (unfactored).

62 Guidelines for Analysis Methods and Construction Engineering of Curved and Skewed Steel Girder Bridges

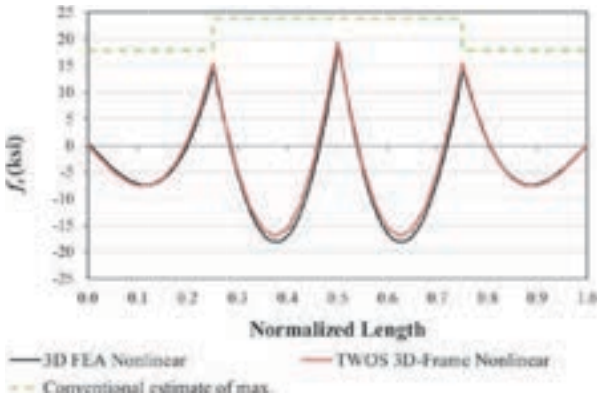

Figure 3-29. FHWA Test Bridge (EISCR1) flange lateral bending stresses in Girder G1 under Service IV load combination (1.5 × total dead load).

length as the flange lateral bending moment value tends to be somewhat conservative in extreme cases where the dimensions *a* and *b* are substantially different.

Figure 3-29 compares the results of simplified calculations of the maximum flange lateral bending stresses for the different unbraced lengths to the 3D FEA benchmark solution for the fascia girder (G1) on the outside of the curve in the FHWA Test Bridge. For curved radially supported I-girder bridges with relatively regular geometry, the basic "conventional" estimate from the AASHTO LRFD equation (C4.6.1.2.4b-1), using a coefficient of $N = 12$ rather than 10, works quite well. In the FHWA Test Bridge calculations, the results from the above improved calculations give essentially the same results as those obtained from the AASHTO equation. However, the AASHTO equation is obviously much simpler. Nevertheless, for bridges having non-zero skew, the improved method is able to account in a rational manner for the skew effects. The net result is a significantly improved estimate of the girder flange lateral bending stresses compared to the coarse values recommended in AASHTO (2010) Article C6.10.1.

It should be emphasized that the AASHTO LRFD equation (C4.6.1.2.4b-1) gives an estimate of the maximum flange lateral bending moment in a given unbraced length. Therefore, in Figure 3-29, the simplified solution is shown just as a constant value within each unbraced length.

Lastly, in Figure 3-29, the TWOS 3D-frame geometric nonlinear solution is provided along with the 3D FEA benchmark result to illustrate the high accuracy achievable with this TWOS solution. However, as stated in the Task 8 report (Appendix C of the contractors' final report), the TWOS approach was not pursued as an improved simplified solution in the NCHRP Project 12-79 research due to the additional complexities associated with its implementation.

3.2.5 Calculation of Locked-In Forces Due to Cross-Frame Detailing

This section addresses the fourth major improvement recommended by the NCHRP Project 12-79 research for the simplified 2D-grid analysis of curved and/or skewed I-girder bridges. However, it is important to note that this improvement also applies to 3D FE design analysis. This section addresses the calculation of locked-in forces due to steel dead load fit (SDLF) or total dead load fit (TDLF) cross-frame detailing. The emphasis here is predominantly on the calculation aspects. Section 3.3 addresses the broader attributes of the behavior and the question of when the locked-in forces due to the detailing of the cross-frames should be considered in the design. Appendix A provides summary definitions of key terms pertaining to cross-frame

detailing. It is essential that the reader understand these definitions to facilitate study and interpretation of the corresponding results and discussions throughout the report.

As noted previously, regardless of whether the analysis is a 2D-grid or a 3D FEA method, it can only give the bridge internal forces associated with no-load fit (NLF) detailing if it is conducted without the modeling of initial lack-of-fit effects. Any locked-in forces, due to the lack of fit of the cross-frames with the girders in the undeformed geometry, add to (or subtract from) the forces determined from the 2D-grid or 3D FEA design-analysis solutions. Fortunately, with some qualifications (discussed subsequently in Section 3.3), the SDLF or TDLF detailing effects tend to be opposite in sign to the internal forces due to the dead loads in straight-skewed bridges. Therefore, the 2D-grid or 3D FEA solutions for the cross-frame forces and the flange lateral bending stresses are conservative when they neglect the SDLF or TDLF initial lack-of-fit effects. Unfortunately, in some cases, these solutions can be prohibitively conservative. In addition, unfortunately, for curved radially supported structures, the cross-frame forces and girder maximum flange lateral bending stresses tend to be increased by the SDLF or TDLF detailing effects (see the subsequent discussions in Section 3.3). For generally curved and skewed bridges, the effects can go both ways.

Technically, it is relatively easy to include the influence of locked-in forces in either 2D-grid or 3D FEA calculations. Basically, the calculation amounts simply to the inclusion of an initial stress or initial strain effect. This is similar to the handling of thermal strains and deflections. Therefore, for cases where the initial lack-of-fit effects are important, including them in the analysis should not provide any significant hardship in terms of modeling effort or computational expense. Of course, as emphasized with the other key improvements recommended in the previous sections, the implementation of the calculations into professional software is essential for the methods to be used efficiently by the design engineer. In addition, it is essential for engineers to understand the methods, calculations, and potential issues; therefore, the software methods need to be well documented.

3.2.5.1 Key Conceptual Configurations Associated with SDLF and TDLF Detailing

To understand the calculation of the locked-in forces due to SDLF or TDLF detailing of the cross-frames, it is essential to first understand the basic geometry calculations associated with these methods. These calculations do not require any structural analysis, but rather, they utilize the specified girder camber profiles to determine the fabricated geometry of the cross-frames.

Figure 3-30 illustrates four different configurations associated with SDLF or TDLF detailing. Geometric factors such as cross-slope, super-elevation, and profile grade line are not shown in the figure for clarity. The cross-frame shown in the figure is assumed to be an arbitrary one within the bridge span (considerations at bearing line cross-frames are addressed subsequently). The two configurations used by structural detailers are Configurations 1 and 4. In Configuration 1, the girders are assumed to be blocked and under zero load with their webs vertical in their initially fabricated (cambered and plumb) geometry. If either TDLF or SDLF detailing is employed, the cross-frame, if connected to the girder on one side, will not fit up with the connection on the other side. This is because the cross-frame geometry is detailed to fit between the girder connection work points, assuming that the girder webs remain vertical while the corresponding camber values are taken out of the girders at the cross-frame location. If TDLF detailing is employed, Configuration 4 is the idealized girder geometry, with plumb webs and with the *total* dead load camber taken out of both of the girders. Correspondingly, if SDLF detailing is used, Configuration 4 is the idealized plumb girder geometry with the *steel* dead load camber taken out of both of the girders. Therefore, given the total dead load or steel dead load camber profiles, the TDLF or SDLF calculation is simply a geometrical one for the detailer and fabricator.

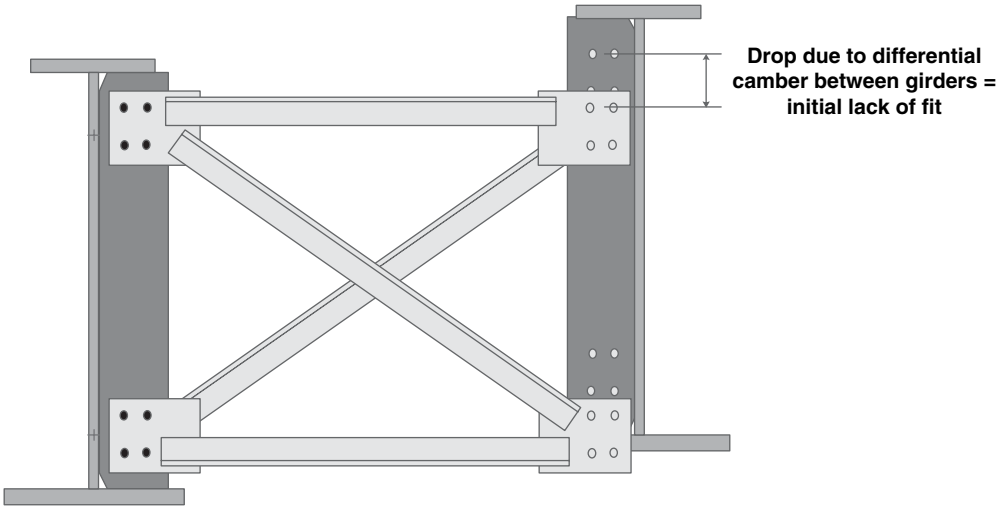

(a) Configuration 1 – No-load geometry before connecting the cross-frames

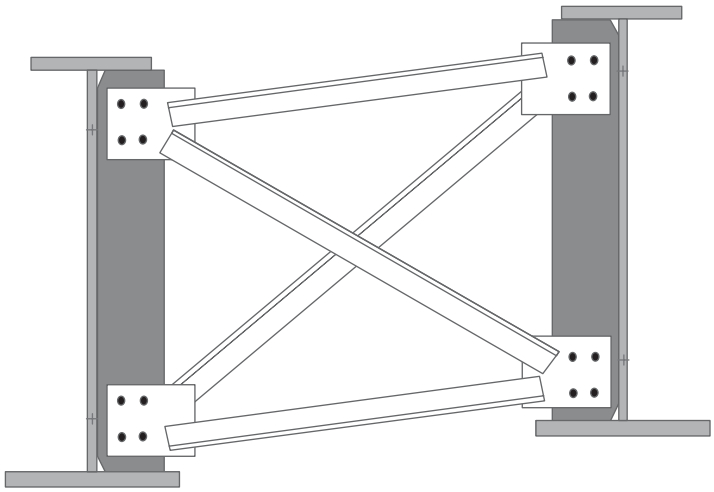

(b) Configuration 2 – Girders "locked" in the initial no-load, plumb and cambered geometry, cross-frames subjected to initial strains and initial stresses to connect them to the girders

Figure 3-30. Important conceptual configurations associated with total (or steel) dead load fit detailing (geometric factors such as cross-slope, super-elevation, and profile grade line are not shown for clarity).

(continued)

In order to include the initial lack-of-fit effects due to the above procedures in the structural analysis, Configuration 2 needs to be considered. It should be emphasized that Configuration 2 is never experienced in the physical bridge. However, this configuration is very convenient for setting up the analysis of the SDLF or TDLF effects. In this configuration, the girders are conceptually "locked" into position in their no-load ideally plumb geometry, and the cross-frames are conceptually deformed (i.e., forced) into the position where they fit up with the corresponding points on the girder connection plates. In many cases, the drops due to the differential camber, labeled in Configuration 1, are sufficiently large such that substantial initial strains need to be induced into the cross-frames in order for the connection points to fit up. This is not a problem, since the girders have been artificially locked in their no-load plumb position in this configuration. This is similar to the conceptual model used in the calculation of thermal loading effects, where the structure "nodes" are initially locked into position, the temperature changes are applied

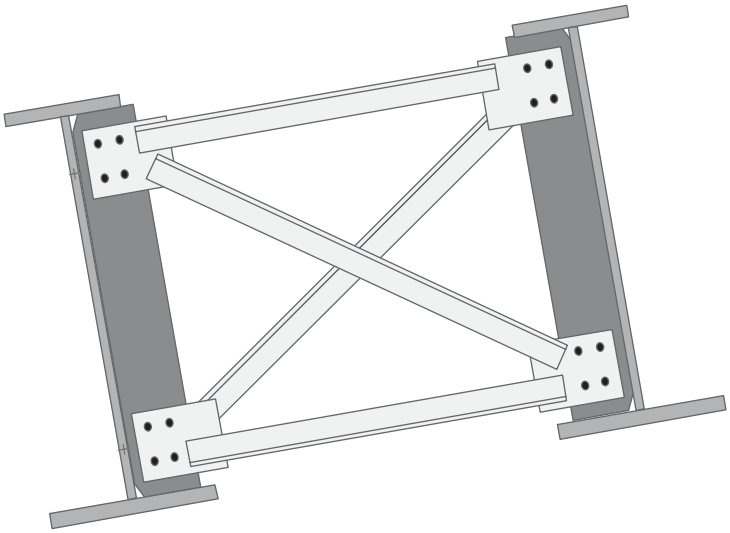

(c) Configuration 3 – Theoretical geometry under no-load (dead load not yet applied), after resolving the initial lack of fit by connecting the cross-frames to the girders, then "releasing" the girders to deflect under the lack-of-fit effects from the cross-frames

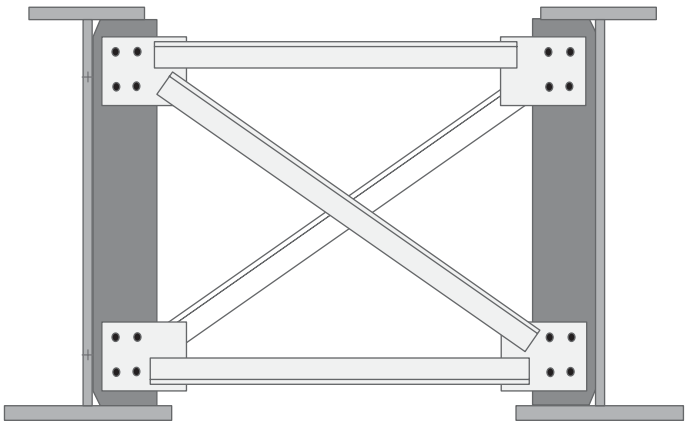

(d) Configuration 4 – Geometry under the combined effects of the total (or steel) dead load plus the locked-in internal forces due to the dead load fit detailing

Figure 3-30. (Continued).

to the model, producing initial stresses, and then the nodes are "released" and the structure is allowed to deform due to the "fixed-end" forces induced at the nodes when everything was initially "locked up."

Configuration 3 represents the geometry achieved by the structure once the girders are "unlocked" and allowed to deform under the fixed-end forces induced from the cross-frames at the connection points in Configuration 2. It should be emphasized that, conceptually, the dead loads (i.e., the self-weight of the steel and the dead weight of the concrete deck) have not been applied to the structure yet in Configuration 3. Therefore, similar to Configuration 2, this configuration also is never directly experienced by the bridge. However, the internal forces and stresses induced in Configuration 3 are the locked-in values due to the SDLF or TDLF detailing effects. When the corresponding steel or total dead load is added to this configuration, Configuration 4 (the state of the bridge under the combined dead load and locked-in force effects) is achieved.

The goal of TDLF or SDLF detailing is to achieve approximately plumb girder webs under the total dead load or the steel dead load respectively. Once the girders are released from their locked

66 Guidelines for Analysis Methods and Construction Engineering of Curved and Skewed Steel Girder Bridges

positions in Configuration 2, the cross-frames tend to "spring back" or "elastically rebound." Since the cross-frames tend to be relatively stiff in their own planes compared to the resistance of the individual girders to lateral bending and twisting, the cross-frames tend to snap-back close to their original undeformed geometry. However, this cannot occur without the twisting of the girders, since compatibility must be maintained between the cross-frame connection points and the corresponding points on the girder connection plates. As a result, the girders are twisted into the position shown in Configuration 3.

When the dead load (i.e., the total dead load or the steel dead load) is applied conceptually to the bridge, starting in Configuration 3, the structure tends to bend and twist under the load such that the geometry shown in Configuration 4 is achieved. The sketch of Configuration 4 shown in Figure 3-30d implies TDLF detailing, since the bridge cross-slopes, etc., are not shown in the figure and the drawing indicates that both of the girders have deflected to the same final elevation. For TDLF detailing, the girder webs are approximately plumb in this condition under the total dead load.

If SDLF detailing is employed, the additional camber associated with the concrete dead load (plus any additional camber for dead load from appurtenances, etc.) still remains in the girders in Configuration 4. However, in this case, the girder webs are approximately plumb under the *steel* dead load.

It should be noted that the twisting induced into the girders in Configuration 3 is largely due to the differential camber between the girders in Configuration 1. Furthermore, the differential camber in Configuration 1 is due to the different vertical displacements that occur in the girders due to the bending and twisting of the structure under the applied loads. Therefore, the displacements that the cross-frames tend to "pull" into the girders in Configuration 3 are approximately equal and opposite to the displacements at these locations under the corresponding total or steel dead load.

3.2.5.2 Calculation of the Initial Strains, Initial Stresses or Initial Forces Associated with SDLF or TDLF Detailing of the Cross-Frames

The calculation of the initial strains generated in the cross-frames in Configuration 2 of Figure 3-30b simply involves the identification of the nodal positions of the girder connection work points in the desired "final" Configuration 4, as well as the corresponding nodal positions of the girder connection work points in Configuration 2. (Note that the Configuration 2 girder nodal positions are the same as the nodal positions in Configuration 1 since the girders are in their undisplaced no-load plumb-web geometry in both of these configurations.) The difference between the nodal positions in Configurations 2 and 4 gives the displacements that the cross-frame is subjected to in order to connect it with the girders in Configuration 2.

- **Calculation of the initial strains, initial stresses, or initial forces in 3D FEA software.** Figure 3-31 shows a spatial representation of Configurations 2 and 4 for a hypothetical location within a bridge span. It should be noted that, if the individual cross-frame members are represented explicitly by truss and/or beam elements, the calculated initial strain is simply the axial extension of the individual members associated with the above displacements. If beam elements are employed for the individual cross-frame members, it is generally sufficient to assume that these elements are "pinned" to the girder connection work points at their ends, such that only axial deformation is produced by the displacements from Configuration 4 to Configuration 2. The engineer may wish to insert rotational releases explicitly in the model at the end of the cross-frame members in many situations where they are modeled by beam elements. However, the bending rigidity of the individual cross-frame members is typically sufficiently small such that including or not including the rotational releases is not of any significance.

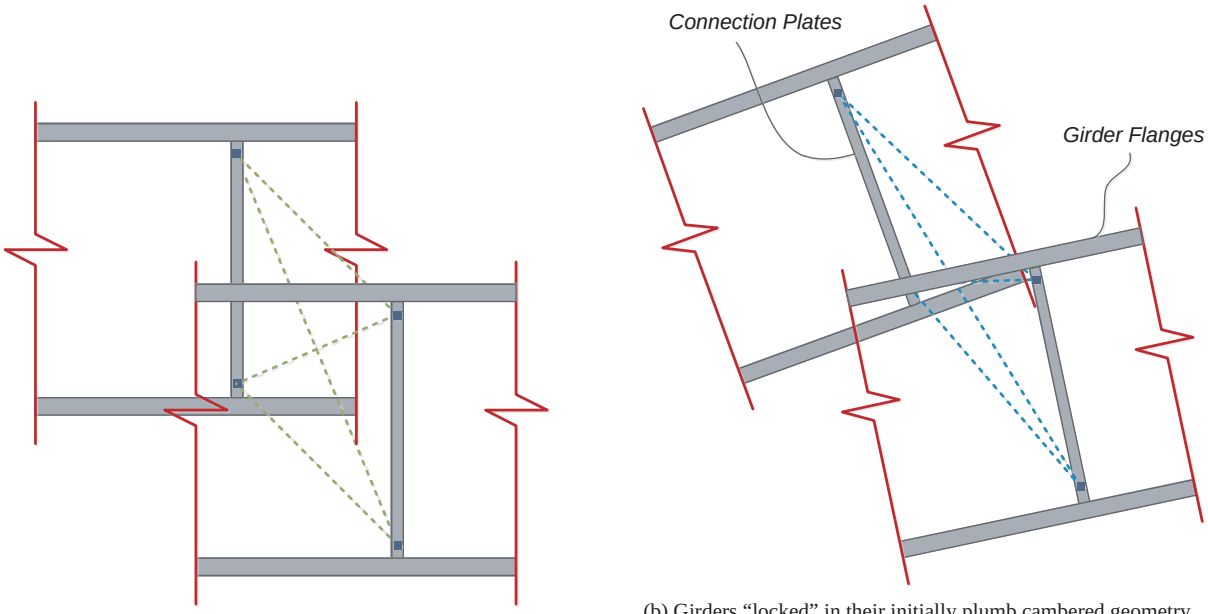

(a) Girders in the final geometry (Configuration 4)

(b) Girders "locked" in their initially plumb cambered geometry, cross-frames subjected to initial strains to connect to the girders (Configuration 2)

Figure 3-31. Configurations used for calculation of initial strains in cross-frame members due to initial lack of fit.

Once the cross-frame element initial (axial) strains are calculated, the corresponding initial stresses are determined simply by multiplying the strains by the elastic modulus of the material. The initial strains and initial stresses are simply a computational device to determine the locked-in force effects. Therefore, even if the initial stress is larger than the material yield strength, the material behavior should be assumed to be linear elastic. The initial cross-frame member forces are determined simply by multiplying the initial stress by the cross-frame area.

It should be noted that the implementation of the above calculations requires that the software, and the structural elements used in the software, must have either initial stress or initial strain capabilities. Any software that already is capable of modeling thermal loading has these capabilities.

Calculation of the initial strains and initial forces in cross-frame equivalent beam elements. If the cross-frames are represented by equivalent beam elements, the calculations are exactly the same as in the above discussion. However, the displacements at the two cross-frame end connection work points are resolved into element end displacements and end rotations. These element end displacements and rotations are then applied to the equivalent beam element. Assuming the use of a structural element for the equivalent beam, the best approach is to calculate the initial forces induced by the above displacements from Configuration 4 to Configuration 2. These forces are then handled as initial fixed-end forces in the equivalent beam element. This procedure requires that the beam element implementation must be able to handle initial fixed-end forces (e.g., fixed-end forces due to thermal loading, fixed-end forces due to internal element loads, etc.). If this is the case, the implementation of the "initial force" effects is relatively straightforward.

As noted above, elements that are able to handle thermal loading already include these effects. In addition, elements that incorporate the calculation of fixed-end forces from internal loading between the nodes already include this type of effect.

68 Guidelines for Analysis Methods and Construction Engineering of Curved and Skewed Steel Girder Bridges

3.2.5.3 Handling of Cross-Frame Initial Strains and Initial Stresses (or Initial Forces) at Skewed Bearing Line Cross-Frames

The computational handling of the initial lack-of-fit or locked-in force effects at bearing line cross-frames is essentially no different than described in the above section. However, the behavior is somewhat different since the girders cannot displace vertically at the bearings and because the skewed cross-frames impose a twist into the girders associated with the girder major-axis bending rotation at the bearings. Figure 3-32 illustrates the rotations, due to applied loads within the bridge span, at the end of a girder connected to a skewed bearing line cross-frame. A fixed bearing is assumed at this position to simplify the discussion.

The girder web and the bearing line cross-frame are assumed to be plumb in the current configuration shown in the figure. The double arrow perpendicular to the girder web represents the major-axis bending rotation of the girder, ϕ_x, about the fixed point. This rotation induces the longitudinal displacement Δ_z at the top flange of the girder. However, since the girder is attached to the skewed bearing line cross-frame, the top flange can only displace significantly in the direction normal to the plane of the cross-frame. This is indicated by the arrow labeled Δ. The cross-frame deflects essentially only by rotating about its longitudinal axis through the fixed point. This is shown by the double-arrow vector ϕ. In order to maintain compatibility between the girder and the cross-frame, the top flange of the girder must deflect by the vector component labeled Δ_x in the figure. Therefore, the girder web lays over by the deflection Δ_x relative to the fixed point. This deflection, divided by the height *h*, gives the girder twist rotation ϕ_z.

Figure 3-33 shows an alternate plan view of the behavior illustrated in Figure 3-32, except that the rotations are in the opposite direction to the rotations associated with the structure's dead loads. If one considers the "deflections" of the girders due to the camber, the typical upward displacement in the spans induces a major-axis bending rotation at the bearing line shown by the double arrows normal to the girders in Figure 3-33 (using the right-hand rule). That is, if the bearing stiffener/connection plate at the bearing is placed normal to the flanges, this stiffener is rotated to a non-vertical position in the initial cambered, no-load, plumb geometry of the girder. This is comparable to Configuration 1 in Figure 3-30a. In order to fit-up with the girders in Configuration 2, the bearing line cross-frames have to be rotated about their

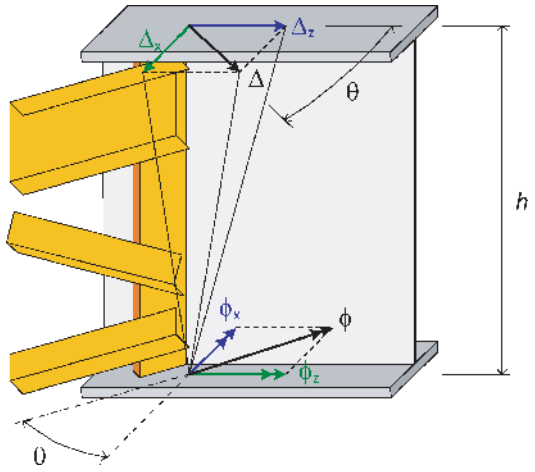

Figure 3-32. Illustration of the girder major-axis bending and twist rotations required for compatibility at a skewed bearing line cross-frame.

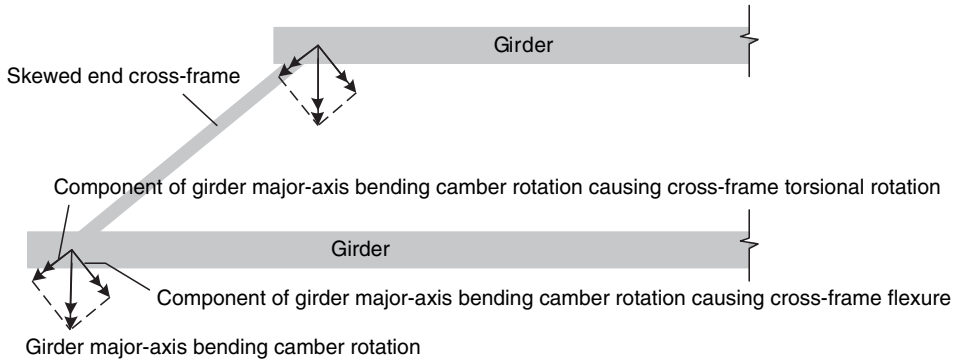

Figure 3-33. Flexural and torsional rotation components at the ends of a skewed end cross-frame due to the girder major-axis bending camber rotations.

longitudinal axis, and then (because of the skewed geometry), strained into position to connect them with the rotated connection plates in the initial cambered no-load, plumb geometry of the girders (i.e., assuming no drops between the girders at the bearing line, the bearing line cross-frames have to be deformed from their rectangular geometry in Configuration 1 into a parallelogram geometry in Configuration 2, assuming equal ϕ at both ends of the cross-frame). When the girders are then "unlocked" and "released," the cross-frames elastically rebound approximately to their initial rectangular geometry and force a twist into the girders opposite to the direction that they twist under the dead loads. This corresponds to Configuration 3 in Figure 3-30c. However, the girders only lay over at the bearing lines. They cannot displace vertically.

It should be noted that skewed intermediate cross-frames involve a combination of the two effects shown in the above for the intermediate cross-frames in Figure 3-30 and for the skewed bearing line cross-frames in Figures 3-32 and 3-33. That is, at skewed intermediate cross-frames, the girders are subjected to twisting due to the differential vertical displacements between the cross-frame connection points on the girders as well as the compatibility of the rotations between the girders and the skewed cross-frames at the connection points.

3.2.6 Simplified Analysis Improvements for Tub-Girder Bridges

Significant improvements also were developed for the simplified analysis of curved and skewed tub-girder bridges in the NCHRP Project 12-79 Task 8B research. These improvements are of a somewhat different nature though, since tub-girder bridges are fundamentally different from I-girder bridges. The key improvements for tub girders were:

1. The development of an improved method for estimating the influence of skew on tub-girder internal torques using basic 1D analysis procedures,
2. The investigation of the influence of skew (and torsion due to skew) on the cross-section distortion of box-girders, and
3. The calculation of local effects from the longitudinal components of the axial forces in the diagonals of the top flange lateral bracing (TFLB) system, which result in "saw-tooth" type local spikes in the longitudinal normal stresses in tub-girder top flanges.

These improvements are described briefly in the following subsections. The NCHRP Project 12-79 Task 8 report (Appendix C of the contractors' final report) and Jimenez Chong (2012) provide more detailed discussions of these improvements.

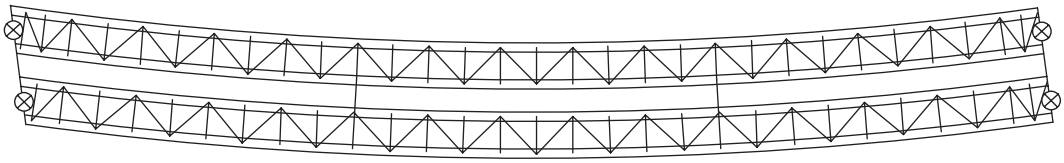

Figure 3-34. Plan view of Bridge NTSCS29.

3.2.6.1 Improved Estimation of Tub-Girder Internal Torques in 1D Line-Girder Analysis Methods

Figure 3-34 shows a plan view of Bridge NTSCS29 analyzed in the NCHRP Project 12-79 Task 7 studies. This is a 225-ft. span simply supported curved and skewed tub-girder bridge with a horizontal radius of curvature of 820 ft., a deck width of 30 ft., and a skew angle of 15.7° at the left-hand abutment. The bearing line at the right-hand abutment is radial. The girders are each supported on single bearings at their ends, and the structure is built with two intermediate external cross-frames. The top flange lateral bracing (TFLB) system in this bridge is a Warren-type truss system.

Figure 3-35 compares the internal torques calculated with two different line-girder analyses of this bridge (including the use of the M/R method for estimating the effects of the horizontal curvature), to two different 3D FEA benchmark simulations. The lighter dotted curve in the figure shows the results for the internal torque calculated solely by using the conventional M/R method without any accounting for the skew effects at the left-hand end. The bold dotted curve shows the combination of this conventional calculation with a separate additional estimate of the internal torque due to the left-hand end skew. The two 3D FEA solutions for the internal torque shown in the plot are:

1. A 3D FEA solution of the bridge as shown in Figure 3-34, indicated by the dark solid line, and
2. A 3D FEA solution of the bridge constructed without any intermediate external cross-frames, indicated by the light dashed line.

One can observe that the M/R solution, combined with the improved method of estimating the internal torque, gives a close representation of the response of the bridge if it did not have any intermediate external cross-frames tying the girders together along the span length. Furthermore, the left-most intermediate external cross-frame appears to cause a shift in the internal torque on

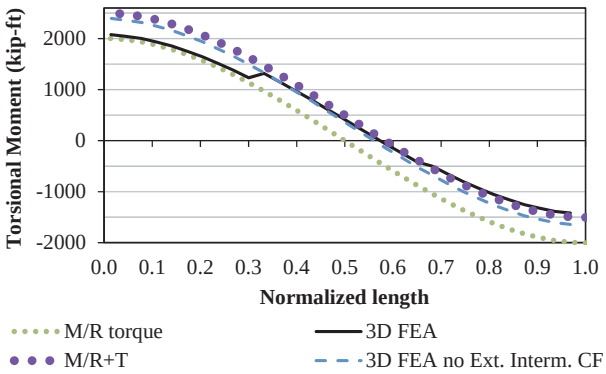

Figure 3-35. Comparison of total dead load torsional moments (unfactored) in the girder on the outside of the horizontal curve of Bridge NTSCS29 predicted by 1D analysis assuming rigid end diaphragms versus 3D FEA.

one side, given by just the M/R method solution, and on the other side, given by the combination of the M/R method with the improved method of estimating the internal torque due to skew. The right-most external cross-frame does not appear to have any significant influence on the internal torque.

The improved method of estimating the internal torque due to skew involves the relatively simple idealization that the bearing line diaphragms (or cross-frames) are rigid in their own plane with respect to torsional stiffness of the tub girders. Although tub girders generally have substantially larger torsional stiffness than I-girders, the bearing line diaphragms or cross-frames are relatively short in length. Therefore, particularly in relatively narrow tub-girder bridges, these components may be approximated reasonably well as acting rigidly in their own plane. As a result, once the major-axis bending rotations are estimated for the tub girders at a bearing line, the same type of rotational compatibility rules as discussed in Section 3.2.5.3 apply.

The NCHRP Project 12-79 research has not addressed analysis of the effect of external intermediate cross-frames or diaphragms via a 1D analysis in the context of the above procedures. A number of the conceptual idealizations used in the development of the V-load method for I-girder bridges may be helpful for the development of such procedures. However, the tedious nature of the adjustments to the 1D solutions may outweigh the benefits of these procedures, given that the use of 2D-grid methods should be quite feasible in current practice (2012).

3.2.6.2 Investigation of the Influence of Skew (and Torsion Due to Skew) on the Cross-Section Distortion of Box-Girders

AASHTO LRFD Article 6.7.4.3 generally requires the use of intermediate internal diaphragms or cross-frames in steel box girders to control cross-section distortion due to torsional loads. Cross-section distortion of box girders is caused by external torsional loads that are not distributed in proportion to the St. Venant shear flow. It is well known that the distortional behavior of a box girder is dependent on the manner in which the external torque is applied to the member. Fan and Helwig (2002) have developed equations for estimating the distortional bracing forces developed in internal diaphragm and cross-frame components by horizontal curvature effects and by eccentric vertical applied loads. However, to the knowledge of the NCHRP Project 12-79 research team, no prior studies have been conducted to understand and to estimate the influence of distortion due to skew.

Evaluations of the tub-girder bridges studied in NCHRP Project 12-79 Tasks 7, 8, and 9 research have indicated that the tub-girder internal cross-frame forces tend to be negligible in straight-skewed tub-girder bridges and that these forces tend to be predicted conservatively by the Fan and Helwig (2002) equations in curved tub-girder bridges. It appears that the development of internal torsional moments in tub girders, due to support skew, is similar to the shear flow associated with St. Venant uniform torsion. This is largely because the support diaphragms restrain the distortion of the girder cross-sections at the skewed supports. As such, the discrete torque induced in the girders at the skewed supports is predominantly a St. Venant torque.

Figure 3-36 shows two basic geometries that can be used to gain some further understanding of this problem: (1) a straight simply supported box girder with a square cross-section and 30° skew at its right-hand end, and (2) a horizontally curved, simply supported box girder having the same cross-section. The span length of these girders is L_s = 150 ft., and the girders are subjected to vertical loads representative of the weight from the placement of a concrete deck. The square box depth is set to $D = L_s/25 = 72$ in. and the web thickness is set to $t_w = 0.5$ in. The top and bottom flange thickness is also set to $t_f = 0.5$ in. for simplicity. The radius of curvature of the second girder is taken as $R = 400$ ft. Solid plate diaphragms with $t = 1$ in. are used at the ends of the boxes, but no intermediate internal diaphragms or cross-frames are employed along the spans. Both box girders are supported continuously across their bottom flange at the supports.

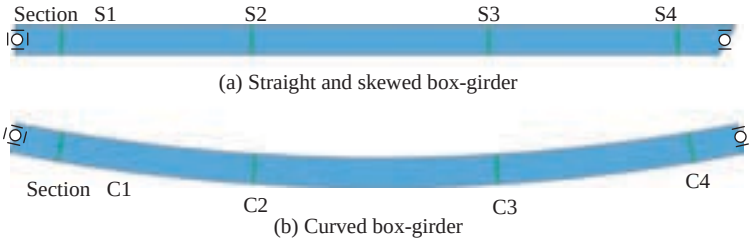

Figure 3-36. Straight skewed and curved box girders used for study of distortion effects.

In Figures 3-37 and 3-38, the cross-section warping deformation is illustrated via a side view and the cross-section distortion is illustrated via a cross-section view from the 3D FEA at the four cross-sections labeled in Figure 3-36. Although the torsion is also smaller in the first case, the warping deformations, as well as the cross-sectional distortion deformations, are also small relative to the torsional deformations. Conversely, in the second case, the distortion of the box is quite evident. This is predominantly due to effective radial forces due to the horizontal curvature coming from the flanges.

3.2.6.3 Calculation of "Saw-Tooth" Longitudinal Normal Stresses in the Top Flanges of Tub Girders

Figure 3-39 shows a simplified free-body diagram illustrating the forces Q and P delivered to one of the top flanges of a tub girder at the connection of the top flange lateral bracing (TFLB)

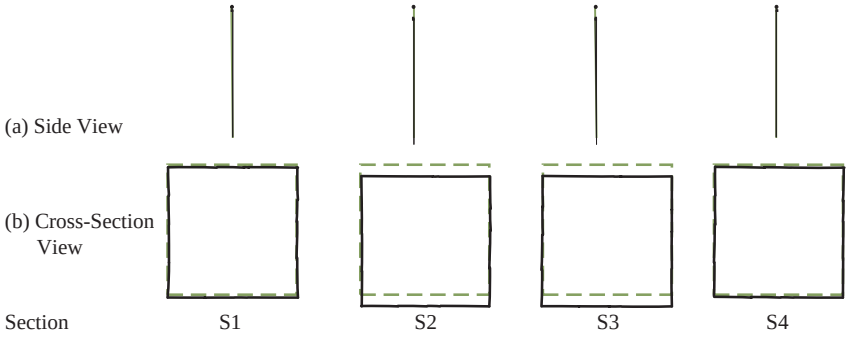

Figure 3-37. Deformed cross-sections in the straight skewed box girder.

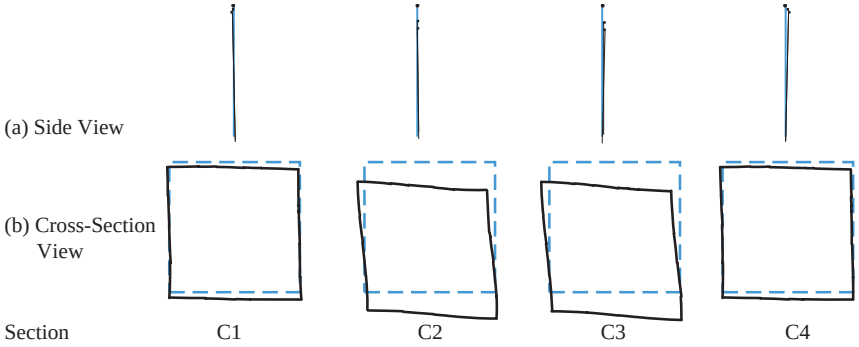

Figure 3-38. Deformed cross-sections in the curved box girder.

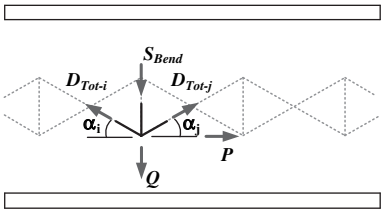

$$P = D_{Tot-i}\cos\alpha_i - D_{Tot-j}\cos\alpha_j$$

$$Q = D_{Tot-i}\sin\alpha_i + D_{Tot-j}\sin\alpha_j - S_{Bend}$$

Figure 3-39. Interaction of forces between top flange lateral bracing and girder top flange for Warren and X-type layouts.

system to the girder. For cases where the tub girder is resisting significant torsion, the diagonal forces often are dominated by the torsion and the forces in the diagonals alternate from tension to compression in the consecutive panels. In these cases, the effects of the tension and compression forces due to the torsion are additive in their contribution to *P*. Therefore, the tub-girder flanges are acted upon by a longitudinal concentrated load at the intersection of the diagonals with the flanges.

Although the predominant flange stress is the major-axis bending stress, which is commonly estimated as $f_b = M/S_{x.top}$, where M is the major-axis bending moment at the cross-section under consideration and $S_{x.top}$ is the elastic section modulus to the top flange, neglecting the contribution of the TFLB system, the above axial load P has an important local effect on the flange stresses. Interestingly, the resulting top flange average normal stress tends to follow a saw-tooth pattern in which the saw-tooth "jump" in stress is essentially $P/b_f t_f$. The saw-tooth effect appears as a $+ P/2b_f t_f$ fluctuation about the "mean" value $f_b = M/S_{x.top}$ (see Figure 3-40). The researchers obtained the best accuracy of the simplified calculations relative to 3D FEA benchmark results when this saw-tooth effect is added to the stress f_b with $S_{x.top}$ determined as explained above.

Figures 3-42 and 3-44 show example results comparing the top flange longitudinal normal stresses (labeled generally as f_b) from 3D FEA simulation models to the "conventional" calculation of the top flange major-axis bending stress as $f_b = M/S_{x.top}$ from a 2D-grid model (neglecting the contribution of the TFLB system in determining $S_{x.top}$). These results correspond to the two simple-span tub-girder bridges shown in Figures 3-41 and 3-43. The first bridge (NTSSS2) is a straight-skewed 150-ft. span tub-girder bridge with 30° parallel skew, a 30-ft. wide deck, and

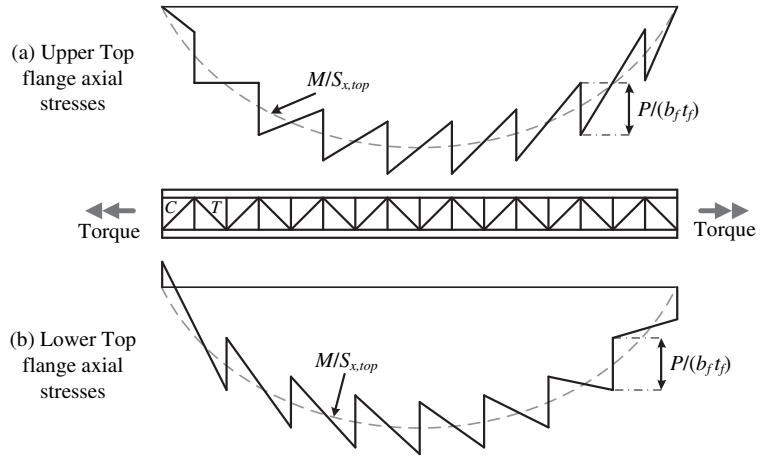

Figure 3-40. Top flange saw-tooth major-axis bending stresses due to interaction with the flange level lateral bracing system.

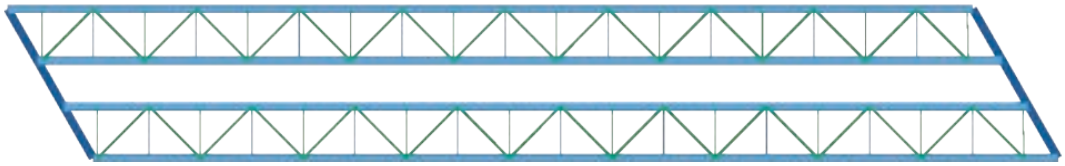

Figure 3-41. Plan view of Bridge NTSSS2.

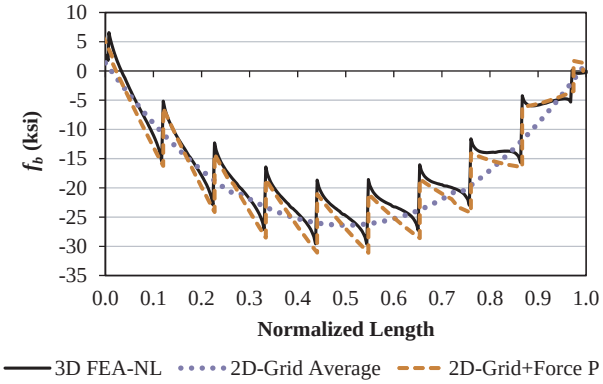

Figure 3-42. Bridge NTSSS2 exterior top flange normal stresses on Girder G1.

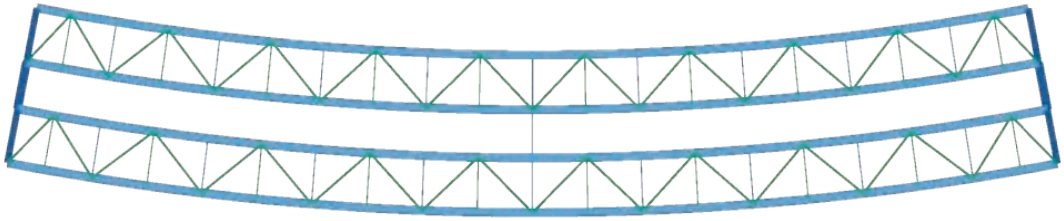

Figure 3-43. Plan view of Bridge NTSCR1.

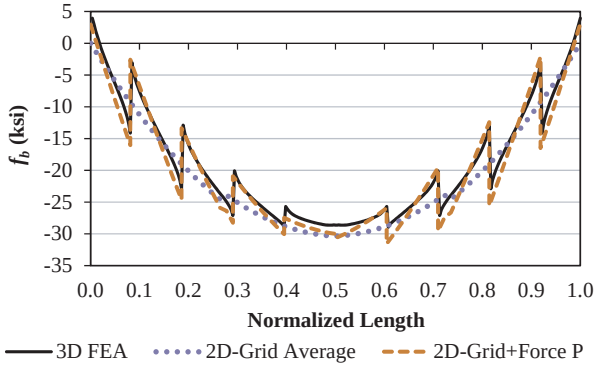

Figure 3-44. Bridge NTSCR1 exterior top flange normal stresses on Girder G1.

no intermediate external diaphragms within its span. The second case (NTSCR1) is a curved 150-ft. span, radially supported structure with a 30-ft. wide deck, and a horizontal radius of curvature $R = 400$ ft.

The 2D-grid estimates of the top flange major-axis bending stresses are excellent in both of these examples. Correspondingly, this result is reflected in the mode grade of A for the calculation of the major-axis bending stresses in straight-skewed and curved radially supported tub-girder bridges in Table 3-2 of Section 3.1.5.

Interestingly, the internal torque is constant (and solely due to the skew) in the straight-skewed bridge. Conversely, the internal torque is maximum at the supports and zero at the mid-span in the horizontally curved structure. These variations in the internal torque are reflected clearly in the saw-tooth patterns shown in Figures 3-42 and 3-44. The "jump" associated with the saw-tooth is constant throughout the length of the bridge in Figure 3-42, while this jump is maximum toward the ends of the bridge and relatively small near the mid-span in Figure 3-44. In cases such as the one in Figure 3-44, the saw-tooth stresses result in a significant local increase in stress above the conventionally calculated f_b in the region of maximum moment. This effect can also occur in the negative moment region of continuous-span bridges.

3.3 Influence of Locked-In Forces Due to SDLF or TDLF Detailing of Cross-Frames

This section provides a summary of the findings of the NCHRP Project 12-79 Task 8B research pertaining to the influence of steel dead load fit (SDLF) and total dead load fit (TDLF) detailing of the cross-frames in curved and/or skewed I-girder bridges. Two examples are extracted from the large suite of structures considered in the Task 7 studies for this purpose. The first example is a simple-span straight bridge with a substantial parallel skew; the second example is a horizontally curved, radially supported structure. The results presented show the impact of the above detailing methods on a relatively complete set of important responses including:

- Bridge displacements (i.e., the constructed geometry),
- Cross-frame forces, and
- Girder flange lateral bending stresses.

This is followed by a broader discussion of key considerations, including the questions:

- When is it important or essential to consider locked-in force effects due to SDLF or TDLF detailing in the design?
- When can SDLF or TDLF initial lack-of-fit effects be considered as incidental?
- To what extent can standard connection tolerances relieve the locked-in internal forces induced by SDLF or TDLF detailing?

Appendix C of the contractors' final report provides a more detailed summary of results for the wide range of bridges studied in the NCHRP Project 12-79 research. Appendix A provides summary definitions of key terms. It is essential that the reader understand these definitions to facilitate study and interpretation of corresponding results and discussions throughout this report.

3.3.1 Straight-Skewed Bridge Example

Figure 3-45 shows the framing plan for a 300-ft. straight simple-span I-girder bridge with a 70° parallel skew of its bearing lines. The bridge has an 80-ft.-wide deck (i.e., $w = 80$ ft.) and 74-ft. spacing between its fascia girders. This geometry produces a skew index of $I_S = 0.68$, which places

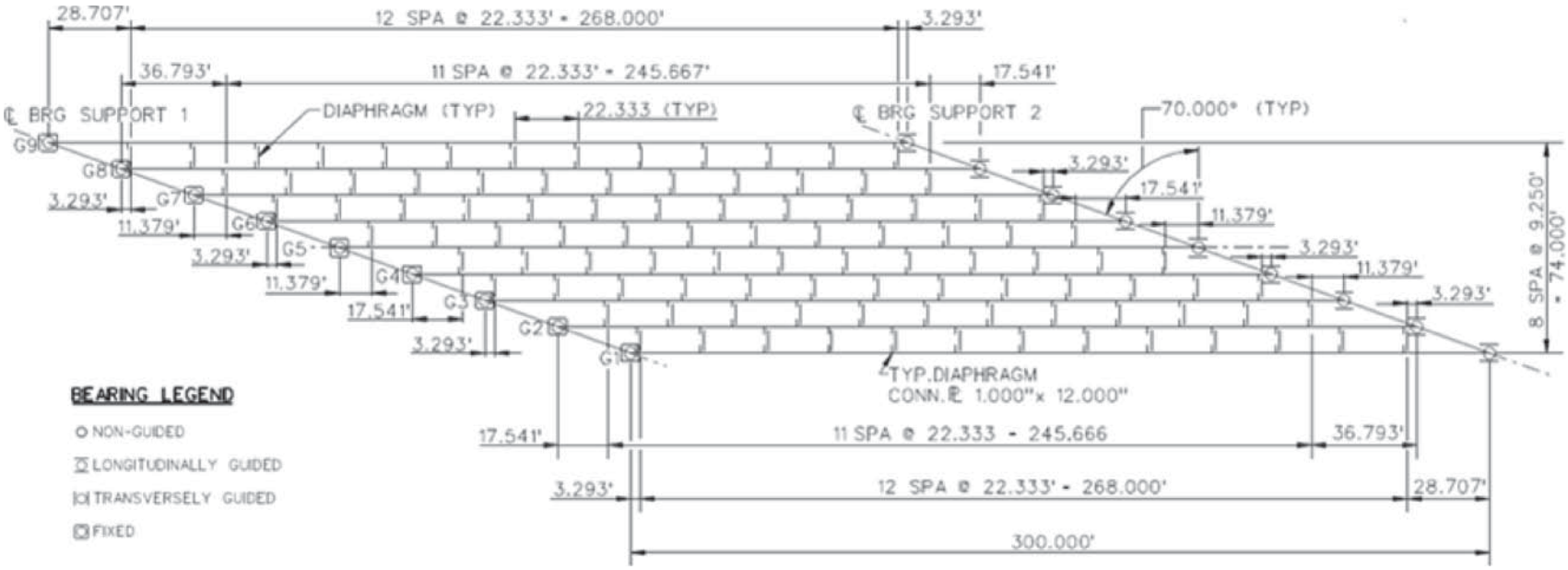

Figure 3-45. NISSS54 framing plan.

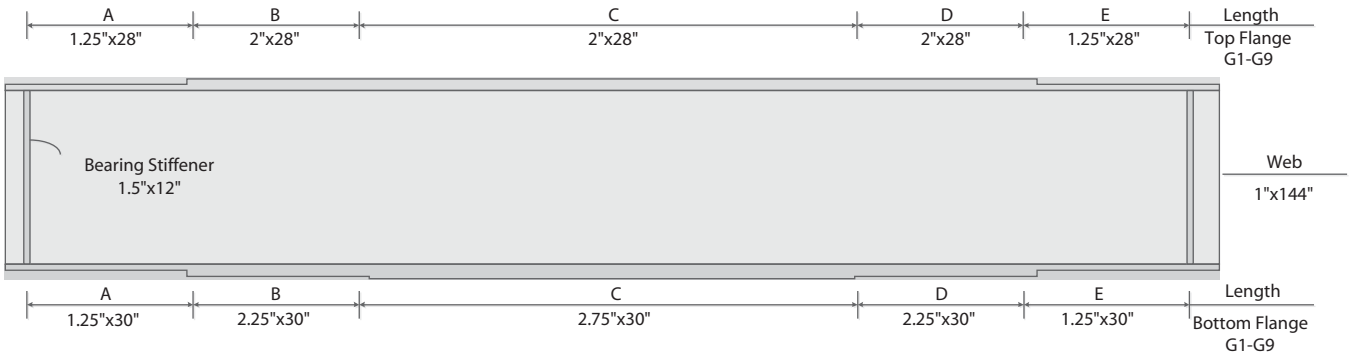

Figure 3-46. NISSS54 girder plate dimensions.

this structure in the third and most difficult "S" category of Table 3-1. Figure 3-46 and Table 3-7 give the girder dimensions, and Table 3-8 gives the cross-frame member sizes. The bridge uses staggered cross-frames to alleviate "nuisance" transverse stiffness effects due to the large skew.

3.3.1.1 Bridge Deflections

It is useful to first consider how this example bridge deflects under its total construction dead load. This can be accomplished by conducting a 3D FEA of the structure assuming no-load fit (NLF) of the cross-frames. Figure 3-47 shows a plan view of the magnified deflected geometry. One can observe that the girders are subjected to substantial layover (i.e., twist rotations) at the bearing lines. This is due to the compatibility between the girders and the heavily skewed bearing line cross-frames, as discussed previously in Section 3.2.5.3. The bearing line cross-frame deflections involve predominantly a rotation about the skewed bearing line, highlighted by the double arrows in the figure (right-hand rule). The large 70° skew induces girder end twists (denoted by ϕ_z in the previous Figure 3-32) approximately equal to $\phi_x \tan(70°) = 2.75\ \phi_x$, where ϕ_x is the girder end major-axis bending rotation. Twists of a similar but different magnitude are induced by the intermediate cross-frames due to the fact that they frame into the girders at different positions along the girder spans. The overall twisting of the girders is a rather complicated pattern, involving twist rotations in opposite directions at the girder ends.

3.3.1.2 Girder Cambers and Camber Differences

Based on the prior discussions in Section 3.2.5.1, it should be clear that the SDLF and TDLF detailing effects are driven largely by the girder camber profiles, or more specifically, by the differences between the camber profiles at each of the cross-frame positions. Figures 3-48 and 3-49 show two different camber profiles for this bridge, the first one based on a 1D line-girder analysis and the second based on a 3D FEA assuming NLF. Figure 3-50 shows the differential values for the 3D FEA girder cambers.

Table 3-7. NISSS54 girder plate lengths (ft.).

Girder	A	B	C	D	E
G1-G9	45	45	45	45	45

Table 3-8. NISSS54, cross-frame member sizes.

Cross-Frame Type	Top Chord	Diagonals	Bottom Chord
Interior (X type)	L6x6x1	L6x6x1	L6x6x1
End (Inverted V)	WT6x53	WT6x60	WT9x38

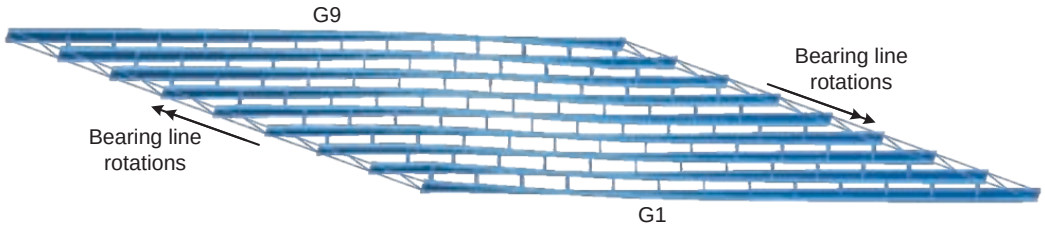

Figure 3-47. Bridge NISSS54 total dead load deflected geometry for the case of NLF detailing of the cross-frames (scale factor = 10x).

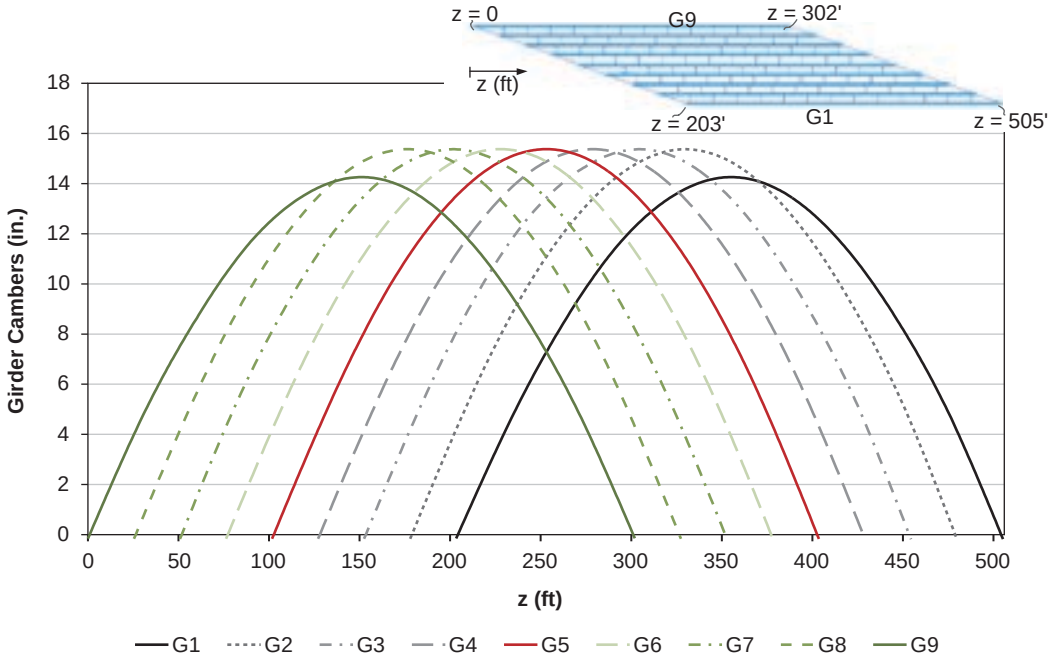

Figure 3-48. Bridge NISSS54 total dead load camber profiles from line-girder analysis.

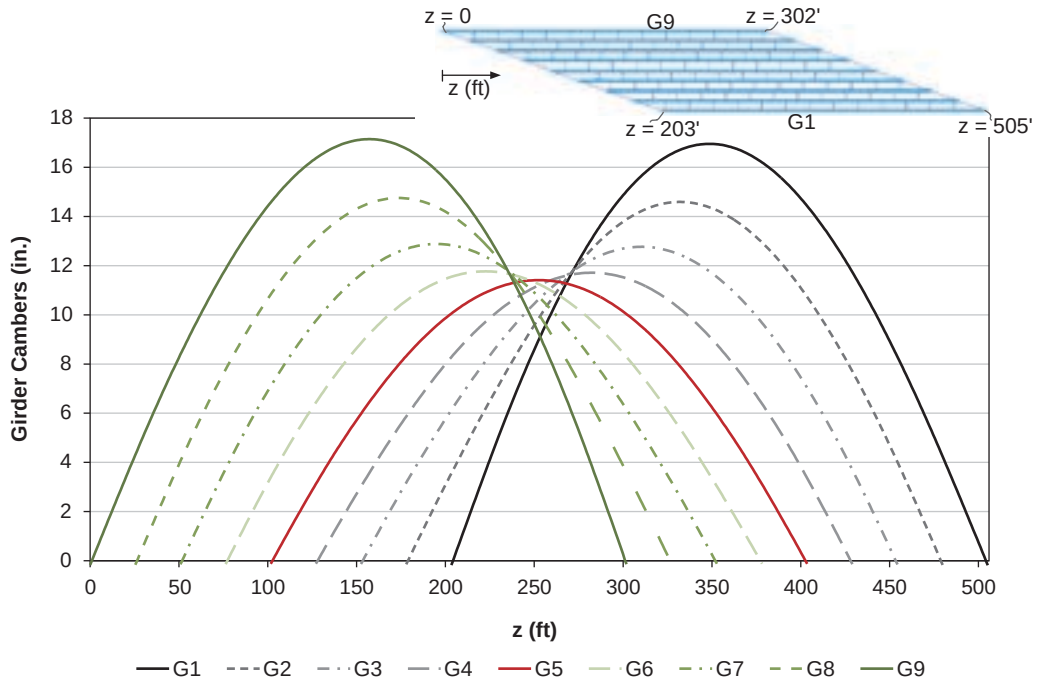

Figure 3-49. Bridge NISSS54 total dead load camber profiles from 3D FEA.

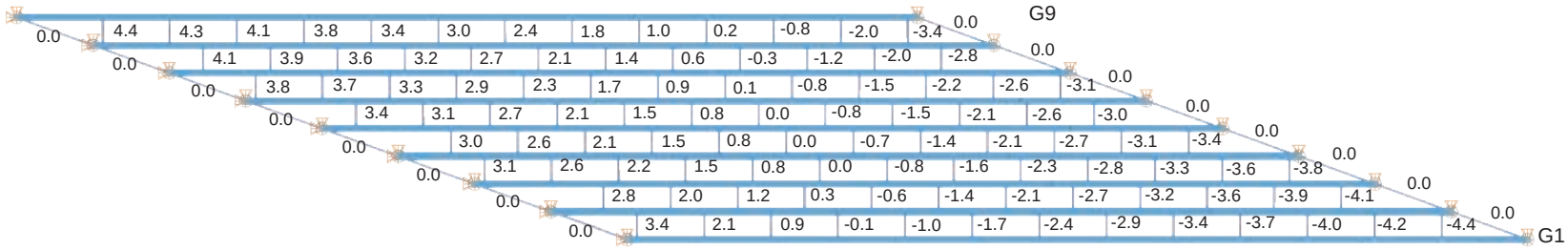

Figure 3-50. Bridge NISSS54 total dead load camber differences (differential camber values) between girders, taken from the camber profiles based on the 3D FEA vertical deflections.

Each of the curves in Figures 3-48 and 3-49 is the total dead load camber profile for a single girder. Only the total dead load cambers are shown to keep the discussion focused and brief. The focus of the subsequent discussions is on the TDLF detailing of the cross-frames and its effects. For TDLF detailing, the cross-frames are fabricated to fit to the girder connection work points in the conceptual geometry where the girder webs are still plumb but the total dead load cambers have been removed from the girders. The TDLF detailing induces twists in the girders in the opposite directions from those shown in Figure 3-47.

The horizontal axis in Figures 3-48 and 3-49 is the longitudinal coordinate "z" along the length of the bridge. The origin for the z coordinate is located at the bearing on Girder G9 at the left-hand acute corner of the structure. Therefore, the left-most curve in the plots is the camber profile for Girder G9. Correspondingly, the right-most curve, ending at $z = 505$ ft., is the camber profile for Girder G1.

One can observe that the 3D FEA camber profiles are substantially smaller for the girders near the center of the bridge width. This is due to the substantial transverse load path between the obtuse corners of the bridge, developed via the cross-frames (even though the cross-frames are staggered throughout the length of the bridge to reduce these effects). The differential cambers shown in Figure 3-50 are based on the girder cambers determined from the 3D FEA vertical deflections. The implications of using the line-girder analysis total dead load vertical displacements versus the 3D FEA vertical displacements for setting the total dead load cambers are discussed subsequently.

3.3.1.3 System Deflections Due to Initial Lack-of-Fit Effects

Figure 3-51 shows the deflections of the NISSS54 Bridge after, first, the cross-frames conceptually are connected to the girders (Configuration 2 of the previous Figure 3-30b), then the girders are "unlocked" and "released" from their initial no-load plumb geometry such that they are deformed by the cross-frames into the Configuration 3 shown in Figure 3-30c. That is, Figure 3-51 shows the "final" deformed geometry due to the cross-frame locked-in force effects (from the TDLF detailing of the cross-frames) if, by some means, the bridge dead load were not yet applied to the structure. One can observe that the bridge deformations in Figure 3-51 are approximately the opposite of the deflections shown previously in Figure 3-47.

Figure 3-52 shows the layover of the girders corresponding to the deflections in Figure 3-51, where the term "layover" is defined as the lateral deflection of the girder's top flange relative to its bottom flange. The plot in Figure 3-52 is similar to the previous plots of the girder cambers in that (1) the horizontal axis is the horizontal z coordinate in the bridge plan view, measured from the bearing at the left-hand acute corner; and (2) each curve gives the layover of a different girder at the various positions along the length.

Upon studying Figure 3-52 carefully, one can observe that the "curvature" of the fascia girder layover curves (i.e., the darkest solid curves in Figure 3-52) is largest near the acute corners

Figure 3-51. Bridge NISSS54 "Configuration 3" deflected geometry under no-load due solely to the initial lack of fit associated with the TDLF detailing of the cross-frames (camber profiles based on 3D FEA vertical deflections).

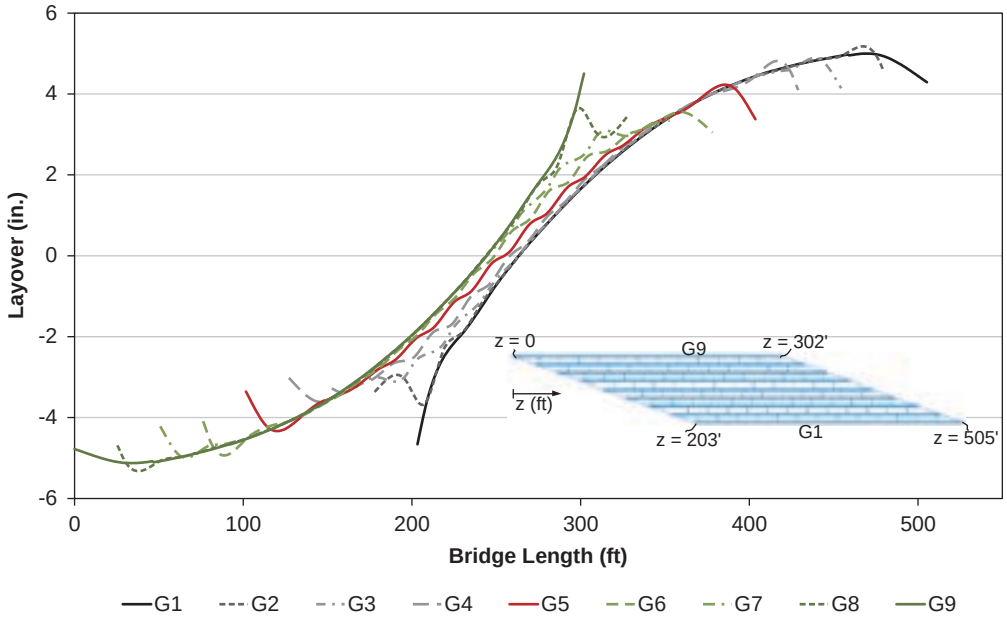

Figure 3-52. Bridge NISSS54 girder "Configuration 3" layovers due to the initial lack of fit associated with the TDLF detailing of the cross-frames.

of the span. This indicates that the TDLF detailing results in substantial "locked-in" flange lateral bending of the fascia girders at the acute corners. In addition, one can observe that the curvature of the layover curves for the interior girders is even more dramatic in the vicinity of the skewed bearing lines at each end of the bridge. Furthermore, if one looks carefully at the curves in the middle of the plot, it can be seen that the inner-most girders are subject to noticeable "back-and-forth" twisting actions. This is due to the use of the staggered cross-frames throughout the bridge, causing the load transfer between the obtuse corners to pass from cross-frame to cross-frame by twisting and flange lateral bending of the girders.

3.3.1.4 Approximate Canceling of Dead Load Layovers by Dead-Load Fit Effects

Figure 3-53 shows the girder layovers in Bridge NISSS54 due solely to the total dead load. That is, these are the layovers associated with the deflected geometry illustrated previously in Figure 3-47. One should note that the girder values in Figure 3-53 are approximately equal and opposite the corresponding girder values in Figure 3-52. However, it should be emphasized that the values in these two plots are not *exactly* equal and opposite to one another.

If one considers the application of the *steel* dead load to the bridge, resulting in the deflections of the girders from Configuration 3 to an intermediate configuration between 3 and 4 shown in the previous Figure 3-30c and d, the resulting girder layovers are the ones plotted in Figure 3-54. As one would expect (once the typical effect of TDLF on the girder layovers is understood), the girder webs are not plumb under the steel dead load. This is because TDLF detailing gives approximately plumb webs under the total dead load, but the total dead load has not been applied at the time of this graph.

Next, if the concrete dead weight is added to the structure (assumed to be applied non-compositely to the bridge for simplicity of the example), the girders finally reach the conceptual Configuration 4 shown previously in Figure 3-30d. The resulting girder layovers corresponding to this configuration are obtained by summing the results from Figures 3-52 and 3-53 and are

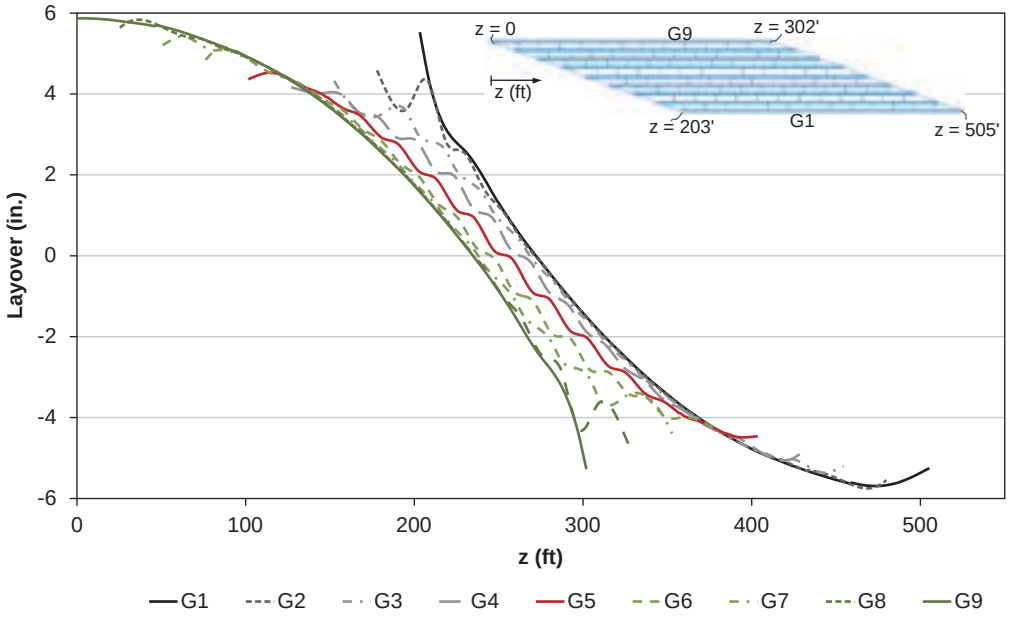

Figure 3-53. Bridge NISSS54 girder layovers solely due to the total dead load.

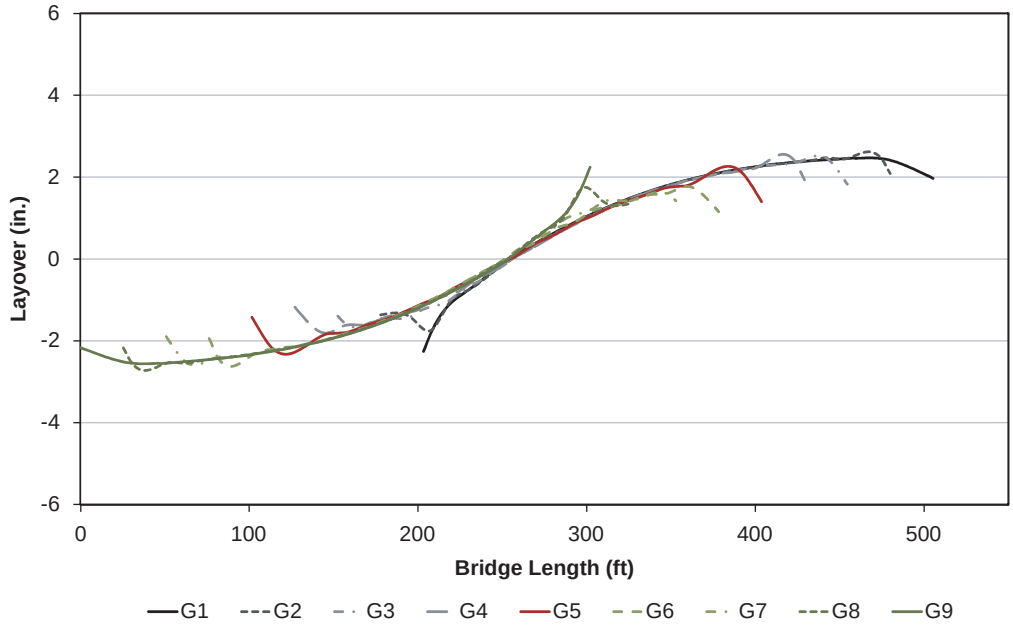

Figure 3-54. Bridge NISSS54 girder layovers under steel dead load (due to the effects of TDLF detailing of the cross-frames plus the steel dead load effects) for the case where the cross-frames are detailed for TDLF.

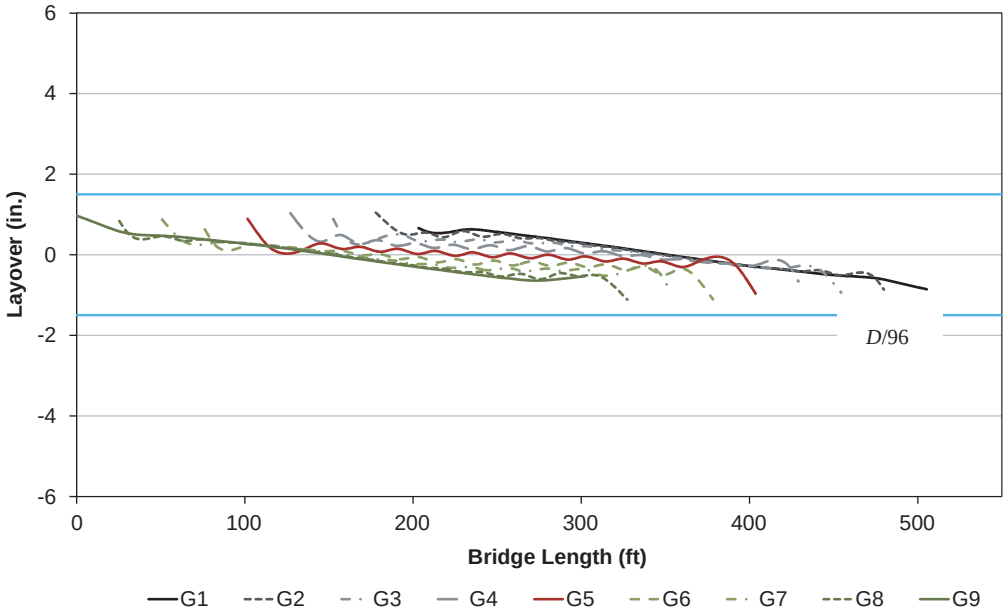

Figure 3-55. Bridge NISSS54 girder "Configuration 4" layovers under total dead load (due to the combined effects of TDLF detailing of the cross-frames and the total dead load effects) for the case where the cross-frames are detailed for TDLF.

shown in Figure 3-55. Many engineers would expect that the girder webs would be perfectly plumb in "Configuration 4" under the total dead load, since TDLF detailing was employed and the same analysis solutions were used consistently throughout the above developments. They would also expect that the girder flange lateral bending stresses would be perfectly zero in this "Configuration 4." However, neither of these assumptions is correct. One can observe from Figure 3-55 that there is still a measurable amount of girder twisting (and corresponding flange lateral bending), particularly in the inner-most girders. Nevertheless, the layover of the webs is within the tolerance of $D/96 = 144$ in./96 = 1.5 in. Therefore, the webs may be considered as "approximately plumb."

The reason why the layovers are not zero in Figure 3-55, as well as why the corresponding girder flange lateral bending stresses discussed subsequently are not zero, is because of the following facts:

- The girders are twisted in the direction opposite to the total dead load displacements (in Figure 3-52) by concentrated lateral loads applied from the cross-frames.
- However, the torsional displacements of the girders under the total dead load, shown in Figure 3-53, are due to the distributed self-weight of the steel as well as the distributed concrete dead load.
- The concentrated lateral loads from the cross-frames, which induce the girder deflections due to the TDLF detailing, cannot possibly produce girder layovers exactly equal and opposite to the effects of the distributed dead loads acting on the girders.

3.3.1.5 Final Girder Vertical Deflections and Vertical Elevations

Figure 3-56 shows the vertical deflections versus the normalized length along the fascia Girder G1 as well as the inner-most Girder G5 for the extreme example skewed I-girder bridge (NISSS54). (The girder normalized length coordinates vary from zero at the bearing at the left end of the bridge to 1.0 at the bearing on right end of the bridge.)

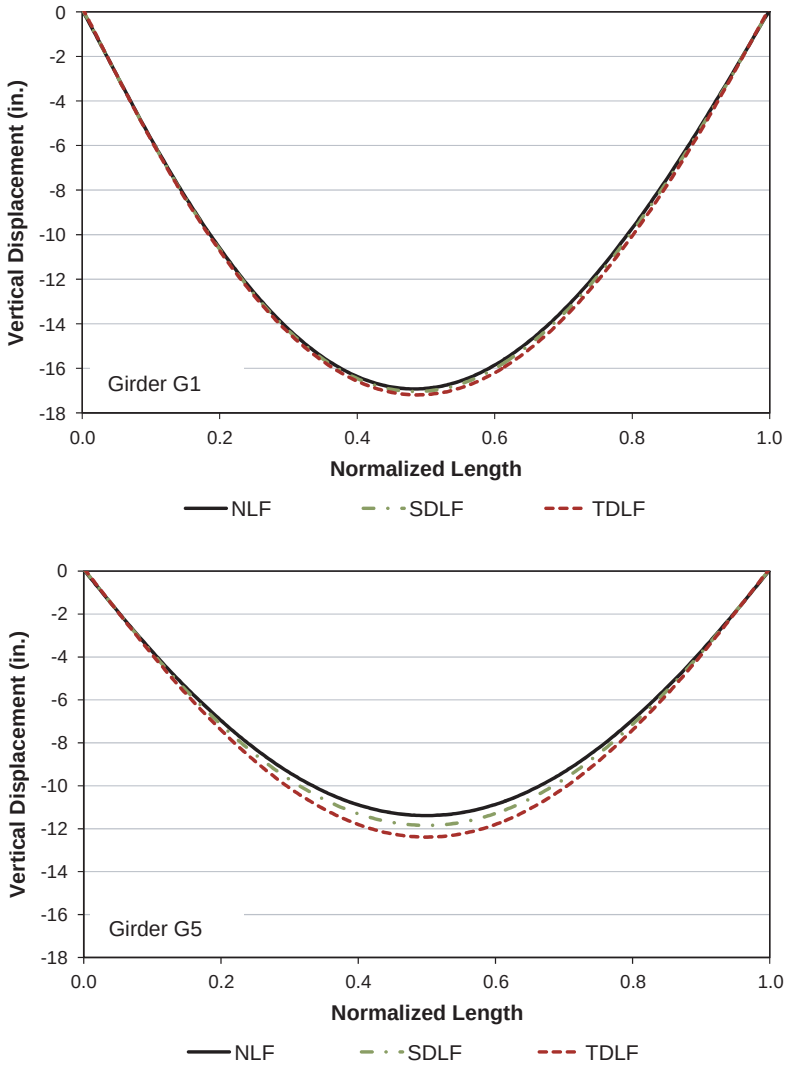

Figure 3-56. Bridge NISSS54 "Configuration 4" vertical deflections under total dead load for different cross-frame detailing methods.

The results for the final (or total) dead load vertical displacements in these plots are shown considering each of the three main cross-frame detailing methods: NLF, SDLF, and TDLF. It can be observed that the mid-span displacements in Girder G5 are slightly smaller at the mid-span when NLF detailing is used. However, the vertical displacements are relatively insensitive to the type of cross-frame detailing. This is generally the case for all straight bridges. The vertical displacements of the fascia girders are essentially the same for all of the detailing methods.

The above displacements can be added to the 3D FEA camber profiles of Figure 3-49 to obtain the final total dead load elevations of the girders. One can observe that the fascia girders are essentially at a "zero" elevation along their full length, whereas the interior Girder G5 has a final "flat" geometry for NLF detailing and is slightly less than 1 in. below the "zero" elevation for TDLF detailing.

3.3.1.6 Cross-Frame Forces

The choice of NLF, SDLF, or TDLF detailing affects more than the girder displacements and stresses. It also can have a significant effect on the cross-frame forces. Figure 3-57 shows the

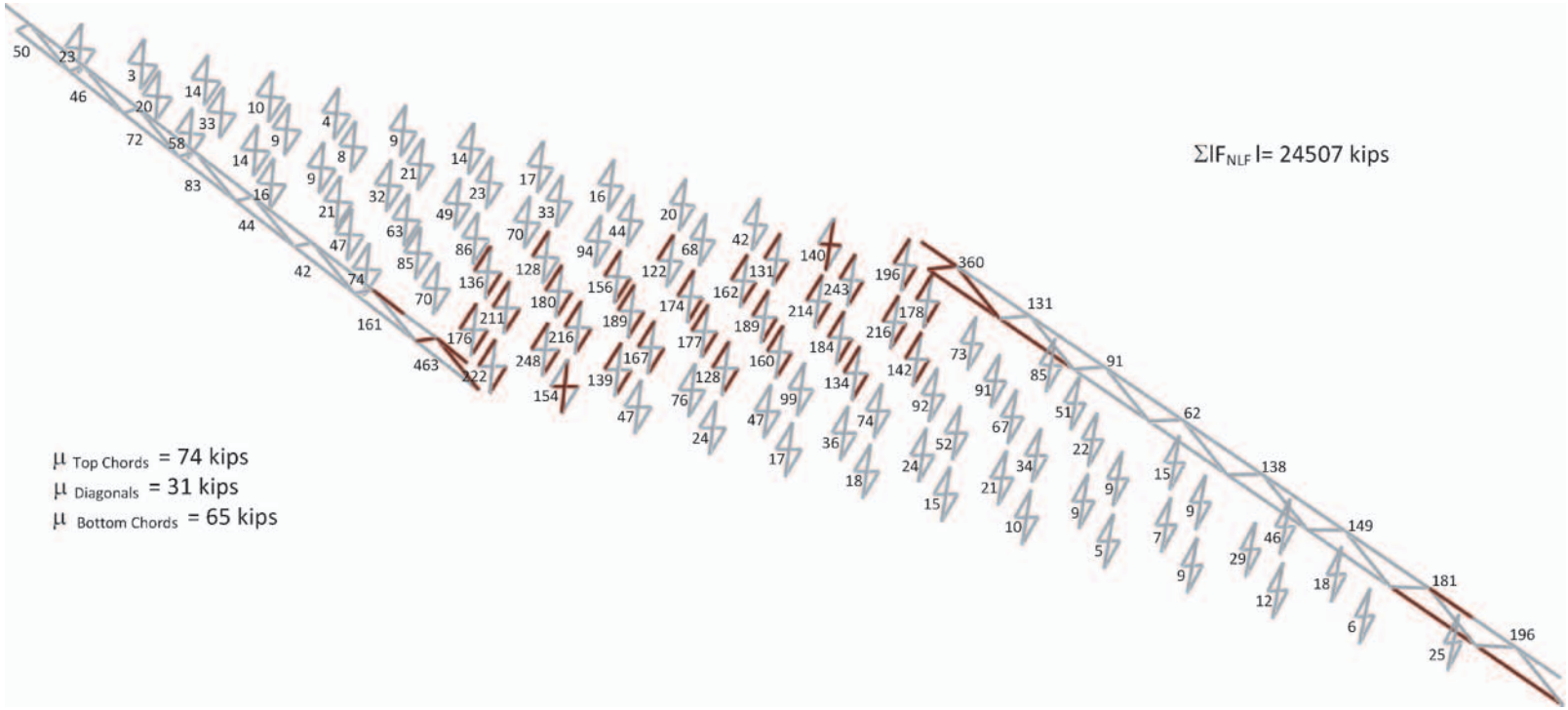

Figure 3-57. Bridge NISSS54 maximum amplitude of the component axial forces in each of the cross-frames under total dead load, NLF detailing of the cross-frames.

86 Guidelines for Analysis Methods and Construction Engineering of Curved and Skewed Steel Girder Bridges

maximum magnitude of the total dead load member axial forces in each cross-frame throughout the NISSS54 Bridge for the ideal case where the cross-frames are fabricated NLF. Figure 3-58 parallels Figure 3-57, but shows the total dead load member axial forces in each of the cross-frames for the situation where the cross-frames are fabricated TDLF. One can observe that, in the NLF case, the cross-frame forces are relatively large in the vicinity of the short transverse load path between the obtuse corners of the bridge. The members having the largest axial force appear in bold in Figure 3-57. It should be noted that the figure also shows the mean of the cross-frame member force magnitudes for the cross-frame top chord, the cross-frame diagonals, and the cross-frame bottom chords. In addition, the sum of absolute value of all the cross-frame member forces, $\Sigma|F_{NLF}|$, is shown in the upper right-hand corner of the figure.

Conversely, in Figure 3-58, the cross-frame member axial forces along the short diagonal direction between the obtuse corners are relatively small (but not equal to zero). In this case, the maximum forces are in the diagonals of several "nuisance stiffness" cross-frames that frame into the girders very close to the skewed bearing lines. If these nuisance stiffness cross-frames are offset a sufficient distance from the bearing lines, as discussed subsequently, all of the final total dead load cross-frame forces are relatively small compared to the forces in the NLF case. However, the cross-frame forces generally are increased due to the TDLF detailing effects in the regions near the acute corners of the deck. One can observe that the chord forces are significantly smaller on average in Figure 3-58, but the average diagonal forces are larger compared to Figure 3-57. This is mainly due to the extremely large forces in the cross-frame diagonals at the acute corners, caused by the small offset distance of these cross-frames from the bearing line. These large forces are due to interactions between the first intermediate cross-frame near the acute corners with the bearing line cross-frames and the corresponding need to introduce a large force into the intermediate cross-frame to "pull" the fascia girders back to an approximately plumb position under the total dead load.

Section 8.2.1 of the Task 8 report (Appendix C of the contractors' final report) recommends that the first intermediate cross-frames should be placed a minimum distance of

$$a = \max(1.5D, 0.4b) \qquad \text{Eq. 15}$$

from the bearing line to alleviate the "nuisance stiffness" effects associated with the above spike in the cross-frame forces, where D is the girder depth and b is the second unbraced length within the span from the bearing line.

Figures 3-59 and 3-60 show solutions comparable to the ones in Figures 3-57 and 3-58, but corresponding to the steel dead load condition. The values for the maximum cross-frame forces in these figures are somewhat representative of the difficulty the erector may encounter in fitting up the cross-frames with the girders in an unshored erection scenario. It is apparent from Figure 3-59 that, for the case with NLF detailing, the greatest difficulty may be encountered with the cross-frames located near the bearing lines and along the short diagonal direction. However, for the case of TDLF detailing, the largest cross-frame forces occur near the acute corners. In particular, it is apparent that some of the cross-frame diagonals near the acute corners may be particularly difficult to install. Again, these "nuisance stiffness" effects can be relieved by using a more appropriate offset distance from the bearing line for these cross-frames. This result demonstrates an important fact that fit-up problems tend to be exacerbated by TDLF detailing of the cross-frames.

From Figures 3-57 through 3-60 as a whole, it is apparent that the locked-in force effects in the cross-frames tend to substantially relieve the cross-frame dead load forces in the short, stiff diagonal direction. However, the "locked-in" cross-frame forces in the vicinity of the acute corners tend to be additive with the dead load effects. Also, it is apparent that the TDLF

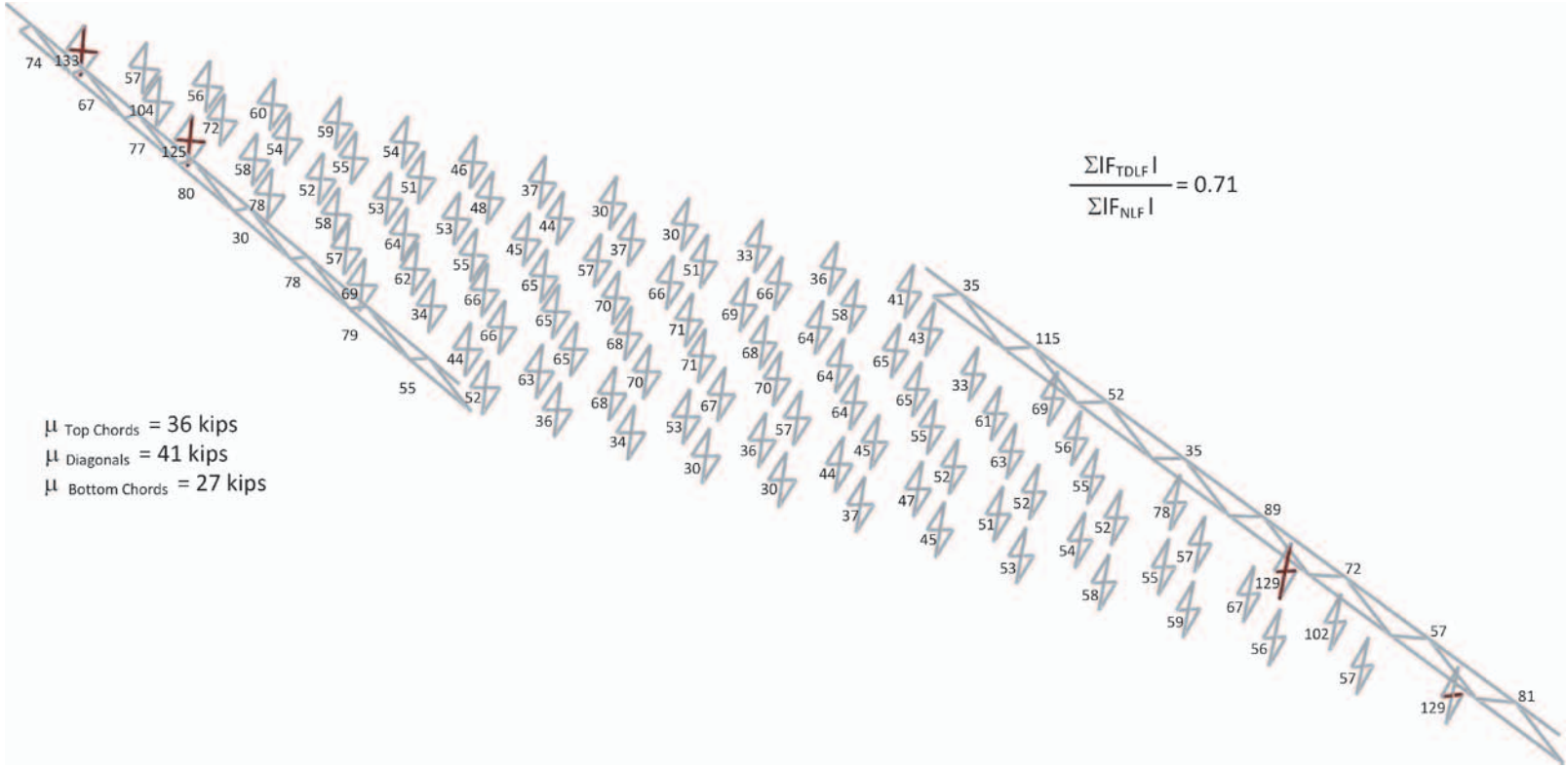

Figure 3-58. Bridge NISSS54 maximum amplitude of the "Configuration 4" component axial forces in each of the cross-frames under total dead load, TDLF detailing of the cross-frames.

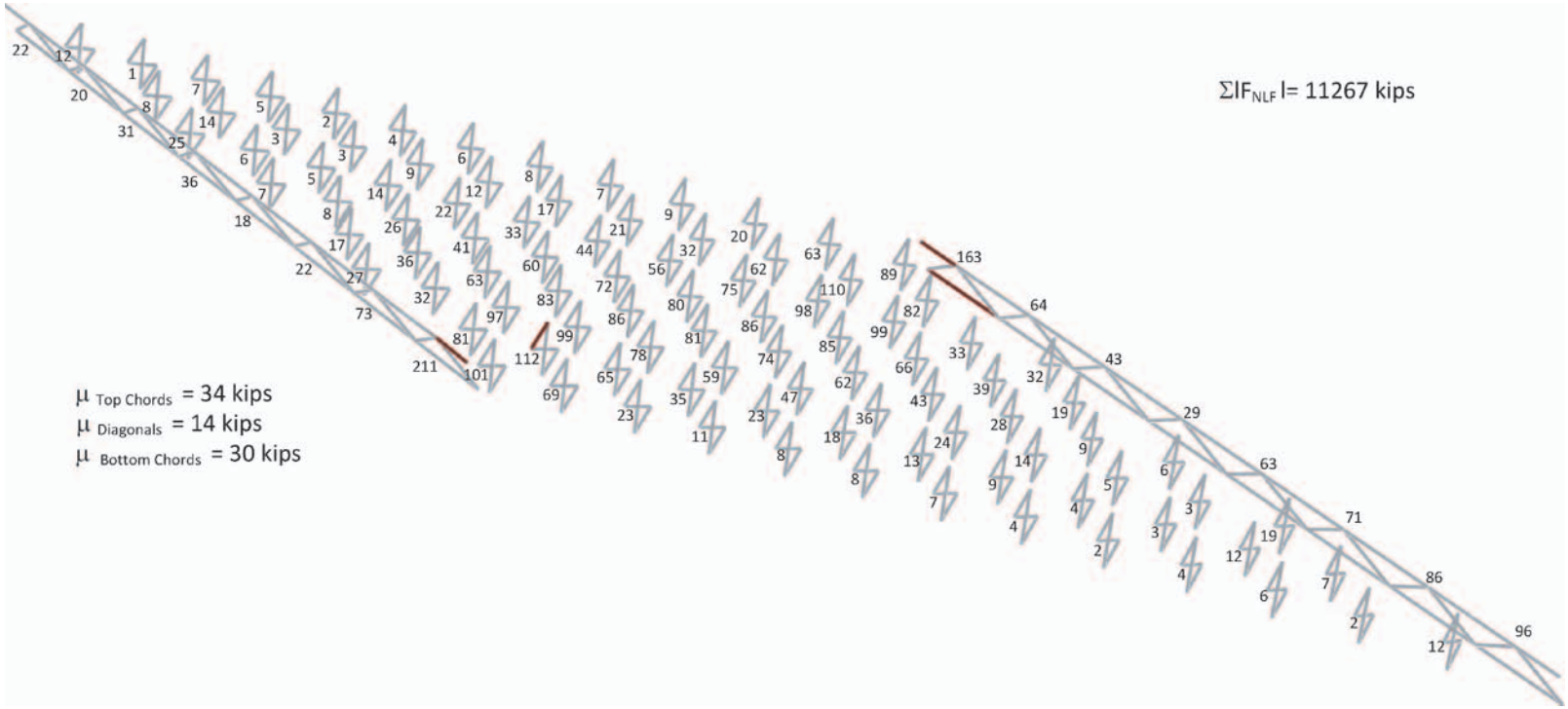

Figure 3-59. Bridge NISSS54 maximum amplitude of the component axial forces in each of the cross-frames under steel dead load, NLF detailing of the cross-frames.

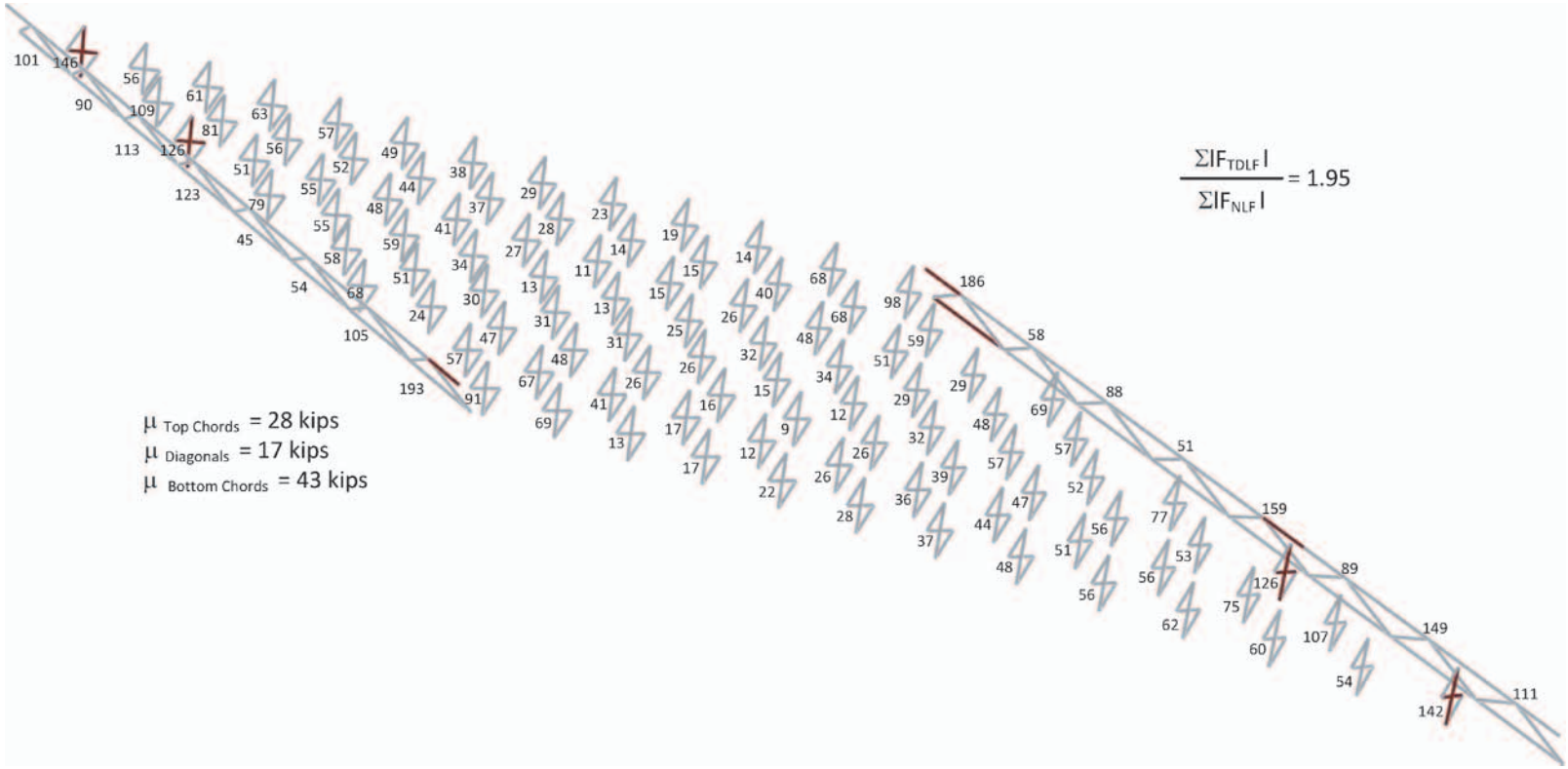

Figure 3-60. Bridge NISSS54 maximum amplitude of the component axial forces in each of the cross-frames under steel dead load, TDLF detailing of the cross-frames.

detailing of the cross-frames tends to exacerbate fit-up problems during the steel erection (due to the fact that the total dead load deflections have not yet been fully taken out of the girders by the application of the total dead loads). Lastly, it should be noted that for NLF detailing of the cross-frames, the forces needed to connect the structure together are theoretically zero if the girders are supported in their no-load position. Therefore, shoring of the girders is a good way to facilitate the erection when NLF detailing is used.

3.3.1.7 Girder Flange Major-Axis and Lateral Bending Stresses

Figure 3-61 shows the top flange major-axis and lateral bending stresses for the fascia Girder G1 and for the inner-most Girder G5 of Bridge NISSS54. The plots in this figure again show the results for all the methods of detailing the cross-frames: NLF, SDLF, and TDLF. Similar to the results for the vertical deflections in G1 and G5, the major-axis bending stresses in these straight girders are relatively insensitive to the type of cross-frame detailing. However, the girder flange lateral bending stresses are substantially affected by whether the detailing of the cross-frames is NLF, SDLF, or TDLF. This should not be surprising given the above results for the girder layovers and cross-frame forces.

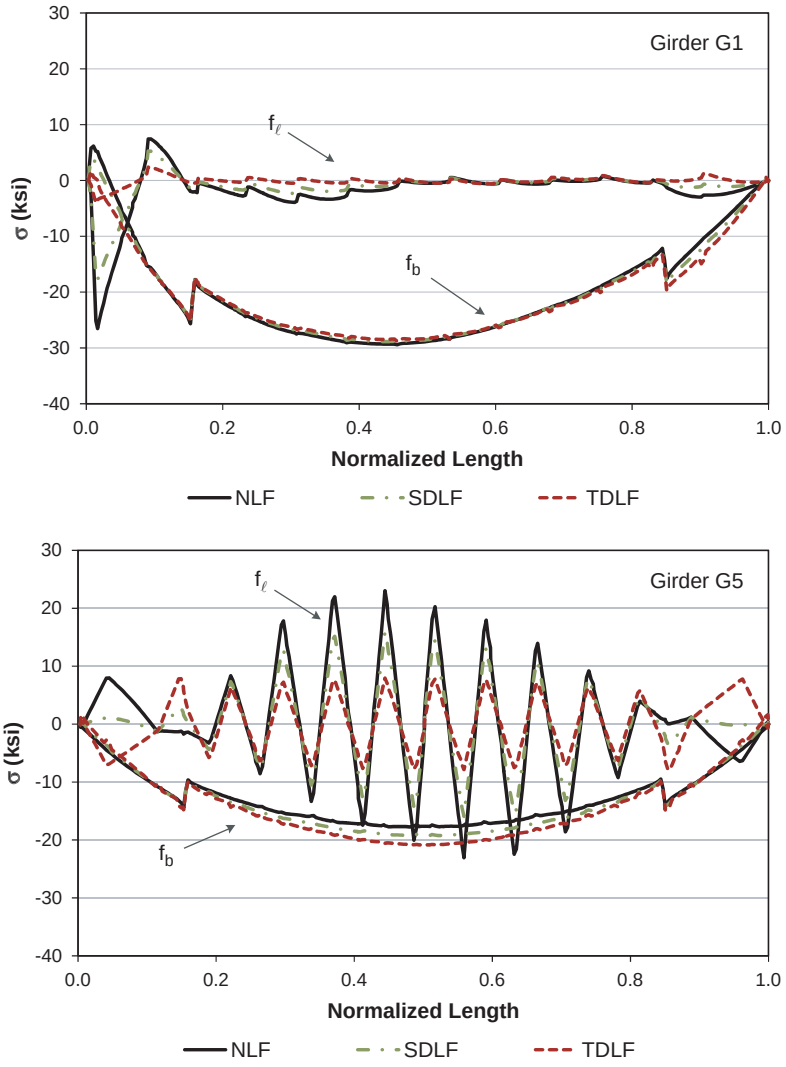

Figure 3-61. Bridge NISSS54 "Configuration 4" top flange stresses under total dead load for different detailing methods.

The girder flange lateral bending stresses are the smallest when TDLF detailing is used. Many engineers expect that if TDLF detailing is used, the flange lateral bending stresses will be essentially zero (under the total dead load condition). This is not generally the case for the same reasons as explained in Section 3.3.1.4. In the fascia girder, the flange lateral bending stress is still approximately 3 ksi near the left-hand end (see the top plot in Figure 3-61). This is related to the same nuisance stiffness effects of framing a number of the cross-frames in too close to the supports observed in Section 3.3.1.6. If the problem cross-frames are offset further from the bearing line, the flange lateral bending stresses in the fascia girder are essentially negligible. It should be noted that some small lateral bending stresses are induced in the top flange of the fascia girder due to the overhang loads.

For the interior Girder G5, significant flange lateral bending stresses are still encountered even for the case of TDLF detailing. These stresses are due to the fact that the locked-in concentrated lateral forces acting on Girder G5 from the cross-frames are not able to cancel the torsional actions of this girder under the distributed total vertical dead load. The maximum flange lateral bending stresses, however, are actually reduced by more than a factor of two by the TDLF detailing effects in Girder G5.

3.3.2 Curved Radially Supported Bridge Example

Figure 3-62 provides the framing plan for a 150-ft. simple-span curved radially supported I-girder bridge with a radius of curvature at its centerline of $R = 438$ ft., a deck width of $w = 30$ ft., and four I-girders spaced at 8 ft. apart. This bridge, named NISCR2, has a connectivity index of $I_C = 4.89$, which places it in the second category of the "C" bridges of Table 3-1. It is expected that a conventional 2D grid analysis may have some difficulty in capturing all the responses of this structure. Figure 3-63 and Table 3-9 give this bridge's plate girder dimensions, and Table 3-10 gives the sizes of its cross-frame members. A number of the attributes of this bridge are simpler than those of the previous example. However, this bridge is important to illustrate several key considerations with respect to SDLF and TDLF detailing effects on horizontally curved geometries.

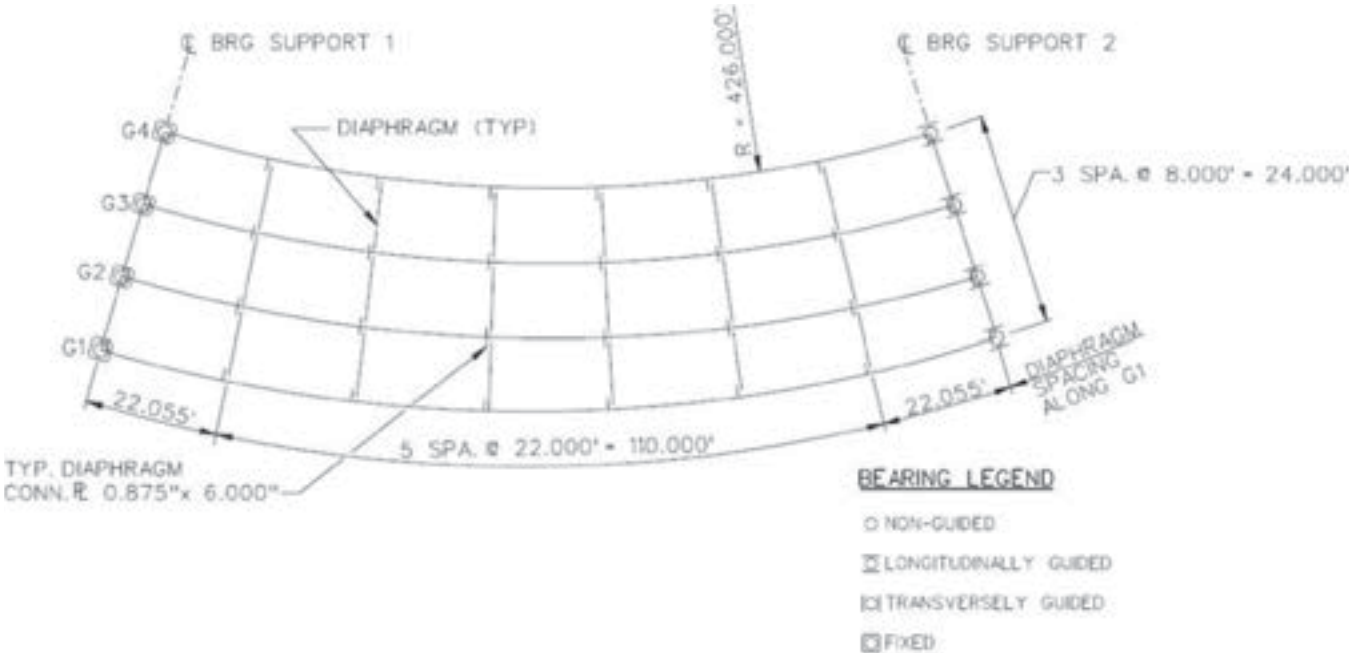

Figure 3-62. Bridge NISCR2 framing plan.

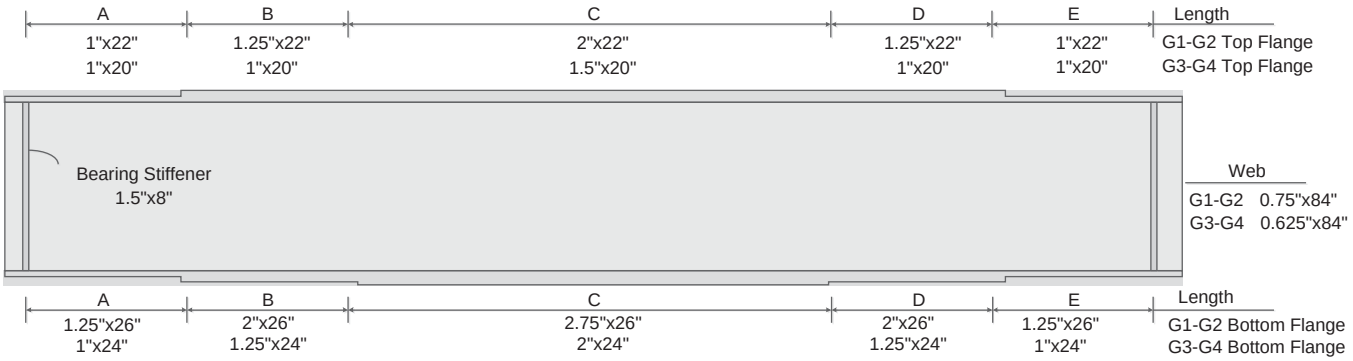

Figure 3-63. NISCR2 girder plate dimensions.

3.3.2.1 Bridge Deflections

Figure 3-64 shows a plan view of the Bridge NISCR2 magnified deformed geometry due to its total dead load. One can observe that there is an overall twisting of the bridge cross-section and all of the girders are laying over in the same direction. However, the layover at the radial supports is zero.

3.3.2.2 Girder Cambers and Camber Differences

As noted in the previous example in Section 3.3.1, SDLF and TDLF detailing are driven by the girder camber profiles or, more specifically, by the differential camber at the cross-frame locations. Figure 3-65 shows the total dead load differential cambers for Bridge NISCR2. One can observe that all the cambers are negative values, indicating that in all cases, the girders with a smaller horizontal radius of curvature have smaller dead load deflections in this bridge. Similar to the previous example, the discussions are focused on the behavior for TDLF detailing of the cross-frames unless noted otherwise.

3.3.2.3 System Deflections Due to Initial Lack-of-Fit Effects

Figure 3-66 shows the deflections of NISCR2 after the cross-frames are first connected to the girders in "Configuration 2" (see Figure 3-30b), second, the girders are "unlocked" and "released" from their initial no-load plumb geometry, and third, the girders are deformed by the cross-frames into Configuration 3 (described in Figure 3-30c). In other words, Figure 3-66 shows the "final" deformed geometry due to the locked-in forces caused by the TDLF detailing of the cross-frames.

Table 3-9. NISCR2 girder plate lengths (ft.).

Girder	A	B	C	D	E
G1	20.0	20.0	74.1	20.0	20.0
G2	19.6	19.6	72.8	19.6	19.6
G3	19.3	19.3	71.5	19.3	19.3
G4	18.9	18.9	70.2	18.9	18.9

Table 3-10. NISCR2 cross-frame member sizes.

Cross-Frame Type	Top Chord	Diagonals	Bottom Chord
Interior (X type)	L6x6x0.75	L6x6x0.75	L6x6x0.75
End (Inverted V)	L6x6x0.75	L6x6x0.75	L6x6x0.75

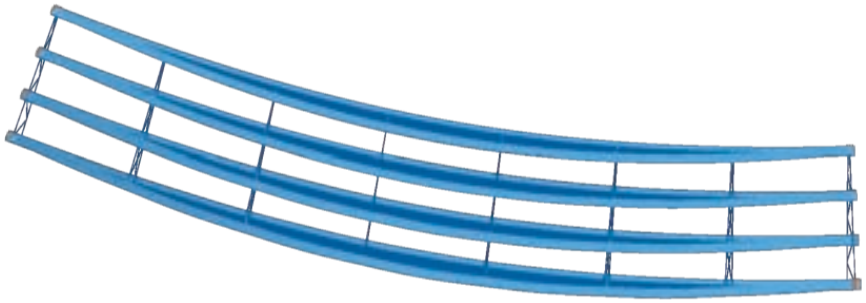

Figure 3-64. Bridge NISCR2 total dead load deflected geometry for the case of NLF detailing of the cross-frames (scale factor = 20x).

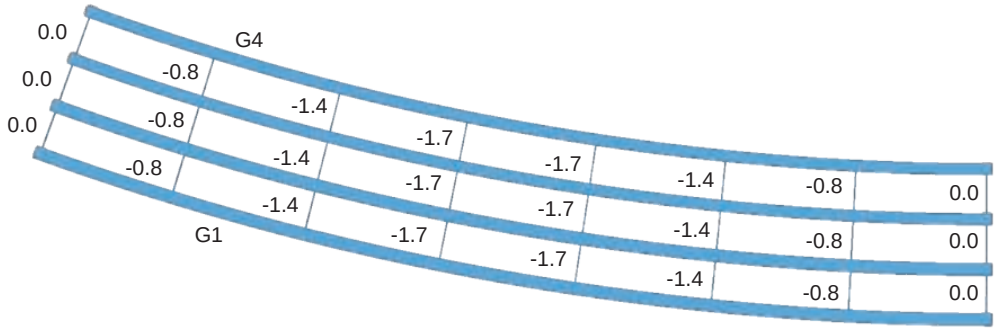

Figure 3-65. Bridge NISCR2 total dead load camber differences (differential camber values) between girders.

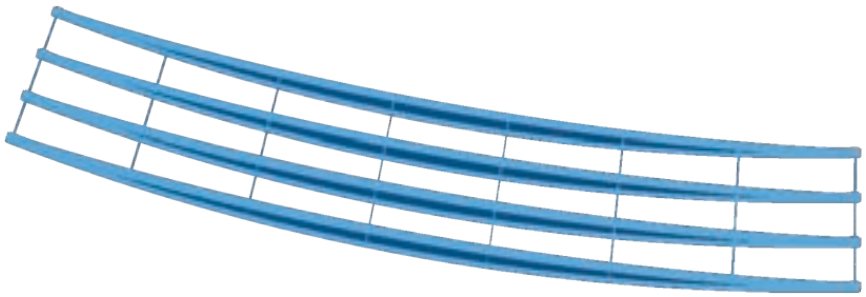

Figure 3-66. Bridge NISCR2 "Configuration 3" deflected shape due to the initial lack-of-fit effects from TDLF detailing of the cross-frames (scale factor = 20x).

One can observe that the bridge deformations in Figure 3-66 are approximately the opposite of the deflections shown in Figure 3-64. Similar to the previous example, they are not exactly equal and opposite.

3.3.2.4 Approximate Canceling of Dead Load Layovers by Dead-Load Fit Effects

Figure 3-67 shows the girder layovers in this bridge once the steel and concrete dead load effects have been added to deflect the structure conceptually from the previously discussed "Configuration 3" to "Configuration 4" (see Figure 3-30c and d). Results similar to those obtained in the previous skewed bridge example are observed in that each of the girder

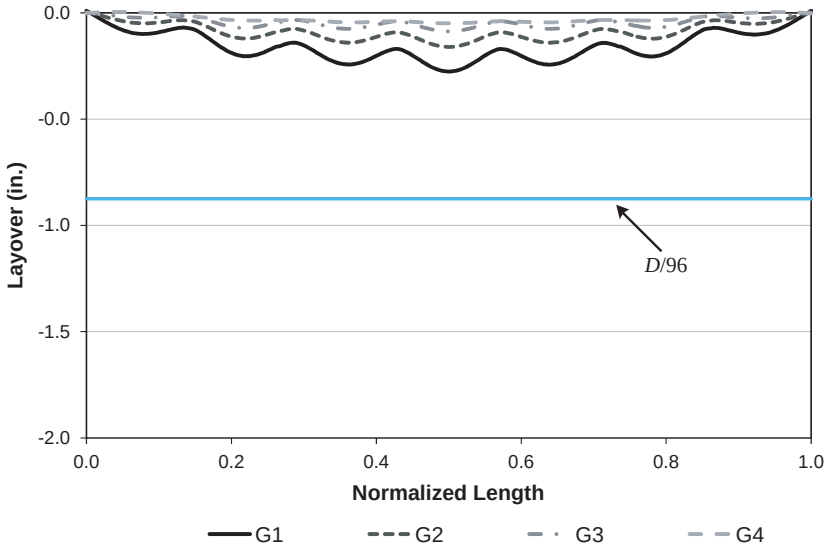

Figure 3-67. Bridge NISCR2 "Configuration 4" girder layovers under total dead load for the case where the cross-frames are detailed for TDLF.

layovers is strictly non-zero; however, the final layovers are well within the typical tolerance of $D/96 = 84$ in./96 = 0.875 in. Also, as stated previously, the layovers cannot possibly be expected to be exactly equal to zero because the TDLF detailing effects are applied to the girders as concentrated lateral loads from the cross-frames, whereas the total dead load layovers are caused by distributed vertical loads.

Figure 3-68 illustrates the girder layovers in Bridge NISCR2 under the steel dead load when TDLF detailing of the cross-frames is used. Clearly, the girders are not plumb under the steel dead load. They are still rotated in the direction opposite to the direction that they twist under the action of the vertical loads. However, these layovers also satisfy the $D/96$ tolerance. Lastly,

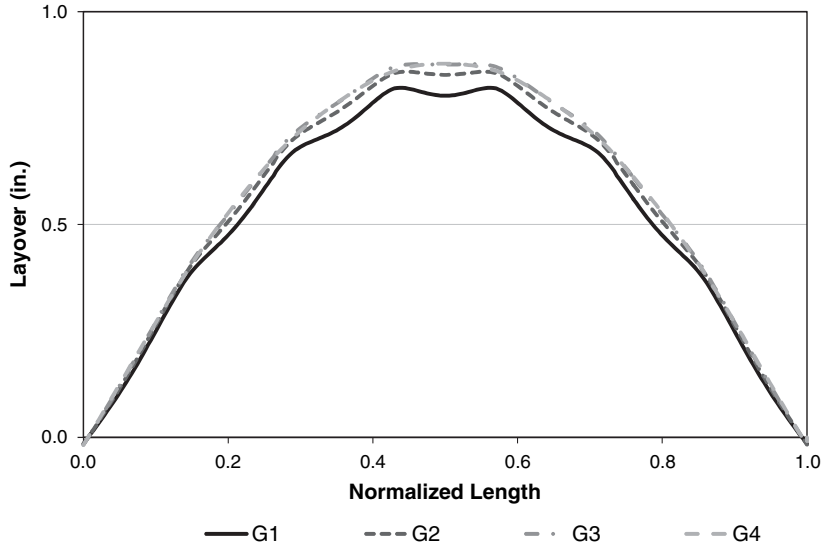

Figure 3-68. Bridge NISCR2 girder layovers under steel dead load for the case where the cross-frames are detailed for TDLF.

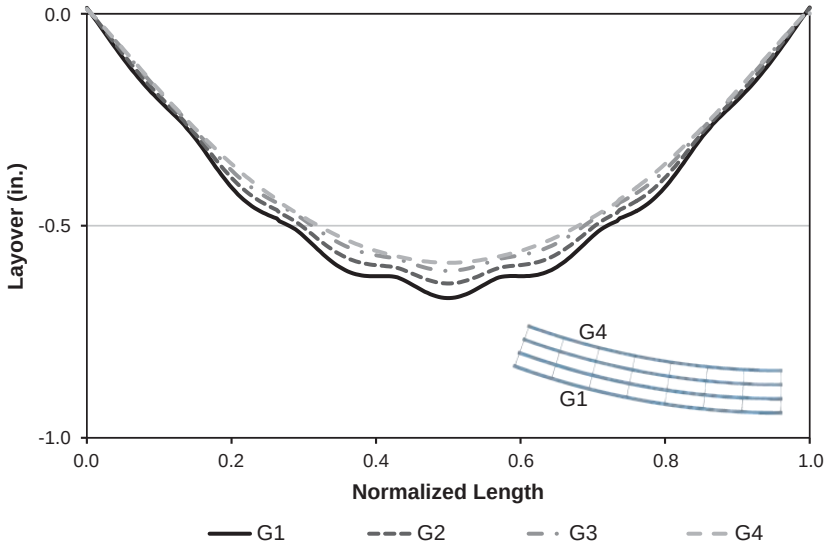

Figure 3-69. Bridge NISCR2 girder layovers under steel dead load for the case where the cross-frames are detailed for NLF.

Figure 3-69 shows the girder layovers under the steel dead load for the case of NLF detailing of the cross-frames, while Figure 3-70 indicates the corresponding layovers under the total dead load. It can be observed that the layovers under the total dead load violate the above *D*/96 tolerance. Nevertheless, rigorous test simulation studies show that this layover does not have any measurable effect on the system capacity.

3.3.2.5 Final Girder Vertical Deflections

Figure 3-71 shows the vertical deflections along the length of the fascia Girder G1 on the outside of the horizontal curve as well as the fascia Girder G4 on the inside of the curve of Bridge NISCR2. The results in these plots are shown for each of the three main cross-frame detailing

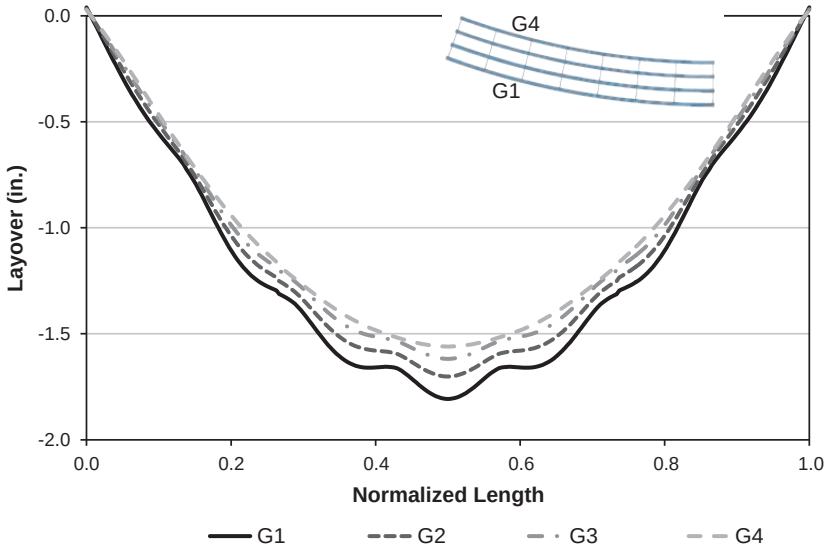

Figure 3-70. Bridge NISCR2 girder layovers under total dead load for the case where the cross-frames are detailed for NLF.

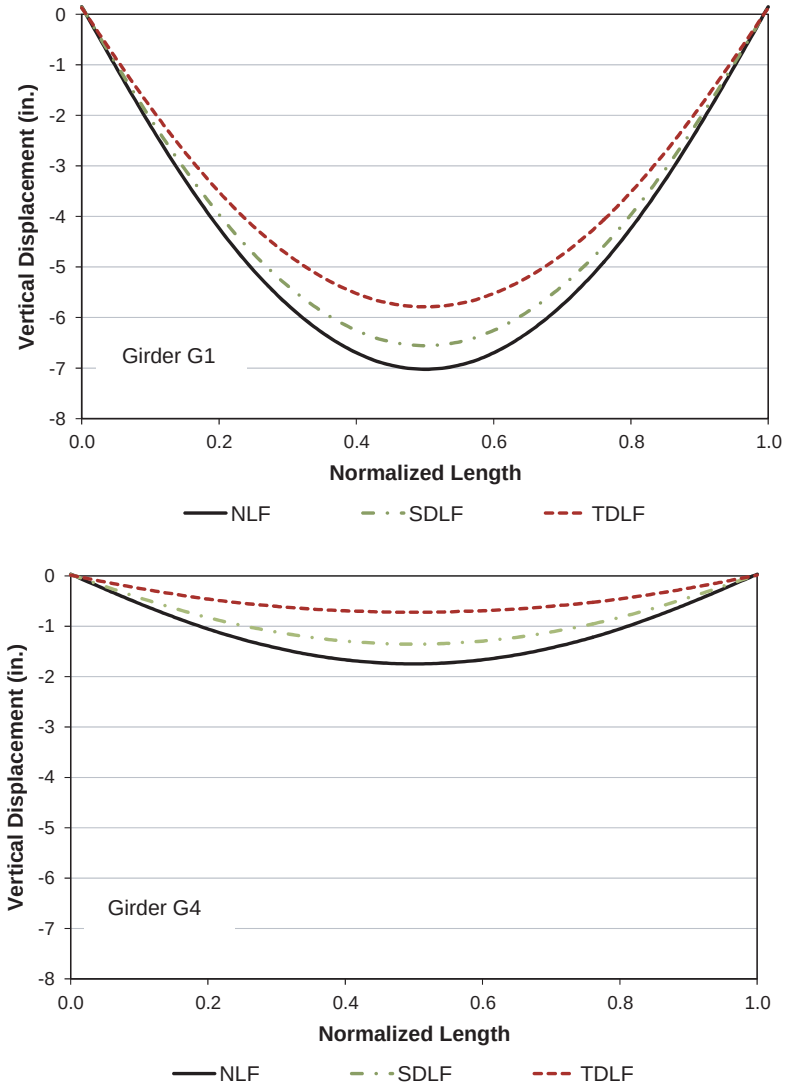

Figure 3-71. Bridge NISCR2 vertical deflections under total dead load for different cross-frame detailing methods.

methods: NLF, SDLF, and TDLF. One can observe that the percentage differences between these vertical displacement solutions are significantly larger than observed in the previous straight bridge example. Generally, the vertical displacements in horizontally curved bridges tend to be affected to a larger degree by the SDLF and TDLF detailing effects than in straight bridges. The mid-span vertical displacement of G1 in this specific example is 7 percent smaller than the solution for NLF when SDLF detailing is used. It is 17 percent smaller when TDLF detailing is employed.

One other important observation that should be made from Figure 3-71 is that the influence on the vertical displacements from the SDLF detailing (i.e., the differences between the SDLF and NLF curves) are similar for all of the girders in the NISCR2 Bridge. The SDLF detailing reduces the displacements of all the girders equally by approximately 0.4 in. This statement also can be made regarding the influence of the TDLF detailing on the girder vertical displacements. The TDLF detailing reduces all the girder displacements by approximately 1.2 in. This is a general finding for all curved radially supported bridges and is demonstrated subsequently for several other bridges of this type.

3.3.2.6 Cross-Frame Forces

Figures 3-72 through 3-74 show the individual cross-frame member axial forces under the total dead load in the NISCR2 Bridge for the cases of NLF, SDLF, and TDLF detailing of the cross-frames, respectively. These figures indicate that the cross-frame chord forces are not significantly affected in this bridge by the type of cross-frame detailing. However, all the diagonal forces are significantly increased. The increase in the mean of the axial force in the diagonals is 35 percent for SDLF detailing versus NLF. The increase is 100 percent for TDLF detailing of the cross-frames.

Correspondingly, Figures 3-75 through 3-77 show the individual cross-frame member axial forces under the steel dead load in the NISCR2 Bridge for NLF, SDLF, and TDLF. As discussed previously, the internal cross-frame forces in these solutions provide an indication of any potential difficulty regarding the fit-up of the cross-frames with the girders during the steel erection. One can observe again that the chord forces are not affected significantly

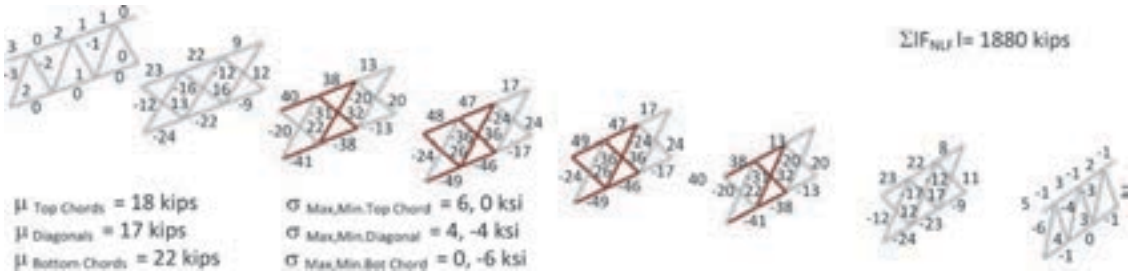

Figure 3-72. Bridge NISCR2 maximum amplitude of the component axial forces in each of the cross-frames under total dead load, NLF detailing of the cross-frames.

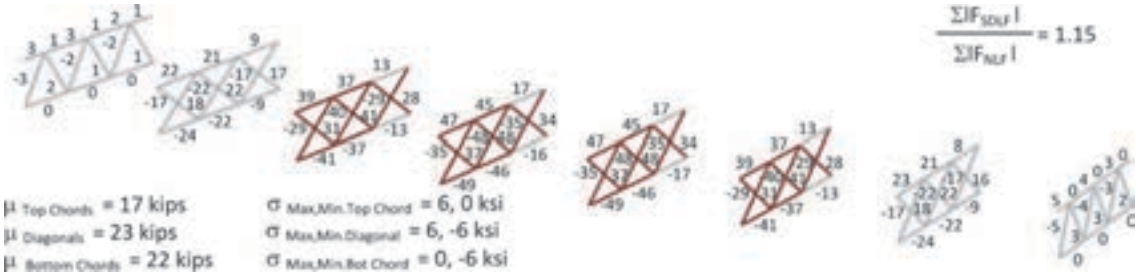

Figure 3-73. Bridge NISCR2 maximum amplitude of the component axial forces in each of the cross-frames under total dead load, SDLF detailing of the cross-frames.

Figure 3-74. Bridge NISCR2 maximum amplitude of the component axial forces in each of the cross-frames under total dead load, TDLF detailing of the cross-frames.

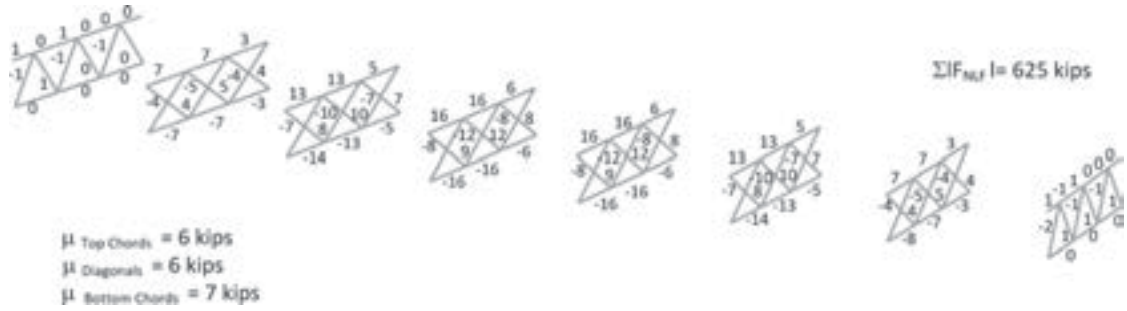

Figure 3-75. Bridge NISCR2 maximum amplitude of the component axial forces in each of the cross-frames under steel dead load, NLF detailing of the cross-frames.

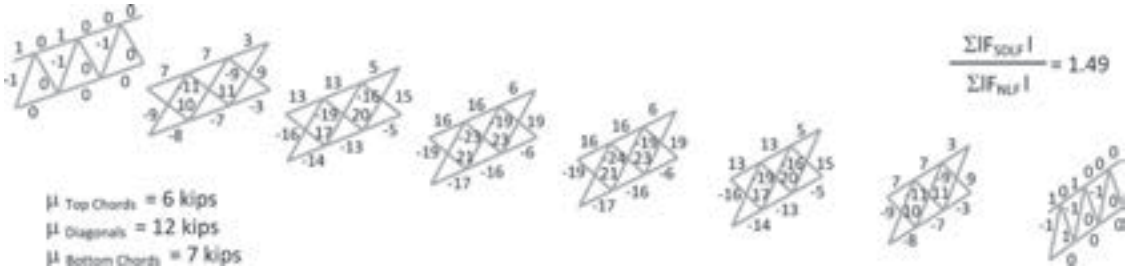

Figure 3-76. Bridge NISCR2 maximum amplitude of the component axial forces in each of the cross-frames under steel dead load, SDLF detailing of the cross-frames.

Figure 3-77. Bridge NISCR2 maximum amplitude of the component axial forces in each of the cross-frames under steel dead load, TDLF detailing of the cross-frames.

by the cross-frame detailing type. However, the mean of the diagonal forces is increased by 100 percent from the NLF detailing to the SDLF case, and 283 percent from NLF to TDLF. Based on the results in Figure 3-77, one can conclude that the span length and radius of curvature for NISCR2 is such that the cross-frame fit-up forces are expected to be manageable for any of the methods. However, for a comparable bridge with a tighter radius curvature and/or a longer span length, the above percentage differences may be of greater significance.

Based on the full set of bridge studies performed within NCHRP Project 12-79, the locked-in forces in the cross-frame diagonals always tend to be additive with the dead load effects when SDLF or TDLF detailing is used on curved radially supported bridge structures. Also, the chord forces tend to be increased, but not as much so. These are important findings. One can conclude that locked-in force effects generally should be considered when sizing the cross-frames in horizontally curved I-girder bridges. (These conclusions are independent of the specific sequence of girder erection, since assuming the structure remains elastic, and neglecting aspects such as

friction at the supports and non-zero connection tolerances, the bridge is a conservative elastic system for which the responses are path independent.)

3.3.2.7 Girder Flange Major-Axis and Lateral Bending Stresses

Figure 3-78 gives the top flange major-axis and flange lateral bending stresses for Girders G1, G2, and G4 in the NISCR2 Bridge. The plots in this figure again show the results for all the methods of detailing the cross-frames: NLF, SDLF, and TDLF. One can observe that the major-axis bending stress in the girders is insensitive to the type of cross-frame detailing. This is a common result for horizontally curved structures, even though the girder vertical displacements exhibit some sensitivity to these attributes. This sensitivity is related to the coupling between the girder vertical displacements and the twist deformations in curved members.

Conversely, the curved I-girder flange lateral bending stresses show some sensitivity to the cross-frame detailing type. This is due to the fact that, in a curved radially supported bridge, the locked-in cross-frame forces due to SDLF or TDLF detailing tend to displace the flanges laterally, and in a direction opposite to the direction the girders are tending to bend and twist under the vertical loads. These actions occur over the full span length of the girders. In the specific case of the NISCR2 Bridge, as well as other generally curved and radially supported structures, the flanges act effectively as continuous-span beams loaded effectively by uniformly distributed lateral loads coming from the horizontal curvature. The cross-frames are the supports for these effective continuous-span beams.

The influence of SDLF or TDLF detailing on the effective continuous span beams is to essentially "pre-stress" the flanges by displacing their supports in the direction opposite to the equivalent horizontal curvature loading. On the inside Girder G4 of NISCR2, this "pre-stressing" is the dominant effect, essentially shifting the entire flange lateral bending moment diagram throughout the span. However in Girders G1 and G2, this pre-stressing effect is manifested predominantly in an increase in the flange "negative bending" moments and flexural stresses (using the above continuous-span beam analogy). These "negative bending stresses" are relatively small in this bridge, but they are increased by a maximum of approximately 20 percent due to SDLF detailing and 66 percent due to TDLF detailing.

3.3.3 General Considerations

3.3.3.1 Key Results from Studies of the Ford City Bridge (EICCR11)

Because of its relative simplicity, Bridge NISCR2 considered in the previous section is useful to illustrate the influence of SDLF and TDLF cross-frame detailing effects on general horizontally curved bridges. Furthermore, this structure is illustrative of the behavior for reasonably "regular" curved I-girder bridges with relatively short-to-moderate span lengths.

The Ford City Bridge (EICCR11) shown in Figures 3-79 through 3-81 represents the most extreme case encountered in the NCHRP Project 12-79 research regarding the influence of the cross-frame detailing method on the girder layovers, vertical displacements, and flange lateral bending stresses. This three-span continuous I-girder bridge has one straight end span of length 321 ft., a straight center span of 445 ft., and a highly curved end span of 292 ft. The minimum radius of curvature in the curved span is 511 ft. Furthermore, the bridge has a relatively narrow deck with $w = 48.2$ ft. given its span lengths. The torsion index on its curved span (Equation 1) is $I_T = 0.87$. In addition, its four girders are 14 ft. deep and are spaced at 13.5 ft. apart. The circles in Figure 3-81 are highlighting a come-along beam that is being used to stabilize the curved girder during lifting. A cable goes up to a lifting beam from each end of the come-along beam.

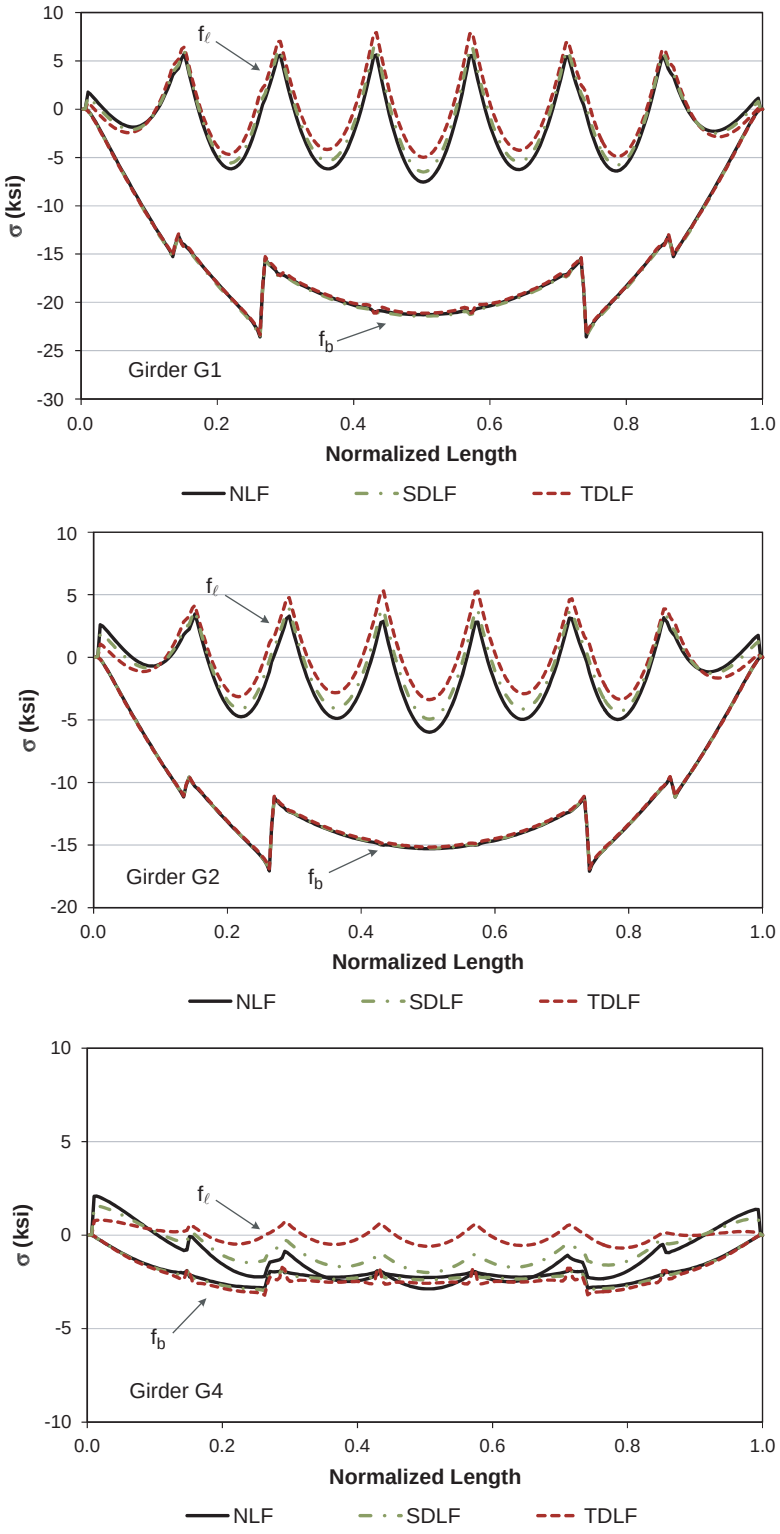

Figure 3-78. Bridge NISCR2 top flange stresses under total dead load for different detailing methods.

Figure 3-79. Ford City Bridge (EICCR11) (Chavel, 2008).

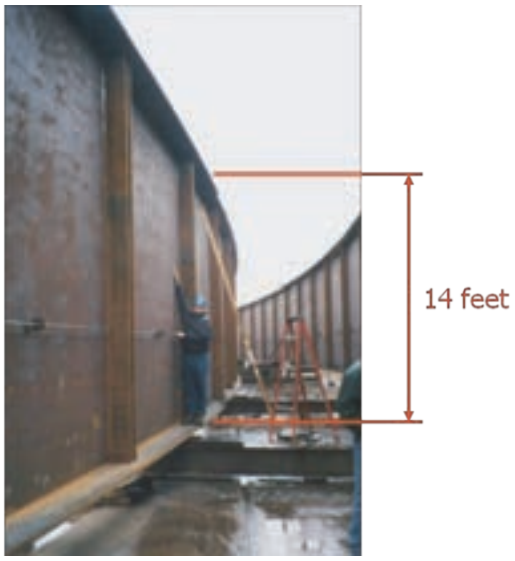

Figure 3-80. Ford City Bridge (EICCR11) girder depth and spacing (Chavel, 2008).

Figure 3-81. Ford City Bridge (EICCR11) installation of drop-in segment (Chavel, 2008).

102 Guidelines for Analysis Methods and Construction Engineering of Curved and Skewed Steel Girder Bridges

The combination of the above attributes, along with various other factors, make the Ford City Bridge possibly one of the most challenging curved I-girder bridges that has ever been erected. This bridge was not originally designed with a top flange lateral bracing (TFLB) system, but one was provided as shown in Figure 3-79 to facilitate the steel erection and concrete deck placement. This bridge was studied without a TFLB system in the NCHRP Project 12-79 research so that legitimate comparisons could be made between the 3D FEA simulations and simplified 1D line-girder and 2D-grid methods (since the 1D line-girder and 2D-grid solutions are generally not sufficient for I-girder bridges with TFLB systems).

Figure 3-82 provides a plan view of three magnified displaced shapes from the 3D FEA simulation model of the Ford City Bridge. These images illustrate the influence of the different methods of cross-frame detailing on the torsional and lateral bending response of the bridge. It is apparent that there are substantial layovers, lateral movements, and span interactions in the bridge if it is constructed with NLF detailing. SDLF detailing reduces these deformations substantially, whereas TDLF detailing gives effectively plumb webs under the total dead load. Unfortunately, because of the size and close spacing of the girders on this bridge, TDLF detailing results in prohibitive fit-up forces. Therefore, SDLF detailing, or possibly detailing for an intermediate condition between NLF and SDLF, is the best option for this bridge. Based on the analytical studies from the NCHRP Project 12-79, NLF detailing tends to minimize the cross-frame internal forces under the intermediate and final steel dead load conditions in curved radially supported bridges and also tends to minimize the forces required to fit-up the steel in these structure types.

Figure 3-83 plots the girder layovers associated with the deflected geometries from Figure 3-82 and shows that the maximum layovers under the total dead load are 3.6 in. when SDLF detailing is used. The NCHRP Project 12-79 research studies show that these displacements do not have any significant impact on the strengths. Generally, if the stability (second-order amplification) checks of Sections 3.1.1.1 and 3.1.1.2 are satisfied and the cross-frames satisfy stability bracing requirements (Helwig, 2012), the influence of girder layover on the structural resistance is sufficiently addressed and does not need to be considered any further.

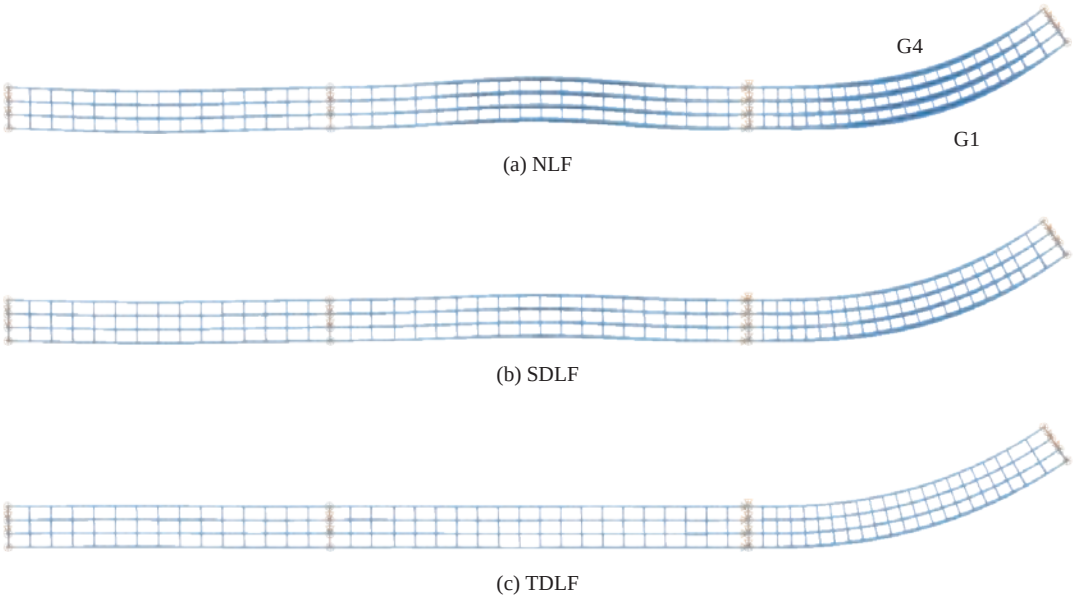

Figure 3-82. Ford City Bridge (EICCR11) deflected shape under total dead load for different detailing methods (scale factor = 10x).

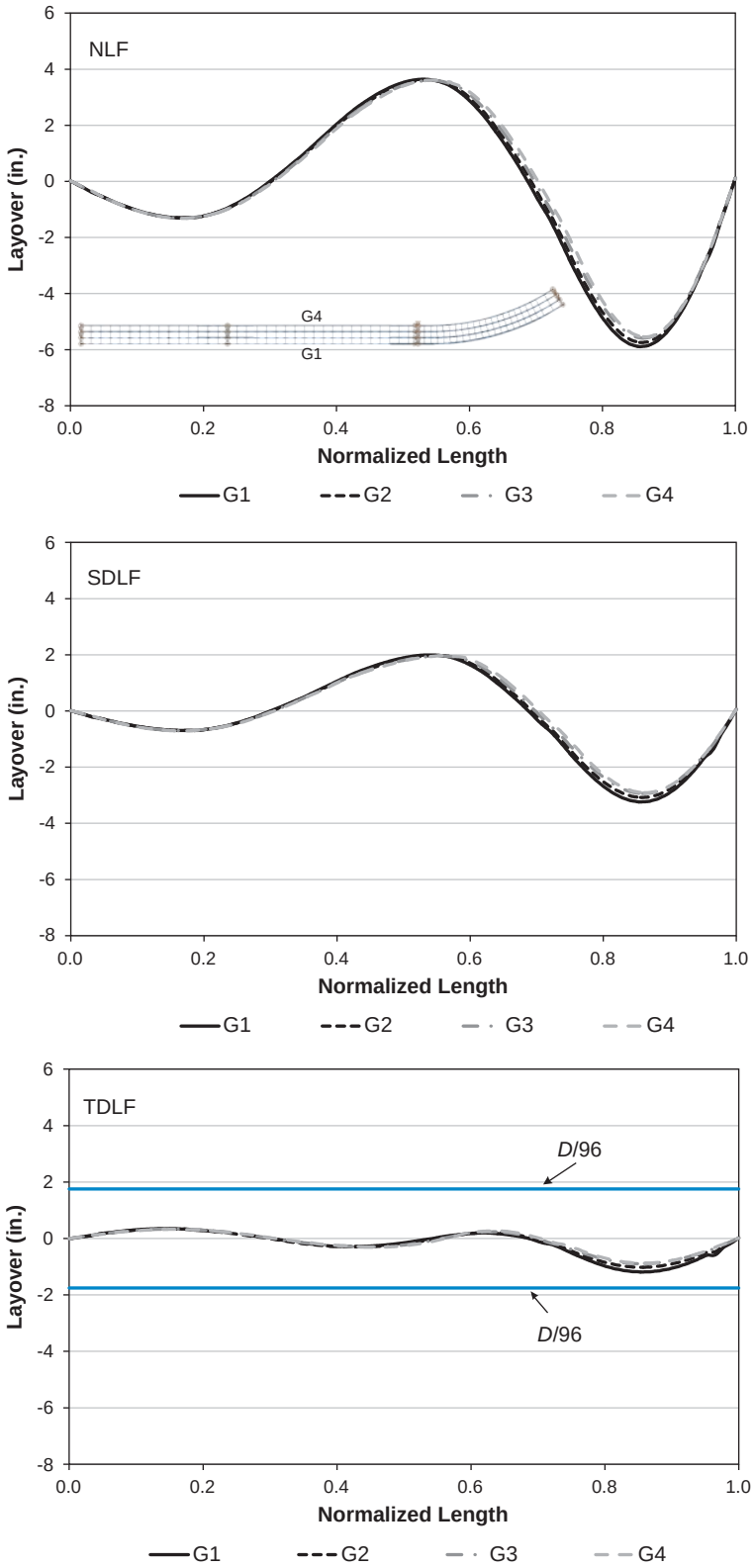

Figure 3-83. Ford City Bridge (EICCR11) girder layovers under total dead load for different detailing methods.

Figure 3-84 shows the vertical deflections from the above 3D FEA simulations of the Ford City Bridge. One can observe that the maximum vertical displacement on Girder G1 under the total dead load is 19.1 in. if NLF detailing were used, 16.9 in. if SDLF detailing were used, and 14.9 in. for TDLF detailing. Girder G4 experiences a more dramatic effect on its vertical deflections due to the span torsional interactions. The curved span on G4 sees a maximum downward displacement of 3.2 in. with NLF detailing of the cross-frames, a maximum upward displacement of 1.7 in. with SDLF detailing, and a maximum upward displacement of 3.4 in. with TDLF detailing. These differences are large enough such that it is clear that the influence of the type of cross-frame detailing would need to be considered in setting the girder cambers in this bridge.

As noted previously for the NISCR2 Bridge (see Section 3.3.2.5 and Figure 3-71), SDLF or TDLF detailing tends to have a similar effect on all of the girder vertical displacements within a given bridge. In Figure 3-84, one can observe that the vertical displacements of all the girders are reduced by the SDLF and TDLF detailing effects in the right-hand curved end-span of the Ford City Bridge. Correspondingly, all the vertical displacements are increased by these effects in the

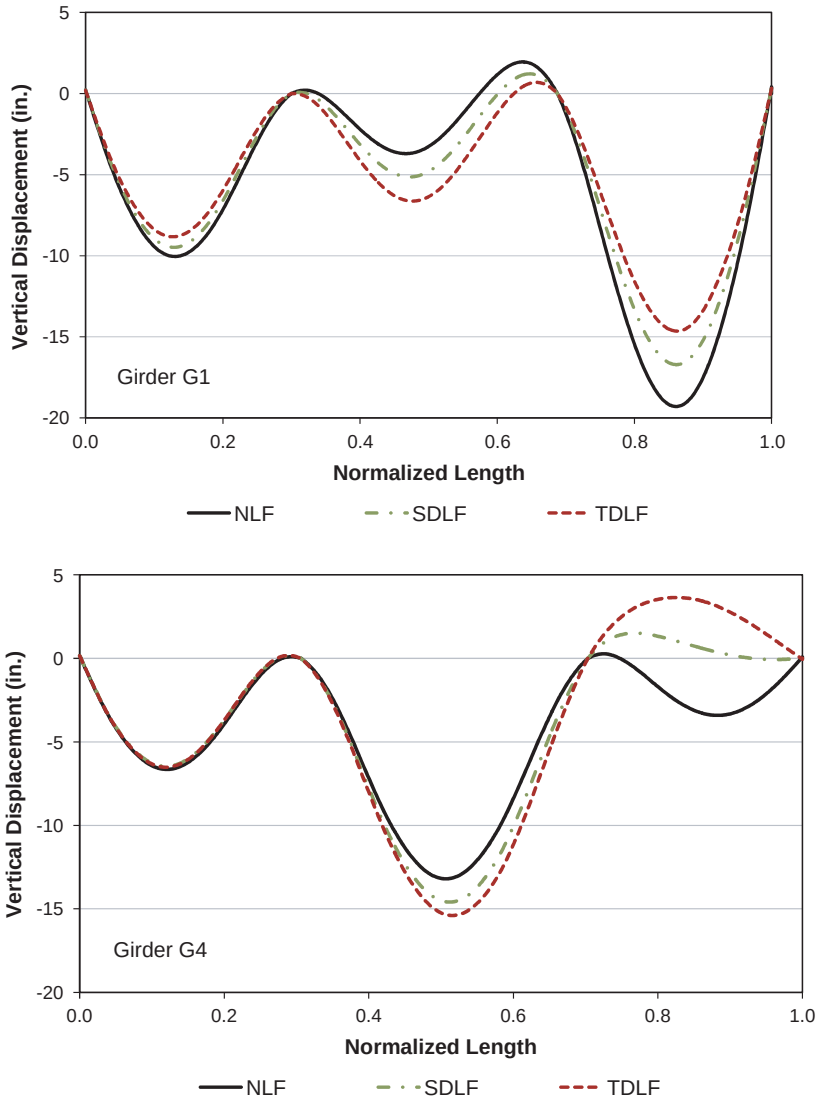

Figure 3-84. Ford City Bridge (EICCR11) vertical deflections under total dead load for different detailing methods.

middle span. The SDLF and TDLF influences on the Girder G1 and G4 displacements, given by the differences between the SDLF and NLF and the TDLF and NLF curves, are somewhat different in the Ford City Bridge however. This is due to the interaction between the continuous spans.

3.3.3.2 Consideration of the Influence of Cross-Frame Connection Tolerances on the Development of Locked-in Forces Due to SDLF or TDLF Detailing

One question that may be asked regarding the influence of SDLF or TDLF detailing is whether small connection tolerances can add up to relieve the locked-in forces to a substantial degree. This question can be evaluated in an informative but simplified fashion using the FHWA Test Bridge (EISCR1) considered in prior Section 3.2. Figure 3-85 shows an isometric view of the 3D FEA simulation model for this structure, illustrating the undeformed geometry as well as the "Configuration 3" geometry explained previously in Figure 3-30c. This is the conceptual configuration in which the girders are "unlocked" and "released" such that the cross-frames impose deformations on them due to the initial lack of fit. However, the vertical loads conceptually have not been applied to the structure at this stage.

Figures 3-86 and 3-87 show the vertical displacements and the flange major-axis and lateral bending stresses under the total dead load (unfactored) for the cases where the cross-frames are detailed for NLF and for TDLF. These results closely parallel the results presented previously in Figures 3-71 and 3-78 for Bridge NISCR2. Basically, the method of detailing can have a significant influence on both of these quantities in horizontally curved I-girder bridge structures.

Figure 3-88 shows the corresponding cross-frame forces in the test bridge associated with NLF and TDLF detailing of the cross-frames. These results show the same trends as illustrated earlier for the NISCR2 Bridge in Figures 3-72 and 3-74 (i.e., the cross-frame diagonal forces can be increased substantially by the use of TDLF detailing in horizontally curved bridges). Similar results are obtained for SDLF detailing, but the increase in the cross-frame forces is smaller.

It is useful to plot the responses induced solely due to the TDLF detailing, to understand their magnitudes before addressing the connection tolerance question. Figure 3-89 shows the vertical displacements induced in Girder G1 on the outside of the horizontal curve and in Girder G3 on the inside of the horizontal curve corresponding to the deformed "Configuration 3" geometry from Figure 3-85. One can observe that comparable vertical displacements are induced in both girders due to the effects of the TDLF detailing (consistent with the previous results shown in Figures 3-71 and 3-84). Figure 3-90 shows the corresponding major-axis and flange lateral bending stresses in the girders due to the initial lack-of-fit effects from the TDLF detailing method, and

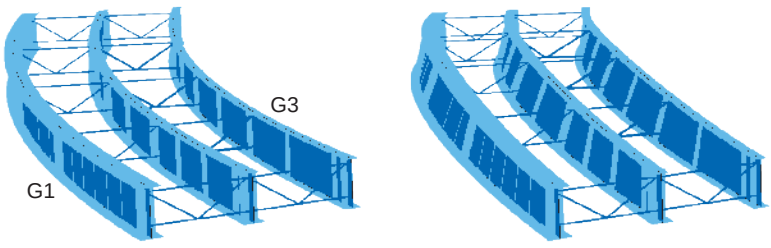

Figure 3-85. FHWA Test Bridge (EISCR1) undeflected geometry and "Configuration 3" deflected geometry due solely to the initial lack of fit from TDLF detailing of the cross-frames.

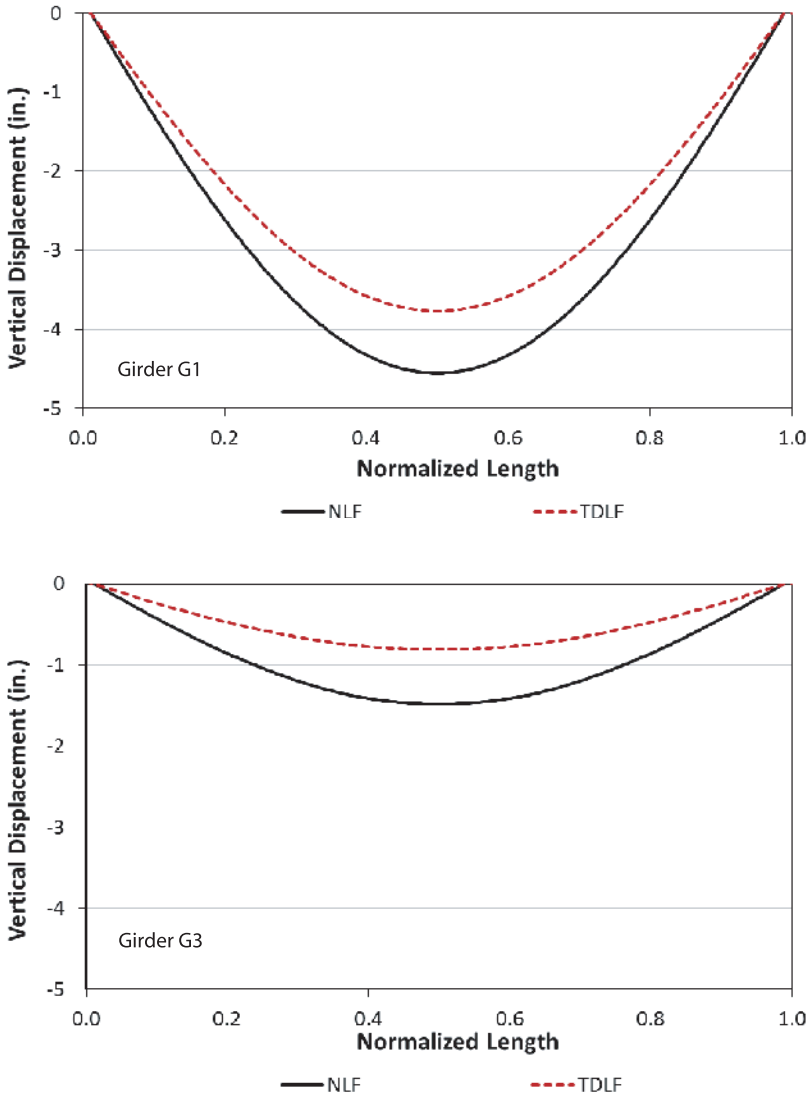

Figure 3-86. FHWA Test Bridge (EISCR1) vertical displacements under total dead load (unfactored) for NLF versus TDLF detailing of the cross-frames.

Figure 3-91 shows the "Configuration 3" cross-frame forces (note that the cross-frame forces in Figure 3-91 are not exactly equal to the difference between the cross-frame forces in Figures 3-88a and 3-88b due to small second-order effects).

Figure 3-92 illustrates the loading mechanism causing a reduction in the downward vertical displacements in all of the girders due to TDLF detailing in the FHWA Test Bridge. Basically, the locked-in forces in the intermediate cross-frames generate an internal couple that is applied to each of the girders at the intermediate cross-frame locations. These couples are balanced by couples in the opposite direction at the bridge bearing lines. The applied internal couples at the intermediate cross-frames twist the girders in the opposite direction from the direction they displace under the total dead load. However, because of the horizontal curvature, the girders cannot twist in this fashion without the girder vertical displacements also being reduced.

In order to obtain a "representative upper-bound" estimate of "slip" at the connections due to small connection tolerances, two scenarios were considered as shown in Figure 3-93. In the first

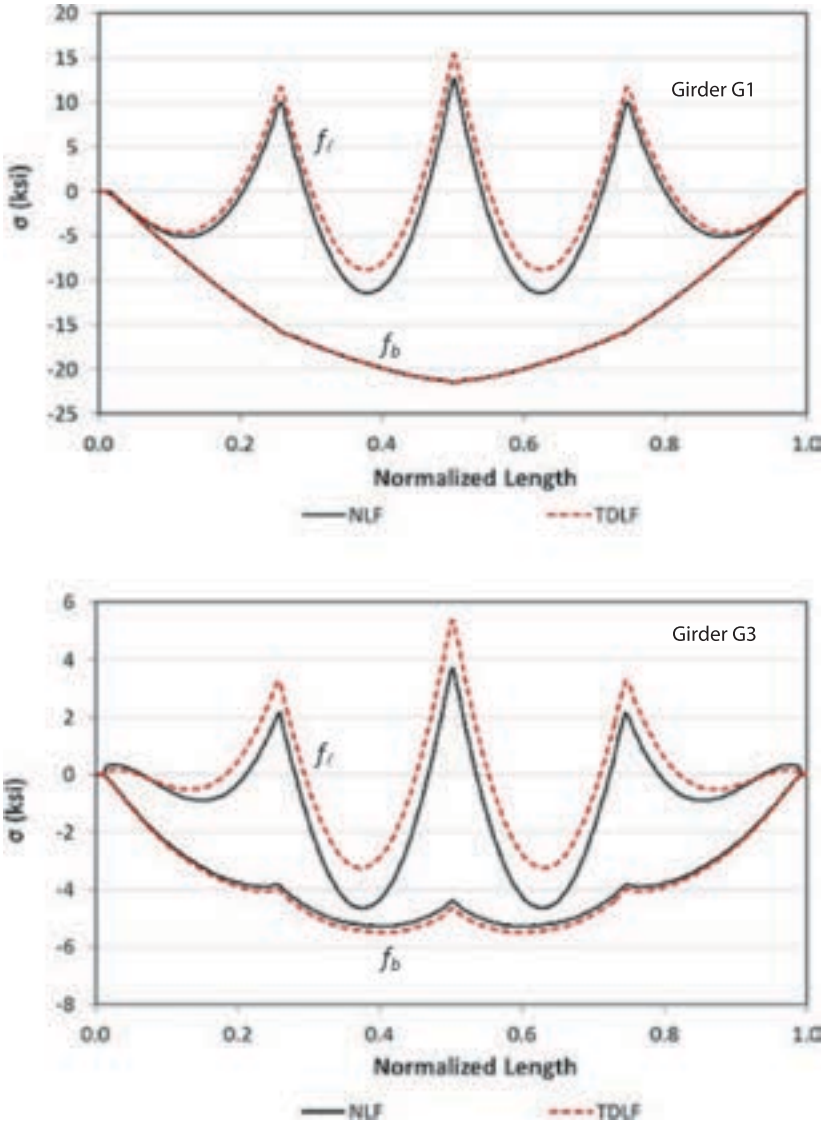

Figure 3-87. FHWA Test Bridge (EISCR1) major-axis bending and flange lateral bending stresses under total dead load (unfactored) for NLF versus TDLF detailing of the cross-frames.

scenario, a ⅛-in. axial movement, or "slip," was assumed in *all* the intermediate cross-frame diagonals of the test bridge. The bridge deformations due to these connection movements are shown in the top image of Figure 3-93. In the second scenario, a ⅛-in. "slip" was assumed in both chords of the three intermediate cross-frames in the direction of their dead load and TDLF axial forces. The deformations corresponding to these movements are shown in the bottom image of Figure 3-93. Figures 3-93 through 3-95 show plots of the corresponding induced girder vertical displacements, flange major-axis and lateral bending stresses, and cross-frame forces due to the first scenario above, and Figures 3-96 through 3-98 show plots of these responses due to the second scenario.

The above ⅛-in. magnitude is obtained by assuming standard size bolt holes 1/16-in. larger than the fasteners and assuming that nominally (or on average) the bolts are in the center of the holes. Then, assuming two plies in every connection, the ideal "slip" that can occur at a given connection is 1/16-in. This value is then multiplied by two to account for the ideal influence of the connection slip at each end on the elongation or shortening of each member.

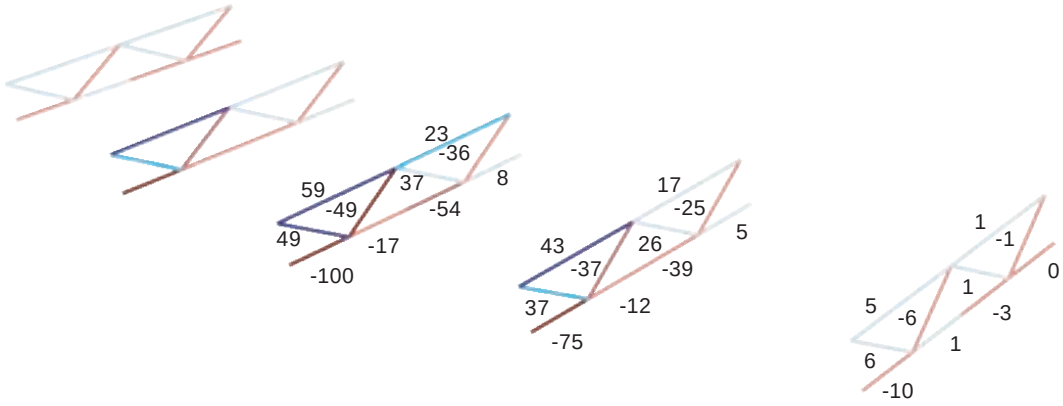

(a) NLF detailing

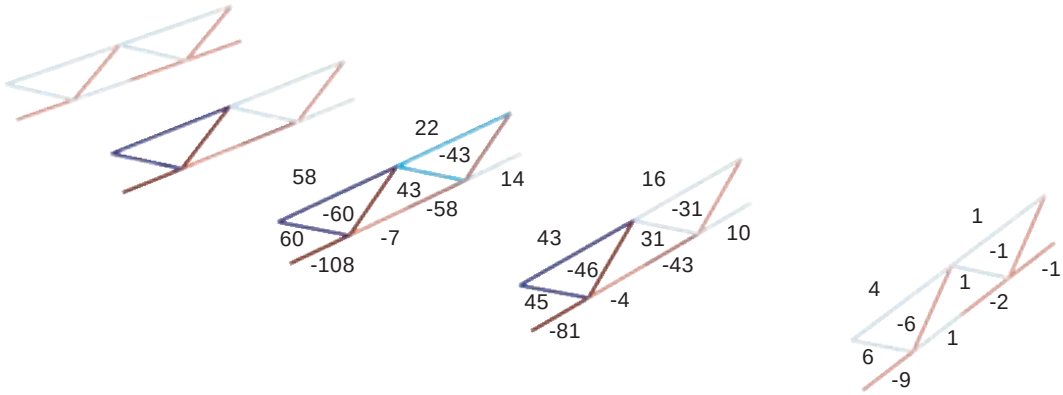

(b) TDLF detailing

Figure 3-88. Cross-frame forces under total dead load (unfactored) for NLF versus TDLF detailing of the cross-frames.

By comparing the values in the above plots, one can observe that the locked-in forces from the TDLF detailing can indeed be reduced to some extent by "joint slip" within standard connection tolerances. However, in this bridge, the TDLF effects are significantly larger than the effects of these "slip" displacements. The other key point that can be noted by considering the above influence of the "slip" displacements is that the use of oversize holes to allow adjustment in the structure basically amounts to giving up control of the geometry by the amount that the connections can move. In addition, the connections have to be engaged before the cross-frames can brace the girders.

This example again shows that the locked-in forces in the cross-frames generally are additive with the dead load effects when SDLF or TDLF detailing is used on curved radially supported bridge structures. Therefore, one can conclude that locked-in forces generally should be considered when sizing the cross-frames in horizontally curved I-girder bridges.

Figures 3-99 and 3-100 provide a combined summary of the above results in terms of the influences of TDLF detailing, as well as the upper-bound connection tolerance movements on the vertical displacements and the girder layovers. The dark solid curve in these figures shows the results for NLF detailing of the cross-frames, and the dashed curve shows the results with TDLF. The light solid curve illustrates the combined results of TDLF detailing along with the ⅛-in. slip in each of the cross-frame diagonals. Finally, the dot-dash curve shows the result of a ⅛-in. slip in all of the internal cross-frame members (diagonals and chords), in the direction of their axial forces, combined with the influence of the TDLF detailing.

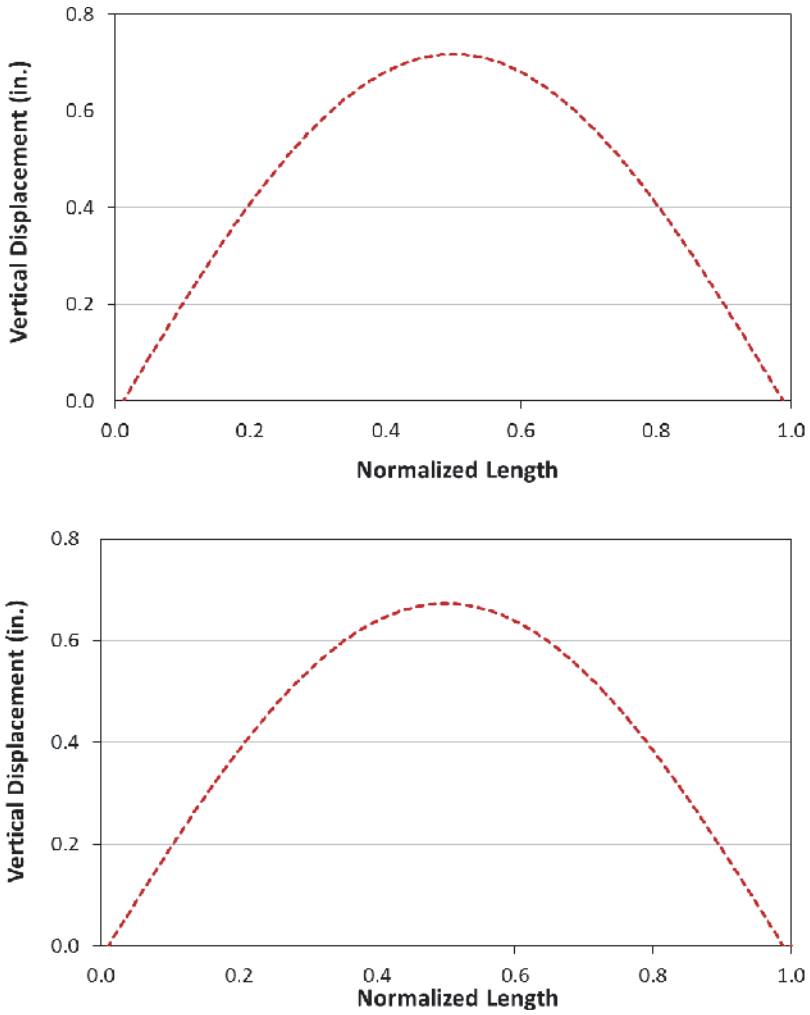

Figure 3-89. FHWA Test Bridge (EISCR1) "Configuration 3" vertical displacements solely due to the initial lack-of-fit effects from TDLF detailing of the cross-frames.

One can conclude that "slip" due to standard connection tolerances within the cross-frames can indeed reduce the influence of TDLF detailing by a significant fraction. However, this is based on a representative upper-bound effect of standard connection tolerances. Indeed, if the TDLF detailing is successful at achieving its objective of approximately plumb webs under the total dead load, then the corresponding girder locked-in vertical deflections, internal stresses, and cross-frame forces would be induced. Similar results are obtained for SDLF detailing, but again, the SDLF effects are smaller (and hence the potential influence of connection tolerances tends to be larger with respect to these effects). In horizontally curved bridges, it can be concluded that TDLF and SDLF detailing effects generally should be included in the structural analysis, since they tend to produce an additive effect on the girder "negative" flange lateral bending stresses and on the cross-frame forces.

3.3.3.3 Potential Influence of Other Connection Tolerances

The previous section considered several scenarios giving an indication of the influence of representative cross-frame connection tolerances on the final constructed geometry, the cross-frame forces, and the girder major-axis and flange lateral bending stresses in the FHWA Test Bridge (EISCR1). It was shown that these connection tolerances can indeed have a measurable effect.

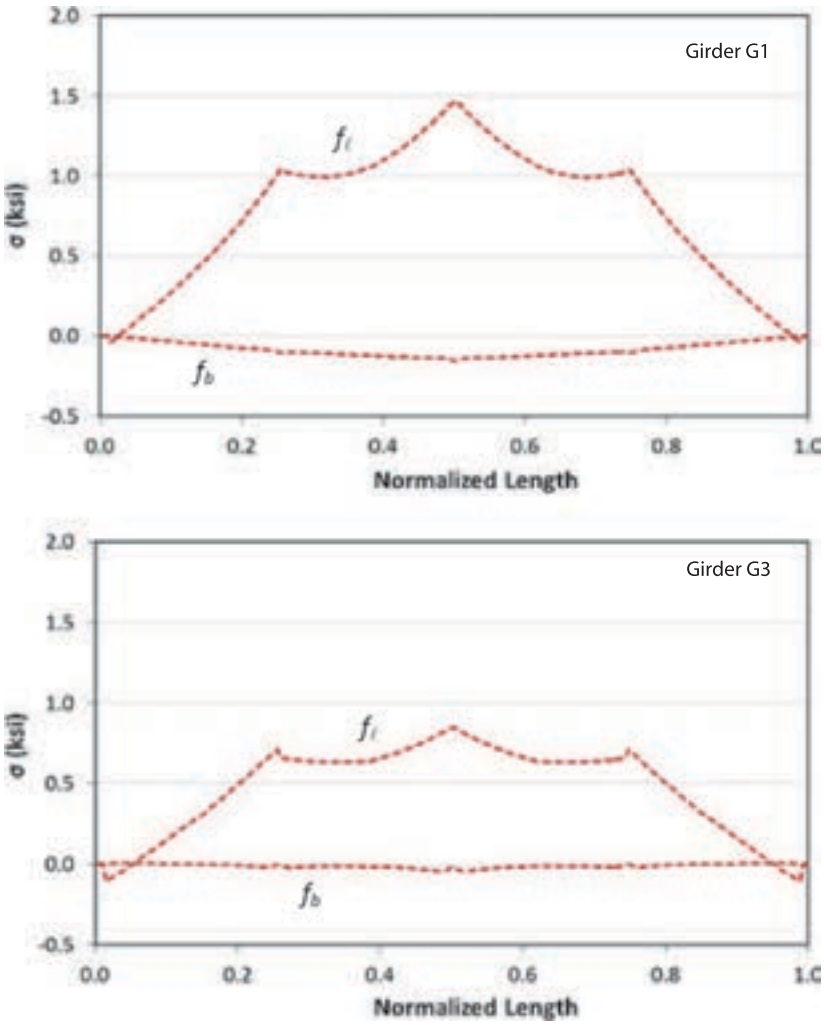

Figure 3-90. FHWA Test Bridge (EISCR1) "Configuration 3" top flange major-axis and lateral bending stresses solely due to the initial lack-of-fit effects from TDLF detailing of the cross-frames.

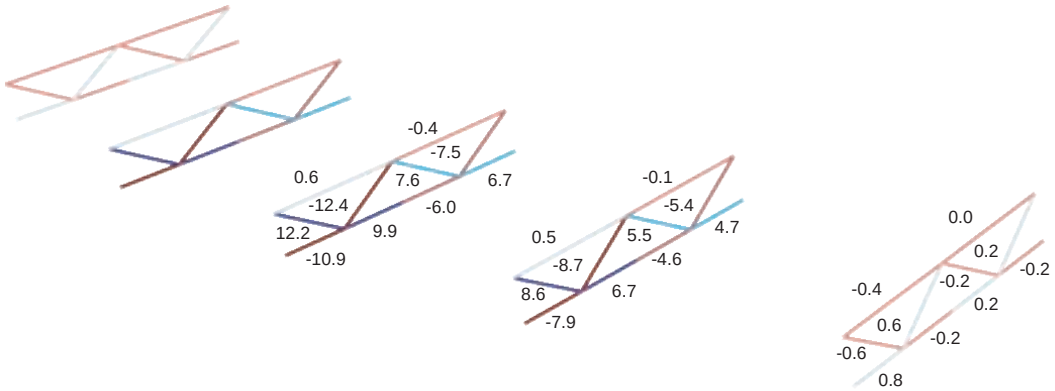

Figure 3-91. FHWA Test Bridge (EISCR1) "Configuration 3" cross-frame forces solely due to the initial lack-of-fit effects from TDLF detailing of the cross-frames.

However, the influence on the overall displacements is not as large as erectors would commonly expect for more general structures based on experience. The discussion below addresses one example scenario where the connection tolerance effects can be significantly larger.

Figure 3-102 illustrates the potential impact of a relative "slip" between the top and bottom of a girder splice. In this case, the impact of the displacement Δ_{slip} between the top and the bottom of the splice is multiplied by the length-to-depth ratio (L/D) of the girder field section. Basically, whenever there is a significant ratio of this sort, there is a lever effect that can have a substantial influence on the constructed geometry. This "lever effect" can also occur across the width of the bridge due to the types of cross-frame connection "slip" displacements discussed in the previous section. However, the FHWA Test Bridge is not wide enough relative to its length to exhibit a significant "lever effect" of the cross-frame connection slip displacements.

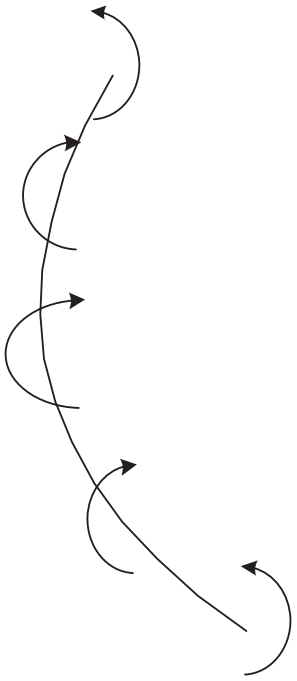

Figure 3-92. Loading mechanism associated with an increase in all the girder vertical displacements due to TDLF detailing in the FHWA Test Bridge (EISCR1).

3.3.4 When Should Locked-in Forces from SDLF or TDLF Detailing be Considered in a Structural Design Analysis?

Table 3-11 summarizes the recommendations and their corresponding rationale from Ozgur (2011) pertaining to the question: When must locked-in forces from SDLF or TDLF detailing be considered in the structural design analysis? Alternately, this question can be phrased as: When can a curved and/or skewed I-girder bridge be designed based on an analysis that assumes NLF detailing, but then the cross-frames are detailed subsequently for either SDLF or TDLF without any significant consequences? The answers are listed in terms of the key bridge responses and are all based on the assumption that the girder cambers are based on

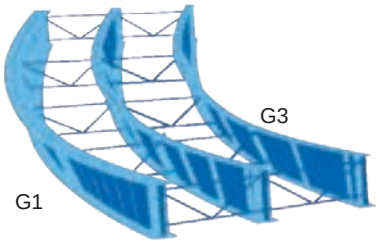

Deformations due to +1/8 inch "slip" in all intermediate cross-frame diagonals (scale factor = 100x)

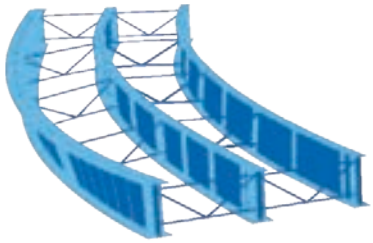

Deformations due to +1/8 inch "slip" in all intermediate cross-frame top and bottom chords (scale factor = 100x)

Figure 3-93. FHWA Test Bridge (EISCR1) deformed geometry solely due to ⅛-in. "slip" in the direction of the internal load in all the intermediate cross-frame diagonals and due to ⅛-in. slip in the direction of the internal load in all the intermediate cross-frame chords.

112 Guidelines for Analysis Methods and Construction Engineering of Curved and Skewed Steel Girder Bridges

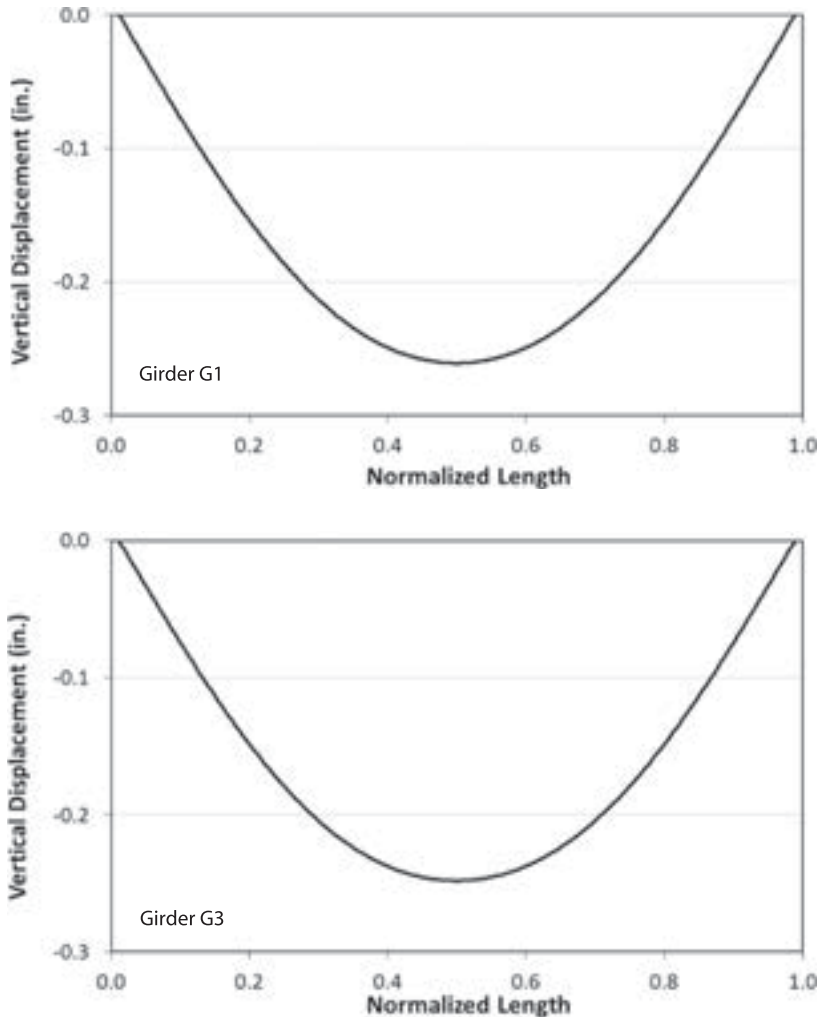

Figure 3-94. FHWA Test Bridge (EISCR1) vertical displacements solely due to ⅛-in. slip in the direction of the internal load in all of the intermediate cross-frame diagonals.

an accurate 2D-grid or 3D FE analysis (see Appendix A for a definition of these terms). These findings are derived from the detailed study of the various bridges analyzed in the NCHRP Project 12-79 Task 8A research.

Based on the basic illustrative examples in Sections 3.3.1 to 3.3.3, one can observe clearly that the answer to the above questions is different for straight-skewed and horizontally curved, radially supported bridges. Furthermore, in short, it can be stated that the influence of SDLF and TDLF detailing on bridges that have both horizontal curvature and skew can involve any combination of the attributes shown for the above distinct bridge types. However, the requirements for when lack-of-fit effects need to be included in the analysis are the same for horizontally curved, radially supported bridges and horizontally curved bridges with skewed supports. Therefore, the rules in Table 3-11 are listed for straight-skewed and skewed and/or curved bridges.

Influence of cross-frame connection tolerances. From the presentations in Sections 3.3.3.2 and 3.3.3.3, clearly connection "slip" displacements can have a substantial influence on the constructed geometry as well as the internal force state in the erected structure. However, this fact

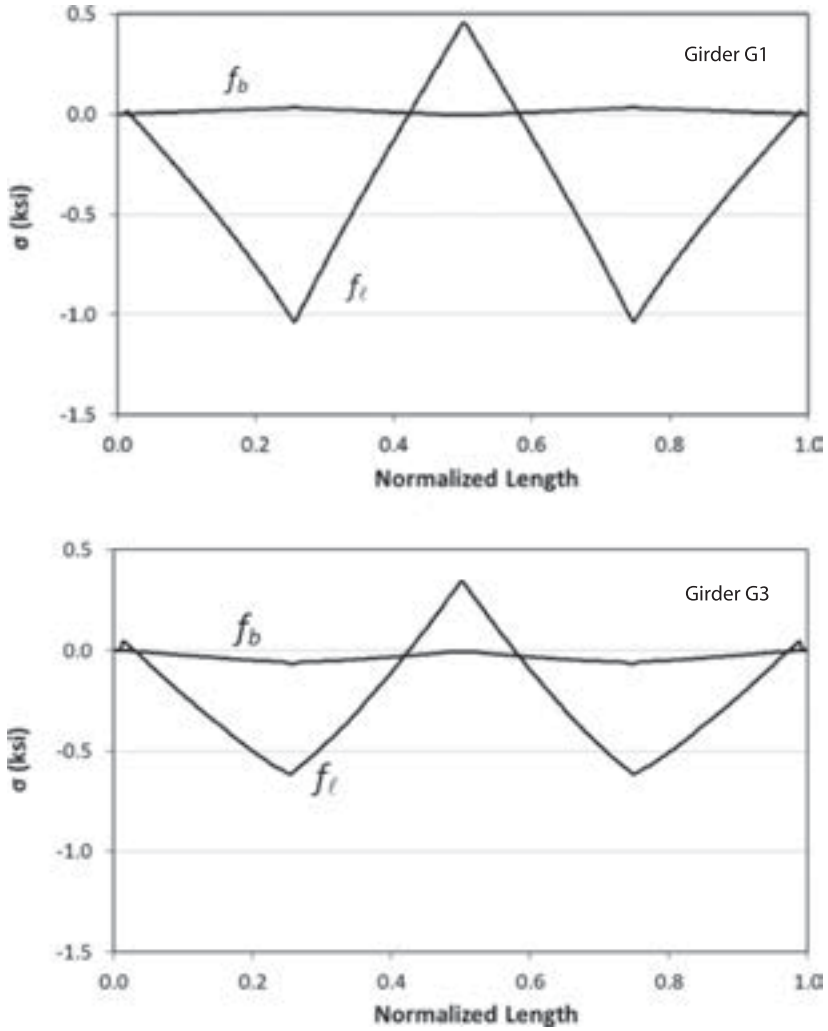

Figure 3-95. FHWA Test Bridge (EISCR1) major-axis bending and flange lateral bending stresses solely due to ⅛-in. slip in the direction of the internal load in all of the intermediate cross-frame diagonals.

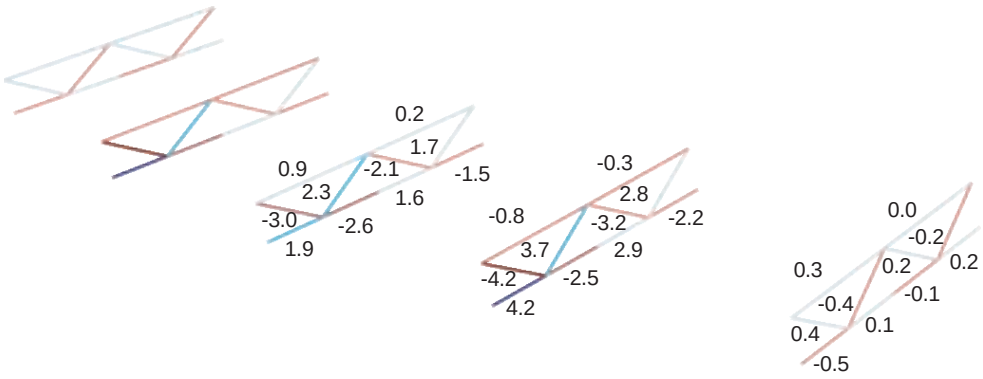

Figure 3-96. FHWA Test Bridge (EISCR1) cross-frame forces solely due to ⅛-in. slip in the direction of the internal load in all of the intermediate cross-frame diagonals.

114 Guidelines for Analysis Methods and Construction Engineering of Curved and Skewed Steel Girder Bridges

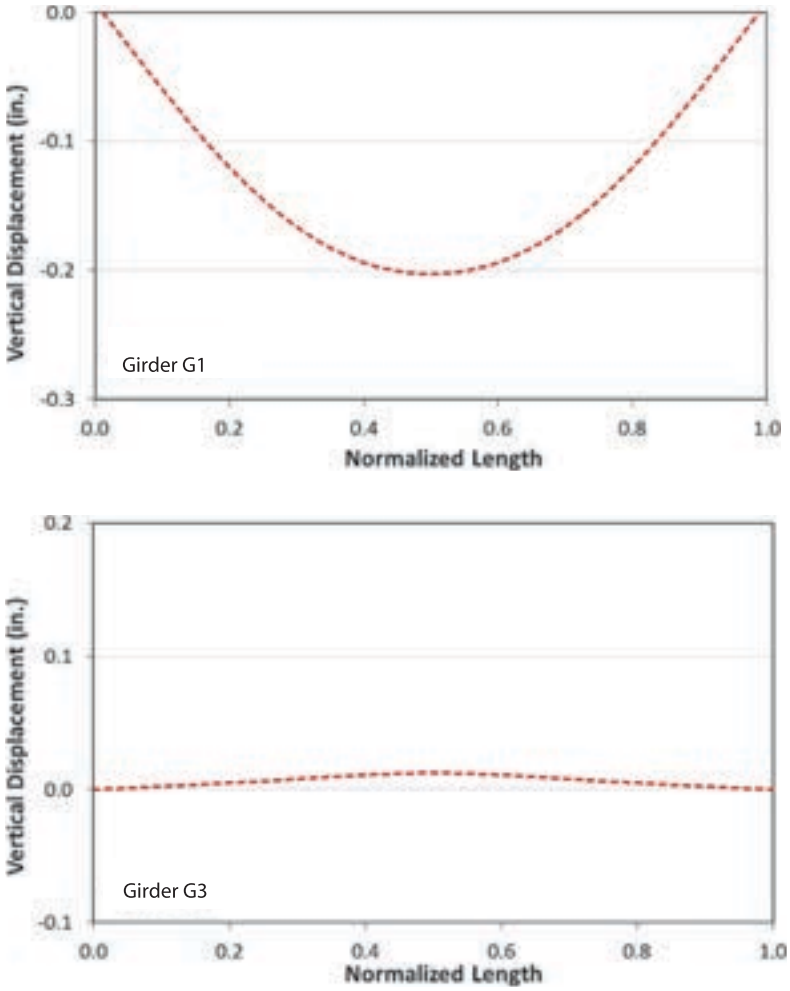

Figure 3-97. FHWA Test Bridge (EISCR1) vertical displacements solely due to ⅛-in. slip in the direction of the internal load in all of the intermediate cross-frame chords.

should not be used as a justification for neglecting initial lack-of-fit effects and the calculation of locked-in forces due to SDLF or TDLF detailing in the structural analysis. Given the above examples and discussions, it is clear that the effects of SDLF and TDLF detailing on the cross-frame forces and girder flange lateral bending stresses are typically additive in curved radially supported I-girder bridges. When these types of structures have longer spans and/or tighter curvatures, the influence of SDLF and TDLF detailing on the girder vertical displacements can be significant. If the cross-frame detailing is indeed successful in controlling the girder layovers, as it is intended to do, these locked-in forces have to exist. However, it is evident that "standard" connection tolerances can nullify much of the SDLF or TDLF detailing effects for bridges with shorter spans or smaller horizontal curvature. Interestingly, when this is the case, the small initial lack of fit is an indication that the cross-frame detailing effects are sufficiently small such that NLF detailing may be a good option.

Impact of using girder cambers from a line-girder analysis in cambering the girders and in SDLF or TDLF detailing of the cross-frames. Table 3-11 is based on the assumption that the girder cambers are determined from an accurate 2D-grid or 3D FE analysis. Some very interesting behavior occurs if the displacements from a line-girder analysis are used in setting the girder

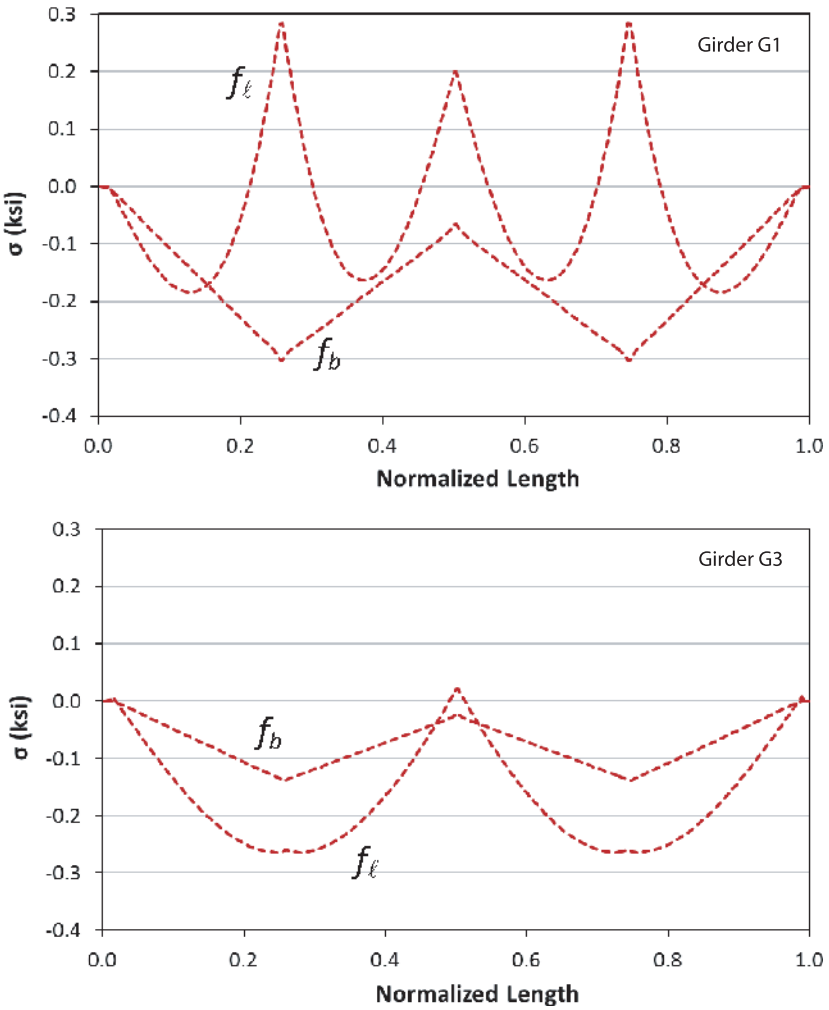

Figure 3-98. FHWA Test Bridge (EISCR1) major-axis bending and flange lateral bending stresses solely due to ⅛-in. slip in the direction of the internal load in all of the intermediate cross-frame chords.

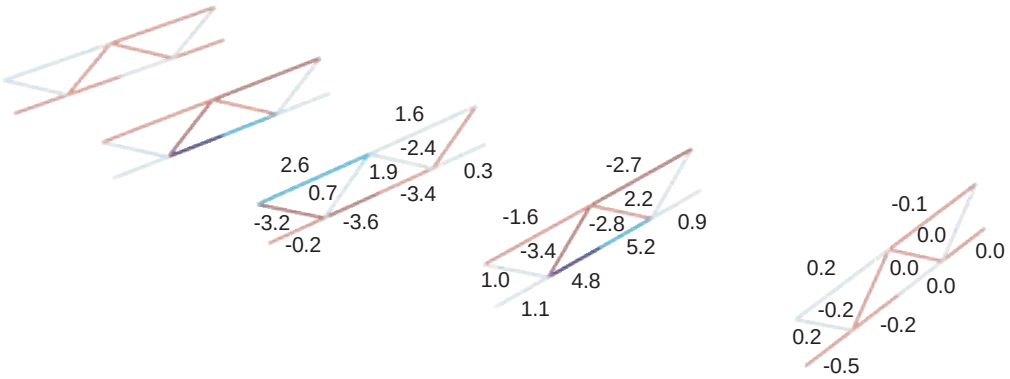

Figure 3-99. FHWA Test Bridge (EISCR1) cross-frame forces solely due to ⅛-in. slip in the direction of the internal load in all of the intermediate cross-frame chords.

116 Guidelines for Analysis Methods and Construction Engineering of Curved and Skewed Steel Girder Bridges

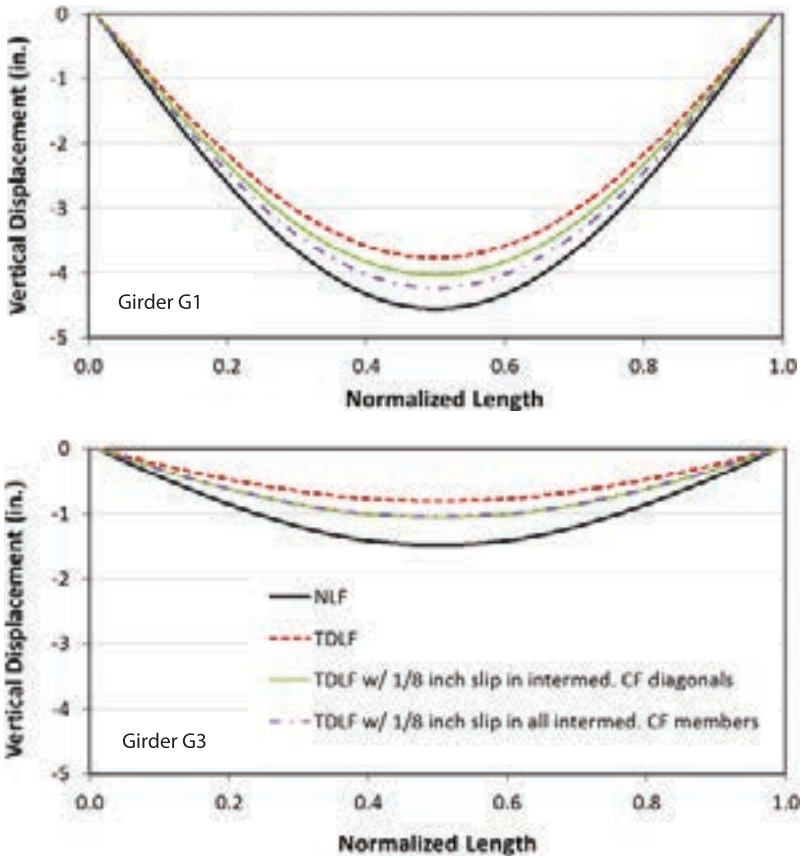

Figure 3-100. FHWA Test Bridge (EISCR1) vertical displacements under the total dead load, based on NLF detailing of the cross-frames, TDLF detailing of the cross-frames with zero tolerance in the fit-up of the connections, and TDLF detailing of the cross-frames with 1/8-in. slip in the direction of the internal load in the intermediate cross-frame diagonals or in all the intermediate cross-frame members.

cambers and detailing the cross-frames for SDLF or TDLF. This behavior, and its implications on the analysis requirements, is detailed below.

- **Steel dead load (SDL) response of straight-skewed bridges with the cross-frames fabricated for SDLF based on line-girder analysis cambers.** For any straight-skewed bridge, if the steel dead load (SDL) cambers are obtained from a line-girder analysis, and if the cross-frames are detailed for SDLF based on these cambers, then theoretically there is zero lack of fit between the girders and the cross-frames *in an idealized unshored SDL configuration* where, prior to engaging the cross-frames, all the girders are placed on the supports and allowed to deflect under the self-weight of the steel. The girder webs are plumb in this configuration, since there is no interaction with the cross-frames. When the cross-frames are detailed for SDLF based on this configuration, they fit-up perfectly with the girders in this configuration without any forcing. Therefore, interestingly, the use of line-girder analysis for SDL gives the "optimum" SDL cambers in that the total cross-frame forces and total flange lateral bending stresses in the SDL condition will be zero. These statements are all predicated on including the correct tributary weights from the cross-frames in the above line-girder analysis.

  Very interestingly, but as should be expected based on a fundamental understanding of the analysis of initial lack-of-fit effects from Section 3.2.5, an accurate 2D-grid or 3D FE analysis

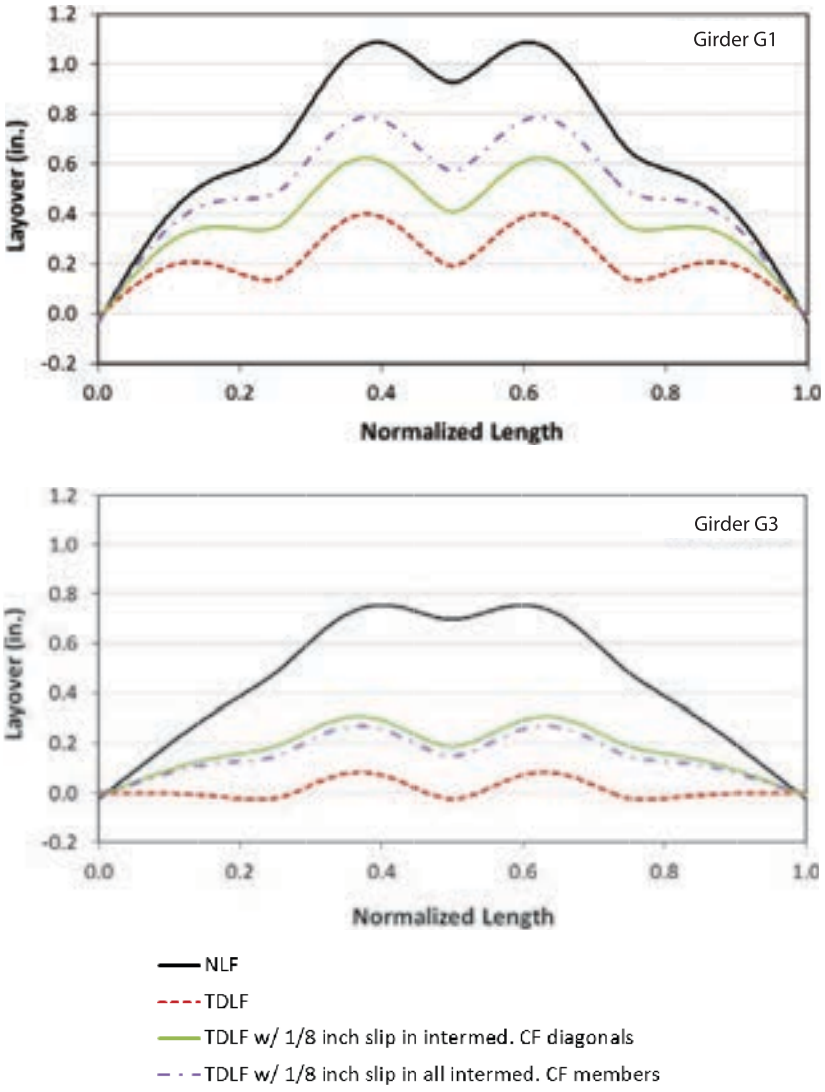

Figure 3-101. FHWA Test Bridge (EISCR1) girder layovers under total dead load, based on NLF detailing of the cross-frames, TDLF detailing of the cross-frames with zero tolerance in the fit-up of the connections, and TDLF detailing of the cross-frames with ⅛-in. slip in the direction of the internal load in the intermediate cross-frame diagonals or in all the intermediate cross-frame members.

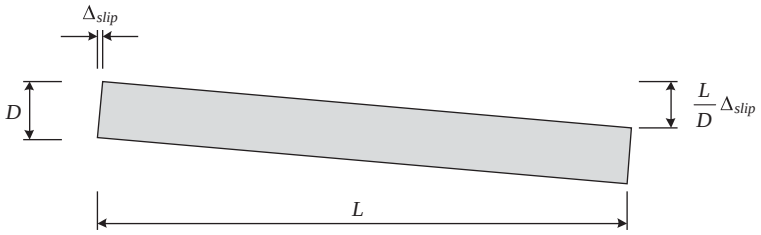

Figure 3-102. Influence of a relative slip between the top and bottom of a girder splice.

118 Guidelines for Analysis Methods and Construction Engineering of Curved and Skewed Steel Girder Bridges

Table 3-11. Summary recommendations and rationale for when the initial lack of fit from SDLF or TDLF detailing should be considered in an accurate 2D-grid or 3D FE analysis (based on the assumption that the cambers are determined from an accurate 2D-grid or 3D FE analysis).

Response	Bridge Type	Lack of Fit Required?	Rationale
Major-axis bending stress f_b	Straight-Skewed Skewed &/or Curved	No	Locked-in f_b is negligible.
General girder vertical displacements, layovers, and final elevations	Straight-Skewed	No	The vertical displacements are insensitive to initial lack-of-fit effects.
	Skewed &/or Curved	Yes	Girder vertical displacements can be affected significantly by cross-frame detailing effects.
Girder layovers in the DL condition corresponding to the type of cross-frame detailing	Straight-Skewed Skewed &/or Curved	No	Approximately plumb webs are obtained.
Cross-frame forces and girder flange lateral bending stresses	Straight-Skewed	Conditionally No	As long as: (1) The first intermediate cross-frames are offset based on Equation 15, and (2) The cross-frames are symmetrical about their mid-length (e.g., no Z-type cross-frames), separate single-size intermediate and bearing-line cross-frames can be designed conservatively and used throughout the bridge based on the maximum member forces obtained from an accurate 2D-grid or 3D FE analysis neglecting lack-of-fit effects (top chord members designed for the maximum tension and the maximum compression determined in the top chord at the cross-frames throughout the bridge, bottom chord members designed similarly, and diagonal members designed similarly). One cross-frame type can be designed for all the intermediate cross-frames, and another for the bearing line cross-frames. In addition, the girder flange lateral bending stresses tend to be predicted conservatively from an accurate 2D-grid or 3D FE analysis neglecting lack-of-fit effects given above caveat Number 1 (e.g., see Figure 3-61). Unfortunately, for bridges with larger skew indices, the conservatism of designing single-size cross-frames in the above fashion can be prohibitive. Since the distribution of the internal cross-frame forces based on NLF detailing (see Figure 3-57) can be very different from that obtained based on SDLF or TDLF detailing (see Figure 3-58), the only alternative if the cross-frames are detailed for SDLF or TDLF is to account for the corresponding locked-in force effects in the analysis. In addition, note that generally, the total forces in the SDL condition (SDL + locked-in, e.g., see Figure 3-60) need to be considered.
	Skewed &/or Curved	Yes	The cross-frame forces and girder flange lateral bending stresses generated by the cross-frame detailing effects tend to be additive with the dead load effects.

of the same straight-skewed bridge matches exactly with the above line-girder analysis results, *but only if initial lack-of-fit effects are considered in the analysis (and only if the lack-of-fit effects are calculated based on the cambers from the line-girder analysis).* Although there is no lack of fit between the cross-frames and the girders in the above SDL condition, there is a lack of fit between the cross-frames and the girders *in the initially fabricated (cambered and plumb) girder geometry.* Therefore, locked-in forces are generated by the SDLF detailing. These locked-in cross-frame forces are exactly equal and opposite to the cross-frame forces from the SDL, and the corresponding locked-in girder flange lateral bending stresses are exactly equal and opposite to the SDL girder flange lateral bending stresses. Assuming that the structural system remains elastic, and neglecting aspects such as friction at the supports and non-zero connection tolerances, the bridge response is unique. That is, regardless of the sequence in which the structure is erected, if the cross-frames are detailed for SDLF based on the cambers from the above line-girder analysis, the total internal cross-frame forces and the girder flange lateral bending stresses are theoretically zero in the final SDL configuration. In summary, *an accurate 2D-grid or 3D FE analysis has to include the initial lack-of-fit effects* (i.e., the corresponding locked-in forces need to be calculated in the analysis) *to properly capture the bridge behavior corresponding to this "optimum" SDL camber-SDLF detailing combination.* The key attributes of this "optimum" combination are summarized again in Table 3-14.

It is important to note that the total dead load (TDL) line-girder analysis responses for a bridge fabricated with the above "optimum" SDL camber-SDLF detailing combination *typically will not be accurate.* The only way to obtain accurate TDL results in general for the above type of bridge is to conduct an accurate 2D-grid or 3D FE analysis *including the initial lack-of-fit effects.*

- **Total dead load (TDL) response of straight-skewed bridges with the cross-frames fabricated for TDLF based on line-girder analysis cambers.** It is very interesting to note that, in many situations, if the TDL cambers are obtained from a line-girder analysis, the total TDL cross-frame forces and girder flange lateral bending stresses tend to be minimized (relative to the results with other cross-frame detailing options). However, these forces and stresses generally are not zero. This is because of (1) the interaction between the girders and cross-frames in the 3D structural system once the cross-frames are engaged, (2) the influence of non-equal loading effects on the fascia girders and the interior girders, (3) the influence of eccentric loads applied to the fascia girders from overhang brackets, and (4) the interaction between the girders and a composite concrete deck, for any construction stages where the deck has gained significant early stiffness and strength. However, in cases with relatively equal load effects on the fascia and interior girders, and if the torsion from eccentric overhang loads on the fascia girders is estimated from a separate analysis, the TDL line-girder analysis results are reasonably accurate for the above case. This fact can be understood by considering the behavior for the "optimum" SDL camber-SDLF detailing combination, and then realizing that the comparable TDL camber-TDLF detailing combination works approximately the same. Similar to the previous summary, *an accurate 2D-grid or 3D FE analysis has to include the initial lack-of-fit effects to properly capture the bridge behavior for this TDLF camber-TDLF detailing combination.* The reader is referred to the Task 8 report (Appendix C of the contractors' final report), Section 7.5.1, for an example illustrating these results. Ozgur (2011) provides additional detailed examples and results.

  Lastly, it is important to note that the steel dead load (SDL) line-girder analysis responses for a bridge fabricated with the above TDL camber-TDLF detailing combination *typically will not be accurate.* The only way to obtain accurate SDL results in general for the above type of bridge is to conduct an accurate 2D-grid or 3D FE analysis *including the initial lack-of-fit effects.*
- **Use of cambers obtained from a V-load analysis on curved or curved and skewed I-girder bridges.** As shown previously in Table 3-1 of Section 3.1.2, the vertical displacements obtained from a 1D line-girder (V-load) analysis can be in error by as much as 20 percent for curved radially supported bridges with $I_C \leq 1$ (C grade in Table 3-1), and by as much as 30 percent for

120 Guidelines for Analysis Methods and Construction Engineering of Curved and Skewed Steel Girder Bridges

curved radially supported bridges with $I_C > 1$ (D grade in Table 3-1). For curved and skewed I-girder bridges, Table 3-1 shows an F grade for the vertical displacements. Therefore, generally the use of a V-load analysis to set the camber profiles in curved or curved and skewed bridges should be discouraged. For curved, or curved and skewed I-girder bridges, the displacements used to set the girder cambers and to establish the cross-frame drops for SDLF or TDLF detailing of the cross-frames generally should be based on an accurate 2D-grid or 3D FE analysis. Regarding whether the initial lack-of-fit effects should be included in the structural design analysis, Table 3-11 then applies.

Section 7.5.2 of the Task 8 report (Appendix C of the contractors' final report) discusses an interesting fact that the V-load analysis results for simple-span radially supported I-girder bridges approximate the physical responses obtained using TDLF detailing better than the responses for SDLF or NLF detailing. This appears to be due to the fact that the girder webs are held in an approximately plumb position at the cross-frame locations when TDLF detailing is used. Ozgur (2011) provides some additional discussion of this behavior.

3.3.5 Estimation of Steel Erection Fit-Up Forces Including SDLF or TDLF Effects

The identification of potential fit-up difficulty during steel erection and the development of erection plans that avoid or alleviate this difficulty is a key task for the erection engineer. This task is often handled based on experience and using relatively simple analysis tools. However, in some situations with longer spans, tighter curves, and sharper skews, a relatively rigorous estimate of the forces required to fit-up the steel may be desirable at certain intermediate stages. This section outlines one recommended process for determining these estimates.

The basic concepts are relatively simple and can be listed as follows:

1. Select a given erection stage where fit-up of the steel is a concern. Numerous factors enter into the decision about which erection stages may need to be evaluated. In very broad terms, fit-up difficulty is typically due to some combination of structural component or unit weights, deflections of the steel components under their self-weight, component resistances to being deformed by come-alongs, jacks, cranes, etc., such that their connections can be made, and site conditions or restrictions that limit the erector's ability to provide temporary supports and/or to apply forces to make a given connection. In many situations, the greatest fit-up difficulty occurs when the connections are made for one of the last girders to be erected in a given span. This is because the incompatibility in the displacements may be significant between the portion of the structure that is already erected, particularly if the structure has significant deflections under its self-weight, and a relatively lightly loaded girder that is being assembled. In addition, the locked-in forces due to SDLF or TDLF detailing of the cross-frames tend to build up as more and more components are connected. It is important to note that there are as many steel dead load configurations as there are erection stages. SDLF detailing commonly is based on the final erected configuration. Therefore, if SDLF detailing is used, the girder webs generally are not close to plumb under steel dead load until all the steel is erected. Particularly when TDLF detailing is used, the locked-in forces can be a significant fraction of the internal forces in the steel during the steel erection.
2. Analyze the structure in the specific configuration attained immediately after the targeted connection is made. The calculated force in the targeted connection at this stage is a direct indicator of the forces that need to be applied to make the connection. This is because, just prior to making the connection, the connection force is, of course, zero. As noted previously, the locked-in forces from any initial SDLF or TDLF lack of fit between the cross-frames and the girders in their initial fabricated (cambered and plumb) geometry can be significant in some cases. These lack-of-fit effects can be included in the analysis with relative ease using

the procedures discussed previously in Section 3.2.5. The actual forces that the erector must apply are, of course, generally different from the above connection force. However, given the connection force that needs to be developed, along with the selection of rigging and other equipment, reasonable estimates can be made of the actual forces the erector will need to apply.

If the estimated fit-up forces are too large, manipulate the temporary supports, holding cranes, and other devices to limit the displacement incompatibility (the lack of fit in the deformed geometry) that needs to be resolved at the stage just prior to making the connection.

3.4 Pros and Cons of Different Cross-Frame Detailing Methods

There is much variety in the industry across the United States regarding practices and preferences pertaining to the detailing of the cross-frames to affect the constructed geometry of curved and/or skewed bridges and to achieve successful erection of the structural steel. In many cases, this variety of practices does not mean that one method is "wrong" or another answer is "better." Rather, there is often more than one right answer, and successful practices vary widely based on local preferences, local strengths, and specific characteristics of a given bridge.

In recognition of the above, this section aims to synthesize the wide range of information about each of the main cross-frame detailing methods (NLF, SDLF, and TDLF) learned from the NCHRP Project 12-79 studies in the form of "pro facts," "con facts," and commentary about these facts and their implications and applications to the two basic types of I-girder bridges addressed in the previous sections: straight-skewed and horizontally curved radially supported. The intent is to provide a reasonably comprehensive accounting of the various factors that can influence the choice of a method, so that designers, detailers, fabricators, erectors, and owners have information readily at hand.

Tables 3-12 through 3-17 provide a synthesis of the pro facts, con facts, and commentary for straight-skewed bridges while Tables 3-18 through 3-23 provide this information for horizontally curved radially supported bridges. These tables are followed by a short discussion of horizontally curved bridges with significant skew of their bearing lines and detailing for special cases such as widening projects, phased construction, and specific tub-girder bridge considerations.

As would be expected, horizontally curved bridges with significant skew generally exhibit a combination of the characteristics detailed in the above tables for straight-skewed and curved radially supported bridges. If the skews increase the girder length on the outside of the curve,

Table 3-12. Pro facts and commentary, straight-skewed I-girder bridges with NLF detailing—no lack of fit between the cross-frames and the girders in the fabricated (cambered and plumb) no-load geometry of the girders (Configuration 1 of Figure 3-30); plumb girder webs in the no-load state after connecting the cross-frames (Configurations 2 and 3 of Figure 3-30).

Pro Facts:	Commentary:
• The steel fits together with zero applied force in the no-load condition.	• This facilitates erection in a shored configuration approximating the theoretical no-load condition. However, erection under other shored or unshored conditions is practically always achievable for straight-skewed bridges, particularly if SDLF detailing is used. Furthermore, NLF detailing leads to other undesirable consequences on straight-skewed bridges as discussed in Table 3-13.
• The locked-in forces are zero.	• As a result, the structural analysis is simpler. When the cross-frames are detailed for NLF, the cross-frame forces are theoretically as analyzed by the designer for SDL, TDL, and LL+I. No additional locked-in forces are present.

122 Guidelines for Analysis Methods and Construction Engineering of Curved and Skewed Steel Girder Bridges

Table 3-13. Con facts and commentary, straight-skewed I-girder bridges with NLF detailing.

Con Facts:	Commentary:
• Due to differential displacements and rotations between the girders, the steel does not fit together in an unshored SDL condition without applying forces.	• This is not a problem for smaller spans and/or smaller skew indices. However, for longer span lengths and larger skew indices, temporary shoring or hold cranes will likely be required. The erector may encounter fit-up difficulty if the girders are not supported by holding cranes or temporary supports such that their dead load deflections are limited. • In some cases, the erector may have to affect the relative vertical elevation of the girders, in addition to twisting a girder, to install a cross-frame. Affecting the relative girder vertical elevations typically is much more difficult to accomplish. In straight-skewed bridges, this problem can be alleviated by (1) temporary shoring or hold cranes, if NLF detailing is used, (2) the use of SDLF detailing and allowing the steel to deflect to its unshored SDL profile (this may require temporary shoring or holding to that profile; also, see the subsequent discussion of the "optimum" girder SDL cambers for SDLF detailing in straight-skewed bridges), and (3) generally, offsetting the first intermediate cross-frames relative to the bearing lines based on Equation 15 of Section 3.3.1.6, $a \geq \max(1.5D, 0.4b)$.
• The girders twist (i.e., lay over) under any dead load conditions. At highly skewed end bearing lines, the TDL layover of the girders tends to be large.	• More expensive bearings may be required in some instances at heavily skewed bearing lines, unless the dead load rotations are accommodated by modifying the bevels of the sole plates (note that beveled sole plates are already common in many bridges to accommodate grade changes along the length of the bridge). • The deck dead load lateral deflections due to girder layover must be addressed in the alignment of any deck joints. • Substantial layover of the girders under the TDL (in the final constructed condition) may be visually objectionable. • The NCHRP Project 12-79 research, as well as other prior research studies, has shown that the influence of girder layovers on the system ***strength*** is negligible as long as the checks for global stability, stability between the cross-frame locations, and bracing of the girders are satisfied. • If desired, the layover of the girders at the completion of the erection can be estimated accurately, based on the Table 3-1 guidance. These layovers may be specified on the engineering drawings to indicate the expected geometry.
• The locked-in forces are zero, since the girders are not "reverse twisted" during the installation of the cross-frames.	• At the end of the construction (i.e., under TDL conditions), the internal cross-frame forces and girder flange lateral bending stresses tend to be larger (compared to the results with other cross-frame detailing methods) due to the effects of torsion, since these forces and stresses are not offset by any locked-in force effects that would have been introduced by initial lack of fit in the no-load condition if the SDLF or TDLF cross-frame detailing methods were used.

the skew effects tend to amplify the horizontal curvature effects (i.e., the bridge tends to exhibit a significant overall twist rotation of its cross-section within the span). If there is a sharp skew that increases the length of the girder on the inside of the curve, the bridge tends to behave more like a straight-skewed structure.

In cases involving widening projects and/or phased construction where new cambered girders are placed next to an existing decked girder line under total dead load, detailing the cross-frames to fit between the steel dead load profile of the new girders and the total dead load profile of the decked girders at the time of the erection is one option. Another option is to not provide any cross-frame diagonals to transfer shear between the new and existing girders until after the deck is placed on the new girders.

Because of the inherent torsional stiffness of the tub girders, and to maintain equal heights of the webs on both sides of the tubs, these girder types are commonly detailed with their cross-section rotated parallel to the bridge cross-slope in the initial no-load configuration. The bearing-line diaphragms are commonly detailed so that they can be subassembled, then fitted

Table 3-14. Pro facts and commentary, straight-skewed I-girder bridges with SDLF detailing—cross-frames fabricated such that they do not fit-up with the girders in their fabricated (cambered and plumb) no-load geometry (Configuration 1 of Figure 3-30); the erector must generally "reverse twist" the girders during the installation of the cross-frames to achieve fit-up (Configuration 3 of Figure 3-30).

Pro Facts:	Commentary:
• Locked-in forces are generated by the initial lack of fit between the cross-frames and the girders in their fabricated (cambered and plumb) no-load geometry.	• The girder webs will be approximately plumb at the end of the steel erection. This results in a web plumb condition, which is easy to measure and inspect at a time when the erector is still on site and the deck has not yet been cast (thus allowing better opportunity to correct any misalignments). • The girder vertical displacements are relatively insensitive to the lack-of-fit effects from SDLF detailing in straight-skewed I-girder bridges. • The internal cross-frame forces and girder flange lateral bending stresses tend to be minimized under the SDL conditions (compared to the results from other methods of cross-frame detailing). The corresponding TDL forces and stresses (at the end of the construction) generally still are significant, but are reduced relative to the results for NLF detailing. • The tendency for uplift at bearings (e.g., uplift at bearings located at the acute corners of a simply supported bridge plan) is minimized under the SDL conditions (compared to the other methods of cross-frame detailing). This is a direct result of the internal cross-frame forces being minimized.
• At highly skewed end bearing lines, the TDL layover of the girders is smaller than that for NLF detailing.	• Depending on the skew angle of the bearing line and the rotation capacity of the bearings, the layover of the girders at the bearing line may be acceptable.
• The lack of fit between the cross-frames and the girders, *under any unshored SDL erection conditions*, tends to be small compared to the results from other methods of cross-frame detailing (this applies only to straight-skewed bridges).	• For straight-skewed bridges, the girder unshored SDL deflections during the steel erection tend to largely offset the SDL cambers, even though the SDL cambers are based on the state at the completion of the steel erection. • The discussion below of the "optimum" SDL cambers requires a thorough understanding of the behavior, but aids in understanding these general statements.

(continued on next page)

to the girder bottom flange and web assemblies in the shop (i.e., they are detailed for no-load fit [NLF]). The stiffeners are kept normal to the bottom flange (AASHTO/NSBA, 2006). At a skewed bearing line, if the diaphragm plate also is kept normal to the flanges, this means the major-axis bending camber rotation of the girders (at the bearing) must be accounted for in determining the fabricated profile of the diaphragm plate. Otherwise, the profile geometry of the diaphragm plate will not fit-up with the profile geometry of the tub girders without some forcing.

Intermediate external cross-frames (or diaphragms) in tub-girder bridges can be installed no-load fit (NLF) or a special steel dead load fit (SDLF) to the tub girders in their unshored deflected position under the steel self-weight (special because both the vertical deflections and the torsional rotations of the tub girders are considered). This latter detailing of the intermediate external cross-frames allows them to be installed theoretically without having to apply any force to the girders, assuming that the girders are in an unshored deflected position at the time of the installation. These cross-frames are subsequently effective to help restrain relative torsional movement between the tub girders during the placement of the deck (although, they are not effective in restraining the relative movements between the tub girders under the steel self-weight). If the cross-frames are detailed for this special SDLF, they will then

(text continues on page 133)

124 Guidelines for Analysis Methods and Construction Engineering of Curved and Skewed Steel Girder Bridges

Table 3-14. (Continued).

Pro Facts:	Commentary:
• Line-girder analysis provides the "optimum" SDL cambers for SDLF detailing of the cross-frames *in straight-skewed bridges*.	• This statement applies only to straight-skewed bridges and only to SDLF detailing. • "Optimum" means that the total cross-frame forces and girder flange lateral bending stresses in the SDL condition, produced by the sum of the SDL forces and the locked-in forces (from the lack of fit in the NL geometry due to SDLF detailing), are minimized. • If the girder SDL camber is obtained from a line-girder analysis, then theoretically, there is zero lack of fit between the girders and the cross-frames *in an idealized unshored SDL configuration* where, prior to engaging the cross-frames, all the girders are placed on the supports and allowed to deflect under the self-weight of the steel. • The girder webs are plumb in this condition, since there is no interaction with the cross-frames. • If the girders are detailed for SDLF based on the above cambers, zero force is required to fit-up the cross-frames with the girders in the above *idealized unshored SDL configuration*. • Correspondingly, once all the cross-frames are fully connected in this configuration to complete the steel erection, the internal cross-frame forces and the girder flange lateral bending stresses will be zero. • Assuming that the structural system remains elastic, and neglecting aspects such as friction at the supports and non-zero connection tolerances, the bridge response is unique. That is, regardless of the sequence in which the structure is erected, if the cross-frames are detailed for SDLF based on the cambers from a line-girder analysis, the internal cross-frame forces and the girder flange lateral bending stresses are theoretically zero in the final SDL configuration. • Although there is no lack of fit in the above idealized SDL condition, there is a lack of fit between the cross-frames and the girders *in the initially fabricated (cambered and plumb) girder geometry*. Therefore, locked-in forces are generated by the SDLF detailing. • If the SDL cambers are obtained based on an accurate 2D-grid or 3D FE analysis, rather than a line-girder analysis, the sum of the SDL and lack-of-fit forces will be non-zero even though the cross-frames are detailed for SDLF. This is because the interaction between the girders and cross-frames in the 3D structural system modifies the girder SDL displacements from the values discussed above. The torsional effects of the distributed vertical loads (the self-weight of the steel) cannot be perfectly offset by the locked-in concentrated forces at the cross-frame locations. Generally, the above sum of the SDL forces and the locked-in forces is not negligible, but tends to be relatively small as long as the first intermediate cross-frames are sufficiently offset from the bearing lines based on Equation 15 of Section 3.3.1.6, $a \geq \max(1.5D, 0.4b)$.

Table 3-15. Con facts and commentary, straight-skewed I-girder bridges with SDLF detailing.

Con Facts:	Commentary:
• Locked-in forces are generated.	• In general, an accurate 2D-grid or 3D FE analysis is required to accurately assess the bridge responses at the end of the construction (i.e., under TDL conditions), as well as for any conditions other than SDL. Generally, for $I_S > 0.30$, accurate calculation of the responses by line-girder analysis is possible only for the SDL condition, and only if the SDL cambers are set based on the line-girder analysis.
• The locked-in forces are not sufficient to offset the TDL forces in the final constructed condition.	• At the TDL level, the cross-frame forces and girder flange lateral bending stresses can be significant, and need to be considered in the design, although they are smaller than when NLF detailing is used. • At the end of the construction (i.e., under TDL conditions), the cross-frame forces and girder flange lateral bending stresses tend to be larger than for the case of TDLF detailing, although these forces and stresses are smaller than for NLF detailing. • Line-girder analysis provides an accurate characterization of SDL vertical deflections and major-axis bending stresses in straight-skewed bridges, if the cross-frames are detailed for SDLF using the line-girder analysis cambers. For any other conditions and/or combinations with SDLF detailing, line-girder analysis can provide erroneous predictions of the girder vertical deflections and major-axis bending stresses. The magnitude of the errors is strongly correlated with the skew index I_S. • When the concrete deck is placed and other appurtenances are added to the bridge, the resulting cross-frame forces can be substantial in bridges with a large skew index, due to the torsional interactions within the system. In general, if SDLF detailing is used, accurate calculation of the cross-frame forces and flange lateral bending stresses in the TDL condition (from the sum of the TDL effects plus the locked-in force effects) requires the use of an accurate 2D-grid or 3D FE analysis including the modeling of the initial lack of fit.
• At highly skewed end bearing lines, the TDL layover of the girders still may be large.	• More expensive bearings may be required in some instances at heavily skewed bearing lines, unless the dead load rotations are accommodated by modifying the bevels of the sole plates (note that beveled sole plates are already common in many bridges to accommodate grade changes along the length of the bridge). • The deck dead load lateral deflections due to girder layover must be addressed in the alignment of any deck joints. • Substantial layover of the girders under the TDL (in the final constructed condition) may be visually objectionable. • The NCHRP Project 12-79 research, as well as other prior research studies, has shown that the influence of girder layovers on the system ***strength*** is negligible as long as the checks for global stability, stability between the cross-frame locations, and bracing of the girders are satisfied.
• For longer spans, the difference between the girder SDL displacements obtained from a line-girder analysis versus an accurate 2D-grid or 3D FE analysis can be significant.	• This is due to the interaction between the girders and the cross-frames in the 3D system. However, as noted in the pros for SDLF detailing, setting the cambers and the SDLF detailing based on a line-girder analysis tends to minimize the lack of fit between the girders and the cross-frames in any unshored SDL erection conditions. • If the SDL camber is based on line-girder analysis, an accurate 2D-grid or 3D FE analysis can reproduce the line-girder analysis (and the physical/actual) vertical deflections, but only if lack-of-fit effects are included in the analysis. An accurate 2D-grid or 3D FE analysis does not give the correct girder vertical displacements for a bridge where the SDL cambers are based on line girder analysis, unless the lack-of-fit effects are included in the analysis.

126 Guidelines for Analysis Methods and Construction Engineering of Curved and Skewed Steel Girder Bridges

Table 3-16. Pro facts and commentary, straight-skewed I-girder bridges with TDLF detailing—cross-frames fabricated such that they do not fit-up with the girders in their fabricated (cambered and plumb) no-load geometry (Configuration 1 of Figure 3-30); the erector must essentially "reverse-twist" the girders during the installation of the cross-frames to achieve fit-up (Configuration 3 of Figure 3-30).

Pro Facts:	Commentary:
• Locked-in forces are generated by the initial lack of fit between the cross-frames and the fabricated (cambered and plumb) no-load geometry of the girders.	• The girder webs will be approximately plumb at the end of the construction (i.e., at the TDL level). • The girder vertical displacements are relatively insensitive to the lack-of-fit effects from TDLF detailing in straight-skewed I-girder bridges. • The internal cross-frame forces and girder flange lateral bending stresses (due to the sum of the dead load effects plus the locked-in force effects) tend to be minimized under the TDL conditions (compared to the results from other methods of cross-frame detailing). • The tendency for uplift at bearings (e.g., uplift at bearings located at the acute corners of a simply supported bridge plan) is minimized under the TDL conditions, compared to the other methods of cross-frame detailing. • The final internal force and stress state and the girder deflections in the TDL condition can be approximated from a line-girder analysis, if the TDL cambers are set based on a line-girder analysis and the cross-frames are detailed for TDLF. However, the accuracy of the line-girder analysis degrades as a function of the bridge skew index. A line-girder analysis predicts zero cross-frame forces and zero flange lateral bending stresses. The sum of the TDL effects plus the locked-in force effects generally is not zero, although this sum tends to be minimized as noted above. • Line-girder analysis provides an accurate characterization of the TDL vertical deflections and major-axis bending stresses in straight-skewed bridges, as long as the cross-frames are detailed for TLDF using the TDL line-girder analysis cambers. For any other loading conditions combined with TDLF detailing (e.g., the SDL vertical deflections of a bridge using TDLF detailing), line-girder analysis can provide erroneous predictions of the girder vertical deflections and major-axis bending stresses. The magnitude of these errors is strongly correlated with the skew index I_S.
• The TDL layover of the girders is approximately zero, even at highly skewed end bearing lines.	• This minimizes the total, long-term (permanent) rotation demand on the bearings. Also, this allows the use of a target TDL geometry in which the girders are assumed to be plumb for the layout of deck joints, etc.
• On bridges with constant cross-slope, detailing for TDLF allows the cross-frames to be built identically, with one fabrication set-up and one piece-mark for multiple frames.	• This makes the fabrication of the cross-frames more efficient and economical and facilitates the handling of the cross-frames during the erection.

Table 3-17. Con facts and commentary, straight-skewed I-girder bridges with TDLF detailing.

Con Facts:	Commentary:
• Significant locked-in forces are generated.	• In general, a more complex analysis is required for any conditions other than TDL. Even for evaluating the TDL condition, an accurate 2D-grid or 3D FE analysis, including the influence of the initial lack of fit between the cross-frames with the girders in their fabricated (cambered and plumb) no-load geometry, is necessary to obtain accurate cross-frame forces and girder flange lateral bending stresses for bridges with larger skew indices. • In some cases, the cross-frame forces and girder flange lateral bending stresses under the SDL (due to the sum of the steel dead weight plus the locked-in force effects) at a given stage of steel erection can be larger than the corresponding TDL values at the end of the construction. If the bridge girders are connected to the cross-frames and supported in a configuration between the SDL and NL conditions, these forces and stresses can be even larger. *Therefore, during interim stages of the steel erection, the locked-in force effects can be significant and should be considered in the design.* It should be noted that the locked-in forces tend to be smaller at the earlier stages of the steel erection. These forces build up as more and more components are assembled into the structural system. • The corresponding forces and stresses under the TDL (at the end of the construction), due to the sum of the dead load effects plus the locked-in force effects, are relatively small compared to the results from the other methods of cross-frame detailing. However, generally, they are not negligible unless the skew index is smaller than $I_S = 0.30$. These non-zero cross-frame forces and girder flange lateral bending stresses are due to the interaction between the girders and the cross-frames (as well as the girders and the slab for construction stages after portions of the concrete deck start to act compositely). The torsional effects of the distributed dead loads cannot be perfectly offset by the locked-in concentrated forces at the cross-frame locations.
• The girder webs will not be plumb under the NL or SDL conditions, once the girders are connected to the cross-frames. The girders will be laid over in the opposite direction from the direction in which they twist under the application of the dead loads.	• The bearings at support lines with significant skew can be subjected to relatively large rotation demands under various NL and SDL conditions during erection and prior to placement of the concrete deck. However, these rotations are temporary and are not additive with the rotation demands due to live loads. If necessary, blocking may be used to protect the bearings at these locations. • If desired, the layover of the girders at the completion of the steel erection can be estimated from an accurate 2D-grid or 3D FE analysis. These layovers can be specified on the engineering drawings to indicate the expected geometry.
• Caution: The girders can be plumb only under one TDL condition.	• If there are significant DC2 loads (such as a substantial utility load, barrier rail load, or wall load), the designer must decide under which TDL the girders should be plumb.
• Caution: Various incidental effects may have an influence on the bridge TDL responses.	• If early stiffness gain on the concrete deck from prior deck casting stages, or from set-up of the concrete during a given stage, is expected to be a factor, these effects would need to be considered in the calculation of the TDL displacements, internal forces, and internal stresses. In addition, other incidental effects such as tipping restraint at the bearings, participation of the metal deck forms, temporary timber struts between girders, welding of rebar between shear studs on adjacent girders, etc., can influence the response and may need to evaluated when ***estimating*** the TDL displacements, internal forces, and internal stresses.
• The lack of fit between the cross-frames and the girders is *maximized under any shored or unshored SDL erection conditions*, compared to the results from other methods of cross-frame detailing.	• For longer spans and larger skew indices, the forces required to fit-up the cross-frames with the girders during the steel erection can be substantial. This is because the TDL major-axis bending deflections have not yet occurred (since only the steel self-weight load is on the structure). Furthermore, for longer spans, the girders tend to be deeper, the girders tend to be more closely spaced relative to their depth, the flanges tend to be larger, and overall, the girders tend to be harder to deform to resolve the incompatibility in displacements between the cross-frames and the girders under the SDL. • The girder SDL deflections typically can be used to reduce the lack of fit between the girders and the cross-frames in an unshored SDL erection condition. In many situations, this may be sufficient to limit the magnitude of the forces the erector will need to apply to get the steel to fit up.

128 Guidelines for Analysis Methods and Construction Engineering of Curved and Skewed Steel Girder Bridges

Table 3-18. Pro facts and commentary, curved radially supported I-girder bridges with NLF detailing—no lack of fit between the cross-frames and the girders in the fabricated (cambered and plumb) no-load geometry of the girders (Configuration 1 of Figure 3-30); girder webs plumb in the no-load state after connecting the cross-frames (Configurations 2 and 3 of Figure 3-30).

Pro Facts:	Commentary:
• The steel fits together with zero applied force in the no-load condition.	• This facilitates erection in a shored configuration approximating the theoretical no-load condition. However, erection under other shored or unshored conditions should be feasible for smaller spans and/or smaller curvature.
• The locked-in forces are zero.	• As a result, the structural analysis is simpler. When the cross-frames are detailed for NLF, the cross-frame forces are theoretically as analyzed by the designer for SDL, TDL, and LL+I. No additional locked-in forces are present.
• NLF detailing tends to minimize the total cross-frame forces, as well as the girder flange "negative" lateral bending moments over the cross-frame locations.	• This is because the locked-in cross-frame forces due to SDLF or TDLF detailing of the cross-frames tend to be additive with the SDL and TDL cross-frame forces in curved radially supported bridges (see the subsequent "con" discussions for SDLF and TDLF cross-frame detailing). • This statement is true both for situations where temporary shoring or hold cranes are used to support the girders in a near NL condition, as well as for unshored SDL or TDL conditions. • The girder flange lateral bending moments tend to be the largest at the cross-frame locations. The girder flanges act in lateral bending effectively like continuous-span beams. The cross-frames act as the supports for these analogous continuous-span beams (see the subsequent "con" discussions for SDLF and TDLF cross-frame detailing). • This statement applies only to curved radially supported bridges.
• NLF detailing tends to minimize the fit-up forces required during the steel erection, since the girders are not "reverse twisted" during the installation of the cross-frames.	• In curved radially supported bridges, since the cross-frame connection forces at any intermediate stage of the steel erection tend to be smallest when NLF detailing is used, the force required to install a given cross-frame at a given intermediate stage also tends to be minimized by NLF detailing. This is because the cross-frame connection force at the intermediate stage is equal to the force that has to be developed into the cross-frame if it were installed just prior to this stage. Before the cross-frame is installed, the connection force is zero, since the cross-frame is unconnected. • This statement is true both for situations where temporary shoring or hold cranes are used to support the girders in a near NL condition, as well as for unshored SDL conditions • This statement applies only to curved radially supported bridges.
• The differential vertical displacements between the girders are comparable for both NLF and SDLF in curved radially supported bridges.	• In some cases, the erector may have to affect the relative vertical elevation of the girders, in addition to twisting a girder, in order to install a given cross-frame. • Curved girders tend to twist as well as deflect vertically under their self-weight. The girder twisting tends to increase the girder vertical deflections. This is beneficial in facilitating the fit-up to steel that has already been erected (if working from the inside of the curve to the outside of the curve in erecting the girders). The steel that has already been erected will be over-rotated relative to its final SDL configuration. If working from the outside to the inside of the curve, the girders can be interconnected first near the mid-span, and the self-weight of the added girder can be used to reduce the over-rotation of the partially erected bridge cross-section. • These attributes work essentially the same in bridges with either NLF or SDLF detailing. • See the subsequent discussion under the pros for SDLF detailing. • This statement applies only to curved radially supported bridges.

Table 3-19. Con facts and commentary, curved radially supported I-girder bridges with NLF detailing.

Con Facts:	Commentary:
• The girders will be twisted (laid over) under any dead load conditions.	• Layover of the girders is restrained essentially to zero by the bearing-line cross-frames at radial bearing lines. • Layover of the girders within the span is more difficult to detect and therefore tends not to be visually objectionable. • The NCHRP Project 12-79 research, as well as other prior research studies, has shown that the influence of girder layovers on the system ***strength*** is negligible as long as the checks for global stability, stability between the cross-frame locations, and bracing of the girders are satisfied.
• Because there are no locked-in forces, the girders see larger "positive" flange lateral bending moments between the cross-frames.	• The "negative" flange lateral bending moments at the cross-frame locations are typically the largest moments. Therefore, NLF detailing of the cross-frames tends to give smaller maximum flange lateral bending moments.

Table 3-20. Pro facts and commentary, curved radially supported I-girder bridges with SDLF detailing—cross-frames fabricated such that they do not fit-up with the girders in their fabricated (cambered and plumb) no-load geometry (Configuration 1 of Figure 3-30); the erector must essentially "reverse twist" the girders during the installation of the cross-frames to achieve fit-up (Configuration 3 of Figure 3-30).

Pro Facts:	Commentary:
• Locked-in forces are generated by the initial lack of fit between the cross-frames and the girders in their fabricated (cambered and plumb) no-load geometry.	• The girder webs will be approximately plumb at the end of the steel erection. This results in a web plumb condition that is easy to measure and inspect at a time when the erector is still on site and the deck has not yet been cast (thus allowing better opportunity to correct any misalignments).
• The layover of the girders within the span will be smaller than that for NLF detailing.	• In curved radially supported bridges, the "reverse twisting" of the girders required to install the cross-frames induces internal forces that twist the girders in the opposite direction from that which they tend to roll under the dead load. This occurs at all of the cross-frames along a given span. As a result, the overall "global" twisting of the girders, and the corresponding lateral bending of the girder flanges, is reduced along the full span lengths.
• The differential vertical displacements between the girders are comparable for both NLF and SDLF in curved radially supported bridges.	• In some cases, the erector also may have to affect the relative vertical elevation of the girders in order to install a given cross-frame. • Curved girders tend to twist as well as deflect vertically under their self-weight. The girder twisting tends to increase the girder vertical deflections. This is beneficial in facilitating the fit-up to steel that has already been erected (if working from the inside of the curve to the outside of the curve in erecting the girders). The steel that has already been erected will be over-rotated relative to its final SDL configuration. If working from the outside to the inside of the curve, the girders can be interconnected first near the mid-span, and the self-weight of the added girder can be used to reduce the over-rotation of the partially erected bridge cross-section. • These attributes work essentially the same in bridges with either SDLF or NLF detailing.
• Some fabricators and erectors believe that bridges with cross-frames detailed for SDLF generally are easier to fit-up under unshored SDL erection conditions.	• The analytical evidence suggests that this is the case for straight-skewed bridges. However, the analytical evidence suggests that the forces required to fit up the steel under unshored SDL erection conditions are somewhat larger when SDLF detailing is used in curved radially supported bridges. • The fit-up forces often are very comparable for curved radially supported bridges with either SDLF or NLF detailing of the cross-frames.

130 Guidelines for Analysis Methods and Construction Engineering of Curved and Skewed Steel Girder Bridges

Table 3-21. Con facts and commentary, curved radially supported I-girder bridges with SDLF detailing.

Con Facts:	Commentary:
• Locked-in forces are developed within the structural system.	• An accurate 2D-grid or 3D FE analysis, including the influence of the initial lack of fit between the cross-frames with the girders in their fabricated (cambered and plumb) no-load geometry, is necessary to account accurately for these effects.
• On average, the locked-in cross-frame forces due to SDLF or TDLF detailing are additive with the SDL and TDL cross-frame forces in curved radially supported bridges.	• For SDLF or TDLF detailing, the girder flanges in curved radially supported bridges work effectively like continuous-span beams over the cross-frames in the lateral direction. The SDLF or TDLF detailing effects are akin to pre-stressing these effective continuous-span beams by displacing their supports (the cross-frames) in the direction opposite to that which these supports displace under the SDL or TDL. This "pre-stressing" increases the continuous-span beam reactions (i.e., the cross-frame forces) and increases the beam negative moments over the supports (i.e., the flange lateral bending moments over the cross-frame locations).
• The girder flange maximum lateral bending stresses tend to be increased by the effects of SDLF or TDLF detailing.	• The predominant SDLF or TDLF detailing effect is in the cross-frame diagonals, and is associated with a racking of the cross-frames that accomplishes the compensating deflections necessary for the girder webs to be plumb in the targeted dead load condition. • Assuming that the bridge remains elastic, and neglecting aspects such as friction at the supports and non-zero connection tolerances, these responses are independent of the sequence of erection. • Generally, the locked-in forces need to be calculated in the analysis to obtain accurate cross-frame forces.
• The girders still will be laid over within the spans under the TDL, although the layover will be smaller than for NLF detailing of the cross-frames.	• Layover of the girders is restrained essentially to zero by the bearing-line cross-frames at radial bearing lines. • Layover of the girders within the span is difficult to detect and therefore tends not to be visually objectionable. • The NCHRP Project 12-79 research, as well as other prior research studies, has shown that the influence of girder layovers on the system ***strength*** is negligible as long as the checks for global stability, stability between the cross-frame locations, and bracing of the girders are satisfied.
• In curved bridges, SDLF detailing tends to reduce the vertical deflections. The required cambers will tend to be over-predicted by an analysis that neglects lack-of-fit force effects.	• The change in the vertical deflections due to SDLF detailing is usually relatively small. However, in extreme cases such as the Ford City Bridge example (see Figure 3-84), this change can be several inches. • This can reduce the concrete deck haunch to a thickness that is not desirable or can lead to problems in achieving the desired deck elevations along the spans. • Generally, the locked-in forces need to be calculated in the analysis to obtain accurate girder cambers.
• The differential vertical displacements between the girders are comparable for both SDLF and NLF in curved radially supported bridges.	• SDLF detailing has approximately the same effect on the vertical displacements for all the girders at any given cross-section of the bridge. The overall rotation of the bridge cross-section tends to not be significantly affected. Therefore, the influence of SDLF detailing on the differential vertical displacements between the girders is small (i.e., there is no significant benefit of SDLF versus NLF, or vice versa, in resolving vertical displacement incompatibilities during erection).
• In curved, radially supported bridges, SDLF detailing tends to increase the fit-up forces required during the steel erection somewhat relative to NLF detailing.	• In curved radially supported bridges, since the cross-frame connection forces at any intermediate stage of the steel erection tend to be increased due to the locked-in forces from SDLF detailing, the force required to install a given cross-frame into the system at a given intermediate stage tends to be increased. This is because the cross-frame connection force at a given intermediate stage is equal to the force that has to be developed into the cross-frame if it were installed just prior to this stage. Before the cross-frame is installed, the connection force is zero, since the cross-frame is unconnected.

Table 3-22. Pro facts and commentary, curved radially supported I-girder bridges with TDLF detailing—cross-frames fabricated such that they do not fit-up with the girders in their fabricated (cambered and plumb) no-load geometry (Configuration 1 of Figure 3-30); the erector must essentially "reverse twist" the girders during the installation of the cross-frames to achieve fit-up (Configuration 3 of Figure 3-30).

Pro Facts:	Commentary:
• Locked-in forces are generated by the initial lack of fit between the cross-frames and the girders in their fabricated (cambered and plumb) no-load geometry.	• The girder webs will be approximately plumb at the end of the construction (i.e., at the TDL level). However, it is most important that the girder webs be plumb at the bearing lines. The cross-frames at radial bearing lines enforce this, regardless of the type of cross-frame detailing. • In curved radially supported bridges, the "reverse twisting" of the girders required to install the cross-frames induces internal forces that twist the girders in the opposite direction from that which they tend to roll under the dead load. This occurs at all the cross-frames along a given span. As a result, the overall "global" twisting of the girders, and the corresponding lateral bending of the girder flanges, is reduced along the full span lengths. For TDLF detailing of the cross-frames, the twisting of the girders is approximately zero at the cross-frame locations at the end of the construction (i.e., at the TDL level). • For curved radially supported bridges, the final internal cross-frame forces and the girder flange lateral bending stresses from a V-load analysis tend to correlate well with the corresponding physical responses associated with TDLF detailing of the cross-frames. However, the accuracy of V-load analysis for predicting the girder vertical deflections degrades as a function of the horizontal curvature.

Table 3-23. Con facts and commentary, curved radially supported I-girder bridges with TDLF detailing.

Con Facts:	Commentary:
• Locked-in forces are developed within the structural system.	• An accurate 2D-grid or 3D FE analysis, including the influence of the initial lack of fit between the cross-frames with the girders in their fabricated (cambered and plumb) no-load geometry, is necessary to account accurately for all of the effects of the locked-in forces. • For curved radially supported bridges, the final internal cross-frame forces and the girder flange lateral bending stresses from a V-load analysis tend to correlate well with the corresponding physical responses associated with TDLF detailing of the cross-frames. However, the accuracy of V-load analysis for predicting the girder vertical deflections degrades as a function of the horizontal curvature.
• On average, the locked-in cross-frame forces due to TDLF or SDLF are additive with the TDL and SDL cross-frame forces in curved radially supported bridges.	• For TDLF or SDLF detailing, the girder flanges in curved radially supported bridges work effectively like continuous-span beams over the cross-frames in the lateral direction. The TDLF or SDLF detailing effects are akin to pre-stressing these effective continuous-span beams by displacing their supports (the cross-frames) in the direction opposite to that which these supports displace under the TDL or SDL. This "pre-stressing" increases the continuous-span beam reactions (i.e., the cross-frame forces) and increases the beam negative moments over the supports (i.e., the flange lateral bending moments over the cross-frame locations).
• The girder flange maximum lateral bending stresses tend to be increased by the effects of TDLF or SDLF detailing.	• The predominant TDLF or SDLF detailing effect is in the cross-frame diagonals and is associated with a racking of the cross-frames that accomplishes the compensating deflections necessary for the girder webs to be plumb in the targeted dead load condition. • Assuming that the bridge remains elastic, and neglecting aspects such as friction at the supports and non-zero connection tolerances, these responses are independent of the sequence of erection. • Generally, the locked-in forces need to be calculated in the analysis to obtain accurate cross-frame forces.

(continued on next page)

132 Guidelines for Analysis Methods and Construction Engineering of Curved and Skewed Steel Girder Bridges

Table 3-23. Continued.

Con Facts:	Commentary:
• Under SDL, the girders will be laid over in the opposite direction from the direction in which they twist under the application of the dead loads.	• These rotations are temporary and are not additive with the rotations due to live load.
• In curved radially supported bridges, TDLF detailing tends to reduce the vertical deflections. The required cambers will tend to be over-predicted by an analysis that neglects lack-of-fit force effects.	• The change in the vertical deflections due to TDLF detailing can potentially be of significance. In the extreme Ford City Bridge example (see Figure 3-84), this change was as much as approximately 5 in. • This can reduce the concrete deck haunch to a thickness that is not desirable or can lead to problems in matching the desired deck elevations at a given location along the spans. • The calculation of locked-in forces generally should be included in the analysis to predict accurate girder cambers.
• The differential vertical displacements between the girders are not significantly affected by TDLF detailing.	• In curved radially supported bridges, TDLF detailing influences the girder twists and the girder vertical deflections. However, the overall rotation of the bridge cross-section tends not to be significantly affected. Therefore, the influence of TDLF detailing on the differential vertical displacements between the girders is small in these types of structures (i.e., there is no significant benefit of TDLF versus NLF or SDLF detailing in resolving vertical displacement incompatibilities during erection).
• In curved radially supported bridges, TDLF detailing tends to increase the fit-up forces required during the steel erection relative to the results for both SDLF and NLF detailing.	• In curved radially supported bridges, since the cross-frame connection forces at any intermediate stage of the steel erection tend to be increased due to the locked-in forces from TDLF detailing, the force required to install a given cross-frame into the system at a given intermediate stage tends to be increased. This is because the cross-frame connection force at a given intermediate stage is equal to the force that has to be developed into the cross-frame if it were installed just prior to this stage. Before the cross-frame is installed, the connection force is zero, since the cross-frame is unconnected.
• The lack of fit between the cross-frames and the girders is *maximized under any shored or unshored SDL erection conditions*, compared to the results from other cross-frame detailing methods.	• For longer spans and larger skew indices, the forces required to fit-up the cross-frames with the girders during the steel erection can be substantial. This is because the TDL major-axis bending deflections have not yet occurred (since only the steel self-weight load is on the structure).
• Caution: The girders can be plumb only under one TDL condition.	• If there are significant DC2 loads (such as a substantial utility load, barrier rail load or wall load), the designer must decide under which TDL the girders should be plumb.
• Caution: Various incidental effects may have an influence on the bridge TDL responses.	• If early stiffness gain on the concrete deck from prior deck casting stages, or from set-up of the concrete during a given stage, is expected to be a factor, these effects would need to be considered in the calculation of the TDL displacements, internal forces, and internal stresses. In addition, other incidental effects such as tipping restraint at the bearings, participation of the metal deck forms, temporary timber struts between girders, welding of rebar between shear studs on adjacent girders, etc. can influence the response and may need to evaluated when ***estimating*** the TDL displacements, internal forces, and internal stresses.

need to be installed with the girders in their deflected steel dead load positions. If the cross-frames are installed before temporary supports or holding cranes are removed, NLF detailing is necessary. Due to the torsional stiffness of tub girders, force-fitting of the cross-frames generally is not an option. In most cases with longer-span tub-girder bridges, there are multiple field sections along the spans and shoring to the approximate no-load condition is preferred.

3.5 Selection of Cross-Frame Detailing Methods for I-Girder Bridges

Based on the summaries in Section 3.4, it is apparent that different methods of cross detailing work well for different I-girder bridge geometries. Furthermore, in many cases, steel I-girder bridges can be built successfully using a wide range of methods. Generally, the appropriate selection of a cross-frame detailing method depends in large part on the priority that one assigns to the various objectives and tradeoffs. Therefore, in the view of the NCHRP Project 12-79 research team, it is important to allow flexibility in any recommendations for selecting cross-frame detailing methods. However, given the detailed pros and cons discussed in Section 3.4, a few basic trends become apparent. These trends are explained in this section.

For straight-skewed bridges with $I_S \leq 0.30$, TDLF detailing is typically a good option:

- The girder webs will be approximately plumb under the targeted TDL.
- The TDL cross-frame forces and girder flange lateral bending stresses will be canceled out in large part by the TDLF locked-in forces. As such, the cross-frame forces and girder flange lateral bending stresses tend to be minimized under the targeted TDL. In addition, these forces and stresses tend to be negligible, given $I_S \leq 0.30$.
- Fit-up concerns during the steel erection should be minimal, given $I_S \leq 0.30$.
- Line girder analysis provides a reasonable estimate of the responses under TDL, given that the cross-frame forces and the girder flange lateral bending stresses are negligible.
- The twist rotation of the girders in the SDL condition can be estimated as $\phi_z = \phi_x \tan \theta$ at skewed bearing lines, where ϕ_x is the sum of the initial camber and the SDL girder major-axis bending rotations and θ is the skew angle, equal to zero for zero skew. The girder SDL twist rotation at cross-frames normal to the girders within the spans may be estimated as $\phi_z = \Delta_y / s$, where Δ_y is the differential vertical displacement between the cross-frame ends due to sum of the initial TDL camber and the SDL displacements. These layovers can be specified on the engineering drawings to indicate the expected geometry at the completion of the steel erection (the direction of the layovers under SDL will be opposite to those due to the TDL).
- Potential "incidental" effects such as non-calculated early stiffness gains of the concrete, tipping restraint at the bearings, participation of metal deck forms, temporary timber struts between girders, welding of rebar between studs on adjacent girders, etc., potentially should be considered when setting the TDL cambers. The accounting for these effects requires engineering judgment regarding specific construction practices and characteristics and cannot be well quantified as of this writing. The engineer may consider reducing the TDL cambers (based on ideal conditions) to ensure that the girders are not "over-cambered" or specifying a cross-frame detailing method somewhere between TDLF and SDLF, but not both of these ad hoc compensating measures. In ordinary practice, these types of effects are often neglected without any apparent detrimental influence.
- The first intermediate cross-frames generally should be positioned at an offset distance $a \geq \max(1.5D, 0.4b)$, where D is the girder depth and b is the second unbraced length within the span adjacent to the offset from the bearing line. This is intended to alleviate local spikes in the cross-frame forces and corresponding potential fit-up difficulty due to nuisance stiffness effects. (In basic terms, the first intermediate cross-frame needs to be far enough away from

134 Guidelines for Analysis Methods and Construction Engineering of Curved and Skewed Steel Girder Bridges

the bearing line so that one end of the girder offset length can be pulled over relative to the other without requiring excessive force.)

For straight-skewed bridges with small-to-moderate span lengths and $I_S > 0.30$, TDLF detailing is typically a good option:

- The girder webs will be approximately plumb under the targeted TDL.
- The TDL internal forces and stresses due to the system torsional effects will be offset in large part by the TDLF locked-in forces. As such, the cross-frame forces and girder flange lateral bending stresses will tend to be minimized under the targeted TDL.
- Fit-up during the steel erection should be feasible, given the small-to-moderate span length.
- Generally, significant cross-frame forces and girder flange lateral bending stresses will exist in the TDL condition and in other loading conditions. Accurate calculation of these values requires an accurate 2D-grid or 3D FE analysis, including the calculation of locked-in forces due to the initial lack-of-fit effects. Since the locked-in forces are comparable in magnitude to the internal forces due to the TDL effects, the internal forces from an accurate 2D-grid or 3D FE analysis neglecting the initial lack-of-fit effects will be substantially in error (e.g., compare the forces in Figure 3-57 versus those in Figure 3-58).
- The twist rotation of the girders in the SDL condition can be estimated as $\phi_z = \phi_x \tan \theta$ at skewed bearing lines, where ϕ_x is the sum of the initial camber and the SDL girder major-axis bending rotations and θ is the skew angle, equal to zero for zero skew. The girder SDL twist rotation at cross-frames normal to the girders within the spans may be estimated as $\phi_z = \Delta_y/s$, where Δ_y is the differential vertical displacement between the cross-frame ends due to the sum of the initial TDL camber and the SDL displacements. These layovers can be specified on the engineering drawings to indicate the expected geometry at the completion of the steel erection.
- Potential "incidental" effects such as non-calculated early stiffness gains of the concrete, tipping restraint at the bearings, participation of metal deck forms, temporary timber struts between girders, welding of rebar between studs on adjacent girders, etc., potentially should be considered when setting the TDL cambers. The accounting for these effects requires engineering judgment regarding specific construction practices and characteristics and cannot be well quantified as of this writing. The engineer may consider reducing the TDL cambers (based on ideal conditions) to ensure that the girders are not "over-cambered" or specifying a cross-frame detailing method somewhere between TDLF and SDLF, but not both of these ad hoc compensating measures. In ordinary practice, these types of effects are often neglected without any apparent detrimental influence.
- The first intermediate cross-frames generally should be positioned at an offset distance $a \geq \max(1.5D, 0.4b)$, where D is the girder depth and b is the second unbraced length within the span adjacent to the offset from the bearing line. This is intended to alleviate local spikes in the cross-frame forces and corresponding potential fit-up difficulty due to nuisance stiffness effects. (In basic terms, the first intermediate cross-frame needs to be far enough away from the bearing line so that one end of the girder offset length can be pulled over relative to the other without requiring excessive force.)

For straight-skewed bridges with large span lengths and $I_S > 0.30$, SDLF detailing, or detailing between SDLF and TDLF, typically are good options:

- In these cases, a potential consideration is the alleviation of fit-up difficulty during the steel erection. SDLF detailing tends to minimize the fit-up difficulty for straight-skewed bridges, but may result in significant layover of the girders at highly skewed bearing lines under the TDL. In the experience of some erectors, long-span straight-skewed bridges with TDLF detailing do not present any major problems with respect to fit-up. Ozgur (2011) discusses a 267-ft. span skewed bridge erection procedure in which TDLF detailing was used and the bridge was erected quite successfully by using the steel dead load deflections to alleviate fit-up problems.

- The tendency for excessive layover at highly skewed bearing lines can be addressed by a combination of the cross-frame detailing, the use of beveled sole plates, and/or by using bearings with a larger rotation capacity. If TDLF detailing is used, the layover is addressed entirely by the cross-frame detailing.
- For SDLF detailing, the girder webs will be approximately plumb under the SDL at the completion of the steel erection.
- For other than SDLF detailing of the cross-frames, the twist rotation of the girders in the SDL condition can be estimated as $\phi_z = \phi_x \tan \theta$ at skewed bearing lines, where ϕ_x is the sum of the initial camber and the SDL girder major-axis bending rotations and θ is the skew angle, equal to zero for zero skew. The girder twist rotation at cross-frames normal to the girders within the spans may be estimated as $\phi_z = \Delta_y/s$, where Δ_y is the differential vertical displacement between the ends of the cross-frame due to the sum of the initial TDL camber and the SDL displacements. These layovers can be specified on the engineering drawings to indicate the expected geometry at the completion of the steel erection.
- Generally, significant cross-frame forces and girder flange lateral bending stresses will exist in the TDL condition and in other loading conditions. Accurate calculation of these values requires an accurate 2D-grid or 3D FE analysis, including the calculation of locked-in forces due to the initial lack-of-fit effects. Since the locked-in forces are comparable in magnitude to the internal forces due to the corresponding dead load effects (e.g., SDL for SDLF and TDL for TDLF), the internal forces from an accurate 2D-grid or 3D FE analysis neglecting the initial lack-of-fit effects will be substantially in error (e.g., compare the forces in Figure 3-57 versus those in Figure 3-58).
- The first intermediate cross-frames generally should be positioned at an offset distance $a \geq \max(1.5D, 0.4b)$, where D is the girder depth and b is the second unbraced length within the span adjacent to the offset from the bearing line. This is intended to alleviate local spikes in the cross-frame forces and corresponding potential fit-up difficulty due to nuisance stiffness effects. (In basic terms, the first intermediate cross-frame needs to be far enough away from the bearing line so that one end of the girder offset length can be pulled over relative to the other without requiring excessive force.)

For curved bridges with radial supports, NLF detailing, or detailing between NLF and SDLF, typically are good options:

- NLF detailing tends to minimize the cross-frame forces as well as the "negative" girder flange lateral bending moments over the cross-frame locations, since there are no additive locked-in force effects due to initial lack of fit.
- Because the cross-frame forces tend to be minimized, the analytical evidence shows that the fit-up forces required to erect the steel tend to be minimized. However, the experience of some fabricators and erectors is that curved radially supported bridges are easier to fit-up under unshored SDL erection conditions if SDLF detailing is used. The use of SDLF detailing on curved radially supported I-girder bridges is a common practice in the industry, although bridges of this type have been detailed and constructed without difficulty using NLF detailing. It is recommended that the expanded use of NLF detailing should be explored and monitored on selected projects to further validate the NCHRP Project 12-79 findings.
- Layover of the girder webs occurs within the spans, but this layover is more difficult to detect visually and is not of any significance with respect to the bridge structural resistance as long as the checks for global stability, stability between the cross-frame locations, and bracing of the girders are satisfied. If the girder layovers within the span are judged to be excessive, the engineer may wish to employ a flange level lateral bracing system to stiffen the structure, particularly for longer span bridges.
- For NLF detailing, the structural analysis is simplified, since there are no initial lack-of-fit effects.

136 Guidelines for Analysis Methods and Construction Engineering of Curved and Skewed Steel Girder Bridges

- For other than NLF detailing, the locked-in force effects in the cross-frames and in the "negative" girder flange lateral bending moments at the cross-frame positions tend to be additive with the dead load effects (compare Figure 3-73 to Figure 3-72, 3-74 to 3-72, 3-76 to 3-75, and 3-77 to 3-75, see Figures 3-78 and 3-87, compare Figure 3-88b to 3-88a, and see Figures 3-90 and 3-91). Accurate calculation of these values requires an accurate 2D-grid or 3D FE analysis, including the calculation of locked-in forces due to the initial lack-of-fit effects. Since the locked-in forces tend to be additive with the internal forces due to the dead load effects, the internal forces from an accurate 2D-grid or 3D FE analysis neglecting the initial lack-of-fit effects tend to underestimate the true forces.

For curved bridges with *sharply skewed* supports, *minor horizontal curvature* and small span lengths, TDLF detailing is typically a good option:

- In these cases, limiting the girder layover at the skewed bearing lines is the overriding consideration.
- The tendency for the cross-frame forces and the girder "negative" flange lateral bending moments (due to horizontal curvature effects) to be increased by the TDLF detailing can be accounted for by conducting an accurate 2D-grid or 3D FE analysis, including the calculation of locked-in forces due to the initial lack-of-fit effects. Since the locked-in forces are comparable in magnitude to the internal forces due to the dead load effects, the internal forces from an accurate 2D-grid or 3D FE analysis neglecting the initial lack-of-fit effects will be substantially in error.
- The first intermediate cross-frames generally should be positioned at an offset distance $a \geq \max(1.5D, 0.4b)$, where D is the girder depth and b is the second unbraced length within the span adjacent to the offset from the bearing line. This is intended to alleviate local spikes in the cross-frame forces and corresponding potential fit-up difficulty due to nuisance stiffness effects. (In basic terms, the first intermediate cross-frame needs to be far enough away from the bearing line so that one end of the girder offset length can be pulled over relative to the other without requiring excessive force.)

For curved bridges with moderately skewed supports, and small to moderate span lengths, detailing of the cross-frames anywhere between NLF and TDLF can be a good option:

- In this case, the engineer should select the cross-frame detailing method to balance between (1) limiting the dead load twist rotations at the skewed bearing lines, (2) alleviating the larger additive locked-in forces associated with TDLF detailing on a curved bridge, and (3) facilitating fit-up during the steel erection.
- Often SDLF detailing is a good "middle of the road" option for these bridge types.
- For other than NLF detailing, the locked-in force effects due to the horizontal curvature in the cross-frames and in the "negative" girder flange lateral bending moments at the cross-frame positions tend to be additive with the dead load effects. Accurate calculation of these values requires an accurate 2D-grid or 3D FE analysis, including the calculation of locked-in forces due to the initial lack-of-fit effects. Since the locked-in forces tend to be additive with the internal forces due to the dead load effects, the internal forces from an accurate 2D-grid or 3D FE analysis neglecting the initial lack-of-fit effects tend to underestimate the true forces.

For curved bridges with skewed supports and large span length, SDLF detailing, or detailing between SDLF and NLF, is typically a good option.

- In these cases, the overriding consideration is the alleviation of fit-up difficulty during the steel erection. SDLF detailing tends to minimize the fit-up difficulty in the vicinity of highly skewed bearing lines and is often preferred by fabricators and erectors for these types of bridges. However, SDLF detailing may result in significant layover of the girders at highly skewed bearing lines under the TDL. NLF detailing tends to minimize the fit-up difficulty

with respect to horizontal curvature effects (based on analytical evidence), but provides no compensation for the layover of the girders at highly skewed bearing lines.
- The tendency for excessive layover at highly skewed bearing lines can be addressed by a combination of the cross-frame detailing, the use of beveled sole plates, and/or by using bearings with a larger rotation capacity.
- For SDLF detailing, the girder webs will be approximately plumb under the SDL at the completion of the steel erection.
- For other than NLF detailing, the locked-in force effects in the cross-frames and in the "negative" girder flange lateral bending moments at the cross-frame positions tend to be additive with the dead load effects due to the horizontal curvature. Accurate calculation of these values requires an accurate 2D-grid or 3D FE analysis, including the calculation of locked-in forces due to initial lack-of-fit effects. Since the locked-in forces associated with the combined skew and horizontal curvature can be comparable in magnitude to the internal forces due to the dead load effects, the internal forces from an accurate 2D-grid or 3D FE analysis neglecting the initial lack-of-fit effects can be substantially in error.
- The first intermediate cross-frames generally should be positioned at an offset distance $a \geq \max(1.5D, 0.4b)$, where D is the girder depth and b is the second unbraced length within the span adjacent to the offset from the bearing line. This is intended to alleviate local spikes in the cross-frame forces and corresponding potential fit-up difficulty due to nuisance stiffness effects. (In basic terms, the first intermediate cross-frame needs to be far enough away from the bearing line so that one end of the girder offset length can be pulled over relative to the other without requiring excessive force.)

3.6 Construction Engineering Recommendations

The main focus of this research was the improvement of analysis methods for erection analysis and prediction of constructed geometry of steel girder bridges. However, the construction engineering recommendations represent perhaps the most important results of this work, and they are likely to be the most easily implemented to provide direct benefit to the industry.

The recommendations in regard to construction engineering are organized into four categories, represented by the subsections of this report presented below. The specific recommendations, however, are best presented in their full and complete form, which appears in the NCHRP Project 12-79 Task 9 report, "Recommendations for Construction Plan Details and Level of Construction Analysis." This document is included as Appendix B of this report. This appendix provides specific guidelines and commentary on recommendations for construction plan details and recommendations for methods of structural analysis and calculations. These guidelines are comprehensive and address all aspects of erection engineering plans and calculations. An owner-agency could adopt the guidelines as a complete specification, could reference the guidelines in their erection specifications, or could adopt all or portions of the guidelines in their specifications.

To further facilitate immediate implementation of these recommendations, this appendix has been deliberately written in a format and with language that can be directly adopted by AASHTO via a revision to the AASHTO/NSBA Steel Bridge Collaboration Guide Specification S10.1 – 2007, *Steel Bridge Erection Guide Specification.*

3.6.1 Recommendations for Construction Plan Details

The reader is referred to Section 2 of Appendix B, which provides detailed and comprehensive recommendations with commentary, organized in a format that would easily lend itself to the

- Plan of work area
  - Permanent and temporary structures shown
  - All roads, railroad tracks, waterways, clearances, utilities, potential conflicts shown
  - Material (steel) storage areas shown
- Erection sequence
  - Step-by-step procedure—figures and narrative dictating work
  - Delivery location of components shown
  - Crane locations shown
  - Temporary support, hold cranes, blocking, tie-downs shown
  - Load restrictions for certain stages (i.e., wind)
- Crane information
  - Crane type, pick radii, boom length shown
  - Approximate crane pick points shown
  - Crane pick weights shown
  - Hold crane loads
- Details of lifting devices and special procedures
- Bolting requirements
- Bearing blocking and tie-down details
- Temporary supports
  - Details of structure shown
  - Load capacities
- Jacking devices and procedures

Figure 3-103. Erection plan and procedures checklist.

development of approval checklists. Figure 3-103 provides the summary checklist developed in this portion of NCHRP Project 12-79's Task 9.

3.6.2 Recommendations for Methods of Structural Analysis and Other Calculations

The reader is referred to Sections 3.1 through 3.6 of Appendix B for summary recommendations on methods of structural analysis and other calculations. Section 3.1 provides an introduction to this topic. Section 3.2 specifically provides quantitative guidance on the accuracy of various analysis methods, organized according to key parameters related to bridge geometry and framing. These analysis accuracy tables are supplemented with examples illustrating their use. Section 3.3 specifically provides guidelines on calculations for structural adequacy and especially stability of the steel framing during construction, as well as guidance on myriad associated issues such as cantilever girders, uplift, temporary hold cranes and support loads, bearing, cross-frames, and bracing. Section 3.5 specifically addresses miscellaneous calculations and recommendations for crane pick locations, alignment of field splice and cross frame connections, and support conditions. Section 3.6 provides a useful calculation checklist. This checklist is shown as Figure 3-104 for ease of reference.

3.6.3 Design and Construction Considerations for Ease of Analysis via Improved Behavior

There are a number of ways to improve analysis accuracy while simultaneously improving the behavior and constructability of steel girder bridges by means of wisely establishing

- Complete analysis of erection sequence
    1. Proper level of analysis used
    2. Support conditions modeled appropriately at all stages
- Correct design criteria employed
- Correct loads investigated
- Complete checks of structural adequacy of bridge components
- Complete checks of stability of girder and bridge system
- Second-order amplification effects addressed as needed
- Girder reactions checked for uplift
- Temporary hold crane loads computed
- Temporary support loads computed
- Bearing capacity and rotation checks
- Cross frame and bracing placement
- Checks of structural adequacy of temporary supports and devices
    1. Falsework towers
    2. Girder tie-downs
    3. Lifting beams
    4. Jacking devices
- Crane pick location calculations
- Checks of displacements at field splices
- Checks of displacements for cross frame placement

Figure 3-104. Calculation checklist.

the framing plan for the structure and by avoiding problematic details. Problematic details are in fact a significant enough topic to warrant separate discussion in Section 3.6.4 of this report.

A wisely established framing plan is one that provides clean, direct load paths and specifically avoids use of secondary bracing members (such as cross-frames) in locations where they would be anticipated to carry significantly high loads as a function of displacement compatibility. Examples include the use of lean-on bracing or omitting selected cross-frames near supports in severely skewed bridges, as cited in Krupicka and Poellot (1993).

3.6.4 Problematic Physical Characteristics and Details to Avoid

The reader is referred to Section 3.7 of Appendix B for a discussion of problematic characteristics and details such as oversize or slotted holes, narrow bridges or bridge units, V-type cross-frames without top chords, bent-plate connections in I-girder bridges, long span I-girder bridges without top flange lateral bracing systems, partial-depth end diaphragms in tub-girder bridges, non-collinear external intermediate diaphragms in tub-girder bridges, and two-girder bearing systems at tub-girder supports.

CHAPTER 4

Conclusions and Recommendations

4.1 Summary

Based on the results of the research conducted on this project, the following conclusions may be drawn:

- Conventional 1D line-girder and 2D-grid methods of analysis are capable of predicting accurate construction responses in many situations; however, there are definite bridge geometries where significant reductions in accuracy can be expected. This research has provided a scoring method engineers can utilize as an aid to gage the accuracy of these simplified tools. Several examples are provided illustrating how the scoring system can be applied most effectively.
- The research identified a number of critical shortcomings in commonly used conventional methods and, in each case, provided mechanistic evaluations of the reasons for the shortcomings and recommended improved procedures that remove or alleviate these flaws. For I-girder bridges, the key critical flaws identified were:
  1. The common dramatic underestimation of I-girder torsional stiffnesses by using solely the St. Venant torsional stiffness GJ/L in 2D-grid analysis methods. This flaw was addressed by the development and use of an equivalent St. Venant torsion constant that approximates the increase in the girder torsional stiffnesses due to the restraint of warping.
  2. The common usage of equivalent beam elements for cross-frames that are unable to capture the physical load-deformation characteristics of these components. This problem was addressed by developing a procedure to obtain relatively accurate equivalent beam properties using a Timoshenko beam approximation rather than a Euler-Bernoulli equivalent beam element. In addition, "exact" equivalent beam elements were developed for a complete range of practical I-girder bridge cross-frame types.
  3. The lack of any direct method of evaluating flange lateral bending stresses due to skew in I-girder bridges. The NCHRP Project 12-79 research developed an approximate procedure that works directly with the more accurate values of the cross-frame forces obtained using the above two improvements.
  4. The lack of consideration of locked-in force effects associated with SDLF and TDLF detailing of the cross-frames. These locked-in forces are due to the lack of fit between the cross-frames and the girders in the initially fabricated (cambered and plumb) girder geometry. This issue was addressed by recommending a streamlined procedure for calculating these effects using cross-frame element initial strains, initial stresses, or initial (fixed-end) forces. Thorough case study examples were presented to provide practical guidance for when the influence of the above locked-in effects should be considered in design.

Several areas of important improvements were also identified for tub-girder bridge analysis:

1. A method was developed for simplified estimation of the internal torques due to skew in tub girders,

2. The impact of skew on box-girder cross-section distortion was directly evaluated and it was shown that the distortion associated with skew effects is typically minor, and
3. A method of accounting for a localized spike or "saw-tooth" in the longitudinal average normal stress distribution in the top flanges of tub girders, caused by the interaction with diagonals in the top flange lateral bracing (TFLB) system, was developed.

- Lastly, this research developed a guidelines document providing recommendations on the level of construction analysis, plan detail, and submittals for curved and skewed steel I- and tub-girder bridges. These guidelines were developed in a specification and commentary format suitable for direct incorporation into other specifications or guideline documents.

4.2 Recommendations for Implementation

The recommendations for implementation of the results of this research are aimed at evolutionary improvements to the current state of practice for steel girder bridge engineering. These recommendations are primarily focused on the following items, which relate directly to the original scope of the research:

1. **Improvements to Conventional Analysis Methods:** Specifically, improvements to the modeling of I-girder torsional stiffness, the modeling of cross-frames' overall stiffness in 2D-grid analyses, the calculation of flange lateral bending stresses from 2D-grid analyses, calculation of fit-up forces due to cross-frame detailing, and simplified analysis improvements for tub-girder bridges.
2. **Definition of Erection Engineering Tasks:** Specifically, a detailed list of recommended items to investigate as part of the erection engineering effort, with commentary, building on existing engineering guidelines as currently published by AASHTO.
3. **Recommendations for Appropriate Level of Analysis Refinement:** Specifically, a set of simple tables providing "letter grade" assessments of the anticipated accuracy of various analysis methods (1D and conventional 2D-grid vs. 3D benchmark solutions) corresponding to the framing and geometry of a given bridge.

The first of these recommendations takes the form of explicit definition of the suggested improvements. The implementation of most of these recommendations would have to be undertaken voluntarily by the structural engineering software industry, but it is hoped that market pressures would encourage implementation. The implementation of the remainder of these improvements would be through education of the design community.

It is recommended that the second and third recommendations would take the form of a guidelines document, published by AASHTO in the form of a guide specification that could be adopted, referenced, or excerpted by the various state DOTs. Various modifications to the AASHTO (2010 and 2010b) Specifications could be provided to make the Specifications consistent with the detailed guidelines.

4.2.1 Improvements to Conventional Analysis Methods

This research produced a number of recommendations for improvements to conventional analysis methods. These recommendations are detailed in Section 3.2 of this report. A summary of these recommendations with implementation strategies is provided in Table 4-1.

4.2.2 Definition of Erection Engineering Tasks

Currently, there is no nationally recognized guideline addressing erection engineering and erection plans for curved and/or skewed steel girder bridges. The closest nationally recognized

142 Guidelines for Analysis Methods and Construction Engineering of Curved and Skewed Steel Girder Bridges

Table 4-1. Analysis improvements and recommendations for implementation.

Improvement	Report Section	Description	Implementation Strategy
Improved I-Girder Torsion Model for 2D-Grid Analysis	3.2.2	Current 2D-grid methods typically neglect warping stiffness, which is a key parameter in the torsional stiffness of an I-girder. Methods for improving the torsional model of an I-girder are provided.	Provide specific methodologies (presented in this report) to the bridge software industry and encourage their implementation in commercial bridge design software. Provide education (through this report and through associated presentations/publications) on this topic to the bridge engineering community. Encourage implementation in commercial bridge design software.
Improved Equivalent Beam Cross-Frame Models	3.2.3	Current 2D-grid methods use simplified models of cross-frame stiffness that mispredict cross-frame load-deformation characteristics. A method for improving the modeling of cross-frame stiffness is provided.	
Improved Calculation of I-Girder Flange Lateral Bending Stresses	3.2.4	Current 2D-grid methods use a simplified approach for calculation of I-girder flange lateral bending stresses and do not provide any direct calculation of flange lateral bending stresses due to skew effects. An improved method is provided.	
Calculation of Locked-in Forces due to Cross-Frame Detailing	3.2.5	Currently, bridge engineers do not typically include locked-in forces in bridge design. Guidance on proper evaluation of lack-of-fit forces is provided.	Provide specific methodologies (presented in this report) to the bridge software industry and encourage their implementation in commercial bridge design software. Provide education (through this report and through associated presentations/publications) on this topic to the bridge engineering community. Encourage implementation in commercial bridge design software.
Simplified Analysis Improvements for Tub-Girder Bridges	3.2.6	2D-grid analysis is not capable of directly predicting all responses in tub girders, particularly with regard to internal framing responses. Improvements for simplified analysis methods are provided.	
Estimation of Fit-up Forces	3.3.5	Currently, bridge engineers do not typically evaluate fit-up forces in a consistently correct manner. Guidance on proper evaluation of fit-up forces is provided.	Provide education (through this report and through associated presentations/publications) on this topic to the bridge engineering community. Software implementation of the recommended improvements from Sections 3.2.2 through 3.2.5 will permit the estimation of fit-up forces using simplified 2D-grid methods in I-girder bridges. Implementation of Section 3.2.5 to 3D FEA methods is essential for comprehensive evaluation of fit-up forces using these methods. The improvements recommended in Section 3.2.6 are not directly related to the evaluation of fit-up forces in tub-girder bridges.

guideline is the AASHTO/NSBA Steel Bridge Collaboration Guide Specification S10.1 – 2007, *Steel Bridge Erection Guide Specification.*

This report addresses this lack of guidance in Appendix B, Recommendations for Construction Plan Details and Level of Construction Analysis. This appendix provides specific guidelines and commentary on recommendations for construction plan details and recommendations for methods of structural analysis and calculations. These guidelines are comprehensive and address all aspects of erection engineering plans and calculations. An owner-agency could adopt the guidelines as a complete specification, could reference the guidelines in their erection specifications, or could adopt all or portions of the guidelines in their specifications.

4.2.3 Recommendations for Appropriate Level of Analysis Refinement

Section 3.1 of this report outlines simplified equations to check for (and prevent) large second-order amplification in I-girder bridges. When tub girders are fabricated with proper internal cross-frames to restrain their cross-section distortion as well as a proper top flange lateral bracing (TFLB) system, second-order amplification of the overall deformations is practically nonexistent. Simplified rules are provided for identifying cases where overall overturning stability and potential uplift at bearing locations is more likely in both I-girder and tub-girder bridges.

A basic scoring table is provided for assessing the anticipated accuracy of 1D line-girder and conventional 2D-grid methods as a function of the framing and geometry of a given bridge. With the implementation of the recommended improvements to the conventional 2D-grid methods, the accuracy of a 2D-grid analysis is improved to the extent that comparable solutions to 3D FEA are obtained for the assessment of gravity-load responses during construction as long as:

- There are at least two I-girders connected together, and
- They are connected by enough cross-frames such that the connectivity index

$$I_C = \frac{15000}{R\left(n_{cf}+1\right)m}$$

is less than 20 ($I_C \leq 20$).

4.2.4 Recommendations for Specific Revisions to AASHTO Documents

The research accomplished by NCHRP Project 12-79 covers both design engineering and erection engineering, as well as detailing, fabrication, and erection of steel girder bridges. As a result, there are some areas where more than one option exists for specific implementation of the recommendations of this project in the form of revisions to AASHTO documents. In some cases, a single recommendation for revisions to AASHTO documents is provided below; in other cases, when appropriate, a second recommendation is listed as an option.

Also, as previously mentioned in Section 4.2.1, the success of the recommendations resulting from this research related to improvements to conventional analysis methods are critically dependent upon implementation in commercial software. Specific updates to provisions in the AASHTO LRFD Bridge Design Specifications are important to provide the endorsement and authority of AASHTO behind these recommendations, while these provisions must be written in a way to maintain freedom for software providers and engineers to use any legitimate method of analysis that provides sufficient accuracy for a given design. Detailed presentation of the procedures in AASHTO guidelines documents is critical for end users to understand the methods and how to use them.

144 Guidelines for Analysis Methods and Construction Engineering of Curved and Skewed Steel Girder Bridges

Thus, the four primary options for implementation of specific revisions to AASHTO documents are:

1. Revisions to the AASHTO LRFD Bridge Design Specifications.
2. Revisions to the AASHTO LRFD Bridge Construction Specifications.
3. Revisions to appropriate AASHTO/NSBA Steel Bridge Collaboration Guideline or Guide Specification documents.
4. Separate publication and dissemination to the bridge industry.

A key advantage to implementation in an AASHTO/NSBA standard is that doing so will offer thorough vetting of practice recommendations with broad representation, including owners, design engineers, engineers who perform erection calculations and analysis, fabricators, and contractors.

The specific recommendations are listed in Table 4-2, with primary (and if appropriate, secondary) implementation suggestions.

4.3 Further Research Needs

The NCHRP Project 12-79 research has provided a relatively comprehensive assessment and synthesis of the adequacy of simplified 1D and 2D analysis methods for prediction of the constructability and of the constructed geometry of curved and/or skewed steel girder bridges. A guidelines document has been developed based on this research, providing recommendations on the level of construction analysis, plan detail, and submittals for curved and skewed steel girder bridges. Nevertheless, there are a number of related areas that merit further study:

- **Fit-up Practices—**A focused, comprehensive investigation of the impact of various decisions and procedures on the fit-up of steel girder bridges during erection would be very fruitful. A fit-up decision is made on every steel bridge project and usually, due to lack of other direction, the decision is made by the fabricator. The decision impacts constructability of the bridge members during erection, loads in the steel bridge system, and the final bridge geometry. This practice has been customary from the earliest days of steel bridge construction, but there has been little study of actual implications of the decision. This investigation should address the various impacts on fit-up forces, locked-in stresses, and final constructed geometry. The collective knowledge of fit-up issues in the steel bridge industry today (2012) is based almost entirely on qualitative experience. Partial knowledge of each aspect of the issues is typically highly compartmentalized: steel detailers, fabricators, and erectors have knowledge and preferences on detailing practices, designers have knowledge and preferences on how to perform structural analysis for final conditions, and owners have knowledge and preferences regarding the final geometry of bridges.

  A comprehensive knowledge of all aspects of these issues by all parties is lacking. Furthermore, all parties only have limited understanding regarding the possible implications of detailing methods on the structural behavior. This research should involve more than just the application and exercise of sophisticated analytical tools; the analytical assessments will be most useful if they are coupled with high-resolution, high-quality field measurements. The emphasis should be placed on I-girder bridges with NLF, SDLF, and TDLF detailing, but some assessment of the specific causes of fit-up issues in tub-girder bridges also would be a valuable contribution.
- **Early Concrete Deck Stiffness and Strength—**More extensive coupled field and analytical evaluation of the effects of early concrete deck stiffness and strength gains, including the influence of staged concrete deck placement would be very valuable. Prior research addressing this consideration shows generally that significant early stiffness and strength gains can exist. However, the studies have been limited to only a few bridges and a few parameters of the

(continued on page 154)

Table 4-2. Recommendations for specific revisions to AASHTO documents.

Recommendation	Report Section	Implementation Suggestion	Comments
Checking for (and Preventing) Large Global Second-Order Amplification	NCHRP Report 725 § 3.1.1.1	PRIMARY: Provide §3 .2.2 to the AASHTO/NSBA Steel Bridge Collaboration for vetting by the industry and for organization and publication in one or more AASHTO/NSBA Steel Bridge Collaboration documents. The initial recommendation of the research team would be for the Collaboration to consider publication of the content of § 3.2.2 in the AASHTO/NSBA Steel Bridge Collaboration Document G13.1, Guidelines for Steel Girder Bridge Analysis. G13.1 does not presently address simplified estimation of global second-order amplification of girder stresses and displacements. Provide a requirement in Article 6.10.1.6 of the AASHTO LRFD Bridge Design Specifications that potential global second-order amplification shall be considered. Provide Eqs. 2 through 4 as one approach for estimating global second-order amplification in Article C6.10.1.6, and provide guidance for when global second-order amplification is apt to be of concern (e.g., long narrow bridge units with a limited number of girders).	There is no significant precedent for prescribing modeling specifics to this high a level of detail in the AASHTO LRFD Bridge Design Specifications. Generally, designers are allowed leeway in choosing specific modeling strategies, provided they understand the implications of their decisions.
		SECONDARY:P rovide education (through this report and through associated presentations/publications) on this topic to the bridge engineering community.	

(continued on next page)

Table 4-2. (Continued).

Recommendation	Report Section	Implementation Suggestion	Comments
Second-Order Amplification of Flange Lateral Bending Stresses between Cross-Frame Locations	NCHRP Report 725 § 3.1.1.2	PRIMARY: Provide § 3.2.2 to the AASHTO/NSBA Steel Bridge Collaboration for vetting by the industry and for organization and publication in one or more AASHTO/NSBA Steel Bridge Collaboration documents. The initial recommendation of the research team would be for the Collaboration to consider publication of the content of § 3.2.2 in the AASHTO/NSBA Steel Bridge Collaboration Document G13.1, Guidelines for Steel Girder Bridge Analysis. G13.1 presently does not address the characteristic of the flange lateral bending amplification illustrated by Figure 3-1. Provide Figure 3-1 and a brief discussion of the behavior for Article C6.10.1.6 of the AASHTO LRFD Bridge Design Specifications.	There is no significant precedent for prescribing analysis specifics to this high a level of detail in the AASHTO LRFD Bridge Design Specifications. Generally, designers are allowed some leeway between choosing to use simpler, more conservative methods vs. more complicated, more refined methods when evaluating second-order effects and when choosing design strategies to minimize or mitigate such effects, provided they understand the implications of their decisions.
		SECONDARY: Provide education (through this report and through associated presentations/publications) on this topic to the bridge engineering community.	
Overturning Stability	NCHRP Report 725 § 3.1.1.3	PRIMARY: Provide a paragraph for Article C6.10.3.1 that introduces the torsion index I_T (Eq. 1) and Figure 2-3 and discusses the use of I_T as a rough indicator of situations when uplift at bearings should be considered.	This is a simple revision to the AASHTO specifications that would be of value to designers.

Improved I-Girder Torsion Model for 2D-Grid Analysis	NCHRP Report 725 § 3.2.2	PRIMARY: Provide § 3.2.2 to the AASHTO/NSBA Steel Bridge Collaboration for vetting by the industry and for organization and publication in one or more AASHTO/NSBA Steel Bridge Collaboration documents. The initial recommendation of the research team would be for the Collaboration to consider publication of the content of § 3.2.2 in the AASHTO/NSBA Steel Bridge Collaboration Document G13.1, Guidelines for Steel Girder Bridge Analysis. G13.1 does not presently address the flaws associated with under-representation of I-girder torsional stiffness by using the conventional *J* and neglecting the flange warping stiffness. Provide a specific paragraph for Article 4.6.2.2.1 of the AASHTO LRFD Bridge Design Specifications indicating that the warping stiffness of steel I-girder flanges shall be considered in the structural analysis when the I-girders are subjected to torsion. Provide a specific paragraph to introduce Eqs. 11 and 12, for J_{eq}, and Eq. 8, for I_C (used to define the limits of applicability of $J_{eq)}$ immediately after the presentation of Eqs. (C4.6.2.2.1-1) through (C4.6.2.2.1-3) in Article C4.6.2.2.1 of the AASHTO LRFD Bridge Design Specifications. Explain that the direct use of open-section thin-walled beam theory, or a general 3D FEA, are other ways of considering steel I-girder flange warping stiffness. Provide a brief explanation of the potential pitfalls of not considering the girder flange warping stiffness in the structural analysis. Provide a reference to the updated AASHTO/NSBA Collaboration Document G13.1 for more detailed information. Provide a discussion of the modeling problem illustrated by Figure 3-9, complete with this figure, in Article C4.6.1.2.4b of the AASHTO LRFD Bridge Design Specifications. Provide a requirement that the flange warping stiffness shall be accounted for in the modeling of curved steel I-section members in Article 4.6.1.2.4b.	There is no significant precedent for prescribing modeling specifics to this high a level of detail in the AASHTO LRFD Bridge Design Specifications. Generally, designers are allowed leeway in choosing specific modeling strategies provided they understand the implications of their decisions.
		SECONDARY: Publish specific methodologies (presented in this report), present them to the bridge software industry, and encourage their implementation in commercial bridge design software.	

(continued on next page)

Table 4-2. (Continued).

Recommendation	Report Section	Implementation Suggestion	Comments
Improved Equivalent Beam Cross-Frame Models	NCHRP Report 725 § 3.2.3	PRIMARY: Provide § 3.2.3 to the AASHTO/NSBA Steel Bridge Collaboration for vetting by the industry and for organization and publication in one or more AASHTO/NSBA Steel Bridge Collaboration documents. The initial recommendation of the research team would be for the Collaboration to consider publication of the content of § 3.2.3 in the AASHTO/NSBA Steel Bridge Collaboration Document G13.1, Guidelines for Steel Girder Bridge Analysis. G13.1 currently presents the "flexural analogy" and "shear analogy" methods of modeling cross-frames without discussion of their flaws. Provide a requirement in Article 6.7.4.1 of the AASHTO LRFD Bridge Design Specifications that flexural and shear deformation should be considered in the modeling of cross-frames as equivalent beam elements, and provide a reference to G13.1 for detailed discussion from Article C6.7.4.1.	There is no significant precedent for prescribing modeling specifics to this high a level of detail in the AASHTO LRFD Bridge Design Specifications. Generally, designers are allowed leeway in choosing specific modeling strategies provided they understand the implications of their decisions. Presently, there is no discussion regarding equivalent beam modeling of cross-frames in the AASHTO LRFD Bridge Design Specifications.
		SECONDARY: Publish specific methodologies (presented in this report), present them to the bridge software industry, and encourage their implementation in commercial bridge design software.	
Improved Calculation of I-Girder Flange Lateral Bending Stresses	NCHRP Report 725 § 3.2.4	PRIMARY: Provide § 3.2.4 to the AASHTO/NSBA Steel Bridge Collaboration for vetting by the industry and for organization and publication in one or more AASHTO/NSBA Steel Bridge Collaboration documents. The initial recommendation of the research team would be for the Collaboration to consider publication of the content of § 3.2.4 in the AASHTO/NSBA Steel Bridge Collaboration Document G13.1, Guidelines for Steel Girder Bridge Analysis. G13.1 presently does not explain how I-girder flange lateral bending stresses can be calculated given the equivalent flange level lateral forces transmitted by the cross-frames. Provide a brief discussion of the recommended calculation of I-girder flange lateral bending stresses in Article C6.10.1 of the AASHTO LRFD Bridge Design Specifications, with reference to G13.1 for detailed discussion.	There is no significant precedent for prescribing modeling specifics to this high a level of detail in the AASHTO LRFD Bridge Design Specifications. Generally, designers are allowed leeway in choosing specific modeling strategies provided they understand the implications of their decisions.
		SECONDARY: Publish specific methodologies (presented in this report), present them to the bridge software industry, and encourage their implementation in commercial bridge design software.	

Calculation of Locked-in Forces Due to Cross-Frame Detailing	NCHRP Report 725 § 3.2.5	PRIMARY: Provide § 3.2.5 to the AASHTO/NSBA Steel Bridge Collaboration for vetting by the industry and for organization and publication in one or more AASHTO/NSBA Steel Bridge Collaboration documents. The initial recommendation of the research team would be for the Collaboration to consider publication of the content of § 3.2.5 in the AASHTO/NSBA Steel Bridge Collaboration Document G13.1, Guidelines for Steel Girder Bridge Analysis. Provide minor updates to Article C6.7.2 of the AASHTO LRFD Bridge Design Specifications to clarify the multiple uses of the term "erected position" and to clarify that locked-in cross-frame forces and negative flange lateral bending stresses are generally additive with the dead load effects in curved radially supported bridges, with references to G13.1 for detailed discussion. SECONDARY: Provide education (through this report and through associated presentations/publications) on this topic to the bridge engineering community. Encourage implementation in bridge design software.	The need for detailed analytical evaluation of locked-in forces due to cross-frame detailing varies from bridge to bridge (as explained in § 3.3.4 of this report), and this type of analysis is currently not commonly performed in practice. At this time, the best strategy is to publicize the issues, provide education on how to address these issues, and seek industry input in formulating policy regarding the need, and best practices, for detailed analytical evaluations.
Simplified Analysis Improvements for Tub-Girder Bridges	NCHRP Report 725 § 3.2.6	PRIMARY: Provide § 3.2.6 to the AASHTO/NSBA Steel Bridge Collaboration for vetting by the industry and for organization and publication in one or more AASHTO/NSBA Steel Bridge Collaboration documents. The initial recommendation of the research team would be for the Collaboration to consider publication of the content of § 3.2.6 in the AASHTO/NSBA Steel Bridge Collaboration Document G13.1, Guidelines for Steel Girder Bridge Analysis. SECONDARY: Provide education (through this report and through associated presentations/publications) on this topic to the bridge engineering community.	There is no significant precedent for prescribing modeling specifics to this high a level of detail in the AASHTO LRFD Bridge Design Specifications. Generally, designers are allowed leeway in choosing specific modeling strategies provided they understand the implications of their decisions. Presently, there is no discussion of the detailed component force equations from Fan and Helwig (1999 and 2002) in the AASHTO LRFD Bridge Design Specifications. These equations are discussed in the AASHTO/NSBA Steel Bridge Collaboration Document G13.1. The research team recommends that G13.1 is the preferred location for discussion of these details.

(continued on next page)

Table 4-2. (Continued).

Recommendation	Report Section	Implementation Suggestion	Comments
Estimation of Fit-up Forces	NCHRP Report 725 § 3.3.5	PRIMARY: Provide § 3.3.5 to the AASHTO/NSBA Steel Bridge Collaboration for vetting by the industry and for organization and publication in one or more AASHTO/NSBA Steel Bridge Collaboration documents. The initial recommendation of the research team would be for the Collaboration to consider publication of the content of § 3.2.2 in the AASHTO/NSBA Steel Bridge Collaboration Document G13.1, Guidelines for Steel Girder Bridge Analysis.	The need for detailed analytical evaluation of locked-in forces due to cross-frame detailing varies from bridge to bridge (as explained in § 3.3.4 of this report), and this type of analysis is currently not commonly performed in practice. At this time, the best strategy is to publicize the issues, provide education on how to address these issues, and seek industry input in formulating policy regarding the need, and best practices, for detailed analytical evaluations. If appropriate discussions are developed by the AASHTO/NSBA Collaboration, references to this material should be provided in commentary to Articles 11.6.4.2 and 11.6.5 of the AASHTO LRFD Bridge Construction Specifications.
		SECONDARY: Provide education (through this report and through associated presentations/publications) on this topic to the bridge engineering community.	
Definition of Erection Engineering Tasks	Task 9 Report § 2	PRIMARY: Provide the Task 9 report to the AASHTO/NSBA Steel Bridge Collaboration for vetting by the industry and for organization and publication in one or more AASHTO/NSBA Steel Bridge Collaboration documents. The initial recommendation of the research team would be for the Collaboration to consider publication of the content of the Task 9 report in the AASHTO/NSBA Steel Bridge Collaboration Guide Specification S10.1, Steel Bridge Erection Guide Specifications.	§ 2 of the Task 9 report is titled Recommendations for Construction Plan Details and addresses all aspects of the documentation of the erection plan for a steel girder bridge, including both drawings and calculations. This section of the Task 9 report is already written in the format of "requirement" and associated "commentary." As such, it can be adopted easily and directly into either the S10.1 Guide Specification or the AASHTO LRFD Bridge Construction Specifications. Adoption in either document would allow national dissemination of the guidelines and provide bridge owners the opportunity to adopt the guidelines directly, by reference as a whole or in parts, or by means of transferring some or all of the provisions into their own specifications and policy documents. The primary recommendation of publication via an AASHTO/NSBA Steel Bridge Collaboration Guideline or Guide Specification reflects the recommendation of the research team to publish a single, cohesive, comprehensive guideline document that addresses the entire set of steel bridge erection documentation requirements, including both erection engineering calculations and plans.
		SECONDARY: Package § 2 of the Task 9 report in its entirety as a ballot item for incorporation into the AASHTO LRFD Bridge Construction Specifications in a revision of § 11.2.2 – Erection Drawings.	

Recommendations for Appropriate Level of Analysis Refinement	NCHRP Report 725 § 3.1 Task 9 Report § 3.2	PRIMARY: Provide the Task 9 report to the AASHTO/NSBA Steel Bridge Collaboration for vetting by the industry and for organization and publication in one or more AASHTO/NSBA Steel Bridge Collaboration documents. The initial recommendation of the research team would be for the Collaboration to consider publication of the content of the Task 9 report in the AASHTO/NSBA Steel Bridge Collaboration Guide Specification S10.1, Steel Bridge Erection Guide Specifications.	The recommendations regarding the appropriate level of analysis refinement are the heart of the research results of NCHRP Project 12-79, and these recommendations should receive as wide and intense a distribution as possible. However, a brief presentation of these recommendations is not feasible. As can be seen in § 3.1 of NCHRP Report 725 or § 3.2 of the Task 9 report, the matrices for recommended level of analysis are large and warrant substantial commentary and examples. For this reason, the primary recommendation of the research team is to publish these recommendations in a document where a more lengthy presentation of the guidelines is more appropriate. The more flexible intent and format of the AASHTO/NSBA Steel Bridge Collaboration documents provides such a mechanism. Publication of these recommendations in the AASHTO LRFD Bridge Design Specifications or LRFD Bridge Construction Specifications is possible, but less desirable due to concerns that the length of the presentation would undesirably encumber the presentation and understanding of the recommendations. The primary recommendation of publication via an AASHTO/NSBA Steel Bridge Collaboration Guideline or Guide Specification reflects the recommendation of the research team to publish a single, cohesive, comprehensive guideline document that addresses the entire set of steel bridge erection documentation requirements, including both erection engineering calculations and plans. These particular analysis recommendations blur the line between design and construction. Therefore the secondary recommendation to publish these recommendations in the AASHTO LRFD Bridge Construction Specifications (rather than the AASHTO LRFD Bridge Design Specifications) reflects the opinion of the research team that this type of analysis is heavily dependent on the individual contractor's chosen erection sequence and erection methods. This type of engineering analysis is not typically the responsibility of the engineer who develops the design documents for bidding, but rather is the responsibility of the contractor's engineer who develops/analyzes the contractor's specific erection plan.
		SECONDARY: Rewrite § 3.2 of the Task 9 report into the format of a ballot item for incorporation into the AASHTO LRFD Bridge Construction Specifications in a revised and re-titled version of § 11.6.4.2. The proposed new title of this section would be Evaluation of Stability, Stresses, and Constructed Geometry During Erection.	

(continued on next page)

Table 4-2. (Continued).

Recommendation	Report Section	Implementation Suggestion	Comments
Guidelines on Calculations for Structural Adequacy and Stability	Task 9 Report § 3.3	PRIMARY: Provide the Task 9 report to the AASHTO/NSBA Steel Bridge Collaboration for vetting by the industry and for organization and publication in one or more AASHTO/NSBA Steel Bridge Collaboration documents. The initial recommendation of the research team would be for the Collaboration to consider publication of the content of the Task 9 report in the AASHTO/NSBA Steel Bridge Collaboration Guide Specification S10.1, Steel Bridge Erection Guide Specifications.	The primary recommendation of publication via an AASHTO/NSBA Steel Bridge Collaboration Guideline or Guide Specification reflects the recommendation of the research team to publish a single, cohesive, comprehensive guideline document that addresses the entire set of steel bridge erection documentation requirements, including both erection engineering calculations and plans. These particular analysis recommendations blur the line between design and construction. Therefore the secondary recommendation to publish these recommendations in the AASHTO LRFD Bridge Construction Specifications (rather than the AASHTO LRFD Bridge Design Specifications) reflects the opinion of the research team that this type of analysis is heavily dependent on the individual contractor's chosen erection sequence and erection methods. This type of engineering analysis is not typically the responsibility of the engineer who develops the design documents for bidding, but rather is the responsibility of the contractor's engineer who develops/analyzes the contractor's specific erection plan.
		SECONDARY: Rewrite § 3.3 through 3.6 of the Task 9 report into the format of a ballot item for incorporation into the AASHTO LRFD Bridge Construction Specifications in a revised and re-titled version of § 11.6.4.2. The proposed new title of this section would be Evaluation of Stability, Stresses, and Constructed Geometry during Erection.	
Guidelines for Structural Adequacy of Temporary Components	Task 9 Report § 3.4	Same as for Task 9 report, § 3.3	Same as for Task 9 report, § 3.3
Miscellaneous Calculations and Recommendations	Task 9 Report § 3.5	Same as for Task 9 report, § 3.3	Same as for Task 9 report, § 3.3
Calculation Checklist	Task 9 Report § 3.6	Same as for Task 9 report, § 3.3	Same as for Task 9 report, § 3.3

Problematic Characteristics and Details to Avoid	Task 9 Report § 3.4	PRIMARY: Provide the Task 9 report to the AASHTO/NSBA Steel Bridge Collaboration for vetting by the industry and for organization and publication in one or more AASHTO/NSBA Steel Bridge Collaboration documents. The initial recommendation of the research team would be for the Collaboration to consider publication of the content of the Task 9 report in the AASHTO/NSBA Steel Bridge Collaboration Guide Specification S10.1, Steel Bridge Erection Guide Specifications. SECONDARY: Rewrite § 3.3 through 3.7 of the Task 9 report into the format of a ballot item for incorporation into the AASHTO LRFD Bridge Design Specifications in a new section, § 6.7.8. The proposed new title of this section would be Problematic Details to Avoid.	The recommendations related to problematic details to avoid are focused on the effect of these details on erection of steel girder bridges. Although this is more clearly a design issue since these decisions are typically made by the design engineer long before the contract is let to a contractor, these specific recommendations do not necessarily rise to the level of prescriptive specification requirements. Thus, the primary recommendation of publication via an AASHTO/NSBA Steel Bridge Collaboration Guideline or Guide Specification reflects the recommendation of the research team to publish a single, cohesive, comprehensive guideline document that addresses the entire set of steel bridge erection documentation requirements, including both erection engineering calculations and plans, and the associated hope that design engineers also will read this document and implement design strategies that will facilitate easy erection of steel girder bridges. The secondary recommendation of publication in the AASHTO LRFD Bridge Design Specifications in a new § 6.7.8 reflects the difficulty in placing these general recommendations in a specific section of the design code. As a compromise, a new section of the code is proposed. A third option could be considered, where the individual recommendations are scattered through the code in sections more directly related to each individual recommendation's specific subject.

154 Guidelines for Analysis Methods and Construction Engineering of Curved and Skewed Steel Girder Bridges

concrete mix design and methods of construction. A more comprehensive understanding of the actual early-age behavior during and after placement of concrete decks is needed if engineers are to take optimum advantage of the early strength gains. Furthermore, as noted in the NCHRP Project 12-79 research, there is no such thing as a conservative displacement prediction. Sufficient measurements and corresponding analytical predictions are needed to allow the calculation of confidence limits for the predicted displacements during and after the concrete deck placement.

- **Innovative Framing Arrangements—**Further studies of innovative framing arrangements to mitigate nuisance stiffness effects in skewed girder bridge construction would be useful. For example, as detailed in the Task 8 report of the NCHRP Project 12-79 research, further research should be conducted to investigate the use of skewed intermediate cross-frames at angles larger than 20°, combined with a split-pipe connection detail to mitigate the problems of connecting to the girders at a sharp skew angle. As demonstrated in the NCHRP Project 12-79 research, nuisance stiffness effects are mitigated best by making the intermediate cross-frames parallel to the bearing lines in parallel-skew bridges and by "fanning" the intermediate cross-frames between the skewed bearing lines in bridges with non-parallel skew. The behavior of straight and curved bridges with these arrangements should be investigated in more detail, including the consideration of other impacts that these cross-frame arrangements may have on the design behavior and construction.
- **Tub Girders with Pratt TFLB Systems—**The impact of Pratt top flange lateral bracing (TFLB) system layouts on the internal forces in tub-girder bridges needs to be better understood. The NCHRP Project 12-79 research showed that a conventional 2D-grid analysis, coupled with commonly used tub-girder bridge component force equations, has particular difficulty in predicting the response of these types of bridges. Further improvements to 2D-grid analysis methods may be possible to make these methods viable for the design of tub-girder bridges with Pratt TFLB systems.
- **Live-Load Effects—**Lastly, the emphasis of the NCHRP Project 12-79 research was on analysis for construction engineering of steel girder bridges. Parallel studies should be conducted to evaluate the accuracy of simplified methods of analysis for the prediction of the live-load response of bridges. Of concern is the tedious nature and limited accuracy of traditional load distribution factor calculations for horizontally curved and/or skewed girder bridges as a function of the complexity of the bridge geometry. Engineers need to better understand the limits of their analysis calculations regarding the live-load response of steel girder bridge systems.

References and Bibliography

AASHTO (2010). AASHTO LRFD *Bridge Design Specifications,* 5th Edition with 2010 Interim Revisions, American Association of State Highway and Transportation Officials, Washington, D.C.

AASHTO (2010b). *AASHTO LRFD Bridge Construction Specifications,* 3rd Edition with 2010 and 2011 Interim Revisions, American Association of State Highway and Transportation Officials, Washington, D.C.

AASHTO/NSBA (2011). *Guidelines for the Analysis of Steel Girder Bridges,* G13.1, AASHTO/NSBA Steel Bridge Collaboration, American Association of State Highway and Transportation Officials, Washington, D.C. and National Steel Bridge Alliance, Chicago, IL.

AASHTO/NSBA (2007). *Steel Bridge Erection Guide Specification,* S10.1, AASHTO/NSBA Steel Bridge Collaboration, American Association of State Highway and Transportation Officials, Washington, D.C. and National Steel Bridge Alliance, Chicago, IL.

AASHTO/NSBA (2006). *Guidelines for Design Details,* G1.4, AASHTO/NSBA Steel Bridge Collaboration, American Association of State Highway and Transportation Officials, Washington, D.C. and National Steel Bridge Alliance, Chicago, IL.

AASHTO/NSBA (2003). *Guidelines for Design for Constructibility*, G12.1, AASHTO/NSBA Steel Bridge Collaboration, American Association of State Highway and Transportation Officials, Washington, D.C. and National Steel Bridge Alliance, Chicago, IL.

Ahmed, M.Z. and Weisberger, F.E. (1996). "Torsion Constant for Matrix Analysis of Structures Including Warping Effect," *International Journal of Solids and Structures,* Elsevier, 33(3), 361–374.

Bridgesoft, Inc. (2010). "STLBRIDGE, Continuous Steel Bridge Design," http://bridgesoftinc.com/

Chang, C.-J. (2006). "Construction Simulation of Curved Steel I-Girder Bridges," doctoral dissertation, School of Civil and Environmental Engineering, Georgia Institute of Technology, Atlanta, GA, 340 pp.

Chang, C.-J. and White, D.W. (2008). "Construction Simulation of Curved Steel I-Girder Bridge Systems," report to Federal Highway Administration, School of Civil and Environmental Engineering, Georgia Institute of Technology, Atlanta, GA, 285 pp.

Chavel, B.W. (2008). "Construction and Detailing Methods of Horizontally Curved Steel I-Girder Bridges," Ph.D. dissertation, Swanson School of Engineering, University of Pittsburgh, Pittsburgh, PA, 357 pp.

Dykas, J. (2012). "Field Measurements during Erection of Ramp B Bridge Over I-40," master's thesis, School of Civil and Environmental Engineering, Georgia Institute of Technology, Atlanta, GA, May.

Fan, Z.F. and Helwig, T. (2002) "Distortional Loads and Brace Forces in Steel Box Girders," *ASCE Journal of Structural Engineering,* V. 128, No. 6, June 2002, pp. 710–718.

Fan, Z.F. and Helwig, T. (1999). "Behavior of Steel Box Girders with Top Flange Bracing," *Journal of Structural Engineering,* August 1999, ASCE, pp. 829–837.

Grubb, M. (1984). "Horizontally Curved I-Girder Bridge Analysis: V-Load Method," *Transportation Research Record 289,* 1984, pp. 26–36.

Hall, D.H., Grubb, M.A., and Yoo, C.H. (1999). *NCHRP Report 424: Improved Design Specifications for Horizontally Curved Steel Girder Highway Bridges*, Transportation Research Board, NRC, Washington, D.C.

Helwig, T. (2012). "Bracing System Design," *Steel Bridge Design Handbook,* Office of Bridge Technology, Federal Highway Administration.

Helwig, T., Yura, J., Herman, R., Williamson, E., and Li, D. (2007). "Design Guidelines for Steel Trapezoidal Box Girder Systems," Technical Report No. FHWA/TX-07/0-4307-1. Center for Transportation Research, University of Texas at Austin, TX, 84 pp.

Jimenez Chong, J.M. (2012). "Construction Engineering of Steel Tub-Girder Bridge Systems for Skew Effects," Ph.D. dissertation, School of Civil and Environmental Engineering, Georgia Institute of Technology, Atlanta, GA, 276 pp.

156 Guidelines for Analysis Methods and Construction Engineering of Curved and Skewed Steel Girder Bridges

Jung, S.K. (2006) "Inelastic Strength Behavior of Horizontally Curved Composite I-Girder Bridge Structural Systems," doctoral dissertation, School of Civil and Environmental Engineering, Georgia Institute of Technology, Atlanta, GA, 811 pp.

Jung, S.K. and White, D.W. (2008) "Inelastic Strength Behavior of Horizontally Curved Composite I-Girder Bridge Structural Systems," report to Federal Highway Administration, School of Civil and Environmental Engineering, Georgia Institute of Technology, Atlanta, GA, 731 pp.

Krupicka, G. and Poellot, B. (1993). "Nuisance Stiffness," *Bridgeline,* 4(1), HDR Engineering, Inc., 3 pp.

LARSA (2010). "LARSA 4D, The Complete Software for Bridge Engineering," http://www.larsa4d.com/products/larsa4d.aspx

MASTAN2 (2011)." MASTAN2, Interactive Structural Analysis Program that Provides Preprocessing, Analysis, and Postprocessing Capabilities," http://www.mastan2.com/

McGuire, W., Gallagher, R.H,, and Ziemian, R.D. (2000). *Matrix Structural Analysis,* 2nd Edition, Wiley, NY.

MDX (2011). "MDX Software, The Proven Steels Bridge Design Solution," http://www.mdxsoftware.com/

NCDOT (2006). *Computing Non-Composite Dead Load Deflections on Steel Bridges,* Memorandum to Project Engineers and Project Design Engineers, G.R. Perfetti, State Bridge Design Engineer, North Carolina Department of Transportation, October 19, 2006, http://www.ncdot.org/doh/preconstruct/highway/structur/polmemo/m101906.pdf

NHI (2011). "Analysis and Design of Skewed and Curved Steel Bridges with LRFD, Reference Manual," NHI Course No. 130095, Publication No. FHWA-NHI-10-087, National Highway Institute, Federal Highway Administration, 1,476 pp.

NSBA (1996). "V-Load Analysis and Check (VANCK), User Manual, Version 1.0," National Steel Bridge Alliance and American Institute of Steel Construction.

Ozgur, C. (2011). "Influence of Cross-Frame Detailing on Curved and Skewed Steel I-Girder Bridges," Ph.D. dissertation, School of Civil and Environmental Engineering, Georgia Institute of Technology, Atlanta, GA, 398 pp.

PennDOT (2004). *Steel Girder Bridges Lateral Bracing Criteria and Details,* BD-620M, Pennsylvania Department of Transportation, http://www.dot.state.pa.us/Internet/BQADStandards.nsf/bd2005?openfrm

Poellot, W. (1987). "Computer-Aided Design of Horizontally Curved Girders by the V-Load Method." *Engineering Journal,* AISC, Vol. 24, No. 1, First Quarter 1987, pp. 42–50.

Richardson, G. and Associates (1963). "Analysis and Design of Horizontally Curved Steel Bridge Girders," United States Steel Structural Report, ADUSS 88-6003-01.

RISA (2011). "Superior Structural Engineering Software for Analysis and Design," RISA Technologies LLC," http://www.risatech.com/

Sanchez, T.A. (2011). "Influence of Bracing Systems on the Behavior of Steel Curved and/or Skewed I-Girder Bridges during Construction," Ph.D. dissertation, School of Civil and Environmental Engineering, Georgia Institute of Technology, Atlanta, GA, 335 pp.

Tung, D. and Fountain, R. (1970). "Approximate Torsional Analysis of Curved Box Girders by the M/R-Method," *AISC Engineering Journal,* July 1970, AISC, pp. 65–74.

TxDOT (2005). *Preferred Practices for Steel Bridge Design, Fabrication and Erection,* Texas Steel Quality Council and Texas Department of Transportation, Austin, TX, 37 pp.

United States Steel Corporation (1965), "Highway Structures Design Book," ADUSS 88-1895-01, Vol. 1.

White, D.W., Zureick, A.H., Phoawanich, N.P., and Jung, S.K. (2001). "Development of Unified Equations for Design of Curved and Straight Steel Bridge I Girders," Final Report to AISI, PSI Inc. and FHWA, October, 547 pp.

Yura, J., Helwig, T., Herman, R., and Zhou, C. (2008). "Global Lateral Buckling of I-Shaped Girder Systems," *Journal of Structural Engineering,* 134(9), 1,487-1,494.

Zureick, A., Naqib, R., and Yadlosky, J.M. (1994). "Curved Steel Bridge Research Project," Interim Report I, Synthesis, FHWA Contract No. DT FG61-93-C-00136, FHWA, McLean, VA, December.

APPENDIX A

Glossary of Key Terms Pertaining to Cross-Frame Detailing

It is essential that the reader thoroughly understand the fundamental meaning of a number of the terms used in this report pertaining to cross-frame detailing, in order to facilitate study and interpretation of the corresponding results and discussions throughout the report. These terms and their definitions are as follows, listed in alphabetical order.

- **Accurate 2D-Grid Analysis.** A 2D-grid analysis that incorporates the improved I-girder torsion model of Section 3.2.2, the improved equivalent beam cross-frame model of Section 3.2.3, the improved method of calculating girder flange lateral bending stresses of Section 3.2.4, and when SDLF or TDLF detailing are employed, the procedure for calculating locked-in forces of Section 3.2.5.
- **Accurate 3D FE Analysis.** A 3D-FEA model that is capable of matching the benchmark 3D FEA responses of the Task 7 report (Appendix D of the contractors' final report) as well as the FHWA Test Bridge benchmarks of Sections 3.2.2.1, 3.2.2.3, 3.2.3.6, 3.2.4, and 3.3.3.2 (Figures 3-85 through 3-91) with a normalized mean error (Equation 6) less than or equal to 6 percent. This corresponds to an A grade in Table 3-1 of Section 3.1.2. When SDLF or TDLF detailing are employed, an accurate 3D FEA must account for the corresponding locked-in forces using a procedure such as the one presented in Section 3.2.5. As shown in Section 3.3, the locked-in forces from the (beneficial) initial lack of fit of the cross-frames and girders generally has a substantial effect on the distribution of internal forces and stresses.
- **Conservative Elastic System.** A structural system in which the response to any loading is unique (i.e., path independent), and in which, if the loading were removed, the system would return to its original undeformed geometry. Steel girder bridges are commonly idealized as conservative elastic systems for their erection analysis. Based on the assumptions that (1) yielding does not occur at any location within the structure, (2) any slip associated with frictional forces developed at the supports is negligible such that the supports may be idealized as non-frictional, and (3) slip within the structural connections (cross-frame connections to the girders, girder splices, etc.) is negligible, a structural analysis model can be developed of all the connected components/members/units for any steel erection stage and the gravity loads can simply be "turned on" to determine the unique response of the structure for that stage. Structural analysis of staged concrete deck placement is not unique because the "strain-free" position of the concrete deck, when its early stiffness first becomes significant for a given stage, depends on the sequence in which the concrete deck is placed. Staged concrete deck placement analysis is commonly handled by considering the bridge as an "incrementally conservative elastic system" in which the structure is analyzed elastically for the concrete loading increment associated with each stage, using a selected constant concrete elastic stiffness for the portions of the deck that have significant early stiffness.
- **Cross-Frame Drop.** The change in elevation between the ends of a fabricated cross-frame. For NLF detailing, the cross-frame drops are taken equal to the drops between the girders in

the initial fabricated (plumb and cambered) geometry. For SDLF or TDLF detailing of the cross-frames, the intermediate cross-frame drops are different from the corresponding girder drops. For SDLF detailing, the steel dead load cambers are subtracted from the above total drops between the girders to obtain the cross-frame drops. For TDLF detailing, the total dead load cambers are subtracted from the above total drops between the girders to obtain the cross-frame drops.

- **Fit-Up Forces.** The forces required to physically bring the components together and complete a connection during the erection of the steel. These forces can be influenced by initial lack-of-fit effects from SDLF or TDLF detailing of the cross-frames, but generally, they are distinctly different from the forces associated with the initial lack of fit between the girders and the cross-frames in their initially fabricated no-load geometry.
- **Initial Lack of Fit.** For analysis of SDLF or TDLF effects, the displacement incompatibility between the connection work points on the cross-frames and the corresponding points on the girders, with the cross-frames and girders in their initially fabricated no-load geometry, and in the context of this report, with plumb cambered initial girder geometry. For SDLF or TDLF detailing of cross-frames in I-girder bridges, the cross-frame may be considered to be connected to the initially plumb and cambered girder on one side, and the initial lack of fit is the displacement incompatibility with the work points on the girder on the other side. It should be noted that for cross-frames that are not normal (perpendicular) to the girders, there are generally two contributions to the initial lack of fit: (1) the difference in the vertical camber between the work points on the connected girders and (2) the major-axis bending rotations of the girders at the girder work points (see Figures 3-31 through 3-33). The initial no-load geometry defines the reference state of the corresponding conservative elastic system at which the strain energy is equal to zero. Hence, the no-load configuration is the only appropriate configuration to use as a basis for determining the corresponding lack-of-fit forces in the structure.
- **Lack-of-Fit Analysis.** A structural analysis in which locked-in forces are determined based on the initial lack of fit between the connection points within the structure. The designer can conduct a lack-of-fit analysis without any applied dead load on the structure to calculate the specific locked-in forces in the structure, or the steel dead load or total dead load may be included in the analysis to determine the total force effects in the structure for the selected steel dead or total dead load loading condition.
- **Lack-of-Fit Analysis Configuration 1.** The physical initial no-load (undeformed, unstrained) geometry of the cross-frames and of the fabricated (cambered and plumb) girders under theoretical zero load (see Figure 3-30a). One should note that defining the initial no-load (undeformed, unstrained) geometry of the structure is key to any structural analysis. The stresses and forces in the system are based on the deformations from this configuration, including any lack-of-fit effects.
- **Lack-of-Fit Analysis Configuration 2.** An idealized (fictitious) configuration, used for the structural analysis, in which the girders are assumed to be "locked" in their initial no-load, plumb and cambered geometry, and the cross-frames are deformed to connect them to the girder connection work points (see Figure 3-30b). For a 3D FEA, the structural analysis calculates cross-frame member initial axial strains or initial axial stresses based on a position vector analysis involving the initial lack of fit of the cross-frames to the girder connection work points. For an accurate 2D-grid analysis, the structural analysis calculates corresponding initial equivalent beam element "fixed-end forces" corresponding to the deformations required to achieve compatibility with the girder connection work points.
- **Lack-of-Fit Analysis Configuration 3.** The idealized deformed configuration reached by the structural system under no-load (dead load not yet applied), after resolving the initial lack of fit by connecting the cross-frames to the girders in Configuration 2, then "releasing" the locked girders to deflect under the lack-of-fit effects from the cross-frames.

- **Lack-of-Fit Analysis Configuration 4.** The final geometry reached under the targeted steel dead load or total dead load condition once the steel dead load or total dead load has been added to the structure, i.e., the geometry under the combined effects of the steel (or total) dead load plus the locked-in forces due to the SDLF or TDLF detailing of the cross-frames.
- **Layover.** The lateral deflection of the girder top flange relative to its bottom flange associated with twisting.
- **Locked-In Forces.** The internal forces induced into the structural system by force-fitting the cross-frames and girders together. These internal forces would remain if the structure's dead load were theoretically removed. In straight-skewed bridges, the locked-in forces due to SDLF or TLDF detailing are largely opposite in sign to corresponding dead load effects, but they can be additive with the dead load effects in some locations. In curved radially supported bridges, the locked-in forces due to SDLF or TDLF detailing largely are additive with the corresponding dead load effects. The locked-in forces are never "removed" by corresponding dead load forces, but when they are opposite in sign to these forces, they can be "balanced" by the corresponding dead load forces.
- **No-Load Fit (NLF) Detailing.** A method of detailing of the cross-frames in which the cross-frame connection work points fit-up perfectly with the corresponding work points on the girders, without any force fitting, in the initial undeformed cross-frame geometry, and with the girders in their initially undeformed fabricated (cambered and plumb) geometry.
- **Steel Dead Load Fit (SDLF) Detailing.** A method of detailing of the cross-frames in which the cross-frame connection work points are detailed to fit-up perfectly with the corresponding points on the girders with the steel dead load camber vertical displacements and rotations subtracted out of the initial total camber of the girders. Also referred to commonly as "erection fit." Detailers and fabricators work solely with the girder cambers specified on the engineering drawings to set the cross-frame drops associated with the SDLF detailing. The girders are assumed to be displaced from their initially fabricated (cambered and plumb) position to the targeted *plumb* steel dead load condition. Any twisting of the girders associated with the three-dimensional interactions with the cross-frames and overall structural system are not directly considered in these calculations.
- **Total Dead Load Fit (TDLF) Detailing.** A method of detailing of the cross-frames in which the cross-frame connection work points are detailed to fit-up perfectly with the corresponding points on the girders with the total dead load camber vertical displacements and rotations subtracted out of the initial total camber of the girders. Detailers and fabricators work solely with the girder cambers specified on the engineering drawings to set the cross-frame drops associated with the TDLF detailing. The girders are assumed to be displaced from their initially fabricated (cambered and plumb) position to the targeted *plumb* total dead load condition. Any twisting of the girders associated with the three-dimensional interactions with the cross-frames, slab, and overall structural system are not directly considered in these calculations. Also referred to commonly as "final fit."
- **Total Forces.** The forces due to the combination of the dead load effects in the targeted condition plus the locked-in force effects from SDLF or TDLF detailing of the cross-frames.
- **Uniqueness.** The attribute of a conservative elastic structural system in which the state of stress and strain in the structure is path independent, i.e., in the context of steel bridge erection, independent of the sequence of erection. This assumption is a common staple of structural analysis for design. The unique solution depends not only on the targeted loading state (e.g., steel dead load or total dead load). It also depends on any specific initial lack of fit between the structural components. The influence of connection slip within tolerances also can be included to obtain a unique solution for a given slip, as demonstrated in Section 3.3.3.2. However, the influence of connection "slip" within standard connection tolerances generally is considered to be negligible for structural design purposes.

APPENDIX B

Task 9 Report—Recommendations for Construction Plan Details and Level of Construction Analysis

NATIONAL COOPERATIVE HIGHWAY RESEARCH PROGRAM

PROJECT NO. NCHRP 12-79

Recommendations for Construction Plan Details and Level of Construction Analysis

TASK 9 REPORT

Prepared for
NCHRP
Transportation Research Board
Of
The National Academies

Brandon W. Chavel
HDR Engineering, Inc.
Chicago, IL

Domenic Coletti
HDR Engineering, Inc.
Raleigh, NC

Donald W. White
Georgia Institute of Technology
Atlanta, GA

February 29, 2012

TRANSPORTATION RESEARCH BOARD

WASHINGTON, D.C.
2006
www.TRB.org

CONTENTS

SUMMARY

Recommendations for Construction Plan Details and Level of Construction Analysis

Difficulties can arise during the construction of curved and skewed steel girder bridges when an erection plan does not contain sufficient details or when the construction analysis does not properly account for the three-dimensional behavior of the structure. The erection plan, construction analysis, and other computations for curved and skewed steel girder bridges must be sufficient to account for the complex behavior of these bridge types.

This document provides recommendations regarding the content of construction plans for curved and skewed steel I-girder bridges. Guidelines for selecting the appropriate methods of analysis for the construction analysis of I-girder and tub-girder bridges are also provided. The guidelines for selecting the appropriate methods of analysis focus on commonly used 1D, 2D, and 3D analytical approaches in current structural engineering practice (2011). Guidelines pertaining to the calculations developed to support the erection plan and procedures also are provided within this document. This document focuses on the plans, analysis methods, and other calculations conducted for the construction engineering of curved and/or skewed steel girder bridges. It does not address the wide range of additional overall considerations in the complete design and analysis of these types of bridges, such as the design of the structure in its final constructed condition for vehicular live load effects.

The major objectives of these recommendations are to help engineers:

1. Ensure that construction plans, methods of analysis, and other calculations for curved and/or skewed steel girder bridges, as affected by the structure's geometry and other construction conditions, are generally sufficient for predicting the constructed geometry (to facilitate fit-up),
2. Ensure stability during all stages of erection, and
3. Achieve better consistency in construction plans, methods of analysis, and other calculations for a given degree of the bridge's geometric, structural, and construction complexity.

Contractors and Contractors' Engineers can use this document as a guide in developing construction plans, performing calculations, and selecting the appropriate analysis methods. Bridge Owners can use this document as a checklist to verify that the Contractor and the Contractor's Engineer have developed an appropriate construction plan and calculation submittal.

CHAPTER 1

Introduction

1.1 Problem Statement

In current practice (2011), the construction of curved and/or skewed steel girder bridges is sometimes hampered by insufficient erection plans and procedures or computations. Within the industry, little has been published in the way of guidelines or recommendations on the level of detail for construction plans for curved and/or skewed steel girder bridges, or on the level of detail regarding engineering calculations for the construction engineering. Furthermore, the industry is lacking guidelines on choosing the proper analytical methods for investigating the steel erection sequence of curved and/or skewed steel girder bridges.

1.2 Objectives

This document outlines key recommendations regarding the level of effort for development of construction plans and calculations for curved and/or skewed steel girder bridges at the construction engineering stage. This document also provides recommendations regarding the appropriate methods of structural analysis for evaluating the structural behavior and predicted geometry of the bridge during the various stages of construction.

This document is written in an effort to make the development of construction plans, calculations, and methods of analysis more consistent for curved and/or skewed steel girder bridges. Contractors and Contractors' Engineers can use this document to guide them in developing construction plans, performing calculations, and selecting the appropriate analysis methods. Bridge Owners can use this document as a checklist to verify that the Contractor and the Contractor's Engineer have developed an appropriate construction plan and calculation submittal.

1.3 Organization

This report is divided into two main sections. Section 2 provides recommendations regarding the level of detail that should be used in the development of erection plans and procedures for curved and/or skewed steel girder bridges. This section is written in a style and format similar to design code provisions, including the development of Commentary sections for many of the erection plan recommendations.

Section 3 defines the levels of construction analysis that should be considered for curved and skewed steel girder bridges based upon the complexity of the structure. These guidelines are summarized from the studies conducted as part of NCHRP Project 12-79, "Guidelines for Analytical Methods and Erection Engineering of Curved and Skewed Steel Deck-Girder Bridges." This section also provides details regarding particular calculations for consideration by engineers developing construction plans and procedures.

CHAPTER 2

Recommendations for Construction Plan Details

2.1 Introduction

The AASHTO/NSBA Steel Bridge Collaboration document S10.1, "Steel Bridge Erection Guide Specification," (AASHTO/NSBA, 2007) highlights the minimum requirements for the development of steel girder erection procedures, including steel erection drawings and calculations. The recommendations provided herein use and build upon this AASHTO/NSBA document based on studies conducted as part of NCHRP Project 12-79. Contractors and Engineers developing erection plans for steel erectors are encouraged to use these recommendations so that erection plans are uniform and complete. Bridge Owners are encouraged to adopt these recommendations as a guide to verify that erection plans submitted by the Contractor contain the necessary details and procedures.

2.2 Erection Procedure Drawings Recommendations

2.2.1 General

The Contractor shall submit a detailed erection plan and procedures to the Owner for each structural unit, prepared by or under the supervision of a licensed Professional Engineer (or a qualified Structural Engineer where applicable). The detailed erection plan and procedures shall contain drawings and calculations (see Section 3) that support the erection plan and procedures. The plan and procedures shall address all requirements for erection of the structural steel into the final designed configuration and satisfy all written Owner comments prior to the start of erection. As a minimum, the erection plan and procedures shall include the items cited in the sections that follow.

2.2.1.1 General—Commentary

The qualifications of the Engineer preparing the erection plan and procedures should reflect knowledge, training, and experience in steel erection, and demonstrated abilities to resolve problems related to steel bridge erection. Complex or monumental structures should have specific requirements noted in the Contract. The erection procedure should be submitted as soon as possible after the Contract award. The submission dates and review period should be agreed upon by the Owner and the Contractor as soon as possible after the Contract award, so that sufficient time is allotted for review by the Owner. Erectors are encouraged to attend prebid and preconstruction meetings to help understand the complexities associated with the steel erection well in advance. Projects that involve complex erection or multi-agency reviews can be expected to require additional time for review of the submitted erection plan and procedure. In these cases, submission dates and review periods should be agreed upon by the Contractor and all agencies conducting reviews. Furthermore, in some cases, coordination with the Fabricator and Detailer may be necessary, as the preparation of shop detailing drawings and geometric calculations will be delayed until the erection plan and procedure is approved.

2.2.2 Plan of Work Area

The erection plan shall contain a plan of the work area showing the bridge, the permanent support structures (piers and abutments), roads, railroad tracks, waterways (including dimensions for navigational channel, and navigational clearance required during construction), overhead and underground utilities, structures and conditions that may limit access, right-of-way and property lines, material (steel) storage areas, and other information that may be pertinent to the steel erection.

2.2.2.1 Plan of Work Area—Commentary

The plan of work area drawing should provide a general overview of the area where the bridge is to be erected. It allows all involved to see site conditions, access routes and staging areas, as well as utilities, roadways, existing structures, or other possible site constraints and better understand why a certain procedure or detail is specified within the erection plans and procedures.

2.2.3 Erection Sequence

The erection plan shall contain the erection sequence for all members noting the use of temporary support conditions, such as holding crane positions, temporary supports, falsework, etc. The erection sequence shall be shown in an illustrative plan view of the bridge for each erection stage, highlighting the structural components to be erected, lifting crane locations for primary member picks, and any temporary support conditions that are necessary during the particular stage. The illustrative plan view shall be accompanied with a written narrative of the procedure to be followed by the steel erector, which shall clearly state items such as structural components to be erected, use of temporary supports, use of temporary bracing, hold cranes, etc. Member reference marks, when reflected on the erection plan, should be the same as used on the shop detail drawings.

2.2.3.1 Erection Sequence—Commentary

The erection sequence should clearly indicate specific structural components to be erected at a given stage, such as the girders, cross frames, lateral bracing, etc. The erection sequence should also clearly indicate lifting crane positions, as well as any temporary support conditions necessary to facilitate a certain erection stage, such as temporary supports, holding crane positions, tie-down stability provisions, blocking of the bearings, etc. The erection sequence drawings should be treated as the detailed instructions for construction of the bridge and should be written as, and followed as, mandatory directives. If an item is not clearly shown or described, problems could arise during steel erection.

2.2.4 Delivery Location

The erection plan shall indicate the primary member delivery location and orientation.

2.2.4.1 Delivery Location—Commentary

The maximum crane lift radius is often controlled by the material delivery location, hence it is necessary to indicate the delivery location on the erection plan.

2.2.5 Crane Information

The erection plan shall show the location of each crane to be used for each primary member pick (see Section 2.2.3), the crane type, the crane pick radius, the crane support methods (mats, barges, etc.), and the means of attachment to the girders being lifted or supported.

The erection drawings also shall show a capacity chart or table for each crane configuration, boom length, counterweight requirements, and pick weights required to do the proposed work. The erection drawings also shall indicate any potential obstructions to crane operations such as existing structures, utilities, etc. Any calculations related to evaluation of crane capacity and crane stability also shall be included. The crane types shall be agreed upon by the Contractor and Contractor's Engineer, to ensure that the crane types are available to the Contractor and can access the work site.

2.2.5.1 Crane Information—Commentary

When the steel erection takes place on a navigable waterway, the configuration of the barge(s), loading sequence, and stability provisions (tie-downs, piles, etc.) shall be provided in the erection plan. Communication between the Contractor and the Contractor's Engineer is vital to ensure the cranes assumed by the Engineer are available to the Contractor. Providing the crane types, pick radii, pick weight, boom lengths, possible obstructions, etc., in the erection plans will help to prevent crane interferences, overloads, or failures during the steel erection.

2.2.6 Primary Member Crane Pick Information

The erection plan shall include the lifting weight of the primary member picks, including all rigging and pre-attached elements (such as cross-frames or splice plates). The erection plan shall also include the approximate center of gravity locations for the primary member picks of curved girders and assemblies.

2.2.6.1 Primary Member Crane Pick Information—Commentary

The lifting weights and the approximate centers of gravity for each pick will provide the steel erector with necessary information to safely lift various components. The centers of gravity provided on the plans should be taken as approximate locations, as these are typically calculated assuming nominal material sizes and approximations of minor items such as bolted connections, etc. The actual center of gravity locations should reasonably match these approximate locations and will aid the steel erector in determining the proper lifting location in the field.

2.2.7 Lifting Devices and Special Procedures

The erection plan shall include the details, weight, capacity, and arrangement of all rigging (beam clamps, lifting lugs, etc.) and all lifting devices (such as spreader and lifting beams) required for lifting primary members. The erection plan also shall specify whether rigging or lifting devices are to be bolted or welded to permanent members, including the method and time (shop or field) of attachment and capacity, as well as methods, time, and responsibility for removal.

As necessary, the erection plan shall provide special lifting/handling procedures for any primary member with potential stability or slenderness issues.

2.2.7.1 Lifting Devices and Special Procedures—Commentary

Assumptions regarding the weight of rigging, spreader beams, etc., should be included in the erection plan. Explicitly indicating all details related to rigging and spreader or lifting beams will help to ensure that the appropriate devices are being properly used in the field.

Straight slender beams, traditionally defined as those having a length of the shipping piece to flange width ratio (L/b) greater than 85, are prone to lateral torsional buckling and require particular attention during lifting/handling operations. This limiting length to flange width ratio for curved beams is smaller than 85, and in some cases has been taken as low as a value of 10. The flange width

(b) should be taken as the smallest width flange within the field section being lifted. Other types of structural members also may have slenderness and/or stability issues that should be addressed in the erection plans as appropriate.

2.2.8 Bolting Requirements

The erection plan shall indicate the bolting requirements for field splices and cross-frame (or diaphragm) connections.

For bolted splice connections of primary members, and bolted connections of diaphragms or cross frames that brace I-girders, fill at least 50 percent of holes in the connection prior to crane release with either erection bolts in a snug tight condition, or full-size erection pins (a.k.a., "drift pins"), using bolts for at least half of the filled holes (i.e., at least 25 percent of all holes). Sufficient erection pins shall be used near the outside corners of splice plate and at member ends near splice plate edges to ensure alignment. The filled holes shall be uniformly distributed across the connection.

2.2.8.1 Bolting Requirements—Commentary

Steel I-girders depend on their connections to adjacent girders through bracing members for their stability and stiffness during steel erection. This is especially true for curved steel girders, as the cross frames serve as primary load carrying members. Therefore, loosely connected cross frames should not be used during steel girder bridge erection, as this may compromise the girder alignment (geometry control) and stability.

The bolting requirements for girder field splices during steel erection need to be considered as well. In accordance with the AASHTO LRFD Bridge Construction Specifications, Article 11.6.5, "splices and field connections shall have one-half of the holes filled with bolts and cylindrical erection pins (half bolts and half pins) before installing and tightening the balance of the high strength bolts." In addition, the Contractor's Engineer developing the erection plan must ensure that the number of bolts or erection pins to be used provides enough capacity for transfer of loads for the given stage of steel erection.

2.2.9 Bearing Blocking and Tie-Down Details

The erection plan shall indicate the blocking and/or tie-down details for the bridge bearings, as necessary.

2.2.9.1 Bearing Blocking Details—Commentary

Depending on their details, bridge bearings may allow movement (translation) in any direction and/or rotation about any axis. During steel erection, in addition to other stability provisions, the bearings may require blocking to prevent or limit the translational movements and rotations. In addition, bearings may need temporary tie-downs to prevent uplift at various stages during construction. The Contractor's Engineer (CE) should determine the blocking and/or tie down requirements such that the structure remains stable during all stages of erection and such that the behavior of the physical structure is consistent with the behavior assumed in the analysis and the erection plans. The CE should ensure that the bearings are not overloaded or over-rotated at any stage during the construction.

2.2.10 Load Restrictions

Restrictions regarding wind and construction dead and live loadings shall be included on the erection plan, as necessary.

2.2.10.1 Load Restrictions—Commentary

Limits may be placed on wind velocities during lifting of girder field pieces or during various stages of erection when the structure is only partially complete. The limitations on wind velocities are intended to prevent girder overstress and/or instabilities that could be caused by certain wind speeds and the associated wind pressure loading. Calculations may show that a girder or girder system may not be stable at a certain wind velocity, and this needs to be communicated to the Contractor and Steel Erector via the erection plan. If appropriate, the erection plans should include instructions and details for temporary support or tie-down of partially completed structures during high wind conditions.

The erection plans should also explicitly state restrictions on construction live loads (vehicles, equipment, personnel, etc.) and construction dead loads (formwork/falsework, stored materials, etc.). Inadvertent overloading by construction loads can affect the geometry control and also can lead to structural collapse.

2.2.11 Temporary Supports

The erection plan shall include the location of any temporary support structures (see Section 2.2.3), as well as details of the temporary support structure itself. If the temporary support is to be prefabricated (selected from a supplier's catalogue), the type and capacity shall be clearly defined in the erection plan; lateral capacity as well as vertical capacity requirements shall be considered as appropriate. If the temporary support is to be constructed by the Contractor on site, a complete design with full details, including member sizes, connections, and bracing elements, shall be provided in the erection plans. In either case, details regarding the upper grillage and temporary bearing assembly (i.e., details of how the steel girders will bear on the temporary support) also shall be included in the erection plan. In addition, all foundation requirements for temporary support structures shall be provided in the erection plan.

The erection plan shall indicate the location of hold cranes used to provide temporary support to the steel assembly (see Sections 2.2.3 and 2.2.5). The hold crane type, capacity, boom lengths, pick radius, and means of attachment to the girders also shall be indicated in the erection plan.

The erection plan shall include the location and details for temporary tie-downs that are required to facilitate the steel erection. At a minimum, the details shall include the tie-down, girder attachment devices, and anchoring devices.

2.2.11.1 Temporary Supports—Commentary

In many cases, temporary supports are essential for the construction of a steel girder bridge. As such, they should be clearly detailed in the erection plan, whether the support is a falsework tower, hold crane, tie-down, bearing blocking, or other support.

2.2.12 Jacking Devices

The erection plan shall indicate jacking devices required to complete the steel erection. Their location, type, size, and capacity shall be clearly indicated on the erection plan, as well as their intended use, sequence of engagement, load level, and any other key parameters of their operation.

2.2.12.1 Jacking Devices—Commentary

In some cases, jacking devices may be required at temporary support structures, or at the permanent supports, for alignment of the structure during the erection process. If the erection plan does indeed require jacking devices, they should be clearly indicated in the erection plan to alert the Contractor to their need, and their intended use should be explicitly presented.

2.3 Erection Plan and Procedures Checklist

- Plan of Work Area
  - Permanent and temporary structures shown
  - All roads, railroad tracks, waterways, clearances, utilities, potential conflicts shown
  - Material (steel) storage areas shown
- Erection Sequence
  - Step-by-step procedure–figures and narrative dictating work
  - Delivery location of components shown
  - Crane locations shown
  - Temporary support, hold cranes, blocking, tie-downs shown
  - Load restrictions for certain stages (i.e., wind)
- Crane Information
  - Crane type, pick radii, boom length shown
  - Approximate crane pick points shown
  - Crane pick weights shown
  - Hold crane loads
- Details of Lifting Devices and Special Procedures
- Bolting Requirements
- Bearing Blocking and Tie-Down Details
- Temporary Supports
  - Details of structure shown
  - Load capacities
- Jacking Devices and Procedures

CHAPTER 3

Recommendations for Methods of Structural Analysis and Calculations

3.1 Introduction

Calculations by the Contractor's Engineer investigating the steel erection sequence are required to substantiate the erection plan and procedures submitted for a given project. This section presents guidelines regarding these calculations. It also provides recommendations on the appropriate methods of analysis to employ when investigating the adequacy of the erection sequence of a curved or skewed steel girder bridge. These guidelines and recommendations are a synthesis of studies conducted as part of NCHRP Project 12-79, "Guidelines for Analytical Methods and Erection Engineering of Curved and Skewed Steel Deck-Girder Bridges." Detailed background to these guidelines can be found in the Task 8 report of Project 12-79, "Guidelines for Selecting Analytical Methods for Construction Engineering of Curved and Skewed Steel Girder Bridges."

3.2 Recommendations on Methods of Analysis

A substantial number of studies were conducted as part of NCHRP Project 12-79 to determine the ability of approximate 1D and 2D methods of analysis to capture the behavior predicted by refined 3D finite element models. To evaluate 1D methods, a commonly available commercial line-girder analysis program, STLBRIDGE (Bridgesoft, 2010), was used to analyze the behavior of straight skewed I- and tub-girder bridges. The 1D analysis of curved, and curved and skewed, I-girder bridges was based on the V-load method (Richardson, Gordon & Associates, 1976; United States Steel, 1980) using the software VANCK (NSBA, 1996). The 1D analysis of curved, and curved and skewed, tub-girder bridges was based on a line-girder analysis coupled with additional calculations based on the M/R method (Tung and Fountain, 1970). To evaluate 2D methods, two commercially available software programs, typically employed by bridge designers, were used to investigate the behavior of these same bridges: the software MDX (MDX, 2011) for analysis using a conventional 2D-grid approach and the capabilities of LARSA-4D (LARSA, 2010) for analysis using a conventional 2D-frame approach. To evaluate linear elastic 3D finite element analysis methods, the software program ABAQUS was used to investigate the behavior of these same bridges. The 1D, 2D, and linear elastic 3D analysis results were compared to benchmark nonlinear "simulation" 3D finite element analysis solutions, also prepared using the software program ABAQUS, including the modeling of 2nd-order effects (geometric nonlinearity). Where possible, extant bridges were evaluated and if those bridges had been instrumented, the nonlinear simulation benchmark analysis results were validated against measured responses.

3.2.1 I-Girder Bridges

A quantitative assessment of the analysis accuracy was obtained by identifying error measures that compared the approximate (1D and 2D methods) solutions to the 3D FEA benchmark

solutions. Using the quantitative assessments, the various methods of analysis were ranked based on a scoring system developed to provide a comparative evaluation of each analysis method with regard to the accuracy of its analysis predictions for various structural responses.

Table 3.1 summarizes the scoring system for the various methods and behaviors monitored. The scoring criteria are as follows:

- A grade of A is assigned when the normalized mean error is less than or equal to 6 percent, reflecting excellent accuracy of the analysis predictions.
- A grade of B is assigned when the normalized mean error is between 7 percent and 12 percent, reflecting a case where the analysis predictions are in "reasonable agreement" with the benchmark analysis results.

Table 3.1 Matrix for Recommended Level of Analysis – I-Girder Bridges.

Response	Geometry	Worst-Case Scores		Mode of Scores	
		Traditional 2D-Grid	1D-Line Girder	Traditional 2D-Grid	1D-Line Girder
Major-Axis Bending Stresses	C ($I_C \leq 1$)	B	B	A	B
	C ($I_C > 1$)	D	C	B	C
	S ($I_S < 0.30$)	B	B	A	A
	S ($0.30 \leq I_S < 0.65$)	B	C	B	B
	S ($I_S \geq 0.65$)	D	D	C	C
	C&S ($I_C > 0.5$ & $I_S > 0.1$)	D	F	B	C
Vertical Displacements	C ($I_C \leq 1$)	B	C	A	B
	C ($I_C > 1$)	F	D	F	C
	S ($I_S < 0.30$)	B	A	A	A
	S ($0.30 \leq I_S < 0.65$)	B	B	A	B
	S ($I_S \geq 0.65$)	D	D	C	C
	C&S ($I_C > 0.5$ & $I_S > 0.1$)	F	F	F	C
Cross-Frame Forces	C ($I_C \leq 1$)	C	C	B	B
	C ($I_C > 1$)	F	D	C	C
	S ($I_S < 0.30$)	NA[a]	NA[a]	NA[a]	NA[a]
	S ($0.30 \leq I_S < 0.65$)	F[b]	F[c]	F[b]	F[c]
	S ($I_S \geq 0.65$)	F[b]	F[c]	F[b]	F[c]
	C&S ($I_C > 0.5$ & $I_S > 0.1$)	F[b]	F[c]	F[b]	F[c]
Flange Lateral Bending Stresses	C ($I_C \leq 1$)	C	C	B	B
	C ($I_C > 1$)	F	D	C	C
	S ($I_S < 0.30$)	NA[d]	NA[d]	NA[d]	NA[d]
	S ($0.30 \leq I_S < 0.65$)	F[b]	F[e]	F[b]	F[e]
	S ($I_S \geq 0.65$)	F[b]	F[e]	F[b]	F[e]
	C&S ($I_C > 0.5$ & $I_S > 0.1$)	F[b]	F[e]	F[b]	F[e]
Girder Layover at Bearings	C ($I_C \leq 1$)	NA[f]	NA[f]	NA[f]	NA[f]
	C ($I_C > 1$)	NA[f]	NA[f]	NA[f]	NA[f]
	S ($I_S < 0.30$)	B	A	A	A
	S ($0.30 \leq I_S < 0.65$)	B	B	A	B
	S ($I_S \geq 0.65$)	D	D	C	C
	C&S ($I_C > 0.5$ & $I_S > 0.1$)	F	F	F	C

[a] Magnitudes should be negligible for bridges that are properly designed & detailed. The cross-frame design is likely to be controlled by considerations other than gravity-load forces.

[b] Results are highly inaccurate due to modeling deficiencies addressed in Ch. 6 of the NCHRP 12-79 Task 8 report. The improved 2D-grid method discussed in this Ch. 6 provides an accurate estimate of these forces.

[c] Line-girder analysis provides no estimate of cross-frame forces associated with skew.

[d] The flange lateral bending stresses tend to be small. AASHTO Article C6.10.1 may be used as a conservative estimate of the flange lateral bending stresses due to skew.

[e] Line-girder analysis provides no estimate of girder flange lateral bending stresses associated with skew.

[f] Magnitudes should be negligible for bridges that are properly designed & detailed.

- A grade of C is assigned when the normalized mean error is between 13 percent and 20 percent, reflecting a case where the analysis predictions start to deviate "significantly" from the benchmark analysis results.
- A grade of D is assigned when the normalized mean error is between 21 percent and 30 percent, indicating a case where the analysis predictions are poor, but may be considered acceptable in some situations.
- A grade of F is assigned if the normalized mean errors are above the 30 percent limit. At this level of deviation from the benchmark analysis results, the subject approximate analysis method is considered unreliable and inadequate for design.

The normalized mean error is calculated as

$$\mu_e = \frac{1}{N \cdot R_{FEA\max}} \sum_{i=1}^{N} e_i$$

where N is the total number of sampling points along the length in the approximate model, R_{FEAmax} is the absolute value of the maximum response obtained from the FEA, and e_i is the absolute value of the error relative to the 3D FEA benchmark solution evaluated at point *i:*

$$e_i = \left| R_{approx} - R_{FEA} \right|$$

The summation in the above is computed for each girder line along the full length of the bridge, and the largest resulting value is reported as the normalized mean error for the bridge. The error measure μe is useful for the overall assessment of the analysis accuracy since this measure is insensitive to isolated discrepancies, which can be due to minor shifting of the response predictions, etc. The normalized local maximum errors, e_i / R_{FEAmax} are generally somewhat larger than the normalized mean error. Also, in many situations, unconservative error at one location in the bridge leads to comparable conservative error at another location. Hence, it is simpler to not consider the sign of the error as part of the overall assessment of the analysis accuracy.

In Table 3.1, the scoring for the various measured responses is subdivided into six categories based on the bridge geometry. These bridge categories are defined as follows:

- Curved bridges with no skew are identified in the Geometry column by the letter "C."
- The curved bridges are further divided into two subcategories, based on the connectivity index, I_C defined as:

$$I_C = \frac{15000}{R\left(n_{cf} + 1\right)m}$$

where R is the minimum radius of curvature, n_{cf} is the number of intermediate cross-frames in the span, and m is a constant taken equal to 1 for simple-span bridges and 2 for continuous-span bridges. In bridges with multiple spans, I_C is taken as the largest value obtained from any of the spans.

- Straight-skewed bridges with no curvature are identified in the geometry column by the letter "S."
- The straight-skewed bridges are further divided into three subcategories, based on the skew index, I_S. where I_S is taken as:

$$I_S = \frac{w \tan\theta}{L_s}$$

where w is the width of the bridge measured between fascia girders, θ is the skew angle measured from a line perpendicular to the tangent of the bridge centerline, and L_s is the span

B-12 Guidelines for Analysis Methods and Construction Engineering of Curved and Skewed Steel Girder Bridges

length at the bridge centerline. In bridges with unequal skew at the bearing lines, θ is taken as the angle of the bearing line with the largest skew.
- Bridges that are both curved and skewed are identified in the geometry column by the letters "C&S."

Two letter grades are indicated for each of the cells in Table 3. The first letter grade corresponds to the worst-case results encountered from either of the two 2D-grid solutions considered in the NCHRP Project 12-79 studies, or from the 1D-line girder calculations, within each of the specified categories. The second letter grade indicates the mode of the letter grades for that category, i.e., the letter grade encountered most often for that category.

Table 3.1 can be used to determine when a certain analysis method can be reasonably expected to produce acceptable results. The following two examples illustrate how Table 3.1 is to be used.

3.2.1.1 I-Girder Bridge Level of Analysis Example 1

Consider a horizontally curved steel I-girder bridge with radial supports, "regular" geometry (constant girder spacing, constant deck width, relatively uniform cross-frame spacing, etc.), and $I_C \leq 1$, for which the engineer wants to perform a traditional 2D-grid analysis to determine the forces and displacements during critical stages of the erection sequence. (It should be noted that if I_C is calculated for an intermediate stage of the steel erection in which some of the cross-frames have not yet been placed, the number of intermediate cross-frames n_{cf} in Eq. 8 should be taken as the number installed in the erection stage that is being checked. In addition, the radius of curvature R and the constant m should correspond to the specific intermediate stage of construction being evaluated, not the bridge in its final erected configuration.)

For the girder major-axis bending stresses and vertical displacements (f_b and Δ), the results are expected to deviate somewhat from those of a 3D analysis in general, because a worst-case score of B is assigned in Table 3.1 for all of these response quantities. The worst-case normalized mean error in these results from the 2D-grid analysis will typically range from 7 to 12 percent, as compared to the results from a refined geometric nonlinear 3D FEA. However, one can expect that for most bridges, the errors will be less than or equal to 6 percent, based on the mode score of A for both of these responses.

Therefore, in this example, if the major-axis bending stress results and vertical displacement results are of prime interest, a 2D-grid model should be sufficient if worst-case errors of approximately 12 percent are acceptable. Given that the bridge has very "regular" geometry, it is likely that the f_b and Δ errors are less than or equal to 6 percent. (The worst-case score is considered as the appropriate one to consider when designing a bridge with complicating features such as a poor span balance, or other "less regular" geometry characteristics.)

It is important to note that the engineer can "compensate" for potential unconservative major-axis bending stress errors in the design by adjusting the target performance ratios desired for the construction engineering analysis. For example, with the above bridge, the engineer may require that the performance ratio be less than or equal to 1/1.12 = 0.89 or 1/1.06 = 0.94 for the girder flexural resistance checks to gain some further confidence in the adequacy of the analysis. Conversely, over-prediction and under-prediction of the vertical displacements can be equally bad. Nevertheless, 12 percent or 6 percent displacement error may be of little consequence if the magnitude of the displacements is relatively small, or if the deflections are being calculated at an early stage of the steel erection and it is expected that any resulting displacement incompatibilities or loss of geometry control can be subsequently resolved. However, if the magnitude of the displacements is large, or if it is expected that the resulting errors or displacement incompatibilities may be difficult to resolve, the engineer should consider conducting a 3D FEA of the subject construction stage to gain further confidence in the calculated displacements. This step

in the application of Table 3.1 is where the bridge span length enters as an important factor, since longer-span bridges tend to have larger displacements.

It should be noted that compared to the creation of 3D FEA models for overall bridge design, including calculation of live load effects, the development of a 3D FEA model for several specific construction stages that may be of concern involves a relatively small amount of effort. This is particularly the case with many of the modern software interfaces that facilitate the definition of the overall bridge geometry.

For calculation of the girder flange lateral bending stresses and the cross-frame forces in the above example bridge, the worst-case errors are expected to be larger, on the order of 13 percent to 20 percent (corresponding to a grade of C for both of these responses). However, the mode score is B, and since the bridge has very regular geometry, it is likely that the normalized mean error in the flange lateral bending stresses and cross-frame forces is less than 12 percent. If these errors are acceptable in the engineer's judgment, then the 2D-grid analysis should be acceptable for the construction engineering calculations. As noted above, the engineer can compensate for these potential errors by reducing the target performance indices. With respect to the flange lateral bending stress, it should be noted that the f_λ values are multiplied by ⅓ in the AASHTO ⅓ rule equations. Therefore, the errors in f_λ have less of an influence on the performance ratio errors than errors in f_b. When checking the AASHTO flange yielding limit for constructability, both f_λ and f_b have equal weights though. Based on these considerations, the best way to compensate for different potential unconservative errors in the f_λ and f_b values is to multiply the calculated stresses from the 2D-grid analysis by 1.20 and 1.12 (or 1.12 and 1.06) respectively prior to checking the performance ratios.

3.2.1.2 I-Girder Bridge Level of Analysis Example 2

Consider a straight steel I-girder bridge with skewed supports and a skew index, $I_s = 0.35$ (corresponding to the intermediate erection stage being evaluated), for which the engineer wants to perform a traditional 2D-grid analysis to determine the forces and displacements during critical stages of the erection sequence.

After reviewing Table 3.1, it is observed that for major-axis bending stresses and vertical deflections, a worst-case score of B is shown for straight skewed I-girder bridges with $0.30 < I_S \leq 0.65$. Furthermore, it can be observed that the mode of the scores for these bridge types is a B for the major-axis bending stresses and an A for the vertical displacements. Therefore, a properly prepared conventional 2D-grid analysis would be expected to produce major-axis bending stress and vertical deflection results that compare reasonably well with the results of a second-order elastic 3D FEA, such that the normalized mean error would be expected to be less than or equal to 12 percent.

If the layout of the cross-frames in the skewed bridge is such that overly stiff (nuisance) transverse load paths are alleviated, the engineer may expect that the error in the displacement calculations may be close to 6 percent or less. In this case, the engineer should be reasonably confident in the 2D-grid results for the calculation of these responses. As noted in the previous example, the potential unconservative errors in the stresses can be compensated for in the construction engineering design checks; however, positive or negative displacement errors are equally bad.

The girder layover at the skewed bearing lines is often of key interest in skewed I-girder bridges. Table 3.1 shows that the girder layover calculations have essentially the same magnitude of errors and resulting grades as the girder vertical displacements. This is because the skewed bearing line cross-frames are generally relatively rigid in their own planes compared to the stiffness of the girders. Hence, the girder layovers are essentially proportional to the girder major-axis bending rotations at the skewed bearing lines.

B-14 Guidelines for Analysis Methods and Construction Engineering of Curved and Skewed Steel Girder Bridges

For the calculation of the cross-frame forces and/or the girder flange lateral bending stresses in the above example, one can observe that the conventional 2D-grid procedures are entirely unreliable. That is, the scores in Table 3.1 are uniformly an F. The reason for this poor performance of the traditional 2D-grid methods is the ordinary modeling of the girder torsional properties using only the St. Venant torsional stiffness GJ/L. The physical girder torsional stiffnesses are generally much larger due to restraint of warping, i.e., flange lateral bending, effects. In addition, for wide skewed bridges and/or for skewed bridges containing specific overly stiff (nuisance) transverse load paths, the limited accuracy of the cross-frame equivalent beam stiffness models used in conventional 2D-grid methods may lead to a dramatic loss of accuracy in the cross-frame forces.

Lastly, conventional 2D-grid methods generally do not include any calculations of the girder flange lateral bending stresses due to skew. Hence, the score for the calculation of the flange lateral bending stresses is also an F in Table 3.1.

Chapter 6 of the NCHRP 12-79 Task 8 report, "Guidelines for Selecting Analytical Methods for Construction Engineering of Curved and Skewed Steel Girder Bridges," recommends several important modifications to conventional 2D-grid procedures that are relatively simple for software providers to implement yet provide substantial improvements in the analysis accuracy. To realize the benefits of these improvements in typical bridge design practice it will be necessary for commercial 2D-grid software providers to implement these types of improvements, since manual implementation of the improvements tends to be cumbersome and time consuming for the engineer. Therefore, this document focuses solely on the accuracy of conventional 2D-grid and 1D line-girder procedures.

3.2.2 Tub-Girder Bridges

Similar to the I-girder bridges, a quantitative assessment of the analysis accuracy of tub-girder bridges was obtained by focusing first on the normalized mean errors in the approximate (1D and 2D method) solutions for the girder major-axis bending stresses, internal torques, and vertical displacements, compared to benchmark 3D FEA results. Using the quantitative assessments, the various methods of analysis were assigned scores in the same manner as the scoring discussed in Section 3.1.1 for the I-girder bridge responses. Table 3.2 summarizes the scores for the above responses in tub-girder bridges.

It is interesting that the Table 3.2 scores for the major-axis bending stresses and vertical displacements are relatively good. However, the worst-case scores for the internal torques are generally quite low. These low scores are largely due to the fact that the internal torques in tub-girder bridges can be sensitive to various details of the framing, such as the use and location of external intermediate cross-frames or diaphragms, the relative flexibility of these diaphragms as well as the adjacent internal cross-frames within the tub-girders, skewed interior piers without external cross-frames between the piers at the corresponding bearing line, incidental torques introduced into the girders due to the specific orientation of the top flange lateral bracing system members (particularly for Pratt-type TFLB systems), etc. Jimenez Chong (2012) provides a detailed evaluation and assessment of the causes for the errors in the girder internal torques for the tub-girder bridges considered in the NCHRP Project 12-79 research.

Similar to the considerations for I-girder bridges, the external diaphragms and/or cross-frames typically respond relatively rigidly in their own plane compared to the torsional stiffness of the girders. Therefore, the girder layovers at skewed bearing lines tend to be proportional to the major-axis bending rotation of the girders at these locations. As a result, the errors in the girder layover calculations obtained from the approximate methods tend to be similar to the errors in the major-axis bending displacements.

Table 3.2 Matrix 1 for Recommended Level of Analysis – Tub-Girder Bridges.

Response	Geometry	Worst-Case Scores		Mode of Scores	
		Traditional 2D-Grid	1D-Line Girder	Traditional 2D-Grid	1D-Line Girder
Major-Axis Bending Stresses	S	B	B	A	B
	C	B	C	A	B
	C&S	B	C	B	B
Girder Torques	S	**F**	**F**	D	**F**
	C	D	D	A	B
	C&S	**F**	**F**	A	B
Vertical Displacements	S	B	B	A	A
	C	A	B	A	A
	C&S	B	B	A	A
Girder Layover at Bearing Lines	S	B	B	A	A
	C	NA[a]	NA[a]	NA[a]	NA[a]
	C&S	B	B	A	A

[a] Magnitudes should be negligible where properly designed and detailed diaphragms or cross-frames are present.

The connectivity index, I_C does not apply to tub-girder bridges, since this index is primarily a measure of the loss of accuracy in I-girder bridges due to the poor modeling of the girder torsion properties. For tub-girder bridges, the conventional St. Venant torsion model generally works well as a characterization of the torsional response of the pseudo-closed section tub-girders. Hence, I_C is not used for characterization of tub-girder bridges in the table. Furthermore, there is only a weak correlation between the accuracy of the simplified analysis calculations and the skew index I_S for tub-girder bridges. Therefore, the skew index is not used to characterize tub-girder bridges in Table 3.2 either. Important differences in the simplified analysis predictions do exist, however, as a function of whether the bridge is curved, "C," straight and skewed, "S," or curved and skewed "C&S." Therefore, these characterizations are shown in the table.

In addition, to the above quantitative assessments, the calculation of bracing component forces in tub-girder bridges is assessed separately in Table 3.3. It is useful to address the accuracy of these response calculations separately from those shown in Table 3.2 since the simplified bracing component force calculations take the girder major-axis bending moments, torques, and applied transverse loads as inputs and then apply various useful mechanics of materials approximations to obtain the force estimates. That is, there are two distinct sources of error in the bracing component forces relative to the 3D FEA benchmark solutions:

1. The error in the calculation of the input quantities obtained from the 1D line-girder or the 2D-grid analysis, and
2. The error introduced by approximations in the component force equations.

Chapter 2 of the NCHRP Project 12-79 Task 8 report provides an overview of the most commonly employed bracing component force equations evaluated here. It should be noted that the calculation of the top flange lateral bending stresses in tub girders is included as one of the bracing component force calculations. This is because these stresses are influenced significantly by the interaction of the top flanges with the tub-girder bracing systems.

The NCHRP Project 12-79 research observed that in many situations the bracing component force estimates are conservative relative to the 3D FEA benchmark solutions. Therefore, it is useful to consider a signed error measure for the bracing component force calculations. In addition, the bracing component dimensions and section sizes often are repeated to a substantial degree throughout a tub-girder bridge for the different types of components. Therefore, it is useful to

quantify the analysis error as the difference between the maximum of the component forces determined by the approximate analysis minus the corresponding estimate from the 3D FEA benchmark, i.e.:

$$e_{\max} = \left(R_{approx.max} - R_{FEA.max} \right) / R_{FEA.max}$$

for a given type of component. The grades for these responses were then assigned based on the same scoring system as that used for the assessments based on normalized mean error with one exception: Separate grades were assigned for the positive (conservative) errors and for the negative (unconservative) errors in Table 3.3. In situations where no negative (unconservative) errors were observed in all of the bridges considered in a given category, the symbol "—" is shown in the cells of the matrix and the cells are unshaded.

The mode of the grades is shown only for the top flange diagonal bracing forces in Table 3.3. The mode of the grades for the other component force types are not shown because of substantial positive and negative errors in the calculations that were encountered in general for the tub-girder bridges, and because, in cases where a clear mode for the grades existed, the mode of the grades was the same as the worst-case grade.

In addition to the above considerations, it should be noted that current simplified estimates of the tub-girder bridge bracing component forces are generally less accurate for bridges with Pratt-type top flange lateral bracing (TFLB) systems compared to Warren and X-type systems. A small number of tub-girder bridges with Pratt-type TFLB systems were considered in the NCHRP Project 12-79 research. Therefore, the composite scores for these bridges are reported separately in Table 3.3.

3.2.2.1 Tub-Girder Bridge Level of Analysis Example

Consider a horizontally curved steel tub-girder bridge with a Warren top flange lateral bracing system and skewed supports for which the engineer wants to perform a traditional 2D-grid analysis to determine the forces and displacements during critical stages of the erection sequence. The bridge has "regular" geometry (constant girder spacing, constant deck width, a relatively uniform top flange lateral bracing [TFLB] system and internal cross-frame spacing, solid plate end diaphragms, single bearings for each girder, etc.).

A properly prepared 2D-grid analysis would be expected to produce major-axis bending stresses and vertical deflections with mean errors less than 12 percent relative to a rigorous 3D FEA solution, since the worst-case score assigned for both of these quantities is a B in Table 3.2 for the subject "C&S" category. Furthermore, it can be observed that the mode of the scores for the vertical displacements is an A, and hence, given the "regular" geometry of the above bridge, it is expected that the vertical displacements most likely would be accurate to within 6 percent.

Unfortunately, the worst-case score is an F for the 2D-grid estimates of the internal torques in the "C&S" bridges. As noted previously, this low score is due to the fact that the internal torques in tub-girder bridges can be very sensitive to various details of the framing, such as the use and location of external intermediate cross-frames or diaphragms, the relative flexibility of these diaphragms as well as the adjacent internal cross-frames within the tub-girders, skewed interior piers without external cross-frames between the piers at the corresponding bearing line, incidental torques induced in the girders due to the specific orientation of the top flange lateral bracing system members (particularly for Pratt-type TFLB systems), etc. Fortunately though, the web and bottom flange shear forces due to the internal torques are often relatively small compared to the normal stresses due to the major-axis bending response of the girders. Furthermore, the mode of the scores for the internal torques is an A from Table 3.2. Therefore, the engineer must exercise substantial judgment in estimating what the expected error may be for the internal

Table 3.3 Matrix 2 for Recommended Level of Analysis – Tub-Girder Bridges.

Response	Sign of Error	Geometry	Worst-Case Scores		Mode of Scores	
			Traditional 2D-Grid	1D-Line Girder	Traditional 2D-Grid	1D-Line Girder
TFLB Diagonal Force	Positive (Conservative)	S	D	D	D	C
		C	D	**F**	B	**F**
		C&S	D[a]	**F**	B	**F**
		Pratt TFLB System	C	**F**	A	**F**
	Negative (Unconservative)	S	**F**[b]	C		
		C	--[c]	--		
		C&S	--	--		
		Pratt TFLB System	--	--		
TFLB & Top Internal CF Strut Force	Positive (Conservative)	S	C	C		
		C	**F**	**F**		
		C&S	**F**	**F**[d]		
		Pratt TFLB System	**F**	**F**		
	Negative (Unconservative)	S	C	C		
		C	--	A		
		C&S	--	C		
		Pratt TFLB System	D	D		
Internal CF Diagonal Force	Positive (Conservative)	S	NA[e]	NA[e]		
		C	**F**	**F**		
		C&S	**F**	**F**		
		Pratt TFLB System	--	**F**[f]		
	Negative (Unconservative)	S	NA[e]	NA[e]		
		C	--	--		
		C&S	--	D		
		Pratt TFLB System	B	--		
Top Flange Lateral Bending Stress (Warren TFLB Systems)	Positive (Conservative)	S	C	C		
		C	**F**	**F**		
		C&S	**F**	**F**[d]		
	Negative (Unconservative)	S	C	C		
		C	--	A		
		C&S	--	C		

[a] Modified from a C to a D considerting the grade for the C and the S bridges.

[b] Large unconservative error obtained for bridge ETSSS2 due to complex framing. If this bridge is considered as an exceptional case, the next worst-case unconservative error is -15 % for NTSSS2 (grade = C).

[c] The symbol "--" indicates that no cases were encountered with this score.

[d] Modified from a B to an F considering the grade for the C bridges.

[e] For straight-skewed bridges, the internal intermediate cross-frame diagonal forces tend to be negligible.

[f] Modified from an A to an F considering the grade for the C and C&S bridges.

torque from a 2D-grid analysis, and in assessing the impact of this error on the bridge design. As noted previously in Section 3.2.1.1 and 3.2.1.2 for I-girder bridges, one can compensate for any anticipated potential unconservative error in the internal force or stress response quantities by scaling up the corresponding responses by the anticipated error, or by adjusting the target values of the performance ratios.

Based on Table 3.3, the worst-case score for the positive (conservative) error in the calculation of the TFLB diagonal forces in the above example bridge is a D whereas the mode of the scores is

a B. The table shows that no unconservative errors were encountered in this calculation for the tub-girder bridges studied in NCHRP Project 12-79. Since the example bridge is "very regular," the engineer may assume that the TFLB diagonal force calculations are conservative, but reasonably accurate, relative to the refined 3D FEA benchmark values.

For both the TFLB and top internal cross-frame strut forces and the internal cross-frame diagonal forces in "C&S" bridges, Table 3.3 shows a grade of F for the conservative error. Also, the table shows that no unconservative errors were encountered in the NCHRP Project 12-79 calculations for these responses. Therefore, the engineer can assume that the forces for these components, as determined from a 2D-grid analysis plus the bracing component force equations, are highly conservative. It should be noted that the forces in the top struts of the internal cross-frames at exterior diaphragm or exterior cross-frame locations can be very sensitive to the interaction of the external diaphragm or cross-frame with the girders. These forces should be determined based on consideration of statics at these locations given the forces transmitted to the girders from the external diaphragm or cross-frame components. NCHRP Project 12-79 did not consider these component forces in its error assessments.

Lastly, Table 3.3 shows that the tub-girder top flange lateral bending stresses tend to be estimated with a high degree of conservatism by 2D-grid methods combined with the bracing component force equations. In addition, no unconservative errors were encountered in the tub-girder bridges studied by NCHRP Project 12-79 for the top flange lateral bending stresses. Therefore, the engineer also can assume that these stress estimates are highly conservative.

3.3 Guidelines on Calculations for Structural Adequacy and Stability

Calculations to substantiate the structural adequacy and stability of the bridge system for each step of the steel erection should be submitted with the erection plan. The calculations should be done in accordance with design criteria established by the Owner, or as stated in the contract plans. This section provides guidelines regarding these calculations. These guidelines should by no means be construed as providing a comprehensive "checklist" of items needing evaluation for erection of any steel girder bridge; each project is unique and may have particular issues requiring the attention of the Contractor's Engineer. Only basic guidelines and suggested evaluation items are presented herein.

3.3.1 Design Criteria

The calculations supporting the erection plan and procedures should be completed in accordance with the AASHTO LRFD Bridge Design Specifications, the AASHTO LRFD Bridge Construction Specifications, and the AASHTO Guide Design Specifications for Bridge Temporary Works, unless otherwise directed by the Owner or the contract documents.

3.3.2 Loads and Load Combinations

The calculations supporting the erection plan and procedures shall consider all applicable loads. Typical load considerations include permanent dead load, construction dead load, construction live load, and wind loads.

Permanent dead loads typically include the self-weight of the structural members and detail attachments. Construction dead and live loads may consist of deck placement machinery, Contractor's equipment, deck overhand brackets, concrete formwork, or other similar attachments applied in the appropriate sequence.

Wind loads shall be considered in each step of the steel erection analysis and are to be computed in accordance with the established design criteria. Provisions should be made by the Contractor's Engineer to ensure that girders are stable in wind events. It is permissible to set limits on maximum wind velocities during steel erection, but these limits must be clearly stated in the erection plan. In some cases, it may be advisable and/or necessary to include provisions in the erection plan for temporary supports and/or tie-downs to address high wind conditions.

Load combinations should be in accordance with the project design criteria, and typically in accordance with the AASHTO LRFD Bridge Design Specifications, unless otherwise agreed to by the Owner.

3.3.3 Girder and System Stability

The calculations supporting the erection plan and procedures shall verify the stability both of individual girders and of the entire erected steel framing for each step of the bridge erection. These calculations are highly dependent upon the particular features of the bridge being erected and also of the particular sequence of erection of each part of the bridge. The assumptions used in the analysis should directly and fully conform to all steps and all details in the erection plan.

The constructability provisions of Article 6.10.3 of the AASHTO LRFD Bridge Design Specifications should be referenced by the Contractor's Engineer when investigating structural adequacy and stability during steel erection. A partial list of suggested evaluation items and guidelines regarding appropriate investigations are as follows.

3.3.3.1 Single Girder Stability

Particular attention should be given to the lateral torsional buckling capacity of a singly erected I-girder. One of the most critical stages during I-girder erection is when the first girder has been erected but not yet connected to adjacent girders in the cross section. Assuming the girder is adequately braced at the supports, and there is no additional bracing within the span, the unbraced length for the girder will be the distance between supports. Long unbraced lengths typically correspond to very low lateral torsional buckling capacity of the girder. Tub-girders typically have much higher lateral torsional buckling capacity, but only if provided with a properly designed top flange lateral bracing system that provides for quasi-closed section behavior of the girder.

Global overturning stability is also a concern for single curved girders, whether I- or tub-girders. The offset of the center of gravity of the girder from a chord line drawn between the support points results in an overturning moment. Single girders are typically afforded little or no torsional restraint at their supports unless tie downs or bracing, or temporary shoring or hold cranes, are provided.

3.3.3.2 Multi-Girder (Global) Stability

A girder system may be vulnerable to global buckling during the steel erection sequence and/or during deck placement. Narrow, long span segments during steel erection are the most susceptible to this global buckling phenomenon. Methods to investigate the global stability of girder systems are available (Yura et al., 2008).

3.3.3.3 Second-Order Amplification Estimates

Second-order amplification of the girder lateral-torsional stresses may cause a loading condition that exceeds the design capacity of the girders or other components. In this situation, the lateral-torsional displacement of the girder results in additional torsional loading in a nonlinear manner. In addition, the displacement amplifications may complicate the prediction and control the structure's geometry during erection. Although second-order amplification should be considered in the

erection analysis of any steel girder bridge, structures that are more susceptible to second-order amplification include widening of an existing bridge with one, two, or a few girders, pedestrian bridges with two-girder systems, phased construction where the various phases may have only one, two, or a few girders erected, and the interim stages of erection of larger bridges where only a few girders are in place in a given erection stage.

A relatively simple method for identifying potentially adverse response amplifications due to second-order effects was developed as part of NCHRP Project 12-79. In this method, the linear response prediction obtained from any first-order analysis is multiplied by the following amplification factor (AF_G):

$$AF_G = \frac{1}{1 - \frac{M_{\max G}}{M_{crG}}}$$

where M_{maxG} is the maximum total moment supported by the bridge unit for the loading under consideration, equal to the sum of all the girder moments, and M_{crG} is the elastic global buckling moment of the bridge unit, which may be estimated using the equation

$$M_{crG} = C_b \frac{\pi^2 sE}{L_s^2} \sqrt{I_{ye} I_x}$$

(Yura et al., 2008). In this equation, C_b is the moment gradient modification factor applied to the full bridge cross-section moment diagram, s is the spacing between the two outside girders of the unit, E is the modulus of elasticity of steel,

$$I_{ye} = I_{yc} + \frac{b}{c} I_{yt}$$

is the effective moment of inertia of the individual I-girders about their weak axis, where I_{yc} and I_{yt} are the moments of inertia of the compression and tension flanges about the weak axis of the girder cross-section respectively, b and c are the distances from the mid-thickness of the tension and compression flanges to the centroidal axis of the cross-section, and I_x is the moment of inertia of the individual girders about their major-axis of bending (i.e., the moment of inertia of a single girder). Yura et al. (2008) provide a number of examples illustrating the calculation of M_{crG}.

3.3.3.4 Cantilever Girders

During the various stages of erection of most steel girder bridges there are often cases where field sections of girders are supported in a cantilevered position. Typically, these intermediate cantilever conditions were not addressed by the Design Engineer during the original bridge design, so it is incumbent on the Contractor's Engineer to investigate these conditions. For long cantilevers, lateral torsional buckling will typically govern over yielding of the section. To examine cantilevers, the lateral torsional buckling capacity can be estimated using the procedures provided in Galambos (1998), Ziemian (2010), or a similar appropriate method. For curved girders, additional consideration needs to be given to the torsional forces that develop due to the offset centroid of the cantilever.

3.3.4 Uplift

Uplift at temporary and permanent supports during steel erection should be accounted for in the development of the erection plan and procedures. Typically, uplift is undesirable and should be prevented, either by changing the erection plan or by providing tie-down restraints. If uplift

is indicated in the analysis but no tie-down restraint is provided, then the analysis should recognize the absence of vertical restraint at that particular support by modeling the boundary condition appropriately. Curved or skewed I-girder bridge systems are particularly susceptible to uplift during various stages of steel erection due to the torsional twisting of the system caused by curvature and/or skew. Incorrect consideration of uplift invalidates the analysis; if not considered correctly, uplift can result in girder alignment and/or other problems as steel erection progresses.

3.3.5 Temporary Hold Cranes

The computations for hold crane loads (if hold cranes are used) should be included in the erection plan calculations. Hold cranes are used to apply an upward load at some location with the span of a girder, thereby reducing the load carried by the girder. Oftentimes, the hold crane load is used to reduce the girder flexural moment due to self-weight (and any other applied loads) to a level at which the moment is less than the lateral-torsional bucking capacity. Typically, a hold crane should not be considered as a brace point in the evaluation of the lateral torsional buckling capacity of a girder; in most cases, the crane cable and crane system are flexible and not capable of providing the lateral resistance necessary to be considered as a brace point.

3.3.6 Temporary Support Loads

The erection plan calculations should include computations for the loads on temporary supports provided at critical stages of the erection sequence. These loads may include vertical and lateral reactions from the superstructure, self-weight of the temporary support, wind loads on the temporary support, etc.

3.3.7 Bearings

Computed bearing rotations during construction should not exceed the rotational capacity of the bearing. The erection plan calculations should include these bearing rotations. Skewed bridges are particularly vulnerable to twisting about the longitudinal axis of the girder. During steel erection, the girder could be rotated beyond the rotational capacity of the bearing, regardless of the vertical load on the bearing.

3.3.8 Cross Frames and Bracing

The placement of the cross frames and other bracing members should be substantiated through calculations that support the erection plan and procedures. The required number of cross frames to be installed before the girders are released from the lifting crane should be verified with calculations and clearly indicated in the erection plan. The cross frames and bracing members and their associated connections must be structurally adequate, and they must also provide sufficient stiffness to the bridge system.

The presence, and correct installation of, cross frames in curved or skewed steel I-girder bridge erection is an important issue. During steel erection, the erector may choose to install the minimum required number of cross frames when initially erecting the girders, so as to decrease erection time, allowing a follow-up crew to install the remaining cross frames later. Therefore, correct determination of the minimum number of required cross frames to prevent lateral torsional buckling of the girders is critical to ensuring the stability of the girders during erection. Yura (1998) provides a general method to check whether cross frames in a girder system provide sufficient bracing for the girders. Additional calculations may be required to check that individual cross frame members and connections have adequate capacity.

3.4 Structural Adequacy of Temporary Components

Calculations to substantiate the structural adequacy and stability of any and all temporary support components for each step of the steel erection should be submitted with the erection plan. Additionally, calculations supporting the use of lifting beams, lifting devices (rigging), and jacking devices should be included in the calculation submittal. The calculations should be done in accordance with design criteria established by the Owner, or as stated in the contract plans.

3.4.1 Temporary Supports

Calculations indicating the load capacity and verifying the stability of any temporary supports should be included in the computations supporting the erection plan and procedures. Temporary support structures should be designed to carry vertical and lateral loads resulting from the proposed erection sequence. As necessary, calculations for the design of an upper grillage, temporary bearings, and foundations should also be included. The elevation of the bearing support (bearing seat elevation) at the top of the temporary support structure should be computed and provided in the erection plan. The bearing seat elevations at the temporary supports can aid the steel erector in controlling the geometry of the structure during steel erection.

3.4.2 Girder Tie-Downs

Calculations indicating the load capacity of girder tie-downs at any location should be included in the computations supporting the erection plan and procedures. The tie-downs may be used to resist wind loads, uplift, lateral dead load forces resulting from horizontal curvature, or other loads.

3.4.3 Lifting Beams and Devices

Calculations verifying the load capacity of Contractor-fabricated lifting devices such as lifting beams, spreader beams, welded lugs, beam clamps, etc., should be provided in the computations supporting the erection plan and procedures. When applicable, manufacturers' certification or catalog cuts for pre-engineered devices should be included with the calculations.

3.4.4 Jacking Devices

Calculations for jacking devices, including jacking loads, jack type, etc., should be included with the erection plan calculations. Also, a detailed jacking procedure should be developed and included in the erection plan.

3.5 Miscellaneous Calculations and Recommendations

3.5.1 Crane Pick Locations

The Contractor's Engineer often provides calculations for the approximate pick locations for girder erection. These approximate crane pick locations should be determined with consideration of the centroid of the entire assembly being lifted into place, including the girder as well as any attached cross frames, splice plates, stiffening trusses, or other attached items.

Figure 3.1 provides equations helpful in the computation of the centroids of various curved shapes.

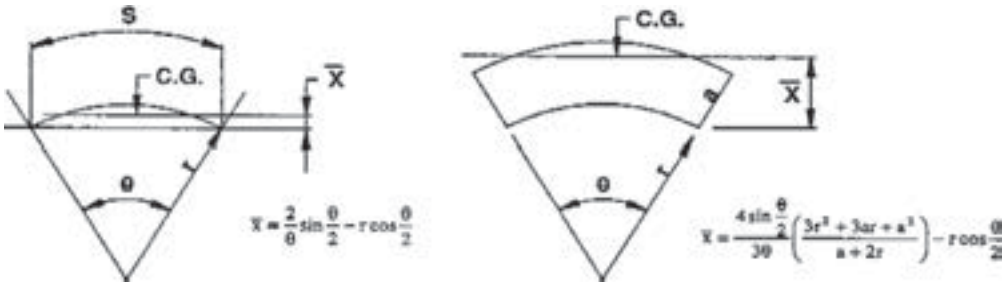

(a) (b)

Figure 3.1 Center of gravity for approximate pick points during lifting: (a) circular arc, (b) sector of annulus.

3.5.2 Alignment of Field Splice Connections

Using the erection analysis results, the Contractor's Engineer should evaluate the lateral and vertical displacements and rotations at field splice locations of previously erected girders in relation to the next girder segment being erected. Oftentimes, the field splice location will be at the end of the girder that is cantilevered over an interior support, and displacements and rotations may be significant enough to hinder the Contractor's attempts to align bolt holes in bolted field splice connections. Vertical displacements and end rotations at the end of the previously placed, cantilevered section may result in the end of the girder being out of position and out of alignment relative to the next field section being erected, which is often in a level, neutral position when being lifted. Lateral displacements are caused by the natural behavior of a curved steel girder to rotate outward from the radius of curvature. Since the next girder piece being lifted into place will typically be in a vertically plumb position, laterally displaced cantilever tips of the previously erected girder could cause alignment issues.

3.5.3 Alignment of Cross Frame Connections

Using the erection analysis results, the Contractor's Engineer should verify that the lateral displacements and girder rotations do not cause problems in erecting cross frames, whether cross frames are installed before or after girders are released from the lifting crane. Long unbraced girder lengths may result in significant out-of-plane rotations and displacements of the top and bottom flanges. Curvature and skew also produce potentially significant girder displacements and rotations. If the rotations and displacements are too large, the Contractor may have difficulty aligning connections.

Contractors typically use various methods to correct these types of misalignments, including the use of temporary hold cranes, jacks, come-alongs, or other means. In certain situations, these means may prove insufficient. In extreme cases, the inherent stiffness of the girders is such that enough force cannot be practically applied to pull the connections into alignment, or alternately the amount of force required to pull the connections into alignment would damage the structure.

3.5.4 Support Conditions

The boundary (support) conditions assumed in the erection analysis should accurately reflect the actual support conditions in the structure at all stages of erection (including accurate consideration of any and all temporary supports). If the character of the support at a location changes during the steel erection, this should be accurately addressed in the analysis model. Improper modeling of boundary conditions leads to erroneous results and invalidates the analysis.

B-24 Guidelines for Analysis Methods and Construction Engineering of Curved and Skewed Steel Girder Bridges

3.6 Calculation Checklist

- Complete analysis of erection sequence
  - Proper level of analysis used
  - Support conditions modeled appropriately at all stages
- Correct design criteria employed
- Correct loads investigated
- Complete checks of structural adequacy of bridge components
- Complete checks of stability of girder and bridge system
- Second-order amplification effects addressed as needed
- Girder reactions checked for uplift
- Temporary hold crane loads computed
- Temporary support loads computed
- Bearing capacity and rotation checks
- Cross frame and bracing placement
- Checks of structural adequacy of temporary supports and devices
  - Falsework towers
  - Girder tie-downs
  - Lifting beams
  - Jacking devices
- Crane pick location calculations
- Checks of displacements at field splices
- Checks of displacements for cross frame placement

3.7 Problematic Characteristics and Details to Avoid

3.7.1 Oversized or Slotted Holes

The use of oversized or slotted holes in gusset and connection plates can decrease significantly the stability bracing efficiency of cross-frames. In addition, the control of the deformed bridge geometry can also be affected since cross-frames are necessary to integrate the girders and make them deform as a unit rather than as independent components. Therefore, it is not recommended to use this scheme as a solution to erecting cross-frames at stiff locations such as the regions near skewed supports.

3.7.2 Narrow Bridges or Bridge Units

In some cases, I-girder bridges can be susceptible to large response amplifications due to global second-order effects. Widening projects of existing bridges, pedestrian bridges with twin girders, phased construction, and erection stages where only a few girders of the bridge are in place, are some examples of structures that can be susceptible to considerable global second-order amplifications. When potential amplifications of the system stress and displacement responses are a concern, it is recommended to study the structure with refined 3D FEA or an approximate method based on amplified responses of a linear analysis solution.

3.7.3 V-Type Cross-Frames without Top Chords

Cross-frames are needed to stabilize I-girders prior to hardening of the concrete deck. In some cases, V-type cross-frames without top chords may not be able to perform this function. The flexural stiffness of this type of cross-frame is substantially smaller than other configurations (i.e. X-type or V-type with top chord). Therefore, its ability to provide stability bracing needs to be con-

sidered carefully during design. Studies conducted on an existing structure that uses V-type cross-frames without top chords illustrates the importance of including the top chord (Sanchez, 2011).

3.7.4 Bent-Plate Connections in I-Girder Bridges

Bent-plate details can introduce excessive flexibility in the system, affecting the stability bracing capacity of skewed cross-frames. Due to this limitation, designers should consider the use of other connection details that do not represent a detriment to the system performance. Details such as the half-pipe stiffener and the reinforced bent-plate are options that can be used to connect skewed cross-frames at angles larger than 20°.

3.7.5 Long-Span I-Girder Bridges without Top Flange Lateral Bracing Systems

Flange level lateral bracing systems are recommended for long-span bridges since second-order amplification and global flange lateral bending effects can be more critical for longer spans as the stresses are more dominated by dead load effects. Flange level lateral bracing systems help to control the bridge geometry and eliminate the second-order effects as these systems cause portions of the structure to act as pseudo-box girders.

3.7.6 Partial-Depth End Diaphragms in Tub-Girder Bridges

Partial-depth end diaphragms often are used when they are the only solution due to the project geometric constraints. When possible, such a detail should be avoided in the practice because it changes the local and global behavior of the system. At the local level, the top flange lateral bracing system will lose continuity close to the end diaphragm. This results in a redistribution of forces through a different load path to reach the end of the girder. Also, the end panel will experience comparatively more deformation with respect to the adjacent panels, thus having a direct impact in the adjacent elements that control the cross section distortion, such as the internal cross-frames. The global consequences include a significant increase of the girder deflections and rotations due to the increased flexibility caused by partial-depth end diaphragms. If partial-depth end diaphragms are used, the resulting behavior of the system needs to be carefully investigated and, in many cases, will require a more refined analysis.

3.7.7 Non-Collinear External Intermediate Diaphragms in Tub-Girder Bridges

When tub-girder bridges require external intermediate cross-frames or support diaphragms to control differential displacements between girders, or reaction force distribution, the internal and external components should be collinear to avoid undesired behavior at the connecting locations.

3.7.8 Two-Bearing System at Tub-Girder Support

The use of twin bearing support under a single tub-girder typically requires a more refined analysis and, in general, should be avoided for curved and/or skewed bridges. In the curved and/or skewed bridges, an ideal twin bearing system could be used to transfer part or all of the associated torque to the support rather than follow the end diaphragm mechanism. In most cases, common bridge bearings are not able to resist upward forces and, consequently, the bridge could experience uplift at one of the twin bearings while the other bearing could be subjected to the entire vertical load, possibly exceeding the bearing design force.

References

AASHTO/NSBA Steel Bridge Collaboration (2007). *Steel Bridge Erection Guide Specification,* American Association of State Highway and Transportation Officials/National Steel Bridge Alliance, Washington, D.C.

AASHTO (2008). Guide Design Specifications for Bridge Temporary Works, 1st edition with Interim Revisions through 2008, American Association of State Highway and Transportation Officials, Washington, D.C.

AASHTO, LRFD Bridge Design Specifications (2010). 5th edition, American Association of State Highway and Transportation Officials, Washington, D.C.

AASHTO, LRFD Bridge Construction Specifications (2010). 3rd edition, American Association of State Highway and Transportation Officials, Washington, D.C.

Bridgesoft, Inc. (2010). "STLBRIDGE, Continuous Steel Bridge Design," http://bridgesoftinc.com/

Galambos, T.V. (1998). *Guide to Stability Design Criteria for Metal Structures*, 5th edition, Wiley, New Jersey.

Jimenez Chong, J.M. (2012). "Construction Engineering of Steel Tub-Girder Bridge Systems for Skew Effects," Ph.D. dissertation, School of Civil and Environmental Engineering, Georgia Institute of Technology, Atlanta, GA, 276 pp.

LARSA (2010). "LARSA 4D, The Complete Software for Bridge Engineering," http://www.larsa4d.com/products/larsa4d.aspx

MDX (2011). "MDX Software, The Proven Steels Bridge Design Solution," http://www.mdxsoftware.com/

NSBA (1996). "V-Load Analysis and Check (VANCK), User Manual, Version 1.0," National Steel Bridge Alliance and American Institute of Steel Construction.

Quadrato, C., Battistini, A., Frank, K., Helwig, T., and Engelhardt, M. (2010). "Improved Cross-Frame Connection Details for Steel Bridges with Skewed Supports," *Transportation Research Record 2200,* 29-35, Transportation Research Board, Washington, D.C.

Richardson, Gordon, & Associates (1976) (now Pittsburgh office of HDR, Inc.), *FHWA Curved Girder Workshop Manual.*

Sanchez, T.A. (2011). "Influence of Bracing Systems on the Behavior of Steel Curved and/or Skewed I-Girder Bridges during Construction," Ph.D. dissertation, School of Civil and Environmental Engineering, Georgia Institute of Technology, Atlanta, GA, 2011.

Tung, D.H.H. and Fountain, R.S. (1970). "Approximate Torsional Analysis of Curved Box Girders by the M/R Method," *AISC Engineering Journal,* Vol. 7, No. 3, 1970.

United States Steel Corporation (1984). *V-Load Analysis (ADUSS 88-8535-01).*

Yura, J., (1993). "Fundamentals of Beam Bracing," *Is Your Structure Suitably Braced? – Structural Stability Research Council Annual Stability Conference Proceedings,* Milwaukee, WI, April 6-7: 1-1.20.

Yura, J., Helwig, T., Herman, R., and Zhou, C., (2008). "Global Buckling of I-Shaped Girder Systems," *Journal of Structural Engineering,* ASCE, 134(9), 1487-1494.

Ziemian, R. (2010). *Guide to Stability Design Criteria for Metal Structures,* 6th edition, Wiley, New Jersey.

Abbreviations and acronyms used without definitions in TRB publications:

AAAE	American Association of Airport Executives
AASHO	American Association of State Highway Officials
AASHTO	American Association of State Highway and Transportation Officials
ACI–NA	Airports Council International–North America
ACRP	Airport Cooperative Research Program
ADA	Americans with Disabilities Act
APTA	American Public Transportation Association
ASCE	American Society of Civil Engineers
ASME	American Society of Mechanical Engineers
ASTM	American Society for Testing and Materials
ATA	American Trucking Associations
CTAA	Community Transportation Association of America
CTBSSP	Commercial Truck and Bus Safety Synthesis Program
DHS	Department of Homeland Security
DOE	Department of Energy
EPA	Environmental Protection Agency
FAA	Federal Aviation Administration
FHWA	Federal Highway Administration
FMCSA	Federal Motor Carrier Safety Administration
FRA	Federal Railroad Administration
FTA	Federal Transit Administration
HMCRP	Hazardous Materials Cooperative Research Program
IEEE	Institute of Electrical and Electronics Engineers
ISTEA	Intermodal Surface Transportation Efficiency Act of 1991
ITE	Institute of Transportation Engineers
NASA	National Aeronautics and Space Administration
NASAO	National Association of State Aviation Officials
NCFRP	National Cooperative Freight Research Program
NCHRP	National Cooperative Highway Research Program
NHTSA	National Highway Traffic Safety Administration
NTSB	National Transportation Safety Board
PHMSA	Pipeline and Hazardous Materials Safety Administration
RITA	Research and Innovative Technology Administration
SAE	Society of Automotive Engineers
SAFETEA-LU	Safe, Accountable, Flexible, Efficient Transportation Equity Act: A Legacy for Users (2005)
TCRP	Transit Cooperative Research Program
TEA-21	Transportation Equity Act for the 21st Century (1998)
TRB	Transportation Research Board
TSA	Transportation Security Administration
U.S.DOT	United States Department of Transportation